Post-transcriptional gene regulation in *Drosophila*: an investigation into the roles of RNA silencing and the DEAD-box helicase Belle

Pavel Natalin

November 2008

Dissertation
submitted to the
Combined Faculties for the Natural Sciences and for Mathematics
of the Ruperto-Carola University of Heidelberg, Germany
for the degree of
Doctor of Natural Sciences

Presented by
Diploma biochemist Pavel Natalin
born in Khabarovsk, Russia.

Oral-examination:

Post-transcriptional gene regulation in *Drosophila*: an investigation into the roles of RNA silencing and the DEAD-box helicase Belle

Referees:
Prof. Dr. Matthias Hentze, EMBL, Heidelberg, Germany;
Prof. Dr. Christine Clayton, ZMBH, Heidelberg, Germany.

Contents

List of Tables

List of Figures

Acknowledgements

I would like to express my sincere gratitude to my thesis supervisor Dr. Elisa Izaurralde for the opportunity to do research in her laboratory. Over the whole period of this work, Elisa was open to discussions and ready to provide me with fresh ideas and any kind of support I needed. I greatly appreciate and admire Elisa's dedication to science.

I would like to thank Dr. Anne Ephrussi, Prof. Dr. Matthias Hentze, and Dr. Stephen Cohen for their support and stimulating suggestions as members of my Thesis Advisory Committee, and Prof. Dr. Christine Clayton, who was my external supervisor at the University of Heidelberg. I am grateful to PD Dr. Ralf Bischoff for his agreement to be in the defense committee.

I would also like to thank Dr. Jan Rehwinkel for the collaborative work on the analysis of mRNAs regulated by Drosha and Argonaute proteins. Many thanks go to Tomi Bähr-Ivacevic and Dr. Vladimir Benes, the members of the GeneCore facility at EMBL, for microarray hybridizations. I wish to acknowledge my collaborators inside EMBL Dr. Julius Brennecke, Dr. Alexander Stark, and Dr. Stephen Cohen.

Special thanks go to Dr. Guido Sauer who has carried out mass spectrometry analysis of proteins associated with Belle and helped me to improve the structure of this manuscript.

I am grateful to Dr. Andreas Lingel, Dr. Jan Rehwinkel, Dr. Viter Marquez, and Dr. Silke Dorner who kindly and patiently introduced me to various experimental techniques. I am very much in debt to Dr. Marina Chekulaeva for sharing her expertise in sucrose gradients. I also wish to thank Daniel Schweizer and Dr. Heinz Schwarz in Max Planck Institute for Developmental Biology for helping me in producing the antibody against Belle.

I feel sincere gratitude to all past and present members of Elisa's laboratory, in particular to Michaela Rode, Dr. David Gatfield, Dr. Leonie Unterholzner, Dr. Tamás I. Orbán, Dr. Isabelle Behm-Ansmant, Dr. Ana Eulálio, Dr. Eric Huntziger, Felix Tritschler, Maria Fauser, Sigrun Helms, Elena Khazina, Evelyn Sauer, Dr. Steffen Schmidt, Jörg Braun, Nadine

Wittkopp, Dr. Isao Kashima, Dr. Tadashi Nishihara, Dr. Latifa Zekri, Dr. Isabelle Tournier, Dr. Gabrielle Haas, Dr. Cátia Igreja, and Daniela Lazzaretti. Their constant readiness to both serious scientific discussion and friendly chat made the daily life in and outside the laboratory an enjoyable time.

I am grateful to Dr. Sarah Danes for her valuable comments and corrections of the manuscript of my thesis. I would also like to thank Dr. Oliver Weichenrieder who helped me to improve some parts of this manuscript.

Finally, I would like to thank my family and all my friends for their endless patience and continuous support without which this thesis could not have been completed.

This work was supported by Jeff Schell Fellowship from the Darwin Trust of Edinburgh.

Summary

Post-transcriptional regulation of gene expression relies on multiple mechanisms to elicit translational control and/or mRNA decay. RNA silencing pathways operate at both stages, targeting a significant fraction of the transcriptome, namely those mRNAs complementary to short interfering RNAs (siRNAs) and microRNAs (miRNAs). Using *Drosophila* S2 cells, I have carried out a genome-wide search for transcripts regulated by these pathways.

mRNA expression profiles were obtained for cells depleted of AGO1, AGO2, PIWI or Aubergine, members of the Argonaute family of proteins essential for RNA silencing, and analyzed alongside profiles from cells depleted of the miRNA-processing enzyme Drosha. Changes in transcript levels in Drosha-depleted cells correlated closely with those in the AGO1 knockdown, demonstrating that miRNA targets change level following inhibition of the miRNA pathway and supporting the idea that miRNAs can cause degradation of the targeted transcripts, and do not just repress translation as previously thought. Furthermore, it was found that a subset of miRNA targets is also regulated by AGO2; together with evidence that AGO1 and AGO2 silence the expression of a common set of mobile genetic elements, this suggests a degree of functional overlap for AGO1 and AGO2 in the *Drosophila* RNA silencing pathway.

I next focused on the *Drosophila* protein Belle, a member of the conserved family of DEAD-box RNA helicases. Most members of this protein family exhibit NTPase activity stimulated by or dependent on RNA binding and use the energy derived from NTP hydrolysis to unwind double-stranded RNA or disrupt RNA/protein interactions. Many DEAD-box proteins localize to RNA granules such as maternal and neuronal transport mRNPs, polar granules, and P bodies. Belle is a component of nuage within nurse cells and polar granules within the oocyte. It is an essential protein required for larval growth, as well as male and female fertility, and has a putative role in RNA silencing.

I show that Belle is required for cell viability. In cells depleted of Belle, general protein synthesis is inhibited. However, a luciferase mRNA reporter

with Belle tethered to the 3′ UTR is translationally repressed without any reduction in mRNA levels. Tethering of Belle to the reporter mRNA induces the formation of heavy mRNP complexes. Translational repression is abolished when Belle contains mutations disrupting the putative helicase activity.

Using a biochemical and computational approaches, I found that in *Drosophila* S2 cells, Belle is part of an interaction network consisting of proteins implicated in general protein synthesis as well as selective translational control mechanisms. Belle interacts with translation initiation factors and ribosomal proteins, supporting the idea that Belle is required for general translation efficiency. However it also associates with translationally regulated mRNAs and proteins involved in mRNA translational control and localization, suggesting that Belle may be implicated in mRNP assembly and transport as well as localized mRNA translation. Finally, I show that Belle interacts with AGO2 and other components of the RISC, suggesting that Belle may function as an auxiliary factor in the RNA silencing pathway.

Zusammenfassung

Bei der posttranskriptionellen Regulation der Genexpression wirken mehrere Mechanismen um die Translation und/oder den mRNA Abbau zu kontrollieren. RNA-Interferenz wirkt auf beiden Ebenen um einen erheblichen Anteil des Transkriptoms zu regulieren; nämlich diejenigen mRNAs, zu welchen es kleine komplementäre short interfering RNAs (siRNAs) und microRNAs (miRNAs) gibt. Um die Transkripte, welche auf diese Art reguliert werden, zu identifizieren, habe ich eine genomweite Suche in Drosophila S2 Zellen durchgeführt.

Es wurden mRNA-Expressionsprofile von Zellen erstellt, in welchen Angehörige der für die RNA-Interferenz essentiellen Argonaut-Proteinfamilie (AGO1, AGO2, PIWI oder Aubergine) depletiert waren. Diese wurden mit dem Profil von Drosha-depletierten Zellen verglichen, einem Enzym das die miRNAs prozessiert. Die Veränderungen im Transkriptionsniveau von Drosha-depletierten Zellen korrelierten eng mit jenen von AGO1-depletierten Zellen. Dies zeigt, dass sich nach einer Blockade der miRNA Produktion die Menge der jeweiligen Zieltranskripte ändert, was wiederum die These stützt, dass miRNAs zum Abbau des Zieltranskriptes beitragen, und nicht nur, wie bisher angenommen, dessen Translation unterdrücken. Weiterhin konnten wir belegen, dass eine Untergruppe von miRNA Zieltranskripten auch über AGO2 reguliert wird. Zusammen mit der Tatsache, dass AGO1 und AGO2 die Expression einer allgemeinen Gruppe genetisch mobiler Elemente unterdrücken, deutet dies darauf hin, dass sich die Rollen von AGO1 und AGO2 bei der RNA-Interferenz überlappen.

Danach konzentrierten sich meine Untersuchungen auf die DEAD-box RNA-Helikase Belle aus Drosophila. Die meisten Mitglieder dieser Proteinfamilie zeigen NTPase-Aktivität, die abhängt oder stimuliert wird durch die Bindung an RNA. Sie benutzen die durch die NTP-Hydrolyse frei werdende Energie, um doppelsträngige RNA aufzuwinden oder um Wechselwirkungen zwischen RNA und Proteinen zu stören. Viele dieser DEAD-box Proteine finden sich in so genannten RNA Körperchen (*RNA granules*), wie z.B. den mütterlichen und neuronalen Transporter-mRNPs, den polaren Körperchen

(*polar granules*) und den prozessierenden Körperchen (*P bodies*). Belle ist ein Bestandteil der "*Nuage*" Struktur in Ammenzellen, und der polaren Körperchen in Oozyten. Es ist ein essentiell notwendiges Protein und erforderlich für das Larvenwachstum und für die Fruchtbarkeit bei männlichen sowie weiblichen Fliegen. Darüber hinaus spielt es eine mutmaßliche Rolle in der RNA-Interferenz.

Ich konnte zeigen, dass Belle für die Lebensfahigkeit der Zelle erforderlich ist. In Zellen, in welchen Belle depletiert wurde, ist die allgemeine Proteinsynthese gehemmt. Ein Luziferase-mRNA Reporterkonstrukt hingegen, in welchem Belle künstlich an das 3′ UTR Ende gebunden wird bleibt mengenmäßig stabil, während die Translation gehemmt wird. Die Bindung von Belle an die Reporter-RNA führt zur Bildung von schweren mRNP-Komplexen. Belle Proteine mit Mutationen, die die mutmaßliche Helikaseaktivität stören, unterdrücken die Translation nicht.

Mit einem kombinierten biochemischen und rechnerischen Ansatz fand ich Belle als Teil eines Interaktionsnetzwerkes, das sowohl Proteine der allgemeinen Proteinbiosynthese enthält, also auch Proteine beinhaltet die an speziellen translationellen Kontrollmechanismen mitwirken. Belle interagiert dabei mit Translationsinitiationsfaktoren und ribosomalen Proteinen, was die Theorie stützt, dass Belle für die Effizienz der allgemeinen Translation notwendig ist. Allerdings assoziiert es auch mit translational regulierten mRNAs und mit Proteinen, welche eine Rolle in der Translationskontrolle und Lokalisation von mRNA spielen. Dies wiederum deutet auf ein Rolle von Belle im Zusammensetzen und Transport von mRNPs und bei der lokalisierten Translation von mRNA. Schlussendlich zeige ich, dass Belle mit AGO2 und weiteren Bestandteilen des so genannten RISC Komplexes interagiert, was darauf hindeutet, dass Belle als zusätzlicher Faktor bei der RNA-Interferenz fungieren könnte.

Abbreviations

Amino acids, ribo- and deoxynucleosides are denoted using the standard single letter code.

A_{260}	absorbance at 260 nm
aa	amino acid
Ac	acetyl
AMV	avian myeloblastosis virus
AP	alkaline phosphotase
APS	ammonium persulfate
ARE	AU-rich element
ATP	adenosine triphosphate
bp	base pair
BSA	bovine serum albumin
cDNA	complementary DNA
DNase	deoxyribonuclease
cpm	counts per minute
C-terminus	carboxyl-terminus
CTP	cytosine triphosphate
dATP	2′-deoxy-adenosine triphosphate
DCP	decapping protein
dCTP	2′-deoxy-cytosine triphosphate
dGTP	2′-deoxy-guanosine triphosphate
DAG	directed acyclic graph
DMSO	dimethylsulfoxide
DNA	deoxyribonucleic acid
dNTP	2′-deoxy-nucleoside triphosphate
dsRNA	double-stranded RNA
DTT	dithiothreitol
dTTP	thymidine triphosphate
EDTA	ethylene diamine tetraacetic acid
EGTA	ethylene glycol tetraacetic acid

EGFP	enhanced green fluorescent protein
eIF	eukaryotic translation initiation factor
EJC	exon junction complex
FBS	fœtal bovine serum
FDR	false discovery rate
Et	ethyl
g	gravitational force
GDP	guanosine diphosphate
GO	Gene Ontology
GST	glutatione-S-transferase
GTP	guanosine triphosphate
HEPES	4-(2-hydroxyethyl)-1-piperazineethanesulfonic acid
IgG	immunoglobulin G
IP	immunoprecipitation
IRES	internal ribosome entry site
kb	kilobase
kDa	kilodalton
LB	Luria-Bertani broth
λN	N-peptide from phage λ
Lsm	Sm-like
M	molar concentration, mol/L
m, Me	methyl
m^7G	7-methyl-guanosine
miRNA	micro RNA
miRNP	micro ribonucleoprotein
M-MuLV	Moloney Murine Leukæmia Virus
MOPS	3-(N-morpholino)propanesulfonic acid
mRNA	messenger RNA
mRNP	messenger ribonucleoprotein
NMD	nonsense-mediated mRNA decay
NP-40	Nonidet P-40, also known as Igepal CA-630
nt	nucleotide
N-terminus	amino-terminus
OD	optical density
ORF	open reading frame
P body	processing body
PABP	poly(A)-binding protein
PAGE	polyacrylamide gel electrophoresis
PBS	phosphate-buffered saline
PCR	polymerase chain reaction
PIPES	1,4-piperazinediethanesulfonic acid

piRNA	PIWI-interacting RNA
PIWI	P-element induced wimpy testis
poly(A)	poly-adenylate
*i*Pr	2-propyl
pre-miRNA	precursor miRNA
pre-mRNA	precursor messenger RNA
pri-miRNA	miRNA primary transcript
PTC	premature termination codon
rasiRNA	repeats-associated siRNA
RBP	RNA-binding protein
RISC	RNA-induced silencing complex
RNA	ribonucleic acid
RNAi	RNA interference
RNAP	RNA polymerase
RNase	ribonuclease
rpm	rotations per minute
RRM	RNA recognition motif
RT	reverse transcription
S	Svedberg unit
SDS	sodium dodecyl sulphate
siRNA	small interfering RNA
snoRNA	small nucleolar RNA
snRNA	small nuclear RNA
TAP	tandem affinity purification
Taq	*Thermus aquaticus*
TBE	Tris/boric acid/EDTA
TE	Tris/EDTA
TEMED	N,N,N′,N′-tetramethyl-methane-1,2-diamine
T_m	annealing temperature
Tris	2-Amino-2-hydroxymethyl-propane-1,3-diol
TRITC	tetramethyl rhodamine isothiocyanate
U	enzyme activity unit
u`AUG`	upstream `AUG` codon
uORF	upstream ORF
UTR	untranslated region
UV	ultra-violet
V	volt

Part I

Introduction

1 Translational control in eukaryotes: *cis*-regulatory sequences and *trans*-acting factors

1.1 Origins of translational control

The main goal of the regulation of gene expression is to determine the levels of proteins in the cell. A protein's level is defined by its rate of synthesis and its rate of degradation. It is also proportional to its mRNA's level which in turn depends on the transcriptional activity and rates of mRNA decay.

Protein synthesis is a sophisticated process that requires a lot of energy (four high-energy bonds per peptide bond) and extensive molecular machinery. It is not surprising that a process of such importance demands close monitoring and control. Translational control can be defined as a way to regulate gene expression by changing the efficiency of utilization of an mRNA in specifying protein synthesis. One of the main features of translation as a site of regulation of gene expression is that it offers the possibility of rapid response to external stimuli without invoking nuclear pathways for mRNA transcription, processing and export.

The idea of translational control emerged very soon after the articulation of the messenger hypothesis. Even before the discovery of the double helix, it was generally assumed that "DNA makes RNA makes Protein", because DNA was in the nucleus and translation took place in the cytoplasm, therefore something had to be a messenger between these two compartments. Early on, ribosomal RNA was thought to carry out this role, until evidence gradually accumulated suggesting that it did not have the characteristics of the postulated messenger. In 1961 Jacob and Monod first coined the term "messenger RNA" [189], and its existence was demonstrated by Brenner, Jacob and Meselson [48], and by Gros and colleagues [154].

The discovery of cytoplasmic free mRNPs which are not bound with ribosomes put forward the idea of masked or blocked mRNA [389, 390]. Subsequent studies on developing embryos, reticulocytes, virus-infected cells, and cells responding to different stimuli ranging from heat to hormones and starvation to mitosis had laid the firm foundation for the hypothesis that mRNA could be subject to differential utilization depending on the circumstances (reviewed in [279]).

The cytoplasm of eukaryotic cells is much more organized structurally than that of prokaryotes. The lack of a nuclear barrier between the sites of mRNA synthesis and translation, the greater speed of macromolecular synthesis in bacteria and their lesser dependence on mRNA processing are

the factors that allow a coupling of transcription and translation which almost eliminates the need for translation control.

Both translation and transcription are critical biosynthetic steps in which the cell makes large investments of energy. Multiple precise mechanisms have evolved to control transcription. Why does translational control exist? Probable reasons for the evolutionary success of translational control are summarized below.

- Translational control is fast and direct. It is applied to the last step of genetic information flow and therefore avoids the delay imposed by mRNA transcription, nuclear processing and export.

- Translational control is reversible. Most mechanisms are brought about by reversible modifications of translational factors (phosphorylation) which can either stimulate or repress translation. Selective mechanisms of translational repression do not require mRNA degradation, therefore de-repressed mRNAs can be translated. The reversible nature of translational control is economical in terms of energy consumption.

- Translational control allows fine-tuning. The changes in transcription efficiency are considerably greater in magnitude than changes in translation efficiency. Thus, regulation of transcription is more coarse, whereas translational control provides a means of fine-tuning gene expression.

- Translational control regulates gene expression in systems that lack transcriptional control. These include *e.g.* reticulocytes, oocytes and RNA viruses, all of which possess little or no opportunity for transcriptional control and in which gene expression is modulated mostly at the translational level. The fact that translational control is widely used during development and by some RNA viruses suggests that this mode of control is more ancient than transcriptional regulation, consistent with the RNA World hypothesis [136].

- Translational control provides higher spatial resolution of regulation of gene expression then transcriptional regulation. It is advantageous over direct protein targeting and allows rapid response to local requirements. Precise localization of protein synthesis within the cell is essential for morphogen gradient establishment in the oocyte during development [99, 107]. Local translation is also required for maintenance of cellular asymmetry of polarized cells such as fibroblasts and endothelial cells [75], as well as neurons, where it enables synaptic plasticity [44].

- Translational control is flexible. A broad spectrum of mechanisms of various specificity exist which allow the regulation of either single genes or whole classes of mRNAs. Such flexibility affords the cell a powerful and adaptable means of regulating gene expression.

Obviously, the outcome of translational control compensates for the the energetic penalties due to the exertion of regulation over a midstream reaction in a long gene expression pathway.

1.2 General principles of translational control

All possible mechanisms of translational control can be divided into global and selective controls. Global controls, such as those operating in oocytes or in cells recovering from stress, affect almost the entire complement of mRNAs within a cell, switching their translation on or off or modulating it in unison. This kind of regulation is usually implemented by substantial alteration in the activity of general components of the translational apparatus that act in a nonspecific manner. Selective controls, on the other hand, affect a subset of the mRNAs within a cell, in the extreme case a single species only. Selective controls in cancer development, metabolic diseases, following stress, and during apoptosis or viral infection utilize the differential sensitivity of mRNAs to more subtle changes in the activity of general components of the protein synthesis machinery, *e.g.*, initiation factors eIF4E and eIF2 [280]. The most specific translational control is achieved through mechanisms relying on mRNA's *cis*-regulatory sequences and *trans*-acting factors or ligands (proteins, RNAs, small molecules) that target individual mRNAs or classes of mRNAs.

This introduction focuses on selective translational control mechanisms in *Drosophila* based on *cis*-regulatory sequences and *trans*-acting factors, since these are most relevant to my work. The introduction leaves outside of its scope other translational control mechanisms as well as regulatory effects on protein degradation, and regulation at the levels of mRNA transcription and decay. However, the relationship between translation and mRNA stability is complex and it is not always possible to segregate one from another (as is indicated, for example, by miRNA-mediated silencing, see § 1.8).

A major response of cells to growth stimuli or stress is to change the availability and/or activity of general translation factors and thereby modulate global translation activity. It is thought that some mRNAs that harbor special *cis*-regulatory sequences in their 5′ UTRs (IRES elements, uORF, secondary structure elements) are able to escape this regulation by bringing into

play alternative mechanisms of translation initiation such as internal initiation, although this view is subject to stark criticism [229, 233, 234, 236, 235].

1.3 Translation initiation in eukaryotes

The rate of translation is mainly controlled at the level of translation initiation (see, *e.g.*, [279]). Initiation efficiency in turn is dependent on the general translational machinery (availability of free ribosomes and amino-acid-charged tRNAs; availability and activity of translation factors) and structural features of mRNAs (*cis*-elements) that influence ribosomal recruitment, scanning to the initiation codon, and initiation codon recognition. Eukaryotic mRNAs exist in cells as mRNPs rather than as free polynucleotides. The mRNAs are dynamically associated with proteins that mediate nuclear export, stability, subcellular localization and translational control [97]. Some of these *trans*-acting protein factors are able to augment or inhibit translation initiation.

This section describes briefly the general translation initiation pathway, given its importance for the majority of global and selective mechanisms of translational control.

Standard translation initiation in eukaryotes is the process of assembly of an 80S ribosome on an mRNA in which the start codon is base-paired to the anticodon of aminoacylated initiator methionyl-tRNA (Met-tRNA$_i^{Met}$) in the ribosomal peptidyl (P) site. According to the current model (see Fig. 1), the initiation pathway includes the steps which are listed below (reviewed in [335, 170]).

- **Ternary complex (TC) formation** is the assembly of eIF2, GTP and Met-tRNA$_i^{Met}$. The TC is responsible for delivering Met-tRNA$_i^{Met}$ to the 40S subunit and is essential for identification of the start codon within the mRNA. After each round of initiation, eIF2·GDP is released as an inactive complex. eIF2B is a guanine nucleotide exchange factor (GEF) for eIF2·GDP which accelerates the replacement of GDP with GTP. eIF2·GTP is an active form that has high affinity for Met-tRNA$_i^{Met}$.

- **Assembly of the 43S preinitiation complex (PIC)** from the TC and a 40S ribosomal subunit is facilitated by eIF1, eIF1A, and eIF3 by a mechanism which includes direct interaction of eIF2 and the 40S subunit, interaction between factors, and induced conformational changes in the 40S subunit.

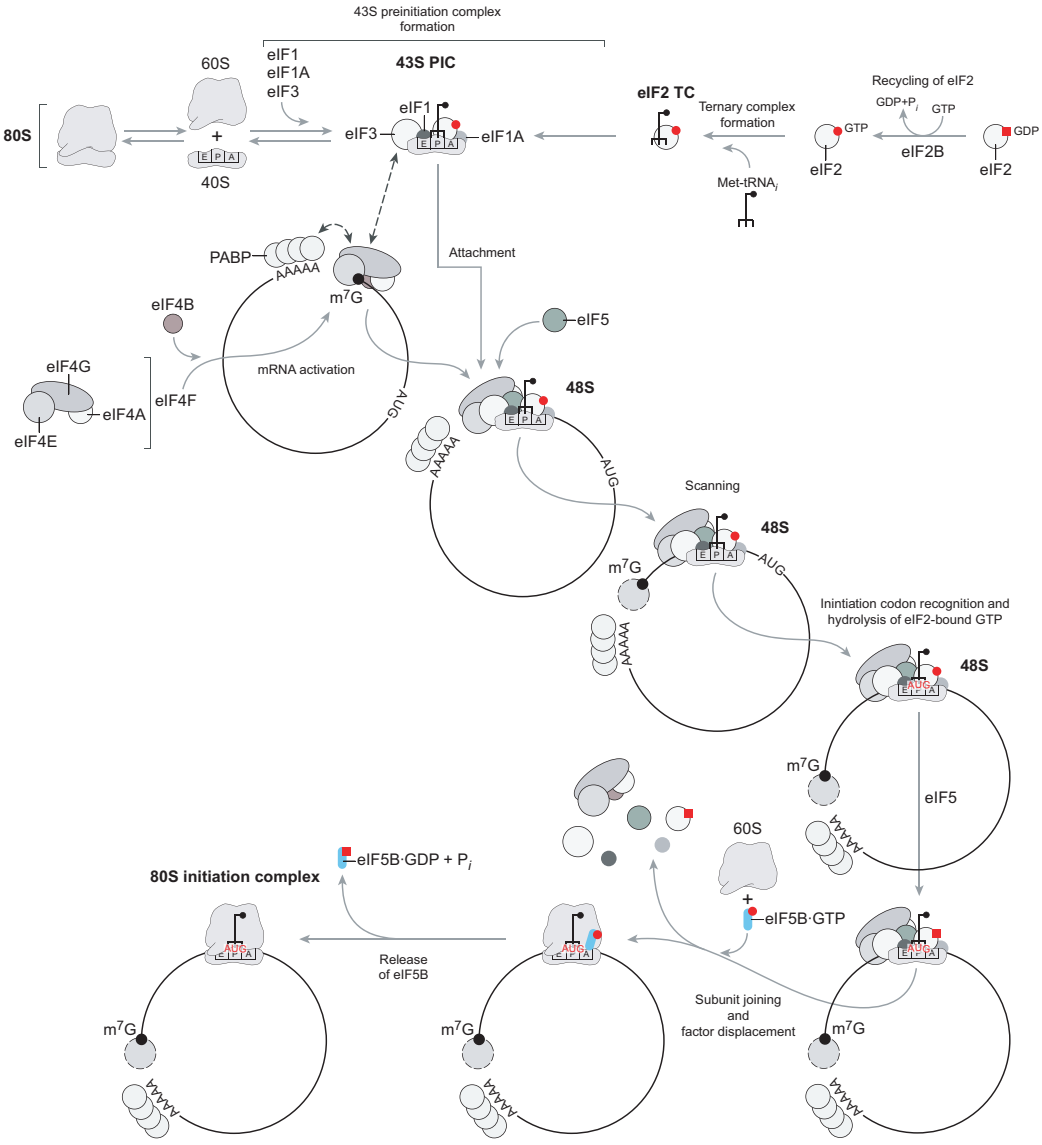

Figure 1. Schematic representation of the assembly of an 80S ribosomal translation initiation complex on a 5′-capped and 3′-polyadenylated mRNA.

The model divides this process into different stages, showing initiation factors at the stage at which they first participate in the process. After completion of initiation, Met-tRNA$_i^{Met}$ is base-paired with the start codon of mRNA in the P site of the 80S ribosome, and the vacant A site is able to accept delivery of the elongator tRNA by eEF1A. Modified from [335].

- **Recruitment of the 43S preinitiation complex to the mRNA** occurs at the 5′ end of the mRNA. The 43S PIC is intrinsically capable of 5′-end-dependent attachment to the mRNA. Most natural mRNAs have considerable secondary structure near the 5′ end. Binding of the 43S complex is greatly stimulated by the cooperative activities of eIF4F, eIF4B, and possibly PABP, which are thought to unwind the 5′-proximal secondary structures to prepare a binding site for the PIC. The 5′ end of all cellular mRNAs is capped with 7-methylguanosine. Via interaction with the eIF4E subunit of eIF4F, the m^7G cap strongly promotes 43S complex binding. eIF4F also contains eIF4A (a DEAD-box RNA helicase) and a large modular protein eIF4G. During PIC recruitment to mRNA, eIF4G enhances the RNA helicase activity of eIF4A (which is also activated by eIF4B) and the cap-binding activity of eIF4E. eIF4G also binds directly to the mRNA and to the eIF3 component of the 43S complex. PABP which binds to eIF4G further enhances the interaction of eIF4F with the cap.

- **Ribosomal scanning on mRNA** starts at the 5′ end of the mRNA and continues linearly in the 5′ → 3′ direction until the 40S ribosome/factor complex encounters the first `AUG` codon, which is recognized by base-pairing with the anticodon in the Met-$tRNA_i^{Met}$. The question of if and when the relay of interactions among the cap, eIF4F, and the PIC is disrupted during scanning has not been answered. Very little is known about the mechanism that actually propels the 40S subunit/factor complex. The 43S complex is capable of ATP-independent scanning on mRNA lacking any secondary structure without eIF4E, eIF4B, and eIF4F, but they are required for scanning if the 5′ UTR contains even weak secondary structure.

- **Recognition of the initiation codon** is principally determined by its complementarity with the anticodon of Met-$tRNA_i^{Met}$. eIF1 is critical for destabilization of premature, partial base-pairing of triplets in the 5′ UTR with the Met-$tRNA_i^{Met}$ anticodon and can also induce dissociation of aberrantly preassembled ribosomal complexes. Experiments in yeast have shown that eIF1A, eIF4G and eIF3 also influence initiation codon recognition, probably via their interactions with eIF1, eIF2, or eIF5.

- **Ribosomal subunit joining** occurs after eIF5-induced hydrolysis of eIF2-bound GTP, which leads to a reduction in eIF2's affinity for Met-$tRNA_i^{Met}$. The combined action of eIF5B and the 60S subunit displace eIF2·GDP and other factors (eIF1, eIF1A, and eIF3) from the 40S subunit surface which contacts the 60S subunit in the 80S ribosome,

during the actual subunit joining event. eIF5 activates GTP hydrolysis by eIF2 only when there is a sufficiently long pause in scanning. That allows the initiation complex to distinguish an authentic AUG start codon (long pause) from other contenders (*e.g.*, short pause at UUG).

Virtually all these steps of the translation initiation pathway can be targeted by global and selective control mechanisms. Availability of translational machinery, modulation of the activity of translation initiation factors by phosphorylation and other post-translational modifications greatly affect translation initiation efficiency. The mRNA structural features (such as 5′-cap, 3′-poly(A), and UTRs) are other key factors that define the translation initiation efficiency.

1.4 Global mechanisms of translational control

1.4.1 Phosphorylation of eIF2

Phosphorylation of the translation initiation factor eIF2 is one of the best characterized mechanisms of general translational control in eukaryotes. eIF2 is a heterotrimer comprised of a large γ subunit and smaller α and β subunits. eIF2γ binds GTP and Met-tRNA$_i^{Met}$ and delivers them to the 40S ribosomal subunit. The assembly of the ternary complex (eIF2·GTP·Met-tRNA$_i^{Met}$) is the first step in translation initiation. The interaction of the ternary complex with the 40S subunit forms the preinitiation complex.

eIF2γ cycles between its GTP-bound (active) state and its GDP-bound (inactive) state. The recycling of inactive eIF2·GDP to active eIF2·GTP is catalyzed by eIF2B which is a guanine nucleotide exchange factor (GEF). Phosphorylation of eIF2α converts eIF2 from a substrate to a competitive inhibitor of eIF2B. The amount of eIF2B is limiting compared to the amount of eIF2. Thus, phosphorylation of a small percentage of eIF2α results in the sequestration of eIF2B in inactive phosphorylated eIF2·eIF2B complexes and in the inhibition of protein synthesis [88].

The phosphorylation event is purely regulatory; it has no direct effect on the function of eIF2 as an initiation factor. Phosphorylation is highly dynamic and regulated by kinases and phosphatases. There are four known eIF2α kinases in vertebrates: GCN2 (responds to amino acid deprivation), PERK (responds to an imbalance between the load of ER client proteins and chaperons, so called ER stress); HRI (responds to unbalanced synthesis of heme and globin); and PKR (responds to the presence of dsRNA in cells). The orthologs of GCN2 and PERK have been identified in *Drosophila* [367, 320, 387, 342].

There are two known phosphatases that dephosphorylate eIF2(αP). One contributes to the high basal eIF2(αP)-directed phosphatase activity, the other ensures recovery of protein synthesis during the later phases of stress responses. It is not known whether these kinases and phosphatases account for all eIF2α phosphorylation and eIF2(αP) dephosphorylation activities of cells [359].

Diverse stress-induced signals are channeled to a single downstream eIF2α phosphorylation step, which is followed by a cascade of translational and transcriptional activation events which are required for the recovery from the stress (Fig. 2).

1.4.2 Phosphorylation of other translation factors

It is now clear that phosphorylation status can regulate the activity not only of eIF2 but also many other translation factors. Recent studies have provided compelling evidence that two signaling cascades in particular have critical roles in this process: the target of rapamycin (TOR) and mitogen-activated protein kinase (MAPK) signaling modules.

The TOR proteins are evolutionarily conserved protein kinases that have key roles in cell growth, proliferation and survival. They are thought to act as a checkpoint for translation, accepting signaling input both from hormone/growth factor receptors and nutrient sensors, and in this way allows translation to occur only in the presence of sufficient nutrients to fuel protein synthesis [349]. In *Drosophila*, the TOR pathway is involved in body size assessment and growth control, and in adaptation to hypoxia (reviewed in [289, 358]).

It has been demonstrated that phosphorylation of the RpS6 kinase (S6K), several translation factors (eIF4B, eIF4G, eEF2), and the eIF4E-binding proteins (4E-BPs) is all mediated by TOR signaling (reviewed in [345]).

The classical MAP kinase signaling pathway is an evolutionarily conserved pathway that is involved in the control of many fundamental cellular processes that include cell proliferation, survival, differentiation, apoptosis, motility and metabolism [222]. Several downstream kinases of the MAPK pathway appear to be important for translational control transducing signals emanating from both growth factor stimulation and stress. These kinases phosphorylate eIF4E, 4E-BP and eIF4B [345].

Although not as well characterized, other signaling modules (calmodulin-dependent protein kinase CaMKI implicated in Ca^{2+}/CaM signaling, casein kinase 2, and cell-cycle-regulated kinase Cdk11) have also been implicated in translational control. It is clear that even more intracellular signaling modules will be implicated in translational control as this process is studied

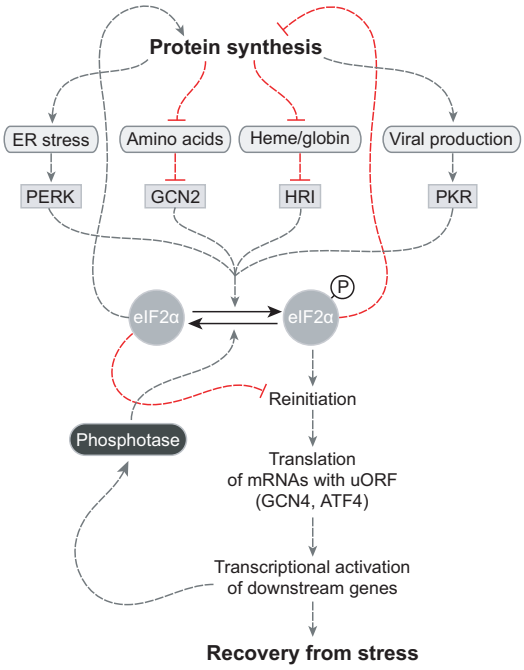

Figure 2. Schematic overview of the eIF2α-phosphorylation-dependent integrated stress response. Modified from [359].

The four kinases—PERK, GCN2, HRI, and PKR—are activated by distinct stress signals, which in turn are dependent on protein synthesis. Stress conditions that lead to eIF2α phosphorylation and inhibition of ternary complex formation derepress translation of mRNAs that contain uORFs by a mechanism of regulated translation reinitiation. It results in expression of some transcription factors (GCN4 in yeast, ATF4 in mammals, and probably some others) that activate transcription of downstream genes. The latter encode transcription factors, chaperons, ER enzymes, enzymes involved in lipid and amino acid metabolism, and also include anti-oxidative stress response genes. Also included is the gene which encodes an eIF2(αP)-specific regulatory subunit of a phosphatase that inhibits the stress-induced cascade [359]. Grey dashed arrows correspond to activating signals; red blunted lines correspond to inhibitory signals.

in more cell types and under other types of physiological conditions.

The phosphorylation state of individual residues in translation initiation factors and the biological function of phosphorylation events have been characterized in many direct studies. The best characterized mechanism is the control of eIF4F formation by the eIF4E-binding protein (4E-BP) family of translational repressors. 4E-BP and eIF4G binding to eIF4E are mutually exclusive, thus 4E-BP binding to eIF4E abrogates eIF4F formation and inhibits cap-dependent translation initiation. Phosphorylation of 4E-BPs affects their ability to interact with eIF4E; hypophosphorylated 4E-BPs efficiently bind to eIF4E, hyperphosphorylated 4E-BPs do not. In the presence of adequate nutrients, mammalian 4E-BP1 is phosphorylated downstream of TOR, resulting in a sufficient pool of eIF4E for incorporation into eIF4F. Under starvation conditions, 4E-BP1 is dephosphorylated and sequesters a proportion of eIF4E to decrease the abundance of active eIF4F and inhibits general protein synthesis [345].

Several extracellular stimuli activate phosphorylation of eIF4E via the MAP kinase pathway, which might be important for regulation of the rate of protein synthesis during certain physiological conditions.

Other translation initiation factors were also found to be phosphorylated (eIF4G, eIF4B, eIF3, eIF2B, eIF5, and eIF5B), but it is not clear yet how these modifications affect translation factor activity and how these changes in activity relate to the control of global translation rates or the translation of the specific mRNAs or mRNA classes [345].

Even though translation is most frequently controlled during the initiation step, accumulating evidence points to the elongation step as a target for control under defined circumstances. The phosphorylation state of eEF2 changes in a way consistent with its having a role in regulating protein synthesis. It becomeshypophosphorylated in response to a wide range of stimuli that activate protein synthesis and hyperphosphorylated under conditions of low cellular energy status.

eEF2 mediates the translocation step of elongation where, following the addition of an amino acid to the growing protein chain, the tRNA attached to the polypeptide translocates from the A site into the P site on the ribosome and the ribosome moves by one codon along the mRNA. This is accompanied by hydrolysis of a GTP molecule bound to eEF2.

The phosphorylation of eEF2 by eEF2 kinase results in a drastic inhibition of polyphenylalanine synthesis in poly(U)-directed translation [364]. It also inhibits eEF2 activity in reticulocyte lysates [346]. Mammalian eEF2 undergoes phosphorylation within its GTP-binding domain, which prevents its binding to ribosomes and thus inactivates eEF2 [53].

Although these and several other studies have reported that eEF2 phos-

phorylation correlates with inhibition of elongation *in vitro*, evidence that that the changes in eEF2 phosphorylation are responsible for the alterations in protein synthesis rates *in vivo* still remains limited [167].

1.5 Principles of selective translational control

In contrast to global translational control mechanisms, selective mechanisms have evolved to target specific mRNAs or mRNA classes. The most "primitive" and efficient mechanisms of this kind preceded more sophisticated regulatory schemes which appeared later during the course of evolution and rely solely on structural features of the mRNA such as the 5′-leader sequence (secondary structures, upstream ORFs or, more correctly, u`AUG` codons) and the context of the initiation codon. These mechanisms interfere with translation initiation in as much as it is the rate-limiting step and because doing so prevents the cell from wasting the energy required for protein synthesis.

Other mechanisms of selective translational control are dependent on mRNA-specific *cis*-sequence elements which on its own have no capability to affect translation. In this case, the recruitment of additional factors (RNA-binding proteins or non-coding small RNAs) is required. Such factors not only directly and stably interact with the aforementioned sequence elements (acting in *trans* to the mRNA) but also with the translational apparatus thereby augmenting or decreasing translation efficiency. Although most of these primary and secondary structure elements lie in the non-coding regions of the mRNA (preferentially in the 3′ UTR), some reside in the coding region.

The scanning mechanism of translation initiation [230] accounts easily for regulation by unusual sequences (u`AUG`s or uORFs, secondary structure elements) or proteins that bind near the 5′ end of the mRNA [232]. In light of the scanning model, it is less clear how sequences located at the 3′ end can affect translation. To explain regulation via the 3′ UTR one has to invoke the closed-loop model (reviewed in [203]), which is based on the discovery that eIF4G can bind simultaneously to eIF4E, at the capped 5′ end of the mRNA, and to the poly(`A`) binding protein (PABP) at the 3′ end [419].

The 3′ UTR regulatory elements affect gene expression in a variety of ways [237]. Nevertheless, it has proved to be difficult to demonstrate unequivocally that one of these ways involves direct participation of the 3′ UTR in translation initiation or any subsequent step [231, 236].

Different possible *cis*-regulatory elements are shown in Fig. 3. A single mRNA can harbour several regulatory elements, which determine the mRNP association and mode of post-transcriptional regulation. Thus, *trans*-acting factors can regulate the same mRNA by cooperating or competing for a

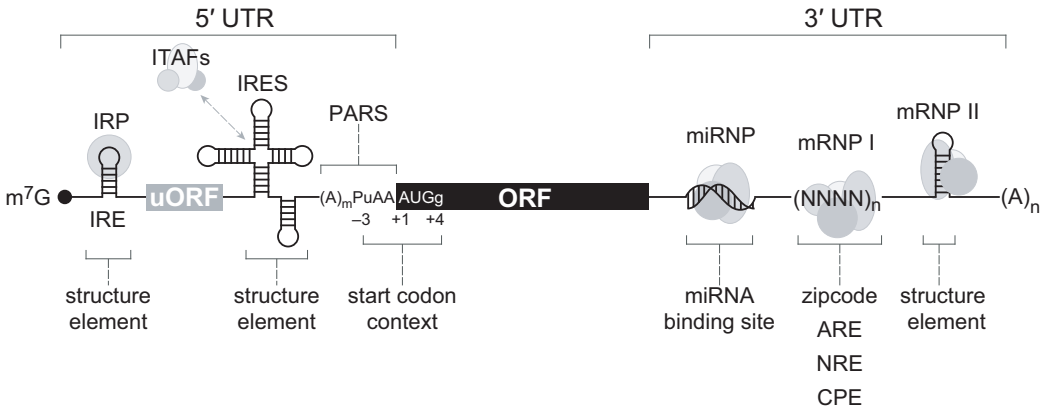

Figure 3. mRNA-specific *cis*-acting regulatory sequences which participate in translational control.

The 5′ end of all cellular mRNAs is protected from exonucleases by the 7-methylguanosine cap structure which also strongly promotes ribosome binding via interaction with eIF4E. Poly(A) tail which is bound by PABP protects the 3′ end of all cellular mRNAs (except histone mRNAs which have a stem loop at the 3′ end) and stimulates translation via the interaction between PABP and eIF4G. Most mRNAs have considerable secondary structures near the 5′ end. A cap-proximal stem loop in the ferritin mRNA, termed iron responsive element (IRE) interacts with IRP, iron regulatory protein, which sterically blocks the binding of the 43S PIC. Upstream open reading frames (uORFs, or uAUGs) reduce the translation of downstream ORFs due to the inefficient reinitiation mode. Certain structure elements in the 5′ UTR can not only inhibit cap-dependent initiation, but also serve as internal ribosome entry sites (IRESs) which promote cap-independent internal initiation. A similar role was recently attributed to polypurine (A)-rich sequences (PARSs). Some IRESs require IRES *trans*-acting factors (ITAFs) to function efficiently. The optimal context of the initiation codon—Pu (A or G) at the −3 position and G at the +4 position—greatly augments translation initiation efficiency. The 3′ UTR often contains several *cis*-regulatory elements: binding sites for proteins and miRNAs, as well as structure elements that govern the spatial and temporal translation and stability of an mRNA. These include: zipcode, AU-rich element (ARE), Nanos responsive element (NRE), and cytoplasmic polyadenylation element (CPE).

regulatory outcome at more than one *cis*-element. Moreover, a single *trans*-acting factor can target multiple mRNAs.

In a broad perspective of post-transcriptional regulation of gene expression, such *cis*-elements and *trans*-factors confer the possibility of precise coordination of mRNA splicing, export, localization, translation and stability.

1.5.1 RNA operon

These views have recently coalesced into the post-transcriptional "RNA-operon" theory, according to which *trans*-acting factors combinatorially regulate multiple functionally related mRNAs along a coordinated pathway of mRNA metabolism, allowing cells to respond better to environmental cues [211, 210, 209]. The RNA operon regulates mRNA stability and translation, guaranteeing the co-regulated expression of a set of proteins that function in the same pathway or form a macromolecular complex. Each mRNA can join different RNA operons as determined by a "*cis*-element code" that governs its fate. Because each mRNA can be a member of more that one RNA operon, if the protein encoded by the mRNA evolves more than one function, it can be dynamically co-regulated with other mRNAs independently to serve a different functional role [209, 210]. Therefore, the genetic information that is represented by multiple copies of each mRNA species, rather than by the gene itself, can be used combinatorially at several levels, and can be regulated as part of multiple mRNPs, simultaneously or sequentially (Fig. 4).

1.6 Selective control: mechanisms that affect initiation of translation

The scanning mechanism of translation initiation postulates that the 40S ribosomal subunit enters at the 5′ end of the mRNA and migrates linearly (scans) downstream along the 5′ UTR. The model predicts that translation should start at the `AUG` codon nearest the 5′ end of the mRNA. The distance from the 5′ end to the first `AUG` codon is irrelevant. The scanning mechanism was shown to operate with no measurable reduction in efficiency even when the first `AUG` codon was more than 1000 nt from the 5′ end of the mRNA [36].

Scanning may be difficult when a long 5′ UTR sequence contains secondary structures. Base-paired structures are most inhibitory when their proximity to the 5′ end blocks ribosome entry. Once bound to mRNA, the 43S PIC has some ability to disrupt base-pairing, although this has limits. Thus, secondary structure can greatly reduce translation efficiency but does not completely block scanning [232].

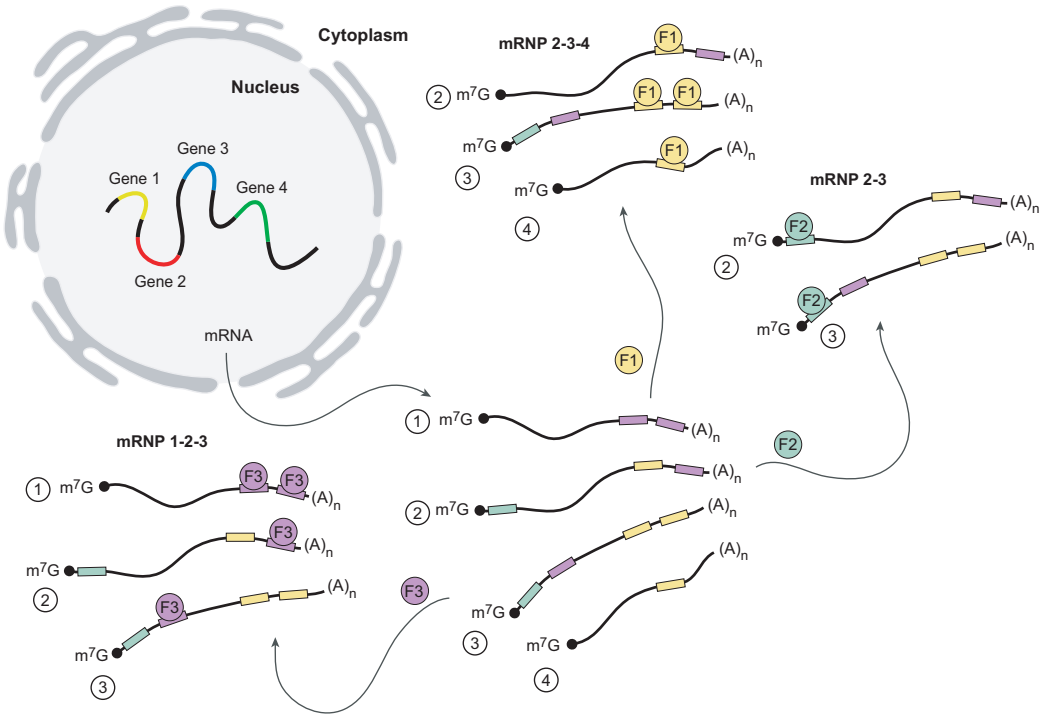

Figure 4. Post-transcriptional RNA operons. Modified from [209].

Coordination os subsets of mRNAs from transcription to translation. Transcription factors activate transcription of a set of genes (Gene 1-4). While they are still being transcribed, the mRNAs are processed, spliced, and exported to the cytoplasm. The four mRNAs shown, when grouped in different combinations, form three different operons, labeled as mRNP 2-3-4, mRNP 2-3, and mRNP 1-2-3. The make-up of each operon is determined by the binding of *trans*-acting factors (labeled F1, F2, and F3) to specific *cis*-regulatory elements, which lead to both co-regulation within each RNA operon and overall coordination of all three operons as high-order combinatorial "regulons". The four transcripts contain different sets of *cis*-elements. Therefore, an mRNA that contains more than one element can be a member of more than one mRNP complex [209].

1.6.1 Upstream AUGs and leaky scanning

If the first AUG codon lies in a poor context, this allows some ribosomes to bypass it and thus reach a start codon further downstream. There are also instances of skipping of the first AUG despite a good context which can happen when it is located too close to the 5′ end to be recognized efficiently. This is called leaky scanning (reviewed in [230, 232]). It enables the production of two separately initiated proteins from one mRNA. Some examples in which two proteins are produced from one mRNA via leaky scanning are listed in the review [230]. The large number of genes that employ leaky scanning indicate the considerable biological significance of this mechanism and of the proteins thereby produced (Fig. 5).

Secondary structures located downstream of a weak initiating codon slow scanning and thus provide more time for codon/anticodon base-pairing. Suppression of leaky scanning by this mechanism requires a critical distance (13-15 nt, which corresponds to half the diameter of the ribosome) between the AUG codon and the downstream structure element. Proteins that stabilize such structure elements might regulate the dual initiation via leaky scanning to achieve for example tissue specific expression of one or the other isoform [230].

1.6.2 Upstream ORFs and reinitiation

Reinitiation occurs with mRNAs that have small ORFs near the 5′ end. The ribosome initiates in the normal way at the first AUG codon, producing the peptide encoded in the small upstream ORF (the term "5′ UTR" in this case is not appropriate, in as much as small ORFs located within "5′ untranslated region" do get translated). When the 80S ribosome reaches the stop codon of the uORF, the 60S subunit is though to be released while the 40S subunit remains bound to the mRNA, resumes scanning and may initiate another round of translation at a downstream start codon. For this to occur, the 40S subunit must reacquire Met-tRNA$_i^{Met}$. Reacquisition of Met-tRNA$_i^{Met}$ appears to be an important point of control and is promoted by lengthening the intercistronic distance, which provides more time for Met-tRNA$_i^{Met}$ to bind, or by increasing the eIF2 ternary complex concentration. Genetic experiments also implicate eIF3 in the Met-tRNA$_i^{Met}$ rebinding step [230]. Another potential point of control is at the termination site of the uORF, where secondary structure might prevent the resumption of scanning or, in some other way, prevent reinitiation.

Although little is known about the molecular mechanisms underlying reinitiation, working rules can be formulated given that certain changes in

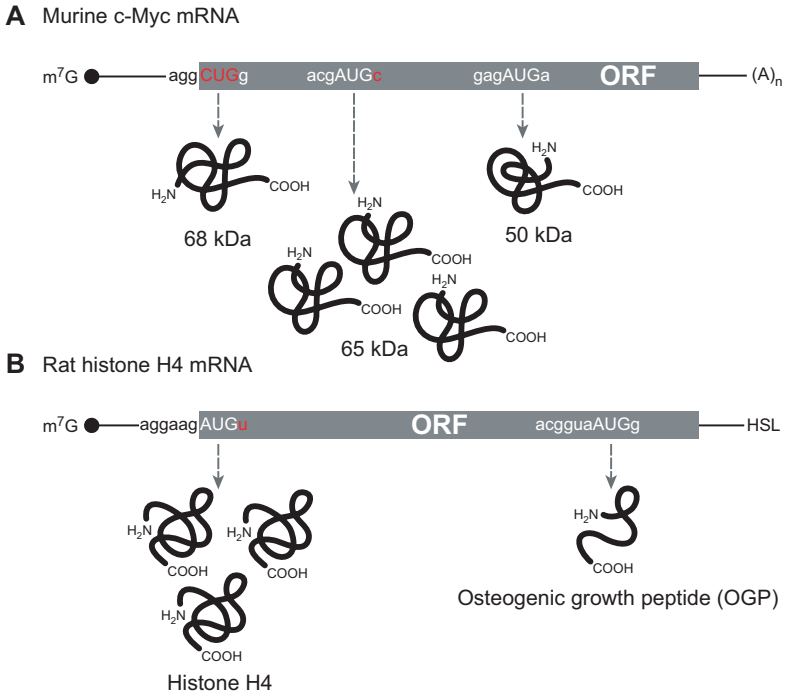

Figure 5. Examples of leaky scanning. Modified from [230].

(A) An example of "maximally" leaky scanning wherein one murine c-Myc mRNA produces three independently initiated proteins. Optimizing the context around the first `AUG` codon suppressed production of the 50 kDa isoform, while changing the upstream `CUG` codon to `AUG` suppressed production of both the 65 and 50 kDa isoforms. **(B)** An example of "minimally" leaky scanning in which a strong, but not quite perfect, context at the first `AUG` causes most ribosomes to initiate there while allowing a low level of initiation downstream. The first `AUG` codon in the rat histone mRNA initiates translation of a full-length protein. The second `AUG`, 85 codons downstream and in the same reading frame, initiates production of a peptide which has growth-regulatory properties. Mutation of `aggaagAUGu` to `gccaccAUGg` suppresses OGP production. Major (three polypeptide chains) and minor (one polypeptide chain) translation products are shown below their respective start codons. Sequences that cause the initiation to be weak, and thus promote leaky scanning, are highlighted in red. The mRNAs are not drawn to scale.

mRNA structure affect reinitiation.

(1) Eukaryotic ribosomes can reinitiate following the translation of a small ORF but not following the translation of a full-length protein-coding ORF. Naturally occurring uORFs are usually only a few codons long. Reinitiation was found to be barely detectable for an experimental construct in which the uORF was 35 codons long [228, 343]. Moreover, it is abolished if an uORF that would otherwise be short enough to allow a reasonable level of reinitiation includes a pseudoknot structure that would be expected to cause the ribosomes translating the uORF to pause [228, 226]. The critical parameter is not the length of the uORF per se, but the time taken to complete its translation. This might be explained if reinitiation depends on retention of certain initiation factors which gradually dissociate from 80S ribosomes during the course of elongation [232].

The only apparent exception occurs with cauliflower mosaic virus, where a protein encoded by the virus appears to promote reinitiation following the translation of a full-length first cistron [329]. The translation of polycistronic mRNAs by what are likely to be termination-reinitiation events requires the immediate-early virus-encoded protein TAV. It has been suggested that TAV interacts with the eIF3g subunit, leading to stabilization of the eIF3-ribosome interaction, so that it persists throughout the elongation phase of translation and thereby facilitates reinitiation [363].

(2) Eukaryotic ribosomes cannot reverse to reinitiate at an `AUG` codon positioned far upstream from the termination site. An extremely low frequency of reinitiation, too low for accurate quantification, was seen when there were four nucleotide residues between the stop and restart codons, but no reinitiation whatsoever with a ten-residue spacer [228]. Many other studies have shown that the strongest inhibition is caused by an uORF that overlaps the start of the downstream cistron [230].

The inefficient reinitiation mode of translation can regulate gene expression in eukaryotes in several ways (Fig. 6). The simplest effect is a reduction in protein synthesis from the major ORF. Small uORFs which force translation to occur by reinitiation are used to limit expression of potent proteins which are required in small amounts. When eIF2 ternary complex levels are low, the slow reacquisition of Met-tRNA$_i^{Met}$ might cause 40S subunits to bypass the closest downstream `AUG` codon and advance farther before reinitiating. Thus, the site where translation reinitiates can be manipulated by the availability of the ternary complex, and this can be manipulated by kinases (§ 1.4.1).

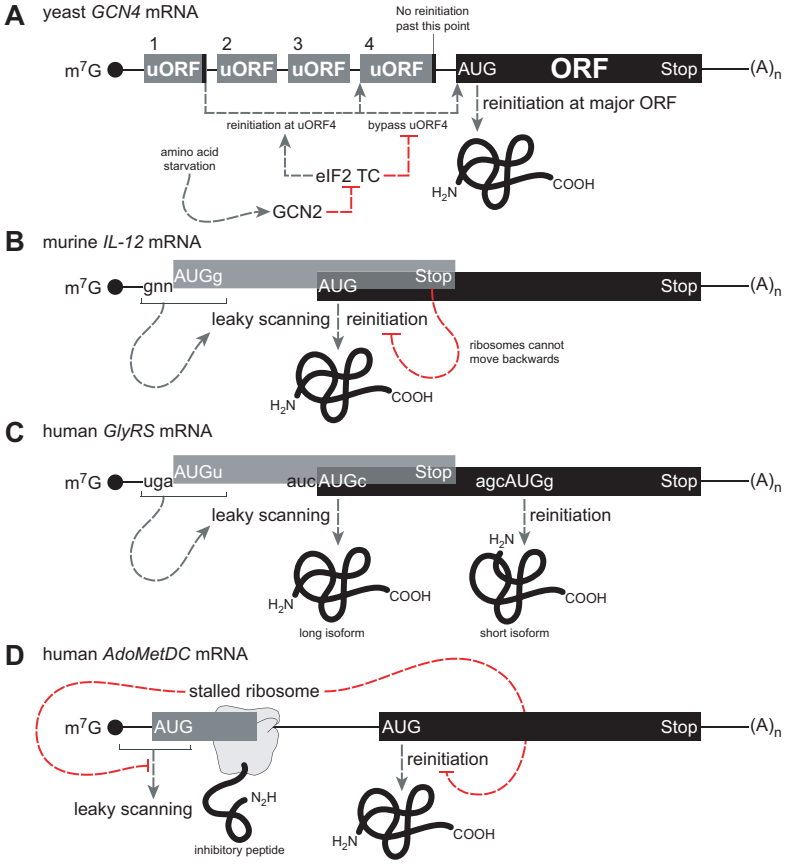

Figure 6. Small uORFs function in various ways to modulate translation. Modified from [230].

(A) The presence of an uORF forces translation of the major ORF to occur by a reinitiation mechanism, which is usually inefficient. The extent of inhibition depends on the number and arrangement of uORFs and whether the context flanking the upstream start codon(s) allows some escape via leaky scanning. Modulation of eIF2 ternary complex levels can affect selection of reinitiation sites. **(B)** Because reinitiation can occur only in the $5' \rightarrow 3'$ direction, an overlapping uORF strongly impairs translation of the major ORF which is translated by low-level leaky scanning allowed by a not-quite-perfect context at start of the uORF. **(C)** This mRNA initiates from two start codons; initiation from the first `AUG` codon of the major ORF occurs by leaky scanning. The uORF serves to divert some ribosomes to the downstream start site of the major ORF. **(D)** Because the uORF start codon is close to the $5'$ end or has suboptimal context, the uORF captures only a fraction of the 43S PICs, leaving the rest able to access the major ORF `AUG` codon by leaky scanning. The ribosomes that translate uORF undergo a prolonged pause or stall at its termination codon, because the peptide encoded by the uORF seems to block the ribosomal nascent peptide tunnel, or interferes with the translation termination process. Stalling prevents any following 43S PICs from reaching the major ORF by leaky scanning and abrogate subsequent resumption of scanning by ribosomes that eventually overcome the stall. Grey dashed arrows correspond to activating signals; red blunted lines correspond to inhibitory signals.

The best studied example involves the yeast *GCN4* gene (Fig. 6A). GCN4 is a transcription factor which turns on expression of genes involved in amino acid biosynthesis. Translation of GCN4 itself is regulated by amino acid availability because the 5′ UTR has four small uORFs, forcing translation to occur via reinitiation; reinitiation is in turn controlled by a kinase activated by uncharged tRNAs for which levels increase during amino acid starvation. The kinase (GCN2) inactivates eIF2α by phosphorylation, and the level of the eIF2 ternary complex drops. This extends the time of reacquisition of Met-tRNA$_i^{Met}$ by the scanning 40S subunit and allows translation to reinitiate from the major ORF (Fig. 6A and [171, 172]).

Stress-induced eukaryotic eIF2α phosphorylation increases translation of the metazoan activating transcription factor 4 (ATF4), activating the integrated stress response, a pro-survival gene expression program. The 5′ UTR of the ATF4 mRNA contains two conserved upstream ORFs. Scanning ribosomes initiate translation efficiently at both uORFs and ribosomes that had translated uORF1 efficiently reinitiate translation at downstream `AUG`s. In unstressed cells, low levels of eIF2α phosphorylation favor early capacitation of such reinitiating ribosomes, directing them to the inhibitory uORF2, which precludes subsequent translation of the ATF4 major ORF. In stressed cells, high levels of eIF2α phosphorylation delays ribosome capacitation and favors reinitiation at the major ATF4 ORF over the inhibitory uORF2 [265].

In the special case of sequence-specific uORFs, the peptide produced from translation of a small uORF has regulatory effects (Fig. 6D and [3, 114, 243]).

1.6.3 Internal translation initiation: IRESs

In some instances, mRNAs utilize an alternative initiation mechanism of internal ribosome binding in which the 5′ UTR of the mRNA has an active role in 40S subunit recruitment. The 5′ untranslated RNA segments responsible for such internal initiation are known as internal ribosome entry sites (IRESs).

The first IRESs were discovered after the analysis of the complete sequences of picornavirus RNAs (reviewed in [193]). The 5′ end of the picornavirus RNA genome is covalently linked to a small protein called VPg. When a newly synthesized viral RNA is destined to engage in protein synthesis, the VPg is removed to yield a viral mRNA with a 5′-terminal `pU` residue, instead of a cap structure [311]. The initiation codon of the viral mRNA is located several hundred nt downstream of the 5′ end, and the intervening sequence may harbor multiple unused `AUG` codons and very stable stem-loop structures, which would greatly decrease, if not completely abolish, scanning of the ribosomal subunit. Nevertheless, such a 5′ UTR from

the encephalomyocarditis virus (EMCV) was shown to very efficiently direct translation of reporter genes in a rabbit reticulocyte lysate. Moreover, insertion of the 5′ UTRs of the poliovirus or EMCV genome RNA between two adjacent coding regions in a bicistronic mRNA construct enabled translation of the downstream cistron independent of the upstream cistron [195, 194, 332].

These findings suggested that cap-independent translation of picornavirus mRNA proceeds by a mechanism whereby ribosomes are recruited to mRNA sequence elements that function as IRESs. Internal initiation was later confirmed by translation of a circular mRNA containing the EMCV IRES element [62], whereas it was shown that RNA circles lacking IRES elements could not be translated [227, 224]. Viral IRES elements possess structures that must be maintained, because small deletion, insertions and point mutations within the IRES elements dramatically reduce their activities (reviewed in [193, 192]). However, there are few similarities in sequence, size, or secondary structure among different viral IRES elements [96].

The minimum set of canonical initiation factors that are required to recruit 40S subunits to the EMCV IRES has been identified. Factors eIF2, eIF3, eIF4G, eIF4A, eIF4B, and Met-tRNA$_i^{Met}$ were sufficient to recruit and to position 43S complexes at the authentic start codon in an ATP-dependent reaction [338, 336]. Other noncanonical translation factors—IRES *trans*-acting factors (ITAFs)—have been implemented in internal translation initiation via IRESs. The hepatitis C virus (HCV) IRES can bind directly to 40S subunits and only requires eIF3 and the eIF2 ternary complex to properly position the ribosome at the AUG start codon [337]. Following 40S recruitment, a number of initiation factors such as eIF5 and eIF5B, as well as GTP hydrolysis are required for 60S subunits to join and generate 80S ribosomes (§ 1.3).

The cricket paralysis virus (CrPV) intergenic region (IGR) IRES mediates translation initiation by a mechanism that is very distinct from the canonical model of translation initiation and other IRES-mediated models. Remarkably, 80S ribosomes can assemble on the CrPV IGR IRES using purified 40S and 60S subunits in the absence of initiation factors and GTP hydrolysis, all of which indicate a novel pathway for 80S assembly [428].

Structural studies of HCV and CrPV IRESs in complex with the ribosome support the idea that despite different sequences, structures, and host-factor requirements, these IRESs stabilize the same conformational state of the 40S ribosomal subunit [96].

EMCV infection leads to dephosphorylation of 4E-BP1, an eIF4E binding protein. In EMCV-infected cells, hypophosphorylated 4EBP1 binds to eIF4E and prevents the interaction between eIF4E and the cap structure, leading to inhibition of cap-dependent translation [139]. This selective in-

hibition of cellular mRNA translation allows almost exclusive utilization of the host's translational resources for production of viral proteins and RNAs, likely contributing to the rapid proliferation of picornaviruses [193].

Numerous RNA viruses and at least two DNA viruses as well as a variety of cellular mRNAs have been shown to utilize IRES mechanisms for translation initiation [193, 165, 223]. Among these are genes involved in cell proliferation, differentiation, and cell death. It is noteworthy that these proteins are biologically effective at rather small concentrations and thus do not need to be expressed at high levels.

Global cap-dependent translation is subjected to transient inhibition under specific physiological conditions, in keeping with cellular requirements (§§ 1.4.1, 1.4.2). The induction of apoptosis is also associated with substantial inhibition of cap-dependent protein synthesis. A number of IRES-containing mRNAs appear to be resistant to reduced levels of the eIF2 ternary complex during stress. It is thought that IRES-mediated translation provides a means for escaping the global decline in protein synthesis and allows the selective translation of specific IRES-containing mRNAs because both apoptosis and survival as well as recovery from stress require *de novo* protein synthesis [174].

It is not understood how the translation machinery binds internally to cellular mRNAs. As with viral IRESs, there are no obvious primary structure similarities that define a consensus sequence. There is no convincing evidence that high-ordered structures are significant or required for cellular IRES function [104].

As with viral IRESs, additional proteins (beyond the canonical initiation factors) are often required for optimal expression from cellular IRES elements. ITAFs may remodel IRES structures by stabilizing a conformation that is active for ribosome recruitment, or may function as a bridge between the RNA and the ribosomes. Examples include La, Unr, hnRNP-C1/C2, and PTB (hnRNP I). At present, the observed effect of the putative ITAFs on IRES activity is usually a 1.5- to 3-fold activation, suggesting that their effect is not the major one [104].

The difficulty in characterizing cellular IRESs that confer very low efficiency of expression and the fact that eukaryotic cells produce no natural bicistronic mRNAs (other than those explicable by leaky scanning) have contributed to scepticism about the credibility of many reported IRESs [233, 235, 236]. Not a single cellular IRES has been rigorously tested employing the circular mRNA test which was used to confirm the function of the viral IRES [62].

However, the discovery of IRES elements has led to important new insights into the biology of viruses and regulation of translation initiation as

an additional level of control of gene expression in response to physiological and environmental signals. Protein synthesis from IRES-containing mRNAs frequently occurs at times when there is a global reduction in cap-dependent translation. The potential utility of cellular IRES-mediated translation as an alternative way to modulate gene expression clearly warrants further investigation.

1.6.4 Translation initiation via PARS

Eukaryotic mRNAs containing polypurine (A)-rich sequence (PARS) or homopolymeric poly-(A) sequence preceding the initiation codon are known to exhibit enhanced cap-independent translation, both *in vivo* and *in vitro*. An example of this is provided by highly expressed poxvirus late mRNAs, which carry an unusual modification. This consists of poly(A) sequences (30-40 nt long, but sometimes shorter) placed at the 5′ ends of these mRNAs, immediately before the initiation AUG codon [37, 372, 330, 430]. *In vivo* translation of poxvirus mRNAs with a poly(A) leader was shown to be at most weakly dependent on the cap-binding complex eIF4F and may be cap-independent [20, 298].

Direct *in vitro* experiments that used uncapped poly(A) sequences (5, 12, and 25 nt long) as the 5′ UTR resulted in an efficient translation of such mRNAs in an eukaryotic cell-free system [157]. A subsequent study has shown that 48S preinitiation complex (PIC) formation at the cognate AUG initiation codon on the mRNA with poly(A) leader does not require eIF3, eIF4A, and eIF4F [379]. This fact implies that ATP-dependent unidirectional scanning of a poly(A) leader is not strictly required for finding the correct initiation codon. It is likely that the poly(A) leader sequence can effectively bind preinitiation 40S ribosomal subunits at random internal sites within the poly(A) sequence and may thus allow the particles to perform energy-independent diffusional movement ("phaseless wandering") along the 5′ UTR until the particle is fixed at the initiation codon [379].

The 48S PIC formed in the absence of eIF3 and eIF4F can join the 60S ribosomal subunit and form the 80S initiation complex. Moreover, such an mRNA has been shown to outcompete a capped mRNA with a 5′ UTR derived from the β-globin mRNA, in a direct competition assay [379].

The factors required for translation initiation on poxvirus poly(A) mRNA leaders are analogous (and in some cases homologous) to prokaryotic IF1, IF1A, and IF2. This implies that poxviruses use the most basic (most ancient) elements of translation initiation machinery that are present in both prokaryotes and eukaryotes.

IRES-like polypurine (A)-rich sequences (PARSs) discovered in crucifer-

infecting tobamovirus (crTMV) may represent another manifestation of the same mechanism [94]. It was shown that the PARSs placed as an intercistronic insert in a bicistronic mRNA exhibit a high frequency of initiation at the second cistron in both *in vivo* and *in vitro* plant and animal translation systems. Remarkably, the activities of crTMV IRES-derived PARSs appeared to be even somewhat higher than that of EMCV IRES in plant and human cells [94].

Typical viral IRESs are characterized by relatively stable tertiary structures and represent compact modules that are capable of specifically binding and positioning the preinitiation 40S ribosomal subunits on the mRNA [96]. The situation with poly(A) leaders or poly(A) internal inserts seem to be quite different: these have no fixed tertiary structure and do not position the ribosomal particle at a strictly determined site in the mRNA. It would be therefore appropriate to consider such enhancers of cap-independent initiation of translation as a special case [379].

Recently it has also been reported that a "minimal" 60 nt IRES that contains an internal poly(A) tract preceding the AUG initiation codon allows a cap-independent translation of mRNAs that are required for starvation-induced differentiation in yeast [138]. This activity requires specific binding of Pab1 (the yeast ortholog of PABP) to the 5′ UTR and the presence of eIF4G [138].

It is possible that the mechanism of the 48S initiation complex formation in the case of an internal poly(A) tract is different from that of a poly(A) leader. Another possibility that was proposed by Shirokikh and Spirin in [379] is that Pab1 and eIF4G are required at later stages of cap-independent translation of mRNAs than is required for the invasive growth in yeast. Such a late eIF4F/eIF4G-dependent stage was suggested by a study of the translation acceleration effect during translation of uncapped mRNAs and may result from a noncovalent circularization of polysomes in the course of their formation[4].

1.6.5 Proteins targeted to the 5′ UTR

Iron-response proteins Ferritin is the major iron-binding protein whose function is to sequester excess intracellular iron, thereby protecting cells from the generation of reactive oxygen and nitrogen free radicals which can damage DNA. Translation of ferritin heavy- and light-chain mRNAs is turned on and off by the iron-response proteins (IRP1 and IRP2). Under conditions of low iron, IRP binds a combined sequence/structure motif (iron-response element, IRE) near the 5′ end of the mRNA (Fig. 7A). Binding of IRP does not affect the association of the cap-binding complex eIF4F to the mRNA but blocks

entry of the 43S ribosomal subunit [297]. The repression is relieved when the IRE is moved away from the cap-proximal position, suggesting that the IRE/IRP complex sterically prevents 43S binding [145].

In addition to controlling translation of ferritin, the IRE/IRP mechanism regulates other genes involved in iron uptake and utilization. In the case of ferroportin, the IRE is near the 5′ end of the mRNA and regulation is at the level of translation. In the case of the transferrin receptor, the IRE is in the 3′ UTR and regulation is at the level of mRNA stability [166].

This steric hindrance mechanism is simple and efficient, and it is not only specific to IRP. It has been shown that other RNA-binding proteins with no role in translational control can repress translation when bound to structures located within *ca.* 40 nt of the cap [398]. It seems surprising that there are not more such examples similar to the IRE/IRP interaction in translational control.

1.6.6 Proteins targeted to the 3′ UTR

The binding sites for many regulatory proteins are located in the target transcript's 3′ UTR. Thus any proposed mechanism must explain how a protein bound to the 3′ end of a mRNA is able to interact with the translation machinery. The idea that interaction between 5′- and 3′-bound proteins might circularize an mRNA (closed-loop model) can be helpful in explaining repression of translation. Inability to translate an mRNA circularized via a protein bridge (wherein one of the proteins is bound very close to the cap) would be expected from the earlier demonstration that 40S ribosomal subunits cannot bind to mRNAs circularized enzymatically by RNA ligase [227]. Alternatively, a protein bound to the 3′ UTR of a circularized mRNA may interact with translation initiation factors bound to the 5′-end and make them unaccessible for their partners.

CPEB and Maskin Many translationally dormant maternal mRNAs become cytoplasmically polyadenylated and translationally activated during oocyte maturation and early embryonic development in *Xenopus*. These mRNAs share the presence of a *cis*-acting regulatory motif in their 3′ UTR called the cytoplasmic polyadenylation element (CPE), with the consensus sequence `UUUUUAU`. The CPE is the binding platform for CPE-binding protein (CPEB), which mediates repression of the translation of CPE-containing mRNAs prior to maturation. CPEB is an RRM- and zinc-finger-containing sequence-specific RNA-binding protein that is found in a wide range of vertebrates and invertebrates [352]. By virtue of its recognition of CPE, CPEB

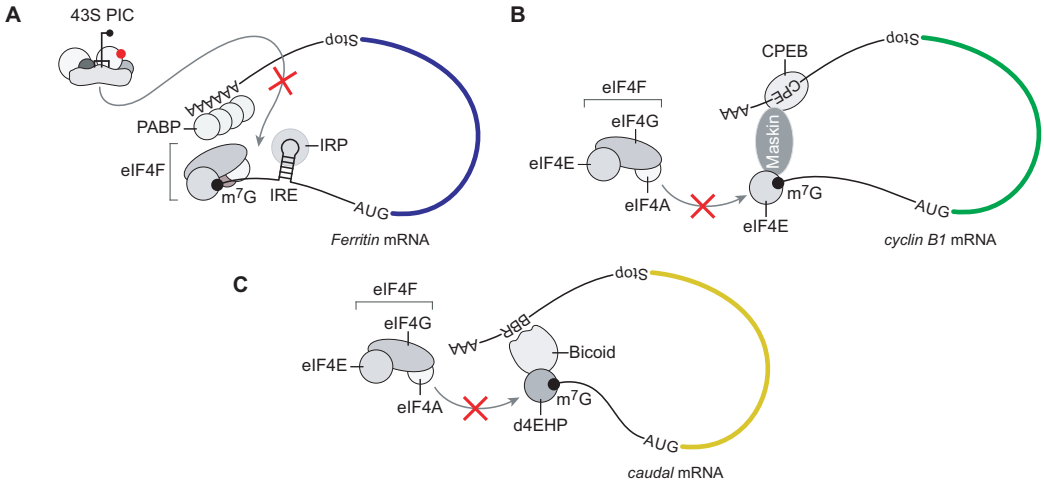

Figure 7. Inhibition of translation initiation by 5′- and 3′-UTR-binding proteins.

(A) IRP binds to IRE, a 5′-proximal stem loop in the 5′ UTR of *ferritin* mRNA, and sterically blocks the association of 43S PIC to eIF4F. **(B)** The CPEB/Maskin complex binds to the *cis*-regulatory cytoplasmic polyadenylation element (CPE) in the 3′ UTR of *cyclin B1* mRNA and competitively inhibits the interaction of eIF4G with eIF4E. **(C)** Bicoid binds to the Bicoid-binding region (BBR) in the 3′ UTR of *caudal* mRNA and recruits the cap-binding d4EHP which blocks the association of eIF4F to the 5′ cap.

is indirectly responsible for both translational repression and translational activation by polyadenylation.

CPEB was found to be associated with Maskin [396]. Maskin also binds eIF4E in the region normally occupied by eIF4G. Thus, Maskin competes with eIF4G for binding to eIF4E and this can inhibit translation by preventing the formation of the cap-binding complex [396, 52], although this has not yet been shown directly (Fig. 7B).

While the poly(A) tail is short, Maskin remains associated with both CPEB and eIF4E. Upon the induction of oocyte maturation, the kinase Aurora A phosphorylates CPEB which stimulates poly(A) tail elongation. The elongated poly(A) tail recruits PABP. PABP, in turn, binds eIF4G and helps it to displace Maskin from eIF4E, the result of which is translation initiation [352].

Although CPEB and Maskin are the key factors for the repression of maternal mRNA in late *Xenopus* oocytes, another mechanism must exist, since Maskin is absent earlier in oogenesis. It was found that in the early *Xenopus* oocyte, CPEB functions in a very large RNP complex with Xp54 (Me31B/DDX6), PAT1, RAP55B (CAR-1/Tral), FRGY2 (Yps/YB-1), 4E-T, and eIF4E1b, an ovary-specific eIF4E which binds the cap weakly [288]. It

was proposed that the repression of CPE mRNAs in *Xenopus* oocytes by the CPEB complex may rely upon the combination of conserved P body components, including Xp54 and 4E-T, alongside a weak cap-binding eIF4E1b protein, which can act as a co-repressor when tethered to the 3′ UTR [288, 392].

CPEs within the 3′ UTR appear to link mRNA translational control and localization through their interaction with CPEB. In neurons, inserting the CPE into an unlocalized message is sufficient to cause the message and CPEB to be transported into dendrites. Overexpression of a truncated CPEB that only contains the RNA-binding domains dominantly interferes with the transport of endogenous messages into dendrites. GFP-tagged CPEB forms particles containing RNA and motor proteins that exhibit microtubule-dependent transport in cultured hippocampal neurons [176]. These particles also contain Maskin, suggesting that CPEB and Maskin can both participate in maintaining localized mRNAs in a translationally quiescent state during transport and in microtubule association of transport particles containing these mRNAs [176]. It is likely that the large CPEB-containing RNP particles identified in *Xenopus* oocytes [288] represent translationally repressed mRNPs similar to transport mRNPs that are found in neurons [24].

Bicoid Anterior-posterior pattern formation in the *Drosophila* embryo during development is dependent on the localization and translation of *bicoid* and *oskar* mRNAs. *bicoid* mRNA is localized at the anterior pole and translated after fertilization to produce a morphogen gradient that patterns the anterior part of the embryo [354]. Bicoid is a homeodomain transcription factor which, in addition to its function in transcription, binds the region in the 3′ UTR of *caudal* mRNA termed the Bicoid-binding region (BBR, 120 nt long) and inhibits its translation [100, 355]. Bicoid contains an eIF4E-binding motif which overlaps with the site for binding the *Drosophila* eIF4E-homologous protein (d4EHP). 4EHP is evolutionarily conserved in metazoans and plants. The amino acid residues of eIF4E which are implicated in its binding to the cap structure are mostly conserved in d4EHP. While 4EHP has 5′-cap-structure-binding activity, it does not interact with eIF4G, suggesting that it could function as a negative regulator of translation since it cannot function in ribosome recruitment. d4EHP interacts with both Bicoid and the *caudal* mRNA 5′ cap structure, while Bicoid binds to BBR in its 3′ UTR. This set of interactions is required for efficient translational repression of *caudal* mRNA by preventing the association of eIF4F to the 5′ cap structure (Fig. 7C, [66]).

It has been shown that d4EHP also inhibits *hunchback* mRNA translation by interacting simultaneously with the mRNA 5′ cap structure and Brat

(Fig. 7D, [65]). Brat is a component of the NRE complex which includes Pumilio and Nanos proteins and binds the Nanos-responsive element (NRE) in the 3′ UTR of *hunchback* mRNA [386].

hnRNP K and E1 Erythroid 15-lipoxygenase (LOX) is a key enzyme which degrades mitochondrial membranes during the late stages of reticulocyte maturation to erythrocytes. LOX protein appears to be produced only in late-stage reticulocytes, although LOX mRNA is transcribed as the most abundant message after globin mRNAs in bone marrow erythroid precursor cells [401]. LOX mRNA translation must thus be temporally restricted. The 3′ UTR of LOX mRNA contains a CU-rich, repetitive sequence motif termed the differentiation control element (DICE), which has been shown to mediate this translational silencing [324]. The KH-domain proteins hnRNP K and E1 bind the DICE in the 3′ UTR which leads to translational repression at the level of initiation [323].

This translational repression is independent of the poly(A) tail and can control cap-dependent translation as well as translation mediated by the EMCV or classical swine fever virus (CSFV) IRES elements, indicating that repression is also independent of the cap structure [323, 322]. Translation initiation via the intergenic region IRES of the CrPV, which solely requires 40S and 60S ribosomal subunits without any eIFs [428], is shown to bypass the silencing mechanism [322]. Sucrose gradient and toeprint analyzes of translation initiation complexes revealed that during the hnRNP-K/E1-mediated translational repression, the AUG codon is reached by the 43S preinitiation complex but 80S complex formation is inhibited [322]. Thus, recruitment of the 60S subunit is blocked during LOX mRNA translational silencing (Fig. 8) which makes this mechanism different to the other known mechanisms described above. hnRNP K also binds to the *c-Src* mRNA 3′ UTR element Src3 and inhibits *c-Src* mRNA translation by blocking 80S ribosome formation [301].

1.7 Selective control: complex mechanisms

Recent studies on selective mechanisms of translational control mediated by mRNA-binding proteins have demonstrated that many of them regulate translation by using more than one mechanism. This ensures the tight translational control and correct localization of maternal mRNAs that encode morphogens establishing the spatial axes of the embryo. Ectopic expression of such proteins leads to severe developmental defects, so multiple translational control mechanisms and RNA localization must cooperate in their deployment.

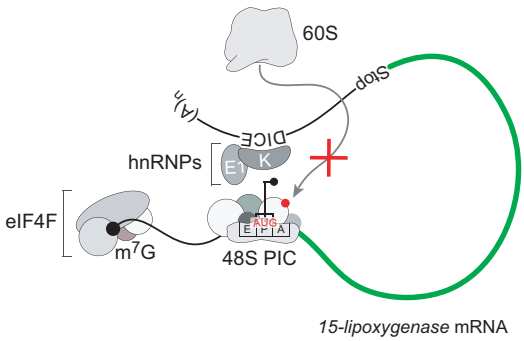

Figure 8. Inhibition of 60S subunit joining by hnRNP K and E.

hnRNPs K and E1 bind to the differentiation control element (DICE) in the 3′ UTR of LOX mRNA and block translation initiation at the step of 60S subunit joining to the 48S preinitiation complex. The same mechanism regulates translation of *c-Src* mRNA.

Bruno and regulation of *oskar* translation During oogenesis in *Drosophila*, Oskar protein is selectively deployed at the posterior of the oocyte, where it directs polar granule assembly and is responsible for posterior body patterning and germ cell formation [200]. *oskar* mRNA is synthesized in the nurse cells and, throughout early oogenesis, becomes concentrated in the oocyte. During early oogenesis (stages 1-6), the mRNA first appears at the posterior of the oocyte, where the minus ends of the microtubule array are concentrated. At stages 7-8, the microtubules reorganize so that the majority of the minus ends become concentrated at the anterior of the oocyte. Tracking the minus ends of the microtubules, *oskar* mRNA transiently localizes to the anterior of the oocyte during these stages. Finally, at stages 9-10, *oskar* mRNA is transported back to the posterior pole in a plus-end directed manner, where it is translated [198]. Localization of *oskar* mRNA is tightly coupled to translational control. Since factors that are involved in localization may also affect translation indirectly, *oskar* mRNA appears to be subject to multiple forms of repression [426].

Prior to its localization at the posterior pole, translation of *oskar* mRNA is repressed by the RNA-binding protein Bruno, which was identified by its ability to bind directly to the *oskar* 3′ UTR [218, 418, 304]. Repression of Oskar synthesis by Bruno involves its binding to Bruno response elements (BREs), which are repeat sequences clustering within two regions of the *oskar* 3′ UTR: one close to the coding sequence and one close to the poly(A) tail. Mutation of the BREs in the *oskar* 3′ UTR results in precocious translation of *oskar* mRNA, but does not interfere with its localization, suggesting that Bruno regulates *oskar* mRNA translation directly [218]. Bruno contains three copies of the RNA recognition motif (RRM). Either of two nonoverlapping

parts of Bruno—RRMs 1 and 2 and RRM 3 plus 42 flanking amino acids—can bind specifically to BRE-containing RNA, but both domains are required for maximal binding [384].

Bruno accumulates in the oocyte and colocalizes with *oskar* mRNA. It has been demonstrated that Bruno shuttles between the nucleus and cytoplasm, and may first bind *oskar* mRNA in the nucleus [384]. A role for Bruno in Oskar regulation *in vivo* was demonstrated through the use of a transgene, which encodes a form of *oskar* mRNA that retains BRE sequences but is mislocalized to the anterior of the oocyte [418]. Ectopic translation of *oskar* mRNA from this transgene leads to embryonic head defects, and this phenotype is enhanced in the Bruno heterozygous flies [418]. Experiments in *Drosophila* cell-free translation systems have demonstrated the direct role of Bruno in *oskar* mRNA translational repression [254, 55].

Bruno has been proposed to inhibit initiation of translation via two routes (Fig. 9): an interaction with the Cup protein (cap-dependent, [425, 304]) and sequestration of *oskar* mRNA in silencing particles (cap- and Cup-independent, [61]).

Sucrose gradient analysis has demonstrated that the BRE/Bruno repression mechanism inhibits 43S preinitiation complex recruitment to *oskar* mRNA [61]. Consistent with this result, it has been shown that Bruno binds the protein Cup which, in turn, binds the 5′-cap-binding eIF4E through a sequence conserved among eIF4E binding proteins. Cup competes with eIF4G for eIF4E binding and therefore prevents cap-binding complex assembly and 43S recruitment to *oskar* mRNA [425, 446, 304].

The second BRE/Bruno-dependent silencing mechanism involves *oskar* mRNA oligomerization and formation of large (50S-80S) silencing particles that cannot be accessed by ribosomes [61]. Such a repression mechanism suggests a mode of mRNA translational control that seems particularly suited to coupling of translational repression with mRNA transport within the cell. The particles could in principle contain other mRNAs regulated and assembled into mRNPs by common components [61].

Interestingly, mutations in *armitage*, *aubergine*, *spindle-E*, and *maelstrom*, which encode proteins with a proposed function in the RNAi pathway, cause precocious accumulation of Oskar protein in the early oocyte [76]. The Armitage protein is a putative RNA helicase with a direct role in the RNAi pathway [404]. Aubergine is a member of the Argonaute family of proteins which are the key components of the RNA-mediated silencing machinery in many organisms [180]. *Spindle-E* encodes a putative DEAD/DEAH-box RAN helicase. Both Aubergine and Spindle-E are required for RNAi in the early embryo, as well as for silencing of *Ste* genes by *Su(Ste)* repeats through a mechanism thought to involve repeat-associated siRNAs (rasiRNAs) [14, 13].

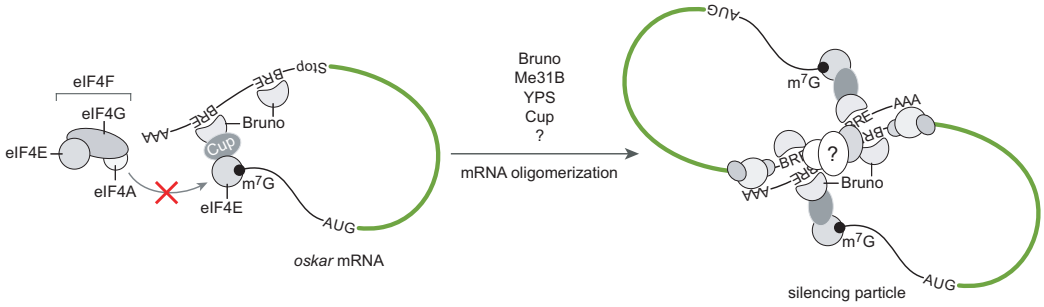

Figure 9. Bruno-mediated translational repression of *oskar* mRNA.

Bruno binds the BREs in the *oskar* 3′ UTR and recruits Cup to inhibit eIF4G binding to eIF4E, which prevents preinitiation complex formation. In addition, Bruno promotes the oligomerization of *oskar* mRNAs through the BRE, which possibly renders the mRNA inaccessible to the translation machinery.

Spindle-E is also implemented in rasiRNA-dependent chromatin silencing of retrotransposons in the *Drosophila* germline [220]. Maelstrom is required for normal localization of the RNAi factors Dicer and AGO2 [120]. Armitage, Aubergine, Spindle-E, and Maelstrom all localize to nuage and are required for rasiRNA production as well as silencing of long interspersed nuclear elements (LINEs) [255].

Intriguingly, all of these mutants in the RNAi pathway display premature translation of *oskar* mRNA before such defects are usually seen in *cup* mutants. This suggests that RNAi-mediated repression may predominate early in oogenesis, while Cup-mediated repression acts later [426]. However, the defects in *oskar* mRNA localization and translation may result from the cytoskeletal defects associated with these mutations [76] or more general defects caused by derepression of genomic repeats and mobile elements. The cytoskeletal and rasiRNA-mediated silencing defects in these mutants underscore the complexity of their phenotypes and raises the possibility that the defects in *oskar* mRNA translation are not direct. Proof that *oskar* mRNA translation is directly regulated by an RNA-silencing mechanism would be achieved by identification of the *cis*-acting elements within the *oskar* mRNA that are required for RNA-mediated repression and the small RNA(s) that recognize these elements [426].

Transport of *oskar* mRNA to the posterior of the oocyte requires many proteins including the exon junction complex (EJC) components Mago, Y14, and eIF4AIII, suggesting that during splicing the EJC is positioned so that it can initiate the assembly of a transport mRNP prior to nuclear export [309, 159, 292, 327]. In the cytoplasm, additional proteins are recruited to

the *oskar* mRNP. Barentsz is recruited through an interaction with eIF4AIII and Cup, and is the only protein apparently functioning solely for posterior transport of *oskar* mRNA [407, 425, 327]. A number of factors, such as Staufen [199, 360, 287], Vasa [45, 273], Apontic [254], Bicaudal C [268, 365], Squid [312], Hrp48 [436, 183], YPS [272], and Me31B [303], have been shown to be required for efficient translational control of *oskar* mRNA *in vivo*, but their mode of action remains unclear.

The dsRNA-binding protein Staufen plays a distinct role, being required not only for transport, but also for anchoring and translation of *oskar* at the posterior end [199, 360, 287]. Similarly to Bruno, Hrp48 and Squid interact with the *oskar* 3′ UTR. The mutations in *hrp48* and *squid* cause defects in *oskar* mRNA localization and ectopic production of Oskar protein [436, 183, 312]. Me31B has been purified as part of a large mRNP complex that contains EXU, YPS, Cup, eIF4E, Bruno, and *oskar* mRNA, indicating that it acts in translational repression of *oskar* mRNA [303, 61].

A long poly(`A`) tail is required for efficient *oskar* translation, both *in vivo* and *in vitro*, but is not sufficient to overcome BRE-mediated repression. Moreover, accumulation of Oskar activity requires Orb, the *Drosophila* homolog of CPEB [54]. Orb-mediated cytoplasmic polyadenylation stimulates *oskar* translation to achieve the high levels of Oskar protein necessary for posterior patterning and germline differentiation [54].

Smaug and *nanos* translation *Drosophila* Nanos is a posterior determinant and translational repressor whose primary function is to regulate translation of maternal *hunchback* mRNA (§ 1.6.6). Once Oskar protein accumulates in the oocyte, it recruits maternal *nanos* mRNA to the posterior by trapping and anchoring *nanos* mRNA that is diffusing throughout the oocyte [414, 128, 413]. This mechanism is inefficient and only a small fraction of the transcripts is localized to the posterior, where it is translated during late oogenesis and embryogenesis. The remaining 96% of *nanos* mRNA is found distributed throughout the bulk of the embryo [35, 129]. Unlocalized transcripts are translationally repressed and degraded [82, 130, 383].

Repression of *nanos* mRNA translation is mediated by *cis*-acting stem-loop translational control elements (TCEs) in the transcript's 3′ UTR. TCE is a bipartite RNA element: one stem-loop appears to represent the binding site for an as yet unidentified translational repressor and is required for translational repression during late oogenesis [79, 122]. The other two stem-loops which harbor a `CUGGC` motif are bound by the sequence-specific RNA-binding protein Smaug, which functions as a translational repressor; such a stem-loop is therefore termed the Smaug recognition element (SRE) [81, 82, 383, 382].

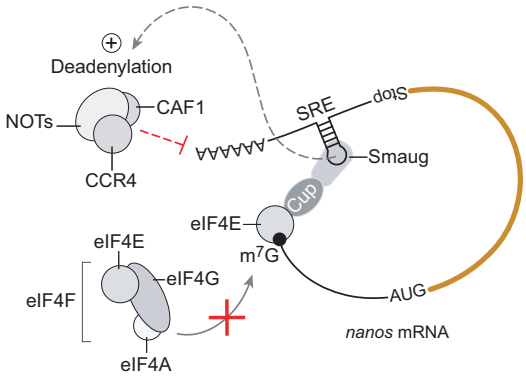

Figure 10. Smaug-mediated translational repression of *nanos* mRNA.

Smaug binds the SRE in the *nanos* 3′ UTR and recruits the 4EBP Cup. Cup binds eIF4E through the conserved sequence that is also found in eIF4G. As a consequence, eIF4G is precluded from the 5′ end, and the preinitiation complex can not form. Smaug also recruits the CCR4-CAF1-NOT deadenylase complex to the mRNA to promote shortening of the poly(A) tail. These two mechanisms lead to an inhibition of translation. The grey dashed arrow corresponds to an activating signal, the red blunted line correspond to an inhibitory signal.

Smaug is conserved from yeast to humans and interacts with the SRE via a sterile α motif (SAM) domain, which is normally involved in protein-protein interactions [19, 146, 147]. The eIF4E-binding protein Cup was identified biochemically as a protein that interacts with the SAM domain of Smaug [307]. Similarly to the role of Cup and Bruno in *oskar* mRNA translational control (§ 1.7), it appears that the Smaug-Cup-eIF4E complex blocks the interaction between eIF4E and eIF4G, as well as preventing eIF4F complex formation at the 5′ cap and 43S PIC recruitment to *nanos* mRNA [307].

However, translationally repressed *nanos* mRNA is also associated with polysomes [70]. One possible explanation for this apparent contradiction is that Nanos synthesis is repressed by at least two *trans*-acting factors that interact with the *nanos* 3′ UTR [79, 122]. In keeping with this model, *nanos* mRNA is translated in the nurse cells and after it has been transported to the oocyte, is first repressed by an unidentified factor in a Smaug-Cup-eIF4E-independent way. This factor bound to the TCE may degrade or destabilize the nascent/released polypeptide chain or block translation at the step after initiation (elongation or termination) [70]. During the first hours of embryogenesis, translational repression becomes Smaug-Cup-eIF4E-dependent [81, 383], but the ribosomes may still remain bound to the mRNA after an initiation block.

It has been shown that Smaug in embryos recruits the CCR4-CAF1-NOT

deadenylation complex to the nanos mRNA, which results in shortening of the poly(A) tail and translational repression [442]. Interestingly, it was found that Oskar prevents Smaug binding the mRNA, and as a result promotes translation of nanos mRNA in the posterior of the embryo. CCR4-CAF1-NOT-dependent deadenylation was shown to be important for both degradation and translational repression of *nanos* mRNA in the bulk of the embryo [442]. Thus it appears that Smaug represses *nanos* mRNA translation by an additional Cup-independent mechanism which relies on recruitment of the deadenylation complex to shorten the poly(A) tail.

SXL and *msl-2* translation Dosage compensation is the process which ensures that equal amounts of X-chromosome-linked gene products are expressed in males that carry one X chromosome and females that carry two [274]. In *Drosophila*, dosage compensation is achieved by increasing the transcriptional output of the X chromosome in males but not in females. Transcriptional activation is mediated by the male-specific lethal (MSL) RNP complex. The MSL complex does not assemble in female flies mainly because they lack one component protein, male-specific lethal-2 (MSL-2). Translation of *msl-2* mRNA in female flies is repressed by the female-specific RNA-binding protein sex-lethal (SXL), containing two RNA recognition motifs which also regulate sex determination (reviewed in [333]). SXL acts as both an alternative splicing regulator to control sex determination and a translational repressor to control dosage compensation. It inhibits *msl-2* expression by first promoting the retention of a facultative intron in the 5′ UTR of *msl-2* mRNA and then repressing its translation [27, 212, 134]. It has been demonstrated that the only function of the retained intron is to provide the binding sites for the SXL protein in the 5′ UTR. SXL binds to poly(U) stretches present in the 5′ and 3′ UTRs of *msl-2* mRNA. In contrast to most other translational regulators, which act from either the 3′ or the 5′ UTR, efficient inhibition of translation requires SXL binding to both UTRs [27, 212, 134].

Sucrose density gradient analysis and toeprint assays revealed that SXL functions via a dual "failsafe" mechanism: SXL bound to the 3′ UTR of *msl-2* mRNA interferes with the initial recruitment of the 43S preinitiation complex to the mRNA, while 5′ UTR-bound SXL stalls any residual scanning 43S complexes that have escaped the first inhibitory mechanism [29].

Scanning inhibition by SXL bound to the 5′ UTR does not seems to operate by a simple steric hindrance mechanism, because mSXL, the *Musca domestica* ortholog of *Drosophila* SLX, binds to the 5′ UTR of *msl-2* mRNA with the same affinity but does not inhibit translation [156, 29]. It is possible that 5′ UTR-bound SXL interferes with the function of a factor required

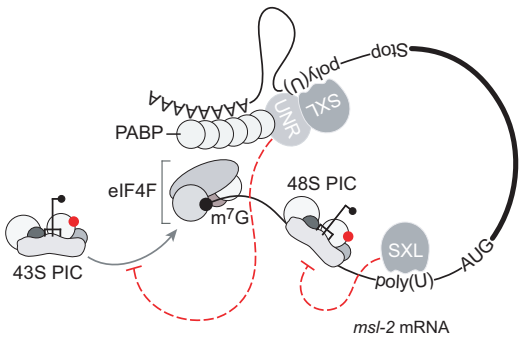

Figure 11. SXL-mediated translational control of *msl-2* mRNA

SXL binds to uridine stretches in the 5′ and 3′ UTR of *msl-2* mRNA. 3′ UTR-bound SXL recruits UNR and probably other proteins to inhibit the initial recruitment of the 43S preinitiation complex to the 5′ end of *msl-2* mRNA. SXL bound to the 5′ UTR inhibits the scanning of those 43S complexes that may have escaped the 3′-mediated inhibition. Red blunted lines correspond to inhibitory signals.

for scanning, or forms a high-order complex of SXL molecules, perhaps in conjunction with other proteins that block 43S PIC transit.

SXL-mediated inhibition of translation initiation is independent of the cap structure, implying that the 43S complex recruitment block imposed by SXL is different from that mediated by Maskin, Cup, or d4EHP, where repression is achieved by blocking the formation of the cap-binding eIF4F complex on the target mRNA [133]. SXL bound to the 3′ UTR requires the RNA-binding protein upstream of N-*ras* (UNR) as a corepressor to efficiently block *msl-2* mRNA translation [156, 1, 101]. Interestingly, UNR protein is expressed at similar levels in both male and female cells in culture and in flies, but only interacts with *msl-2* mRNA to modulate its translation when SXL is present [101]. Presumably the SXL-UNR corepressor complex directly interacts with factors that affect small ribosomal subunit recruitment, or may do so through additional bridging factors as part of a larger "corepressor assembly". A candidate factor is *Drosophila* PABP, since mammalian PABP interacts with UNR [59]. Although *msl-2* mRNA translational inhibition does not require a poly(A) tail [132], PABP appears to have a critical function in initiation that is independent of the poly(A) tail [204], raising the possibility that UNR might interfere with PABP-mediated recruitment of the 43S complex to *msl-2* mRNA [101].

Additional factors that specifically co-purify with the repressed mRNP have been identified biochemically [101]. These include several known components of translationally quiescent mRNPs: DEAD-box RNA helicases Me31B and Rm62, YPS, dFMR1, and Rasputin (a *Drosophila* homolog of G3BP2,

an RNA-binding protein). 3′ UTR-mediated translational inhibition by SXL-UNR involves the accumulation of the repressed mRNA within unusually heavy RNP particles, although no RNA oligomerization activity has been detected, in contrast to Bruno-mediated *oskar* mRNA repression [29, 61]. Additional studies will be required to elucidate the mechanism by which SXL and UNR bound at the 3′ end of *msl-2* mRNA block translation initiation at the 5′ end.

PUF domain proteins *Drosophila* Pumilio and *C. elegans* FBF (fem-3 binding factor) proteins are founder members of the evolutionary conserved family of RNA-binding proteins known as the PUF family [388, 422]. PUF proteins are typically characterized by a C-terminal RNA-binding domain, known as the Pumilio homology domain (PUM-HD), composed of eight tandem imperfect repeats, each of approximately 40 amino acids, flanked by conserved N- and C-terminal regions [447, 445, 25]. The crystal structures of the PUM-HD domains have revealed that the repeats are aligned in tandem to form an extended curved crescent-like molecule [417, 103]. The crescent provides two extended surfaces: one contacts RNA, and the other proteins. The RNA binds to the concave surface of the domain in a sequence-specific manner [388, 422]. Each of the eight repeats makes contact with a different RNA base via stacking and backbone interactions provided by three aromatic and basic amino acid residues positioned in the middle of the repeat [417, 103, 158].

PUF proteins bind specific sequence elements present in the 3′ UTR of target mRNAs to control mRNAs' translation and stability. Analysis of many mRNAs associated with PUF proteins in different species has led to a consensus eight-nucleotide sequence `UGUANAUA` which is recognized by PUF proteins [135, 126, 294].

In *Drosophila*, Pumilio and Nanos are required for proper posterior segmentation and abdomen formation of the embryo and are necessary for establishment of the posterior-anterior gradient of the transcription factor Hunchback [173, 187, 399]. Pumilio binds to the Nanos responsive element (NRE) within the 3′ UTR of maternal *hunchback* mRNA and causes a translational arrest [300, 429, 385]. Pumilio and Nanos are involved in the translational control of maternal *cyclin B* mRNA in *Drosophila* [16, 202, 408]. In *Xenopus* oocytes, Pumilio overexpression inhibits *cyclin B1* mRNA translation and anti-Pumilio antibody injection induces it. In addition to interacting with CPEB, Pumilio also has binding sites of its own in the *cyclin B1* 3′ UTR, which contribute to the translational repression [302].

Recent studies on yeast and *Drosophila* have provided a general frame-

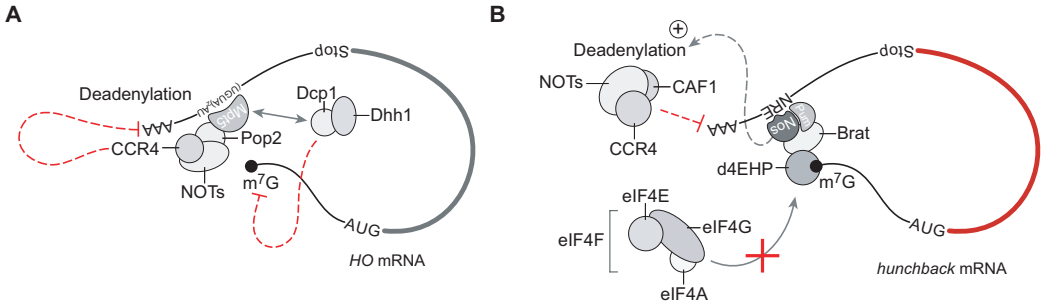

Figure 12. PUF-protein-mediated translational control mechanisms.

(A) Direct interaction between the Pop2/CAF1 deadenylase and a PUF domain protein (here, budding yeast Mpt5) recruits the CCR4-Pop2-NOT deadenylase complex to the 3′ UTR of *HO* mRNA. Pop2-promoted deadenylation prevents the binding of PABP, thereby repressing translation of the mRNA. Mpt5 also recruits the complex containing Dhh1/Me31B and Dcp1 which can cause decapping, translational repression or both. **(B)** In *Drosophila*, the ternary NRE complex comprised of Nanos (Nos), Pumilio (Pum), and Brain tumor (Brat) assembles on the Nos-responsive element (NRE) in the 3′ UTR of *hunchback* mRNA and recruits d4EHP which blocks the eIF4F/5′-cap interaction. In addition, the NRE complex can recruit the CCR4-CAF1-NOT deadenylase complex. Red blunted lines correspond to inhibitory signals.

work for understanding how PUF proteins control mRNA translation and stability [142, 143, 202, 421]. Pumilio nucleates formation of the complex by recognizing the NRE in the 3′ UTR of *hunchback* mRNA and recruiting Nanos [385]. The subsequent recruitment of Brain tumor to the Pumilio-NRE-Nanos complex [386] results in translational inhibition via poly(A)-dependent and poly(A)-independent mechanisms [58]. The yeast PUF protein Mpt5 interacts directly with Pop2p/CAF1 and recruits the deadenylase complex. Moreover, PUF-Pop2 interaction is conserved in *C. elegans* and humans [142, 143]. In *Drosophila*, Nanos has been shown to interact directly with the NOT4 subunit of the CCR4-CAF1-NOT deadenylase complex [202]. These results suggest that a quaternary NRE complex consisting of Pumilio, Nanos, Brain tumor, and *hunchback* mRNA may recruit the CCR4-CAF1-NOT deadenylase complex and promote deadenylation of *hunchback* mRNA. Brain tumor can also interacts with d4EHP and inhibit translation initiation via a cap-dependent mechanism (§ 1.6.6, [65]).

Interestingly, it has been found that yeast PUF protein Mpt5 is physically associated with the decapping enzyme subunit Dcp1 and the DEAD-box RNA helicase Dhh1, which is the yeast ortholog of Me31B/RCK [142]. Dcp1 and Dhh1 are protein components of P bodies and other repressed mRNPs, which are conserved from yeast to humans [109, 8]. In the *C. elegans* germ

line, repressed maternal mRNAs and PUF proteins localize to P-body-like mRNP granules together with DCAP-1/Dcp1, DCAP-2/Dcp2, CAR-1/Tral, and CGH-1/Me31B [310]. Human Pum1 has been shown to be localized in stress granules after arsenite treatment [294]. These findings suggest that translational control mediated by PUF domain proteins may cause movement of the repressed mRNPs to specific cytoplasmic RNA granules such as P bodies, stress granules, or "germ line RNP granules related to P bodies (grP bodies)" [310].

Fragile X mental retardation protein FMRP is an RNA binding protein highly expressed in the brain. Absence or mutation of FMRP leads to Fragile X syndrome, an X-chromosome-linked dominant disorder and the most frequent cause of inherited mental retardation [23]. FMRP belongs to a family of heterogeneous nuclear ribonucleoproteins (hnRNPs) that are involved in many aspects of mRNA metabolism and biology. The protein contains several RNA binding domains including two KH motifs and one RGG box. As expected from this domain structure, FMRP binds RNA homopolymers and mRNAs *in vitro* [18, 380]. *In vivo*, FMRP forms part of a large mRNP complex that is involved in the transport and translation of mRNA in neurons [23].

Most isoforms of FMRP contain both a functional nuclear localization signal (NLS) and a nuclear export signal (NES), which indicates that it can shuttle between the nucleus and the cytoplasm [102, 381]. In the nucleus, one role of FMRP could be to associate with mRNAs and escort them out of the nucleus.

The majority of cytoplasmic FMRP is associated with polysomes throughout the length of the neurons, including dendritic spines [10, 117]. Microtubule-associated FMRP is predominantly retained in translationally dormant mRNP complexes. FMRP may shuttle between the mRNPs and polysomes depending on the translational state of the cell [415]. Consistent with these results, FMRP relocates out of polysomes and into stress granules subsequent to oxidative stress or heat shock [282, 216]. FMRP is also found in transport mRNP granules, which travel in dendrites on microtubules and are thought to be translationally arrested complexes of ribosomes, RNA-binding proteins and RNAs [11, 206, 260, 24]. According to the current model, FMRP regulates transport efficacy by regulating the association between mRNA cargo and microtubules. It acts as a molecular adaptor to bind mRNA targets and suppress their translation during kinesin-mediated transport to synaptic sites [89, 108].

The mechanisms which FMRP uses to regulate translation are not clear.

The fact that FMRP has been found to co-sediment with actively translating polysomes and with free mRNPs has complicated the issue. Several observations suggest that FMRP regulation might involve miRNAs. *Drosophila* FMRP has been characterized as a component of the RISC (RNA-induced silencing complex) [188, 56], and shown to interact with Rm62, the DEAD-box helicase present both in the RISC and in the Microprocessor complex involved in pre-miRNA processing [188, 149, 124]. Mammalian FMRP has been shown to interact with mammalian AGO2 and miRNAs [197]. Both FMRP and miRNAs are associated with polysomes [215, 308, 313, 340, 275].

Another small non-protein-coding RNA called *BC1*, unrelated to miRNAs or other components of the RNAi pathway, was proposed to be involved with FMRP-controlled translation. In this model, it has been proposed that *BC1* RNA that localizes to synaptodendritic domains operates as a requisite adaptor by specifically binding to both FMRP and, via direct base-pairing, to FMRP target mRNAs. The FMRP RNP is thereby brought into the vicinity of the initiation codon and blocks the translation [444].

In contrast to these results, interactions of *BC1* RNA with the FMRP could not be documented by Wang *et. al* [416]. It has been shown that *BC1* RNA inhibits a rate-limiting step in the assembly of the translation initiation complex. A translational repression element is contained within the unique $3'$ domain of *BC1* RNA. Interactions of this domain with eIF4A and PABP mediate repression, indicating that the $3'$ *BC1* domain targets a functional interaction between these factors [416, 225]. Moreover, it was found that *BC1* RNA specifically blocks the RNA duplex-unwinding activity of eIF4A but, at the same time, stimulates its ATPase activity [257]. Thus, it is thought that *BC1* RNA acts as a general inhibitor of translation which directly interacts with translation initiation factors, rather than an mRNA-specific inhibitor as suggested by Zalfa *et. al* [444].

Recently, in a study conducted independently, five laboratories have re-examined the issue of FMRP-*BC1*-mRNA interactions *in vivo* and *in vitro* [184]. They have reported that specific *BC1*-FMRP interactions could be documented neither *in vitro* nor *in vivo*. Significantly, the association of FMRP with *bona fide* target mRNAs was independent of the presence of *BC1* RNA *in vivo*. The authors conclude that *BC1* RNA is not required as an adaptor to link previously reported target mRNAs to FMRP [184].

Although most investigators in the fragile X field agree that one function of FMRP is to repress translation, the exact mechanisms by which it does so have not been elucidated. One possible mechanism of translation initiation inhibition has been proposed recently [305]. It has been shown that FMRP-mediated repression of translation requires an interaction with the cytoplasmic FMRP-interacting protein CYFIP1/Sra-1, which

also binds the cap-binding factor eIF4E. The eIF4E-interacting domain of CYFIP1 forms the characteristic "reverse L shaped" structure that is also assumed by the canonical eIF4E-binding motif. CYFIP1 forms a complex with specific FMRP-target mRNAs and blocks eIF4F assembly, interfering with the eIF4E-eIF4G interaction [305].

1.8 Selective control: post-transcriptional regulation by miRNAs

MicroRNAs (miRNAs) are short RNAs of approximately 22 nucleotides that silence gene expression post-transcriptionally by binding to the 3′ UTRs of target mRNAs. They have been implicated in a broad range of biological processes including development, cellular differentiation, proliferation and disease. In animal cells, miRNAs regulate their targets by translational inhibition and mRNA destabilization. Although much is known about miRNA biogenesis and biological function, the mechanistic details of the function of miRNAs in repressing protein synthesis are still poorly understood (Fig. 13).

More than a hundred miRNA genes have been identified in *Drosophila*, and 500-1000 in vertebrates and plants. According to several computational predictions of miRNA targets, each miRNA regulates hundreds of mRNAs, and one target mRNA could be combinatorially regulated by multiple miRNAs, suggesting that miRNA molecules may constitute a new layer of regulatory control over gene expression programs in many organisms [26, 50].

1.8.1 miRNA and miRISC biogenesis

Most miRNA genes are transcribed by RNAP II[1] to generate a primary miRNA (pri-miRNA) transcript, which are capped and polyadenylated, and can range in size from hundreds of nucleotides to tens of kilobases [51, 249]. In mammals, the majority of miRNA loci are encoded within intronic regions and transcribed as part of their hosting transcription units. Such intronic miRNAs can be processed from unspliced introns before splicing catalysis [217].

Pri-miRNAs fold into hairpin structures which are processed within the nucleus by a multiprotein complex termed the Microprocessor. The core components of this complex are the RNase III enzyme Drosha and the dsRNA-binding domain (dsRBD) protein Pasha/DGCR8 [247, 85, 149, 160, 241, 124]. Drosha cleavage of the pri-miRNA stem produces an approximately

[1] An exception are miRNAs lying within repetitive *Alu* elements, which are transcribed by RNAP III [41].

70-nt hairpin precursor miRNA (pre-miRNA) that contains 2-nt 3′ overhang, characteristic of RNase III-mediated cleavage [160].

An alternative biogenesis pathway exists for miRNAs derived from short intronic hairpins termed "mirtrons". Their nuclear processing appears to bypass Drosha cleavage. Instead, mirtron hairpins are defined by the action of the splicing machinery and lariat-debranching enzyme, which yield pre-miRNA-like hairpins [34, 362, 317].

The mirtron pathway merges with the canonical miRNA pathway during hairpin export by Exportin-5 which transports the pre-miRNA into the cytoplasm via a Ran-GTP-dependent mechanism [39, 266, 438].

In the cytoplasm, pre-miRNAs are cleaved by another RNase III enzyme, Dicer [181, 213], which forms a complex with the dsRBD proteins Loquacious/TRBP and PACT [64, 123, 366, 196, 248]. The final processing yields the mature $\sim$ 22-nt miRNA:miRNA* duplexes with protruding 2-nt 3′ overhangs. The Dicer-Loquacious complex recruits the Argonaute protein (AGO1 in *Drosophila*) and they form a trimeric complex that initiates the assembly of the miRNA-induced silencing complex (miRISC) [148, 271]. The miRNA strand with relatively lower thermodynamic stability of base-pairing at its 5′ end is incorporated into the miRISC, whereas the miRNA* strand is typically degraded [371, 98, 214]. Strand separation and miRISC loading has been proposed to occur by unwinding of the miRNA:miRNA* duplex via an unidentified RNA helicase followed by transfer of the miRNA strand to AGO1 [403, 339].

The most important and best-characterized components of miRNPs are proteins of the Argonaute family (reviewed in [180, 339]). There are five Argonaute proteins in *D. melanogaster* (AGO1-3, PIWI, and Aubergine). AGO1 is dedicated to the miRNA pathway, and AGO2 mainly functions in RNAi. Apart from the Argonaute proteins, miRISCs often include other proteins, which probably function as miRNP assembly or regulatory factors, or as effectors mediating the repressive miRNP functions [339]. In *Drosophila*, AGO1 directly interacts with GW182, an RNA-binding protein, and this interaction is required for miRNA-mediated translational repression and mRNA decay [347, 30, 112]. This requirement can be bypassed by tethering GW182 directly to mRNA in cells depleted of AGO1 [30]. Thus, GW182 (possibly in conjunction with other proteins) appears to be capable of inducing translational repression and mRNA degradation acting downstream of AGO1 (reviewed ind [90]). Consistent with this conclusion is the finding that depleting mammalian cells of the GW182 paralog TNRC6B impairs the ability of miRNAs to downregulate gene expression [190, 261, 284].

Once incorporated into the miRISC, the miRNA guides the complex to its mRNA targets by base-pairing interactions. In cases of perfect or near-

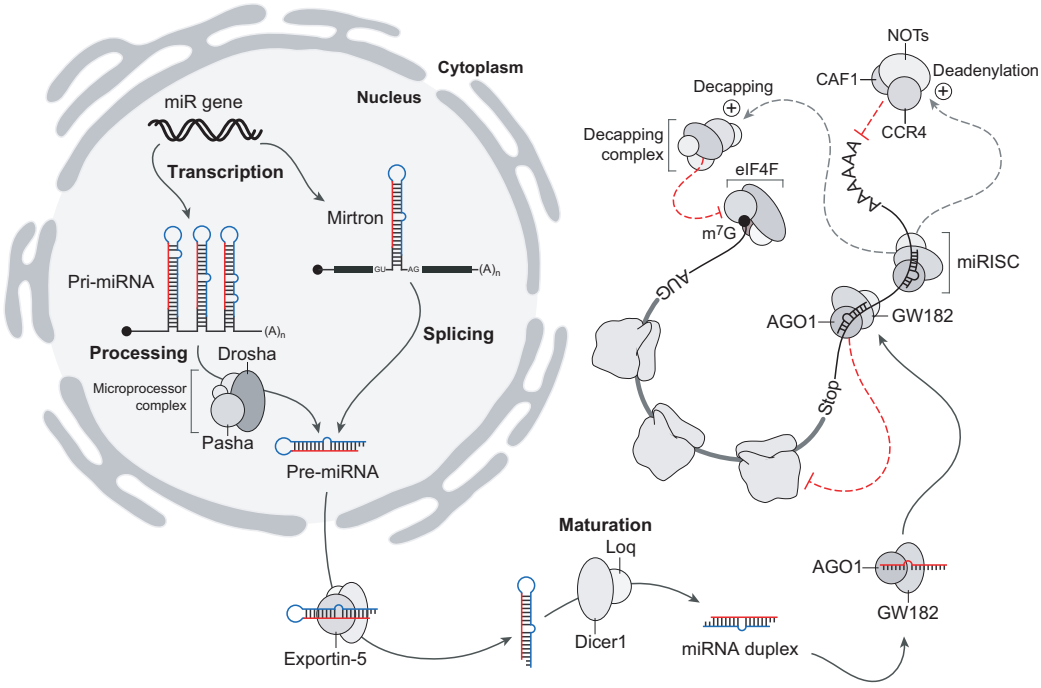

Figure 13. miRNA-mediated silencing pathway in *Drosophila*.

miRNAs are processed from primary transcripts (pri-miRNAs), which are either transcribed by RNAP II from independent miRNA genes or are portions of intronic sequences of mRNAs. A single pri-miRNA transcript often contains several different miRNA hairpins. These hairpin structures with imperfectly base-paired stems are processed by the RNase III type endonuclease Drosha which is a component of the Microprocessor complex that also includes the dsRNA-binding protein Pasha/DGCR8. The Microprocessor complex processes pri-miRNAs to $\sim$ 70-nt hairpins known as miRNA precursors (pre-miRNAs). Some spliced-out introns correspond precisely to pre-miRNAs (mirtrons), thus circumventing the requirement for Drosha-mediated processing. Pre-miRNAs are then transported to the cytoplasm by Exportin-5, where they are cleaved by another RNase III-like enzyme, Dicer1 (complexed with the dsRNA-binding protein Loquacious/TRBP) to yield $\sim$ 21-bp miRNA duplexes. After unwinding of the duplexes, one strand is selected to function as a mature miRNA, while the other miRNA* strand is degraded. Occasionally, both strands give rise to mature miRNAs. Dicer1-mediated processing is coupled with the assembly of mature miRNAs into RNP complexes called miRNPs or miRNA-induced silencing complexes (miRISCs). The key protein components of the miRISC are AGO1 and GW182. It can also contain further proteins that function as regulatory factors or effectors mediating the inhibitory function of miRNPs. The miRISC binds to the 3′ UTR of target mRNAs and prevents the production of proteins in different possible ways. These include: induction of target mRNA deadenylation and decapping, inhibition of translation initiation or elongation, and stimulation of nascent polypeptide degradation. Grey dashed arrows correspond to activating signals; red blunted lines correspond to inhibitory signals.

perfect complementarity to the miRNA, target mRNA can be cleaved and the fragments degraded; otherwise, the mRNA expression is inhibited by a complex mechanism ([182, 92, 278] and see below). Repression normally requires perfect contiguous base-pairing of the mRNA target with the "seed region" of the miRNA (residues 2-8) [93, 47]. In contrast, base-pairing between the mRNA target site and the 3′-proximal part of the miRNA is much less critical, although good base-pairing here can compensate for a suboptimal "seed match".

Recent studies suggest that the exact configuration of the mismatches defines whether miRNAs elicit decay or translational repression [5]. In addition, the mRNA sequences flanking the target sites, the number of target sites, the distance separating them and their position in the 3′ UTR may all influence the efficiency of repression [153].

1.8.2 miRNA-mediated control of mRNA translation and decay

mRNA decay Initial studies in *C. elegans* showed that the miRNA *lin-4* binds to the 3′ UTR of the *lin-14* mRNA and this causes a strong decrease of lin-14 protein levels without affecting the mRNA levels, indicating that *lin-4* inhibits gene expression at the level of translation [246, 321, 423]. Subsequent studies, however, have clearly demonstrated that animal miRNAs do induce significant degradation of target mRNAs in addition to translational repression [432, 141, 30, 22].

The mechanism of miRNA-mediated mRNA destabilization is best understood in *Drosophila*. MicroRNAs cause target mRNA decay by directing them to the general mRNA degradation machinery (reviewed in [127]). This process requires miRISC components AGO1 and GW182, the CCR4-CAF1-NOT deadenylase complex, the decapping enzyme DCP2, and several decapping activators including DCP1, Ge-1, EDC3, and Me31B/RCK (Fig. 13; [30, 113]). According to the current model, GW182 is recruited to miRNA targets through direct interaction with AGO1, where it contributes to translational repression and marks the transcript for degradation via deadenylation and decapping [30, 113].

In eukaryotic cells, the general mRNA degradation pathway is initiated by poly(A) tail shortening. This step is reversible—deadenylated transcripts that bear the correct *cis*-regulatory signals, in principle, can be re-adenylated and return to polysomes [127]. The deadenylated mRNAs that must be destroyed undergo irreversible decapping by the DCP2-DCP1 decapping complex, which exposes them to $5' \rightarrow 3'$ exonucleolytic degradation, presumably by Xrn1. Alternatively, the unprotected 3′ end lacking the poly(A) tail can be attacked by a large complex of $3' \rightarrow 5'$ exonucleases called the exosome

(reviewed in [127, 90, 111]).

The relative contribution of accelerated mRNA decay to the overall influence of miRNAs varies widely from message to message. In some instances, it appears to be the principal mechanism of downregulation, whereas in others its effect can be quite modest compared to that of translational repression [30].

Accelerated deadenylation with subsequent mRNA decay appears to be an independent mechanism by which miRNA-mediated silencing is accomplished, and can be uncoupled from translation and translational control. Blocking translation by introducing a large stem loop into the 5′ UTR does not itself trigger poly(A) removal or impair the ability of miRNAs to do so [434]. Likewise, an ApppN-capped miRNA target which was not translated due to the defective cap structure was rapidly deadenylated, indicating that deadenylation promoted by miRNAs is not caused by the lack of translation initiation and does not require active translation [290, 411]. It has also been shown that in *Drosophila* cells and human cell extracts, miRNA-mediated mRNA decay can occur even when translation is inhibited by cycloheximide [411, 113].

Although deadenylation of the target mRNA abrogates the cap/poly(A) synergy and reduces the efficiency of its translation, it is not the only mechanism which miRNAs employ to control translation. The observation that mRNAs lacking a poly(A) tail, or containing a 3′ histone stem-loop in place of a poly(A) tail, also undergo miRNA-mediated translational repression suggests that a poly(A) tail *per se* is not absolutely required for the repression [341, 178, 434].

Controversy over modes of translational control Although miRNAs have been known for some time to downregulate translation [423], the exact mechanism used to achieve this is still under debate. Indeed, published studies indicate that miRNAs may repress protein expression in several distinct ways, raising the possibility that more than one mechanism is involved (Fig. 14):

- inhibition of translation initiation, including inhibition of cap recognition and 43S PIC recruitment [178, 341, 412, 281, 219, 400, 411], and inhibition of the 60S subunit joining [63];
- inhibition of elongation or premature termination of translation [373, 275, 340];
- cotranslational protein degradation [321, 313].

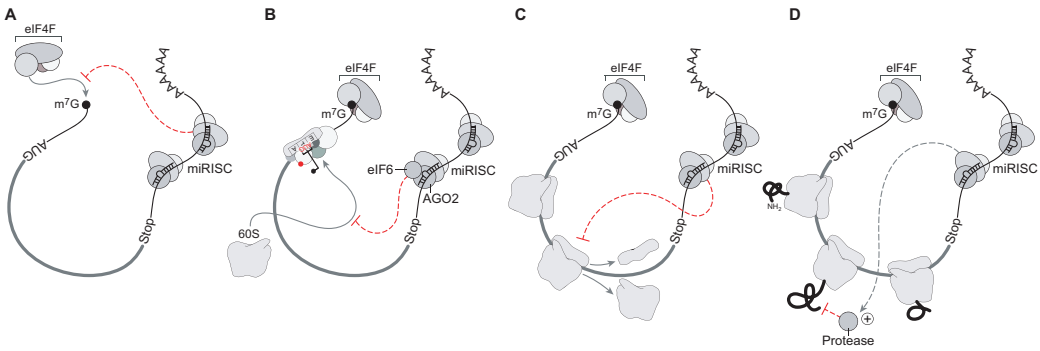

Figure 14. Hypothetical mechanisms of translational repression by miRNAs

(A) Inhibition of translation initiation by blocking cap recognition and subsequent 43S reinitiation complex recruitment. Competition between RISC and eIF4E for cap binding is one possible mechanism. **(B)** Inhibition of translation initiation by impeding the association of the small and large ribosomal subunits. **(C)** Inhibition of translation elongation or premature ribosome termination (drop-off). **(D)** Recruitment of a protease which cause cotranslational degradation of nascent polypeptides. The grey dashed arrow corresponds to an activating signals; red blunted lines correspond to inhibitory signals.

A number of observations suggests that miRNAs inhibit the initiation of translation (Fig. 14A, B). First, it has been shown that miRNAs and their targets are not associated with the polysomal fraction in sucrose gradients but rather with the free mRNP pool in mammalian cells, which is a characteristic sign of impaired initiation [341]. Second, experiments utilizing *in vitro*-transcribed mRNAs transfected into cells, or translated in cell-free systems recapitulating miRNA silencing, have demonstrated that cap-independent IRES-mediated translation initiation may be insensitive to repression by miRNAs, suggesting that miRNAs inhibit translation initiated by a cap-dependent mechanism [178, 341, 281, 400, 411]. Finally, it has been reported that adding purified cap-binding translation initiation complex eIF4F counteracted miRNA-mediated repression [281].

The discovery that the central domain of human AGO2 exhibits sequence similarities to eIF4E and binds to m^7GTP on Sepharose beads has suggested a concrete mechanism by which miRNAs may inhibit translation initiation: competition between the RISC and eIF4E for cap binding [219]. Two conserved phenylalanine residues were identified, which when mutated abolished both the cap binding and the silencing activity of the human protein [219]. However, substitutions of the corresponding phenylalanines in *Drosophila* AGO1 do not affect m^7GTP Sepharose binding but do disrupt interactions with GW182 and miRNAs [112]. These results suggest that the function of the conserved phenylalanines is unrelated to cap binding and underscore the

essential role of GW182 in miRNA-mediated translational repression [112].

An alternative mechanism of miRNA action was recently proposed in [63]. AGO2 has been found in a multiprotein complex containing eIF6 (which binds the 60S subunit to prevent its precocious interaction with the 40S subunit) and the 60S ribosomal proteins. The authors showed that partial depletion of eIF6 in either human cells or *C. elegans* rescues mRNA targets from miRNA inhibition. According to their model, AGO2 recruits eIF6, then the large and small ribosomal subunits might not be able to associate, causing translation to be repressed (Fig. 14B, [63]). This model has been challenged recently by a study that demonstrated that eIF6 is not generally required for silencing in *Drosophila* [112]. In addition, the role of eIF6 in 60S ribosomal subunit biogenesis suggests that the depletion of this protein may have secondary effects.

In contrast to all the above results, which are consistent with inhibition of an initiation step, early investigations into silencing mediated by *C. elegans* lin-4 and let-7 miRNAs and recent studies in mammalian cells have suggested that repression operates at a post-initiation step [321, 373, 275, 313, 340]. Unlike the results that support the initiation block hypothesis, these studies have reported that miRNAs and their targets are associated with polysomes. These polysomes were shown to be actively translating mRNA targets because they were sensitive to a variety of antibiotics that inhibit translation [275, 313, 340]. In addition, despite reports to the contrary, it was observed that reporter target mRNAs driven by the HCV or CrPV IRESs were susceptible to miRNA-mediated silencing. This implies that the repression mechanism operates at some stage after the initiation step [340, 267].

These observations have led to proposals that miRNAs might cause retarded elongation by the translating ribosomes, possibly coupled to premature termination (ribosome drop-off, Fig. 14C, [340]), or induce cotranslational degradation of nascent polypeptides (Fig. 14D, [373, 313]).

Although these conflicting findings are difficult to reconcile, and neither an initiation block mechanism nor a post-initiation block mechanism is easily dismissed, the two modes of regulation are not mutually exclusive, and some experiments designed to detect one may have obscured the other (reviewed in [111, 433, 391, 119]. For example, it is possible that initiation is always inhibited, but when the elongation step is also repressed, ribosomes would queue on the mRNA, thereby masking the effect of an initiation block. It seems reasonable that miRNA-mediated repression is manifested in multiple ways, including one that inhibits the earliest events of cap-dependent initiation and another that affects later, post-initiation steps in translation.

P bodies and stress granules are known to be temporary sites of storage for repressed mRNAs (reviewed in [109, 8]. The detection of AGO proteins,

miRNAs and mRNAs repressed by miRNAs in P bodies and stress granules implicated these cytoplasmic compartments in miRNA repression and in the fate of repressed mRNAs [341, 38, 30, 190, 284, 262, 251]. However, it was demonstrated that the miRNA pathway remains unaffected in cells lacking microscopically visible P bodies [439, 110]. Thus, P bodies are not required for miRNA-mediated repression which is initiated in the soluble cytoplasmic fraction, and that the localization of the silencing machinery in P bodies is a consequence rather than a cause of silencing [439, 110, 178, 341].

It is worth noting that under certain conditions, or in specific cells, miRNA-mediated repression can be effectively reversed or prevented, which makes this regulation much more wide-ranging and dynamic [38, 290, 370, 175]. The context of the 3′ UTR is important since it can contain multiple *cis*-regulatory elements, such as binding sites for RNA-binding proteins which might counteract, modulate, or influence the extent and mode of miRNA regulation in a target-specific manner (reviewed in [252]).

Part II

Results

2 Genome-wide analysis of mRNAs regulated by Drosha and Argonaute proteins in *Drosophila*

RNA silencing pathways are conserved mechanisms that regulate gene expression at both the transcriptional and post-transcriptional levels in a sequence specific manner (reviewed in [50, 150, 285]). These pathways are triggered by the presence of dsRNA of diverse origin, which may originate from viral replication, transcription of endogenous miRNA genes, pseudogenes and repetitive sequence elements or during transposition of mobile genetic elements [50, 150, 285, 319]. dsRNAs can also be introduced into the cell artificially. To enter silencing pathways, dsRNA molecules and pri-miRNAs are first processed by the RNase III-like enzymes Drosha and/or Dicer [50, 150, 285]. In *Drosophila*, Dicer-2 converts long dsRNAs into 21-22-nucleotide siRNAs [250, 50]. Processing of pri-miRNA hairpins encoded in the genome into *ca.* 22-nt-long miRNAs requires the consecutive action of Drosha and Dicer-1 [85, 149, 247, 250].

The siRNAs and miRNAs are incorporated into multimeric RNA-protein complexes referred to as siRNA- or miRNA-induced silencing complexes (siRISCs or miRISCs), which elicit decay or translational repression of complementary mRNA targets [50, 285]. siRNAs are fully complementary to their targets and elicit mRNA degradation via a pathway known as RNA interference. Similarly, plant miRNAs are often fully complementary to their targets and elicit mRNA decay. In contrast, animal miRNAs are only partially complementary to their targets and either elicit mRNA decay or repress translation without affecting transcript levels [50, 111].

Argonaute proteins are essential components of RISC [180]. The *Drosophila* genome encodes five AGO paralogs (AGO1-3, PIWI and Aubergine). This family of highly basic proteins is characterized by a central PAZ domain and a C-terminal PIWI domain [180]. The PAZ domain is involved in the specific recognition of the 2-nt 3' overhangs of siRNAs and miRNAs. The PIWI domain adopts an RNase H-like fold. The PIWI domains of human and *Drosophila* AGO2, and of *Drosophila* AGO1 are catalytically active and can cleave mRNAs fully complementary to siRNAs or miRNAs [180].

Current evidence suggests that despite their similar domain organizations, Argonaute paralogs are not redundant in *Drosophila* [78, 87, 291, 318, 326, 344, 427]. Indeed, *Drosophila* PIWI, and Aubergine have been initially implicated in heterochromatin formation and are required for the establishment and maintenance of the germline [78, 326]. Recent studies have demonstrated that these two Argonaute paralogs together with AGO3 are

the key components of the Piwi-associated RNA (piRNA) pathway (reviewed in [12, 314, 162]). In addition to miRNAs and siRNAs, a third small RNA silencing system has been uncovered that prevents the spreading of mobile genetic elements in the germ line. The nature of the primary piRNA-generating transcript is still not clear, but RNAi-like cleavage events are likely to define the 5′ ends of mature piRNAs [12, 314, 162].

Drosophila AGO2 mediates siRNA-guided endonucleolytic cleavage of mRNAs, whereas *Drosophila* AGO1 plays a role in translational repression or mRNA decay triggered by miRNAs. This lack of redundancy is further supported by the observation that mutations or knockouts of Argonaute paralogs in *Drosophila* have different phenotypes [87, 318, 427].

The results presented in this section have been published [348].

2.1 Identification of transcripts regulated by RNA silencing pathways

To identify transcripts regulated by the Argonaute proteins, expression profiles of *Drosophila* Schneider cells (S2 cells) individually depleted of AGO1, AGO2, PIWI or AUB were analyzed using whole genome oligonucleotide microarrays. To distinguish clearly transcripts whose levels are regulated by the miRNA pathway, RNA expression levels in cells depleted of Drosha were also profiled. The efficacy of the depletions were assessed by Western blot analysis. Four days after addition of dsRNA, the steady-state expression levels of Drosha, AGO1, AGO2 and AUB had declined to about 10% of the levels detected in untreated cells (Fig. 15A, lane 4 versus lane 1).

On day 9, the residual levels of the proteins were less than 10% of those observed in control cells (Fig. 15A, lanes 5). Depletion of Drosha, AGO1 or AGO2 also inhibited cell proliferation, confirming the effectiveness of the dsRNAs (Fig. 15C). In the absence of specific antibodies against PIWI, I determined the extent of its depletion by RT-PCR (Fig. 15B). Importantly, depletion of AGO1 did not affect the expression of AGO2 or Drosha. Conversely, AGO2-depletion had no effect on AGO1 or Drosha expression levels (data not shown).

The following section of work was done in conjunction with Jan Rehwinkel. For each depleted protein, we obtained two (Drosha, AUB and PIWI), three (AGO2) or six (AGO1) independent expression profiles from RNA samples isolated on day 9 (see Materials and Methods for a description of the RNA samples). For AGO1, whose depletion leads to more widespread changes in RNA levels, a time course was also performed and expression profiles from RNA samples collected on days 3, 5 and 9 of the same knock-

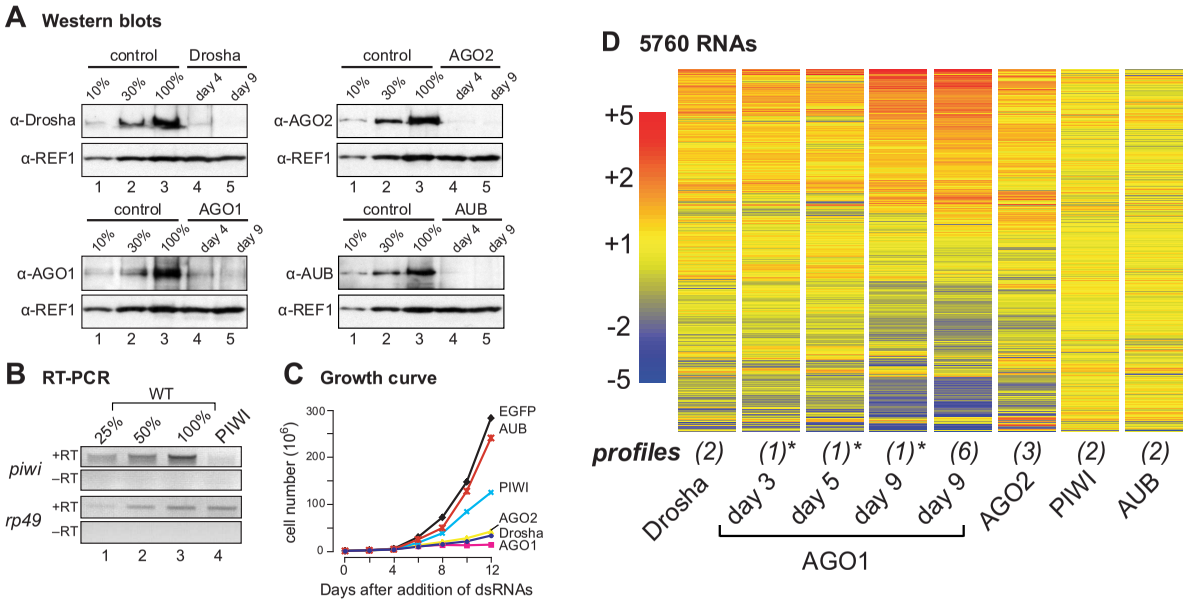

Figure 15. Expression profiles of *Drosophila* S2 cells depleted of Drosha or Argonaute proteins.

(A) S2 cells were treated with the dsRNAs indicated above the lanes. The effectiveness of the depletions was analyzed by Western blotting with the antibodies indicated on the left. In lanes 1-3, dilutions of the sample isolated on day 0 were loaded to assess the efficacy of the depletion. Antibodies against the nuclear antigen REF1 were used as a loading control. **(B)** The effectiveness of PIWI depletion was analyzed by RT-PCR. The positive or negative signs on the left of the panels indicate that the reverse transcriptase was included (+RT) or omitted (-RT). The rp49 mRNA served as an internal control. **(C)** Inhibition of cell proliferation in Drosophila cells depleted of Drosha, AGO1, AGO2, PIWI or AUB. S2 cells growing in suspension were treated with dsRNAs specific for Drosha, AGO1, AGO2, PIWI, AUB, or GFP. Cell numbers were determined every two days up to 12 days after addition of dsRNAs. On day 4, cells were re-treated with the corresponding dsRNAs. **(D)** Comparison of the average expression levels of detectable transcripts (5760 RNAs) in all profiles. The number of independent expression profiles obtained per protein is indicated between brackets in italics. Asterisks indicate profiles derived from a single knockdown.

down were analyzed (Fig. 15D, asterisks). Total RNA was isolated from mock-treated cells as a reference (control) sample. To identify mRNAs regulated non-specifically in response to the dsRNA treatment, mRNA profiles in cells treated with enhanced green fluorescent protein (EGFP) dsRNA were examined (data not shown).

Detectable transcripts were assigned to three classes according to their relative expression levels. These were: (1) transcripts at least 1.5-fold under-represented compared to the reference sample (blue); (2) not significantly changed (less than 1.5-fold different from the reference, yellow); and (3) at least 1.5-fold over-represented (red). A transcript was considered only if its class assignment was the same for all the independent day 9 profiles (or the same in 5 of 6 profiles for AGO1). I validated changes in RNA levels for selected mRNAs by Northern blot (see below and data not shown).

Fewer than 2% of transcripts showed altered expression in cells depleted of PIWI or AUB (Fig. 15D and Supplementary Table I in [348]). Most of these transcripts have low levels of expression in wild type cells and we did not investigate them further. In cells depleted of Drosha, AGO1 or AGO2, between 6% and 18% of transcripts were differentially expressed (Fig. 15D).

The expression profiles in cells depleted of Drosha or AGO1 (day 9) were significantly correlated (rank correlation $r = 0.7$; Fig. 15 D), indicating that depletion of these proteins affects the expression of a common set of RNAs. Some of the RNAs in this set changed levels concordantly in AGO2 depleted cells (Fig. 15 D). In agreement with this, the rank correlation coefficient between AGO2 and AGO1 (day 9) profiles was $r = 0.7$ and between Drosha and AGO2 profiles $r = 0.4$, indicating that Drosha, AGO1 and AGO2 regulate the expression levels of common targets.

2.2 Depletion of Drosha and AGO1 leads to similar expression profiles

To investigate further the similarity of the cellular response to the depletion of Drosha, AGO1 or AGO2, mRNAs belonging to specific classes in the Drosha knockdown (at least 1.5-fold over- or under-represented, respectively) were selected and their levels analyzed in the AGO1 or AGO2 knockdowns. It was observed that of the 233 transcripts at least 1.5-fold over-represented in Drosha-depleted cells, 58% and 16% were at least 1.5-fold up-regulated in the AGO1 (day 9) and AGO2 knockdowns, respectively (Fig. 16A and Supplementary Table II in [348]). Similarly, of the 233 down-regulated RNAs in Drosha-depleted cells, 61% and 16% exhibited the same effect on regulation in AGO1 (day 9) and AGO2 depleted cells, respectively (Fig. 16 A and

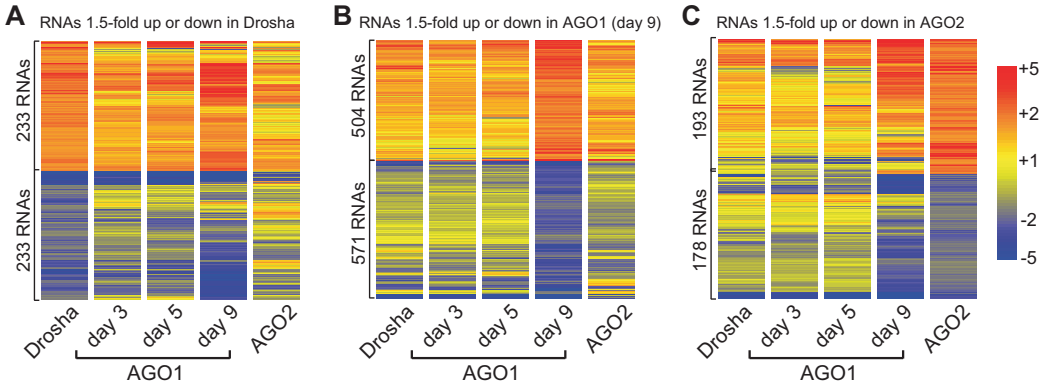

Figure 16. RNAs regulated by Drosha, AGO1 or AGO2.

(A) Expression profiles of RNAs at least 1.5-fold over- or under-represented in the two independent profiles obtained for Drosha ([348], Supplementary Table II). **(B)** Expression profiles of RNAs at least 1.5-fold over- or under-represented in at least five of six profiles obtained for AGO1 on day 9 ([348], Supplementary Table III). **(C)** Expression profiles of RNAs at least 1.5-fold over- or under-represented in the three independent profiles obtained for AGO2 ([348], Supplementary Table IV). In all panels, transcripts detectable in Drosha, AGO1 and AGO2 depleted cells (5868 RNAs) are considered.

Supplementary Table II in [348]).

Likewise, RNAs showing differential expression in AGO1-depleted cells (days 3, 5 and 9) had expression profiles similar to those in the Drosha knockdown, although the relative changes in expression levels were more pronounced in AGO1-depleted cells on day 9 (Fig. 16 B and Supplementary Table III in [348]). These results indicate that Drosha and AGO1 regulate common targets, in agreement with the role of these proteins in the miRNA pathway [85, 149, 247, 318]. As mentioned above, a subset of transcripts regulated by AGO2 showed similar expression levels in cells depleted of Drosha or AGO1 (Fig. 16 C and Supplementary Table IV in [348]), suggesting functional overlap between the three proteins.

2.3 Predicted miRNA targets are significantly enriched among up-regulated transcripts

Given the role of Drosha and AGO1 in the miRNA pathway [85, 149, 247, 318], changes in mRNA levels observed after their depletion are most likely to be caused by the inactivation of this pathway. We therefore decided to investigate whether the transcripts up-regulated in Drosha- or AGO1-depleted cells were among predicted miRNA targets. The overlap between both sets can be used to distinguish between transcripts whose levels are

directly or indirectly affected by miRNAs. The *Drosophila* genome encodes 152 miRNAs [152]. At the time of this analysis *ca.* 100 miRNAs were known [14, 151, 238, 239] of which 53 had been cloned [14, 238, 239], and 39 had unique (non-redundant) seed sequences (i.e. eight most 5′ nucleotides). We tested the enrichment for targets of non-redundant cloned miRNAs predicted in [394] using an algorithm based on experimentally derived rules for miRNA-target recognition [47], and found a significant enrichment for predicted miRNA targets among transcripts up-regulated in the Drosha knockdown ($p = 5.8 \cdot 10^{-24}$) and AGO1 knockdown ($p = 3.0 \cdot 10^{-34}$). Interestingly, transcripts up-regulated in the AGO2 knockdown were also significantly enriched in miRNA predicted targets ($p = 1.8 \cdot 10^{-9}$), suggesting that some miRNAs may not discriminate between AGO1- or AGO2-containing RISCs (Supplementary Table V in [348]). Targets predicted in other studies were also represented in the list of up-regulated genes [106, 356, 395]. No significant enrichment for predicted targets was found amongst down-regulated transcripts (p-values of order unity), suggesting that these transcripts represent secondary targets of the miRNA pathway.

2.4 Identification of a core set of transcripts regulated by the miRNA pathway

To identify potential miRNA targets, we generated a list of transcripts up-regulated at least 1.5-fold in the two profiles obtained for Drosha and in at least 5 of 6 profiles obtained for AGO1 (day 9). 136 mRNAs fell into this class, representing 2.3% of detectable RNAs (Fig. 17A and Supplementary Table VI in [348]). Although the cut-off ratio of 1.5 is low relative to the standard deviation of all detectable spots in the array[2], the stringent filtering criterion (i.e. regulation in at least 7 of 8 independent profiles) reduces the likelihood of selecting false positives. Consistent with this, only 4 of these transcripts changed levels more than 1.5-fold in cells treated with AUB, PIWI or GFP dsRNA ([348], Supplementary Table VI). These RNAs were defined as core transcripts, whose levels are regulated by the miRNA pathway.

The list of core transcripts includes *hid* and *reaper* mRNAs, which are validated miRNA targets [47, 395]. Indeed, it was found that both *hid* and *reaper* mRNAs were at least 2-fold up-regulated in cells depleted of Drosha or AGO1 (day 9; Supplementary Table VI in [348]). Unexpectedly, both *hid* and *reaper* were at least 1.7-fold up-regulated in AGO2-depleted cells ([348], Supplementary Table VI). Furthermore, among the 136 core transcripts, 31

[2]When two independent total RNA samples were compared all spots had an average ratio of 1.07 ± 0.50 after intensity-dependent normalization.

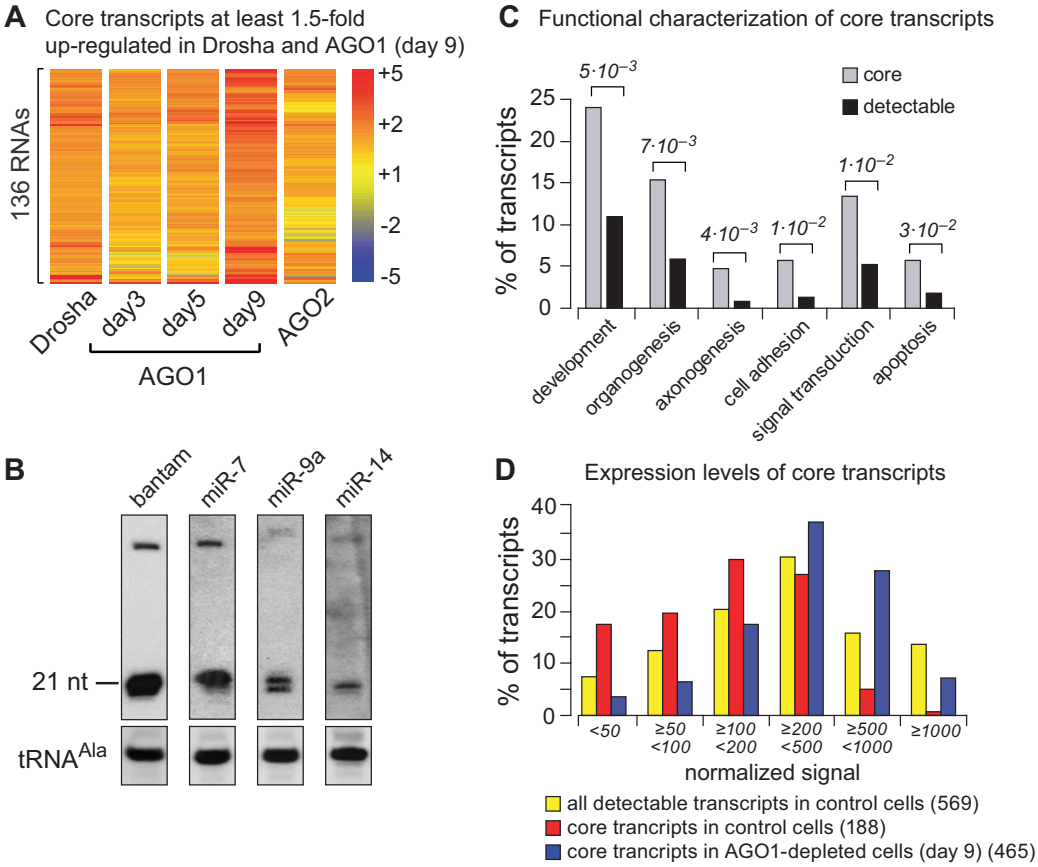

Figure 17. Core transcripts regulated by the miRNA-pathway.

(A) Expression profiles of RNAs at least 1.5-fold over-represented in Drosha and AGO1 (day 9) depleted cells (core transcripts; Supplementary Table VI in [348]). **(B)** Northern blot analysis of total RNA samples isolated from S2 cells. Probes specific to the miRNAs indicated above the lanes were used. tRNAAla served as a loading control. **(C)** Gene ontology (GO) terms significantly enriched within the lists of core transcripts (grey bars). Black bars indicate the percentage of detectable transcripts associated with a specific GO term. Numbers in *italics* indicate p-values. **(D)** The histogram shows the distribution of signal intensities for all transcripts detected in samples isolated from control cells (yellow bars), and for the list of core transcripts in control cells (red bars) or in AGO1-depleted cells (day 9; blue bars). The vertical and horizontal axes represent the fraction of probe sets and the normalized signal intensities, respectively. Numbers in *italics* indicate average signal intensities.

were at least 1.5-fold up-regulated in the three independent profiles obtained for AGO2 (Fig. 17A and [348], Supplementary Table VI). This lends additional support to the hypothesis that some miRNAs may not discriminate between AGO1- or AGO2-containing RISCs.

The miRNAs with the most significant target gene enrichment among the core transcripts were the K-Box miRNAs (i.e. miRs-2/13, miR-6 and miR-11, $p \sim 10^{-12}$–10^{-6}, Table 1). Targets of miR-308, miR-8 and miR-314 were also significantly enriched ($p \sim 10^{-9}$–10^{-6}). The enrichment for miR-14 targets ($p = 6 \cdot 10^{-4}$) and miR-9a/b ($p = 1 \cdot 10^{-2}$, Table 1) was also significant, although these miRNAs have not been shown to be expressed in S2 cells. These results suggest that miR-9 and miR-14 might be expressed in S2 cells under these experimental conditions. Indeed, these miRNAs are detectable in S2 cells (Fig. 17B).

Table 1. Enrichment of predicted miRNA targets amongst core transcripts.

p-value	miRNA	No. of targets (core/detectable)
$1.2 \cdot 10^{-22}$	Cloned miRNAs redundant	90/1674
$2.6 \cdot 10^{-22}$	Cloned miRNAs non-redundant	89/1645
$1.8 \cdot 10^{-12}$	miR-6	23/148
$8.2 \cdot 10^{-12}$	miR-13b	22/144
$8.2 \cdot 10^{-12}$	miR-2a	22/144
$8.2 \cdot 10^{-12}$	miR-2b	22/144
$1.1 \cdot 10^{-11}$	miR-13a	22/146
$2.3 \cdot 10^{-9}$	miR-314	15/82
$1.5 \cdot 10^{-8}$	miR-308	18/142
$2.7 \cdot 10^{-6}$	miR-8	16/162
$4.3 \cdot 10^{-6}$	miR-11	11/78
$2.4 \cdot 10^{-4}$	miR-184	5/22
$4.9 \cdot 10^{-4}$	miR-92b	12/155
$6.0 \cdot 10^{-4}$	miR-14	8/75
$6.5 \cdot 10^{-4}$	miR-317	7/58
$3.3 \cdot 10^{-3}$	miR-92a	9/121
$3.7 \cdot 10^{-3}$	miR-34	6/59
$4.0 \cdot 10^{-3}$	miR-279	6/60
$4.0 \cdot 10^{-3}$	miR-286	6/60
$7.3 \cdot 10^{-3}$	miR-263b	6/68
$8.6 \cdot 10^{-3}$	miR-9b	8/116

Analysis of the biological function of the proteins encoded by core transcripts using gene ontology terms [17] reveals that some functional groups are over-represented in the list of core transcripts in comparison to the detectable transcripts (Fig. 17C and [348], Supplementary Table VI). In particular, a significant enrichment was observed of genes involved in developmental processes ($p = 5 \cdot 10^{-3}$), axonogenesis ($p = 4 \cdot 10^{-3}$), organogenesis ($p = 7 \cdot 10^{-3}$), cell adhesion ($p = 1 \cdot 10^{-2}$), and signal transduction ($p = 1 \cdot 10^{-2}$).

Compared to the distribution of abundance of detectable transcripts (Fig. 17D, yellow bars), core transcripts show a bias towards low abundance in wild

type cells (Fig. 17D, red bars), but an almost normal distribution in AGO1-depleted cells (blue bars). This suggests that the low abundance of these transcripts seen in wild type cells is due to down-regulation by the miRNA pathway.

2.5 Core transcripts represent authentic miRNA targets

To investigate whether predicted miRNA targets in the list of core transcripts represent authentic targets, 3′ UTRs derived from eight core transcripts were cloned into a firefly luciferase sensor reporter [347]. Transcripts were selected that were also regulated by AGO2. Four of them were predicted miR-9a/b targets. A previously validated miR-9b target, Nerfin [394], served as a positive control. When co-transfected with at least one of the predicted cognate miRNAs, six out of eight of the 3′ UTRs led to a reduction of luciferase activity (relative to the activity observed in the absence of the miRNA; Fig. 18 A, asterisks).

It was found that predicted miR-9 targets were often regulated exclusively by either miR-9a or miR-9b (Fig. 18 A; *e.g.* CG10011 and Nerfin), indicating that these miRNAs are not redundant, despite their sequence similarity. Also, for some reporters (*e.g.* CG4851, Sema-1b, and CG12505), co-expression of an miRNA led to an increase in luciferase protein expression (Fig. 18 A). One possible explanation for these results is that these miRNAs silence the expression of a negative regulator.

The results described above raised the question of whether predicted miRNA targets not included in the list of core transcripts also represent authentic targets. We therefore tested two 3′ UTRs derived from transcripts (CG30337 and CG33087) that were regulated in Drosha and AGO1 depleted cells, but were not in the list of core transcripts because they were not detectable in two experiments. These reporters were also down-regulated by at least one of the miRNAs predicted to recognize these 3′ UTRs (Fig. 18 A). This observation confirms the assumption that the filtering criterion to select core transcripts (regulation in 7 of 8 independent profiles, and detectable in all profiles) is stringent and some genuine targets are excluded.

In addition, nine 3′ UTRs were selected from predicted targets of miR-9a/b, miR-13a/b and miR-14, whose expression levels remained unchanged in depleted cells and were comparable to those of the core transcripts in wild-type cells. Four out of nine 3′ UTRs tested repressed luciferase expression in the presence of the cognate miRNA (Fig. 18 B, asterisks). Note that for these 3′ UTRs, not all miRNAs predicted to have binding sites have been tested,

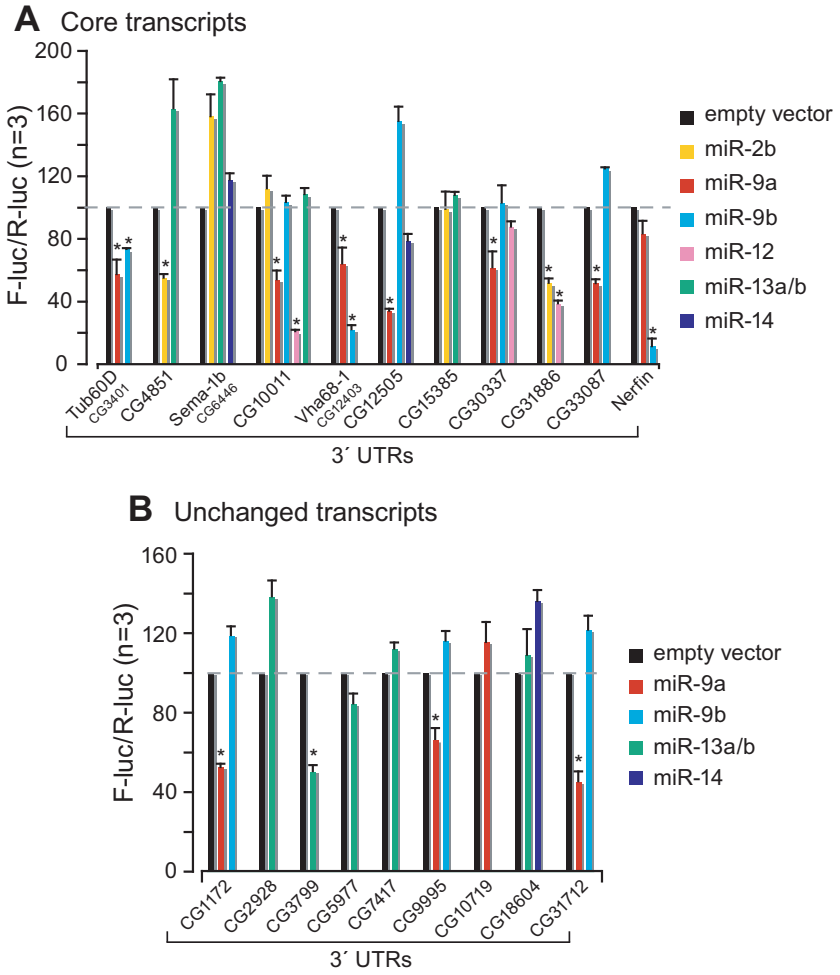

Figure 18. Core transcripts represent authentic miRNA targets.

(A, B) Reporter plasmids constitutively expressing firefly luciferase flanked by the 3′ UTRs of predicted miRNA targets and plasmids expressing miRNA primary transcripts were co-transfected in S2 cells as indicated. *Renilla* luciferase was included as a transfection control. Firefly luciferase activity was normalized to that of the *Renilla* luciferase activity in 3 independent experiments ($n = 3$). Normalized firefly luciferase activities in the absence of miRNAs were set to 100%. Mean values are shown. Error bars represent standard deviations. Asterisks indicate a significant reduction of firefly luciferase activity. In panel **(A)** all miRNAs predicted to have binding sites in a given 3′ UTR are tested, while in panel **(B)** only a subset of miRNAs having potential binding sites are tested per reporter.

so the fraction of these transcripts representing authentic miRNA targets is likely to have been underestimated.

Taken together, this shows that although the majority of predicted miRNA targets in the list of core transcripts are genuine targets of the miRNA pathway, this list is not comprehensive and additional targets may be identified when less stringent criteria are applied. Furthermore, not all miRNA targets are subject to down-regulation of mRNA levels, or might not be regulated at all in S2 cells.

2.6 AGO2 associates with miRNAs

Previous studies from our laboratory have showed that expression of firefly luciferase from the reporters harboring Vha68-1 or CG10011 3′ UTRs in the presence of miR-9b or miR-12 could be restored in cells depleted of AGO1, but not of AGO2 [347], despite Vha68-1 and CG10011 mRNA levels being changed in AGO2-depleted cells. Similar results were obtained for the reporter containing the Nerfin 3′ UTR (Fig. 19A). Depletion of Drosha also led to a partial restoration of firefly luciferase expression from these reporters, providing further evidence for a regulation of these reporters via the miRNA pathway (Fig. 19A). The lack of restoration in AGO2-depleted cells is not caused by an inefficient depletion, because silencing of firefly luciferase expression by co-transfecting a fully complementary siRNA (Luc-siRNA) is impaired in these cells ([348], Supplementary Fig. 1B and [347]). Thus, depletion of AGO2 inhibits siRNA-guided, but not miRNA-guided gene silencing as reported in [318].

These results contrast with the observation that AGO1 and AGO2 regulate the expression levels of a common set of miRNA targets. We therefore reasoned that regulation by AGO2 may not be observed with the reporter assays described above as in this case both the reporter and the miRNAs are over-expressed. To investigate whether AGO2 associates with endogenous miRNAs, Jan Rehwinkel performed immunoprecipitations from total lysates of S2 cells expressing an HA-tagged version of AGO1, AGO2 or, as a control, maltose binding protein (MBP). The presence of miRNAs associated with the precipitated proteins was analyzed by Northern blot. Although the expression levels of these proteins was comparable, HA-AGO1 immunoprecipitated very inefficiently (Fig. 20A). Nonetheless, miR-13b and bantam coimmunoprecipitated with HA-AGO1 (Fig. 20B). HA-AGO2 also immunoprecipitated these miRNAs above background levels, indicating that a small fraction of endogenous miRNAs can be found in association with AGO2 (Fig. 20B). These results provide an explanation for the observation that a subset of miRNA targets is regulated by AGO2.

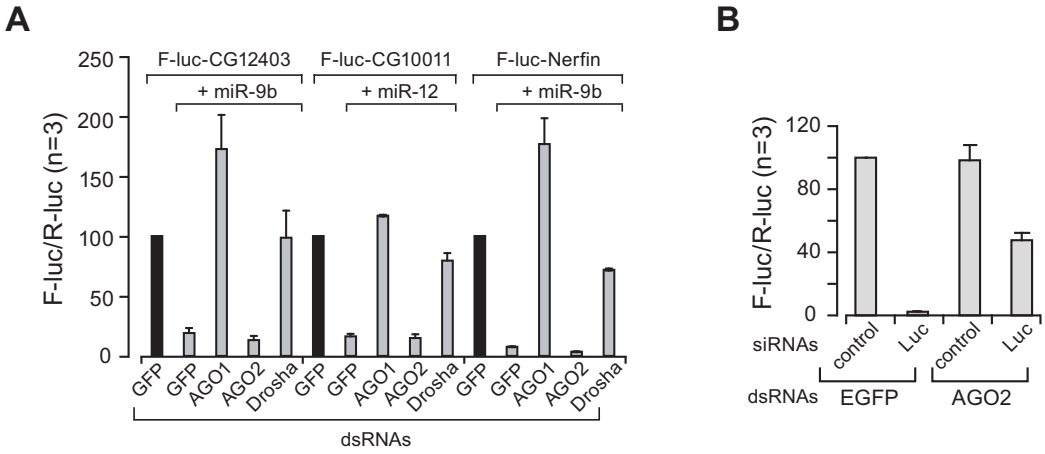

Figure 19. Depletion of AGO2 inhibits siRNA-guided, but not miRNA-guided gene silencing.

(A) S2 cells were treated with the indicated dsRNAs on days 0 and 4. On day 6, cells were transfected with a mixture of plasmids comprising: plasmids expressing firefly luciferase (F-luc) flanked by the indicated 3′ UTRs, plasmids expressing miRNA primary transcripts (grey bars) or the corresponding empty vector (black bars) and a plasmid expressing *Renilla* luciferase (R-luc). F-luc and R-luc activity were measured four days after transfection. F-luc activity was normalized to that of the R-luc and set to 100 in cells transfected with the empty vector and treated with EGFP dsRNA (black bars). Mean values are shown. Error bars represent standard deviations from 3 independent experiments. **(B)** S2 cells were treated with the indicated dsRNAs (on day 0 and day 4). On day six, cells were transfected with plasmids expressing firefly and *Renilla* luciferase. siRNAs targeting F-luc (Luc) or a control siRNA (control) were co-transfected as indicated. F-luc and R-luc activity were measured four days after transfection. F-luc activity was normalized to that of the R-luc and set to 100 in cells treated with the control siRNA and EGFP dsRNA. The following siRNA sequences were used: luciferase siRNA (5′-`CGUACGCGGAAUACUUCGAdTdT`), control siRNA (5′-`GGACAGAUUCAAAUAACAAdTdT`). The siRNAs were transfected at a final concentration of 26 nM.

2.7 A few transcripts are regulated exclusively in the individual knockdowns

To determine whether Drosha, AGO1 and AGO2 have evolved specialized functions, we searched for transcripts exclusively regulated in one of the knockdowns but clearly unaffected (less than 1.3-fold) or showing inverse correlation in the other knockdowns. Only four transcripts were found to be exclusively regulated in Drosha-depleted cells (Fig. 21 A, E).

Initial cleavage of pri-miRNAs is catalyzed by Drosha, which exists in a multiprotein complex. Along with Drosha the complex also contains Pasha (partner of Drosha), a double-stranded RNA binding protein [85]. I tested

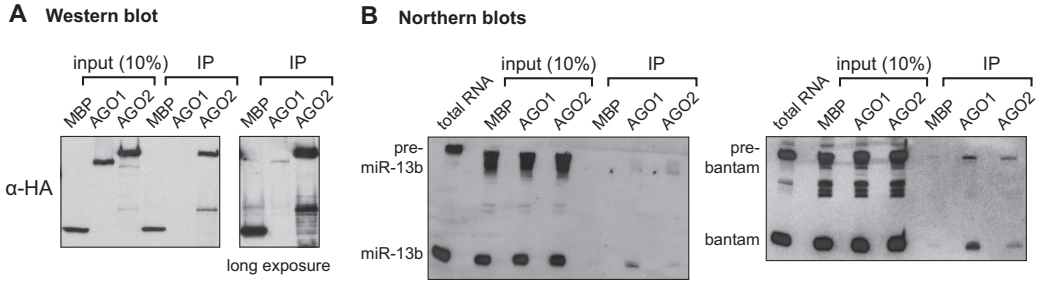

Figure 20. AGO2 associates with miRNAs.

(A) Immunoprecipitation of HA-tagged AGO1, AGO2 or MBP from total cell lysates. The right panel shows a longer exposure of the immunoprecipitated samples to visualize the presence of AGO1. **(B)** The presence of miR-13b or bantam in the immunoprecipitates shown in **(A)** was analyzed by Northern blot.

the expression levels of the two up-regulated genes (CG15861 and CG31642) in the Pasha knockdown (Fig. 22A). I found that the genes were also up-regulated in the cells depleted of Pasha.

In baker's yeast, dsRNA stem-loop structures found in intronic regions of some transcripts trigger degradation of unspliced pre-mRNAs and lariat introns. The dsRNA regions are cleaved by Rnt1p, the yeast ortholog of RNase III, which creates an entry site for complete degradation by the Xrn1p and Rat1p exonucleases and by the nuclear exosome [83]. Rnt1p also selectively inhibits Mig2 gene expression by directly cleaving a stem-loop structure within the mRNA coding sequence [131].

A similar mechanism might be involved in the regulation of CG15861 and CG31642 by Drosha and Pasha. Interestingly, CG31642 resides in the intron 4 of the gene Stathmin-14 (CG31641), see Fig. 22C. If this hypothesis is true and the mechanism of regulation does not rely on miRNAs, then unspliced pre-mRNA levels of these genes would be increased in cells depleted of Drosha and Pasha. To test this I performed RT-PCR using primers specifically detecting unspliced pre-mRNAs.

I found that the pre-mRNA levels of the genes regulated by Drosha were increased in Drosha- and Pasha-depleted cells (Fig. 22B, C). The levels of Stathmin-14 (CG31641) pre-mRNA containing intron which flanks the sequence of CG31642, were also elevated in cells depleted of Drosha and Pasha (Fig. 22B, C, primers E and F).

Transcripts were also identified which are exclusively regulated by AGO1, but not by Drosha or AGO2, and transcripts regulated by AGO2, but not by Drosha or AGO1 (Fig. 21B, C, F). The latter would be explicable if AGO2 regulates the expression of these transcripts by a mechanism involving, for

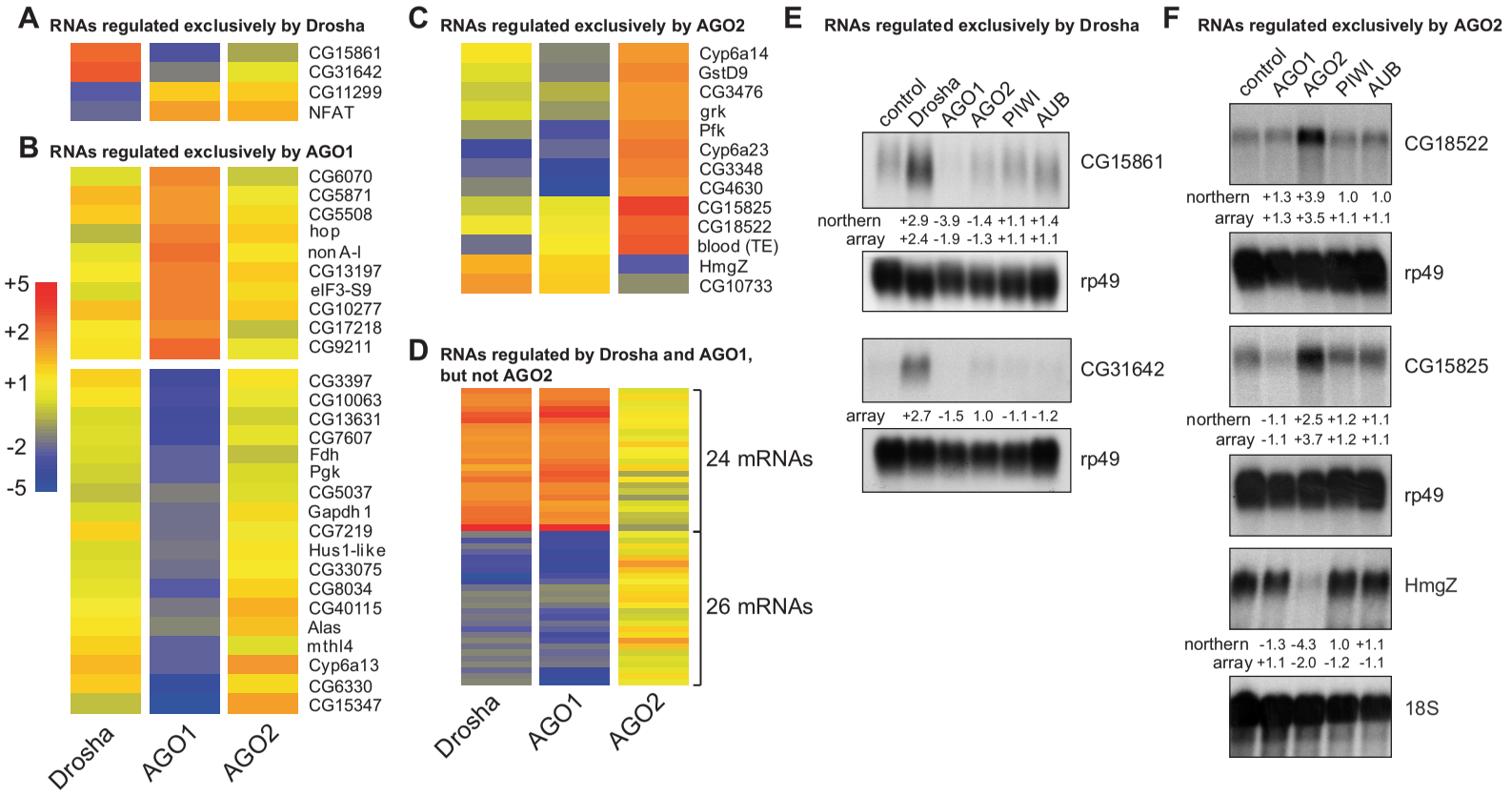

Figure 21. RNAs exclusively regulated in the individual knockdowns.

RNAs exclusively regulated by Drosha **(A, E)**, AGO1 **(B)** or AGO2 **(C, F)** showing non-correlated expression in the other knockdowns. **(D)** RNAs exclusively regulated in the four profiles obtained for Drosha and AGO1 (day 9). In panels **(E, F)** the signals from the Northern blot were normalized to rp49 mRNA or 18S rRNA. These values were compared with the values measured by microarray (average of three or six independent profiles). Values are given relative to the values obtained in mock treated (control) cells (positive values, over-represented; negative values, under-represented).

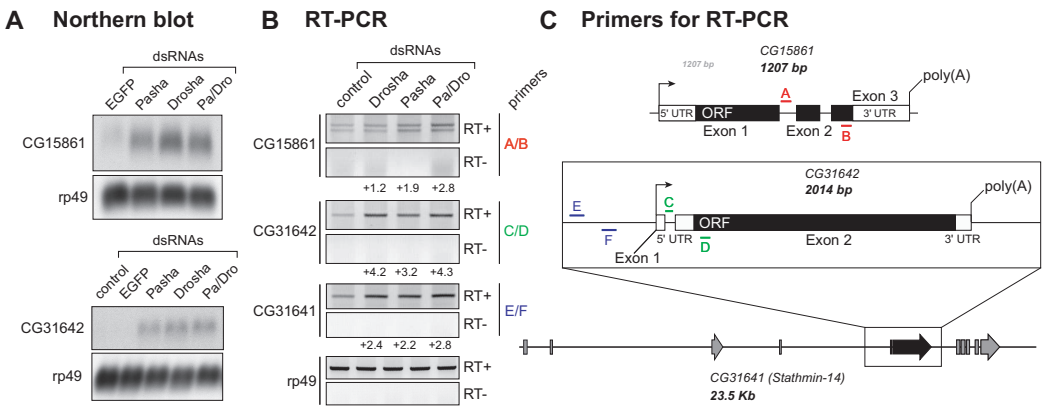

Figure 22. RNAs exclusively regulated in the Drosha knockdown.

(A) The levels of the RNAs exclusively up-regulated by Drosha were analysed by Northern blot in cells depleted of Drosha, Pasha, and both Drosha and Pasha. **(B)** RT-PCR was used to specifically detect unspliced pre-mRNA. Primer pairs for each pre-mRNA amplicon are indicated on the right. The positive or negative signs on the right of the panels indicate that the reverse transcriptase was included (RT+) or omitted (RT-). The rp49 mRNA served as an internal control. Numbers below the panels show the quantification with the control signal set to 1. **(C)** Schematic representation of the gene structures. Binding sites of the primers used for RT-PCR are shown as coloured bars.

example, siRNAs that are not processed by Drosha.

Furthermore, transcripts were identified which were regulated exclusively by Drosha and AGO1 but unaffected in AGO2-depleted cells (Fig. 21D), or transcripts regulated by AGO1 (showing correlated expression in AGO2-depleted cells) but unaffected by Drosha-depletion (not shown). Finally, it was observed that Dicer-1 and Dicer-2 mRNAs were at least 1.5-fold up-regulated in AGO1-depleted cells (in four of six profiles). Drosophila Dicer-1 mRNA has one target site for miR-314 and Dicer-2 mRNA has sites for miR-280 and miR-315 (note that these sites are not conserved in *D. pseudoobscura*). This suggests that a feedback mechanism regulates the expression of genes involved in RNA silencing. This feedback mechanism appears to be conserved, as expression of Dicer-like 1 (DCL1) is regulated by miR-162 in *Arabidopsis thaliana* [435], and the expression of AGO1 is regulated by miR-168 [410].

Among the transcripts exclusively regulated by AGO2-depletion, I found the transposable element (TE) blood (Fig. 21C). This prompted an investigation into whether additional transposon-derived transcripts are regulated in depleted cells. There are 96 families of transposable element in Drosophila, which represent 22% of the genome [205, 207]. TEs are represented by 85 probe sets on the microarray, most of which correspond to LTR (long ter-

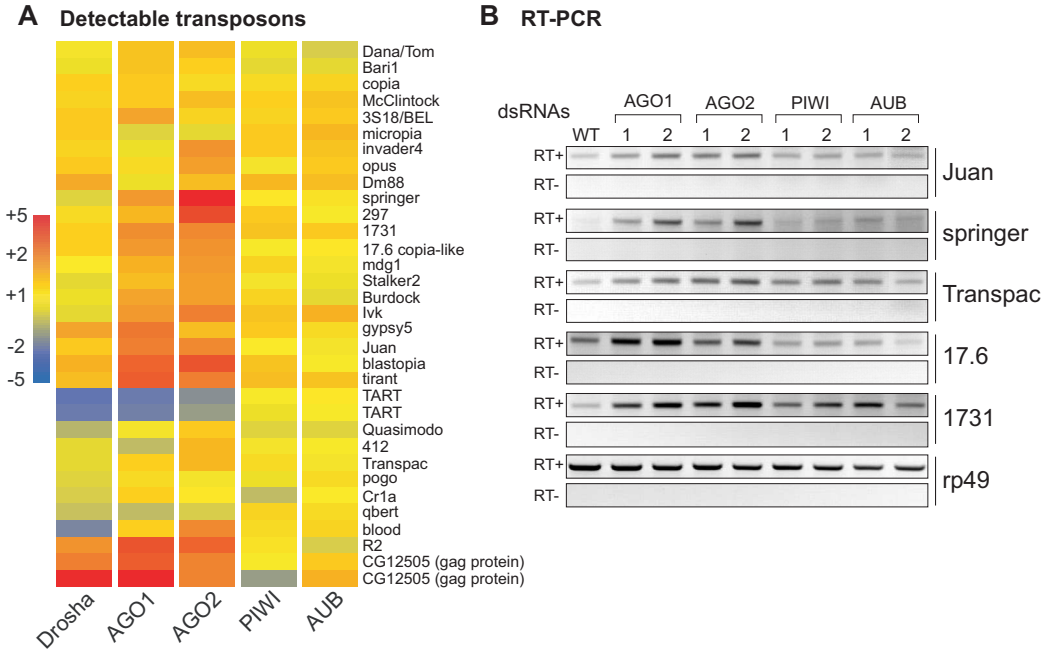

Figure 23. Argonaute proteins regulate expression of transposons in S2 cells.

(A) Expression profiles of detectable transposons. **(D)** The expression levels of selected transposons were analyzed by RT-PCR. The numbers 1 and 2 above the lanes indicate that RNA samples were isolated from cells treated with two non-overlapping dsRNAs (1 and 2) for each protein. The positive or negative signs on the left of the panels indicate that the reverse transcriptase was included (RT+) or omitted (RT-). The rp49 mRNA served as an internal control.

minal repeat) and non-LTR retrotransposon families. I found that 21% and 41% of detectable TEs were at least 1.5-fold up-regulated in cells depleted of AGO1 or AGO2, respectively (Fig. 23A, B and [348], Supplementary Tables III and IV). With two exceptions, transposons up-regulated in cells depleted of AGO1 were also up-regulated in the AGO2 knockdown, providing further evidence for functional crosstalk between these proteins.

3 A role for *Drosophila* RNA-helicase Belle in translational control

3.1 Belle is a cytoplasmic protein that does not localize to P bodies

To study the subcellular localization of Belle protein, *Drosophila* S2 cells were transfected with a plasmid encoding HA-tagged Belle. In immunofluorescence experiments using primary anti-HA antibody and secondary TRITC-coupled antibody, I observed that HA-tagged Belle localizes to the cytoplasm (Fig. 24A). The localization of the protein was heterogenous, suggesting that Belle might partially localize to some RNA granules. To determine whether Belle localizes to P bodies, co-localization experiments were performed using S2 cells co-transfected with HA-Belle and EGFP-tagged Me31B, which is a known component of P bodies in *Drosophila*. The two proteins showed no co-localization in the foci (Fig. 24B). In addition to this, I observed that the foci formed by EGFP-DCP1, another known P body component, did not contain HA-Belle (Fig. 24C).

I obtained similar results with an EGFP-fusion of Belle co-transfected with HA-Ge-1, which is yet another P body component in *Drosophila* S2 cells. Subcellular localization of EGFP-tagged Belle was different from the HA-tagged protein. EGFP-Belle formed discrete cytoplasmic foci of varying number and size, and showed considerably less diffused cytoplasmic staining. Consistent with the result obtained with HA-Belle, these foci showed no co-localization with Ge-1 (Fig. 24D).

3.2 Belle is required for cell viability

To understand the functions of Belle in *Drosophila*, I performed an RNAi-mediated knock-down experiment in S2 cells using dsRNA spanning *ca.* 700 nt of Belle mRNA. To ensure the maximum reduction of the endogenous protein level, dsRNA treatment of S2 cells was done twice (on day 0 and later on day 4 of the experiment). I confirmed the efficiency of the depletion by Western blot analysis using rabbit polyclonal anti-Belle antibody produced in our laboratory (Fig. 25B).

S2 cells depleted of the essential translation initiation factors eIF4E and the DEAD-box RNA helicase eIF4A, which are required for efficient cell proliferation, served as a positive control. Me31B, another DEAD-box helicase, decapping co-activator and translation regulator was also depleted from S2 cells.

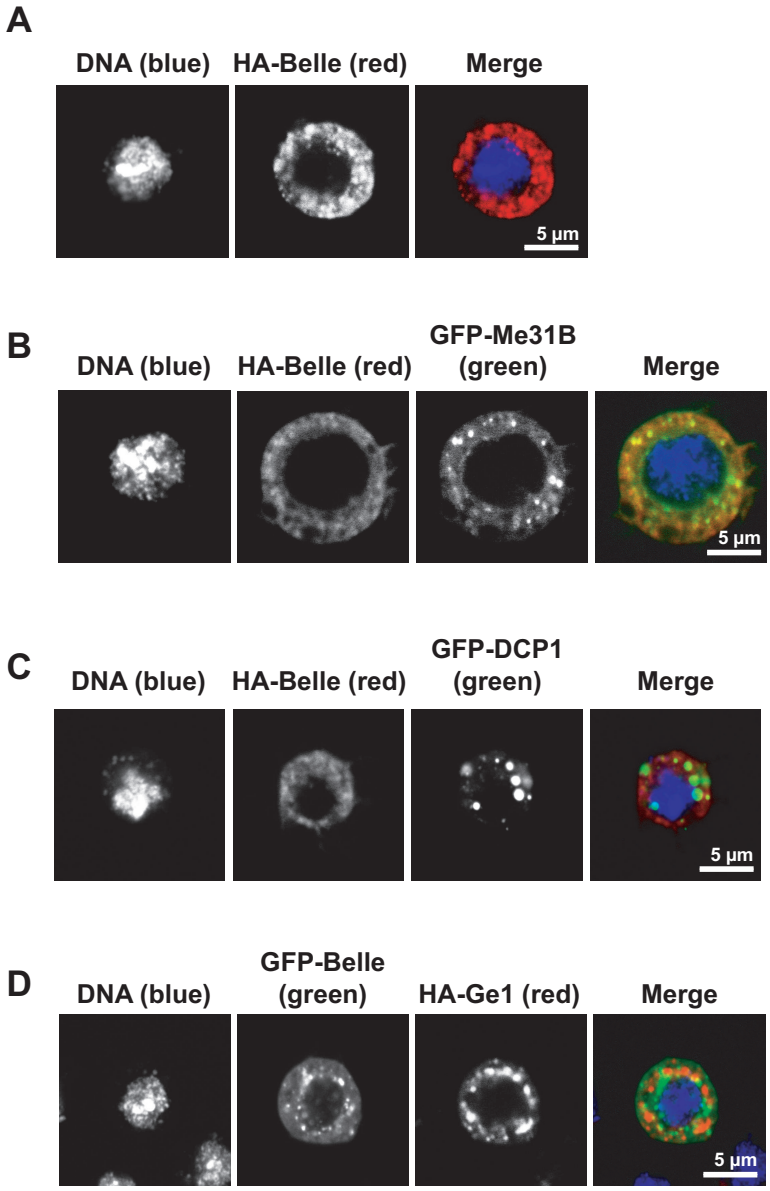

Figure 24. Subcellular localization of Belle in S2 cells.

(A) Confocal fluorescent microphotograph of S2 cell expressing HA-tagged Belle. Cells were fixed and stained with anti-HA primary antibody and then with TRITC-coupled secondary antibody (red signal). DNA was stained with Hoechst 33342 (blue). **(B)** Confocal image of fixed S2 cell co-expressing HA-Belle and EGFP-fusion of Me31B. The HA-tag signal is shown in red and the EGFP signal is green. Overlap of the two colours appears yellow. DNA was stained with Hoechst 33342 (blue). **(C)** Confocal image of fixed S2 cell co-expressing HA-Belle (red signal) and EGFP-DCP1 (green signal). **(D)** Confocal fluorescent microphotograph of fixed S2 cell co-expressing EGFP-Belle (green signal) and HA-Ge-1 (red signal). Scale bar is 5 μm.

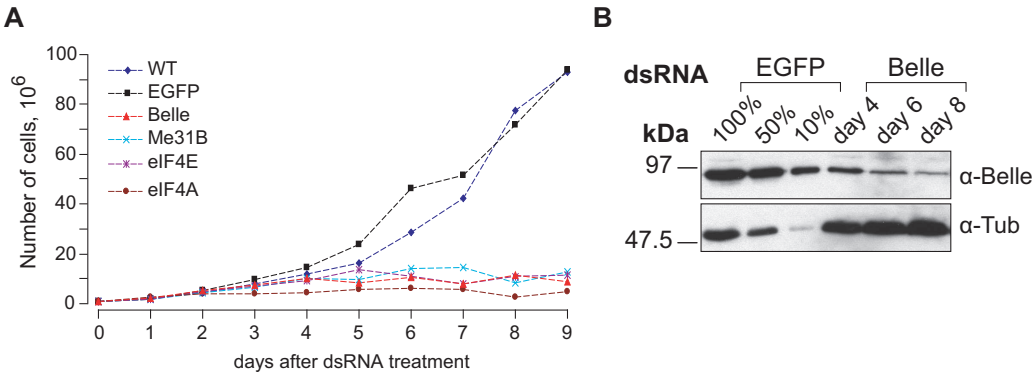

Figure 25. Belle is required for S2 cells proliferation.

(A) S2 cells growing in suspension were treated with dsRNAs specific for Drosophila Belle, Me31B, eIF4E, eIF4A, and EGFP. Depletion of Belle inhibits cell growth, similar to the depletions of Me31B, eIF4E, eIF4A. (Experiment was done three times, a representative growth curve is shown.) **(B)** Cells from the same experiment were analyzed by Western blotting with polyclonal antibody against Belle. Dilutions of the sample from EGFP dsRNA treated cells isolated on day 8 were loaded to assess the efficiency of the depletion. Tubulin served as a loading control.

I found that the depletion of Belle inhibit proliferation of S2 cells, similarly to the depletions of Me31B, eIF4A and eIF4E, as shown in Fig. 25A. This result is in line with a previous study that demonstrated that Belle is required for larval growth, as well as male and female fertility [201].

3.3 Protein synthesis is inhibited in cells depleted of Belle

Previous studies on Ded1p, the yeast homolog of Belle, had demonstrated that this protein is required for translation initiation [68, 84, 186]. Recent results from Roy Parker's laboratory suggested that the yeast homolog of the DEAD-box helicase Me31B, Dhh1p, is required for global translational repression in response to stress (glucose deprivation or amino acid starvation), during which the vast majority of mRNAs undergo translational repression [73].

To test whether Belle is required for translation control in *Drosophila*, I studied the efficiency of general protein synthesis by metabolic labeling in S2 cells individually depleted of Belle, Me31B, eIF4A and eIF4E by RNAi. The experiment was performed at normal growth conditions (25°C) and during heat-shock-induced stress (at 37°C) (Fig. 26). I observed that in cells depleted of Belle, the incorporation of [^{35}S]-methionine into newly synthesized

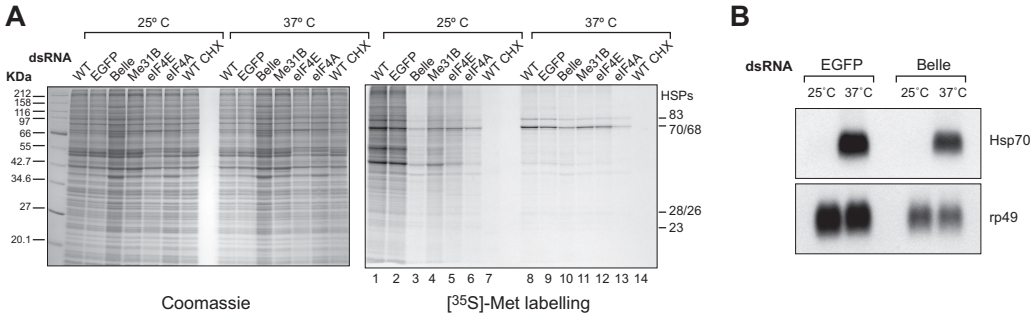

Figure 26. Belle is required for efficient translation in S2 cells.

(A) S2 cells from the same experiment shown Fig. 25 were pulse labeled with [^{35}S]-methionine for 1 h. Total lysates from equivalent numbers of cells were analyzed by SDS-PAGE followed by Coomassie blue staining (left panel) and autoradiography (right panel). Wild type cells, treated with protein synthesis inhibitor cycloheximide, served as a control for translation shut down. The position of heat shock proteins is indicated on the right. **(B)** Northern blot analysis of Hsp70 mRNA levels in the control (EGFP dsRNA treated) and Belle-depleted S2 cells before (25°C) and after (37°C) induction by the heat shock.

proteins decreased significantly relative to the control cells (Fig. 26A, lane 3 versus lane 1 and 2). Moreover, the expression of HSP70 protein following heat stress was also reduced (Fig. 26A, lane 10 versus lane 8 and 9) despite the fact that the corresponding mRNA was strongly induced (Fig. 26B). Although all knock-down cells showed similar growth inhibition (see Fig. 25A), depletion of Belle had the strongest effect on protein synthesis, comparable to the effect of depletion of the translation initiation factor eIF4A. This result suggests that the effect of the depletions on general protein synthesis is not only due to cell growth arrest, and that Belle is required for efficient translation in S2 cells.

To confirm this result, I analyzed polyribosome profiles of S2 cells individually depleted of Belle, eIF4A and eIF4E (Fig. 27). The profiles were obtained from cytoplasmic lysates, prepared from equivalent amounts of cells. The lysates were loaded on 15%-45% sucrose density gradients, and lysate components were separated in the gradient according to their sedimentation coefficients by ultracentrifugation. The polysome profiles from depleted cells were compared to a control profile from S2 cells treated with EGFP dsRNA. The profile from cells treated with Belle dsRNA was similar to the profiles obtained from eIF4E- and eIF4A-depleted cells. All three profiles were characterized by an increase of the 80S (monosome) peak and a decrease of the polysome peaks, suggesting that translation was impaired in these cells (Fig. 27).

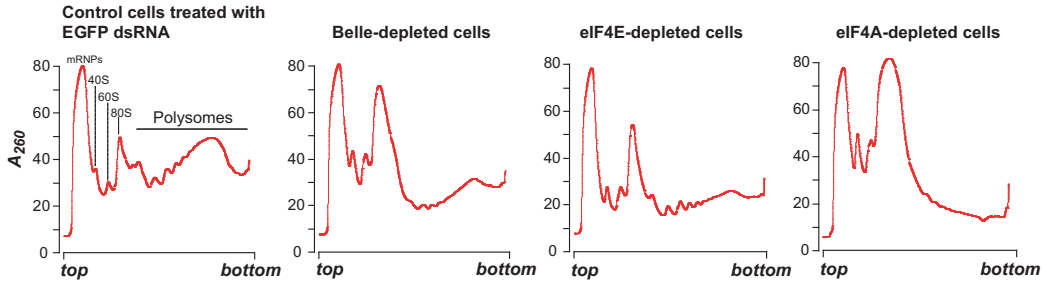

Figure 27. Polyribosome profiles of S2 cells treated with dsRNAs specific for *Drosophila* Belle, eIF4E, eIF4A, and EGFP.

The positions of peaks, corresponding to ribosome-free mRNPs, ribosomal subunits (40S and 60S), monosomes (80S) and polysomes, are indicated on the control profile, obtained from EGFP dsRNA treated S2 cells. "Top" and "bottom" mark the top (15% sucrose) and the bottom (45% sucrose) of the sucrose density gradient, respectively.

3.4 Belle represses translation of bound mRNA

The next question to be answered was whether Belle is able to elicit translation control when it is bound to a reporter transcript. To address this, I decided to make use of the tethering assay described in [30]. This assay involves the expression of λN-HA-fusion proteins that bind with high affinity to five BoxB sites (5BoxB) in the 3′ untranslated region (UTR) of a firefly luciferase reporter mRNA (F-luc-5BoxB reporter) (Fig. 28A). S2 cells were transiently transfected with the F-luc-5BoxB reporter, a plasmid expressing Belle fused to the λN-HA peptide (λN-HA-Belle), and a plasmid encoding *Renilla* luciferase (R-Luc) as a transfection control. 48 hours after transfection, cells were harvested and the steady-state levels of reporter luciferase activities were quantified by the dual luciferase assay. The firefly luciferase activity levels were normalized to that of *Renilla* to compensate for possible differences in transfection efficiencies.

The tethering of Belle caused a reduction in the level of firefly luciferase activity to *ca.* 40% of the level detected in cells expressing the λN-HA peptide alone (Fig. 28B). To determine whether Belle silences firefly luciferase expression by inhibiting translation directly or indirectly by reducing mRNA levels, I analyzed the steady-state levels of the F-luc-5BoxB mRNA by Northern blot and normalized to the levels of the control R-Luc mRNA. Surprisingly, expression of the λN-HA-Belle fusion caused an increase in the levels of the reporter mRNA (*ca.* 1.6-fold relative to the levels detected in cells expressing the λN-HA peptide alone) (Fig. 28B).

To test whether the ability of Belle to repress translation of bound mRNA was dependant on its helicase activity, I introduced single amino acid sub-

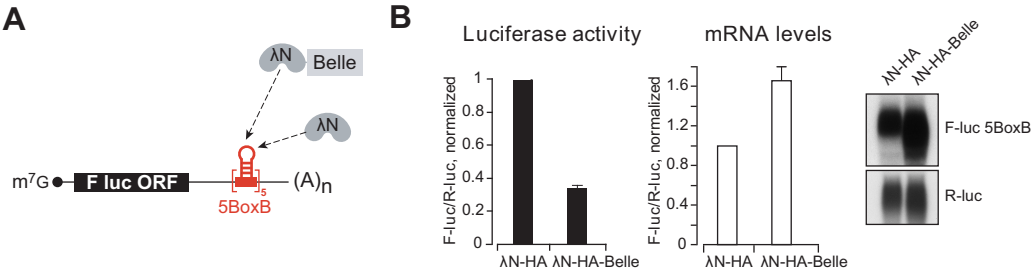

Figure 28. Tethering of λN-HA-Belle represses translation of firefly reporter.

(A) Schematic representation of the firefly luciferase (F-luc) 5BoxB reporter. **(B)** S2 cells were transfected with a mixture of plasmids comprising the F-luc-5BoxB reporter, a plasmid expressing *Renilla* luciferase (R-Luc) and plasmids encoding the λN-HA peptide and λN-HA-Belle. Protein levels were measured by luciferase assay (black bars). The reporter mRNA levels (white bars) were analyzed by Northern blot with the probes against F-luc and R-luc. The levels of the F-luc-5BoxB reporter were normalized to the levels of R-luc reporter. Normalized values were set to 1 in cells expressing the λN-HA peptide alone. Mean values ± standard deviation of three independent experiments are shown.

stitutions in its putative helicase domain. The selection of amino acids was based on the mutational analysis of mammalian DEAD-box RNA helicase eIF4A, reported in [331], given the highly conserved nature of the helicase core domain. Analogous mutations in mammalian eIF4A completely abolished the unwinding activity of the protein, but had different effects on ATP-binding and hydrolysis activities (Table 2). The domain architecture of Belle is shown in Fig. 29A with mutated residues indicated in red. I expressed these mutants of Belle in S2 cells (Fig. 29B) and tested in the tethering assay (Fig. 30).

Table 2. Biochemical activities of eIF4A mutants.

Motif	eIF4A	ATP-binding (%)	ATPase (%)	Unwinding (%)
Walker A (AXXXXGKT)	WT	100	100	100
Walker A (AXXXXGKT)	AXXXXGNT	2	0	0
Walker B (DEAD)	DQAD	60	0	0
C-terminal VI (HRIGR)	QRIGR	60	30	0

Modified from Pause and Sonenberg, 1992.

I found that two mutants (K345N and E460Q) were unable to repress translation of the firefly reporter mRNA (Fig. 30A). The third H645Q mutant showed the same effect on reporter translation as the wild type Belle. The inhibitory effect of λN-HA-Belle affected only tethered mRNA, while an F-luc reporter lacking the 5BoxB sites was translated even more efficiently in

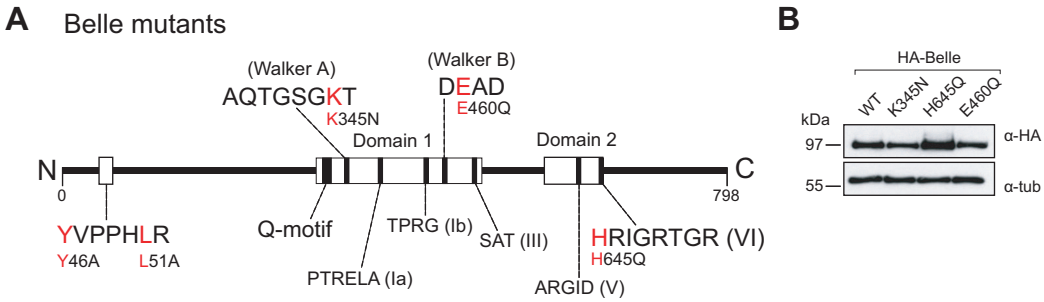

Figure 29. Expression of Belle mutants in S2 cells.

(A) Schematic representation of the domain organization of Belle. Mutated amino acid residues are indicated in red. **(B)** The expression of Belle mutants was confirmed by Western blot. HA-tagged proteins were detected using anti-HA antibody.

the presence of over-expressed protein (Fig. 30A).

I measured the steady-state levels of the F-Luc-5BoxB mRNA by Northern blot analysis and normalized to the levels of the control R-Luc mRNA. Expression of the wild type λN-HA-Belle and the two mutants (E460Q and H645Q) caused a marked increase in the levels of the reporter mRNA (around 1.8-2-fold relative to the levels detected in cells expressing the λN-HA peptide alone) (Fig. 30C, black bars). Tethering of the K345N mutant increased the F-luc-5BoxB reporter level only *ca.* 1.2-fold. No stabilizing effect was seen on transcripts lacking the tethering sites (Fig. 30C, white bars).

After normalizing firefly luciferase activity to the corresponding mRNA levels, the bound wild type λN-HA-Belle led to a net 4-fold reduction in protein expression (Fig. 30D), and the same net effect was observed for the H645Q mutant. The other two mutants (K345N and E460Q) had no net effect on reporter protein expression. The differences between the activities of Belle mutants in the tethering assay correlated with the properties of eIF4A mutants, summarized in Table 2.

This result suggests that the putative ATPase activity of Belle is required for translation repression of bound F-luc-5BoxB mRNA.

3.5 Tethering of Belle induces the formation of heavy mRNPs which are different from polysomes

Actively translated mRNAs form polysomes which sediment faster during ultracentrifugation, and appear in the "heavy" gradient fractions, close to the bottom of the gradient. The result of inefficient translation initiation or elongation is that less ribosomes are associated with the mRNAs, so the

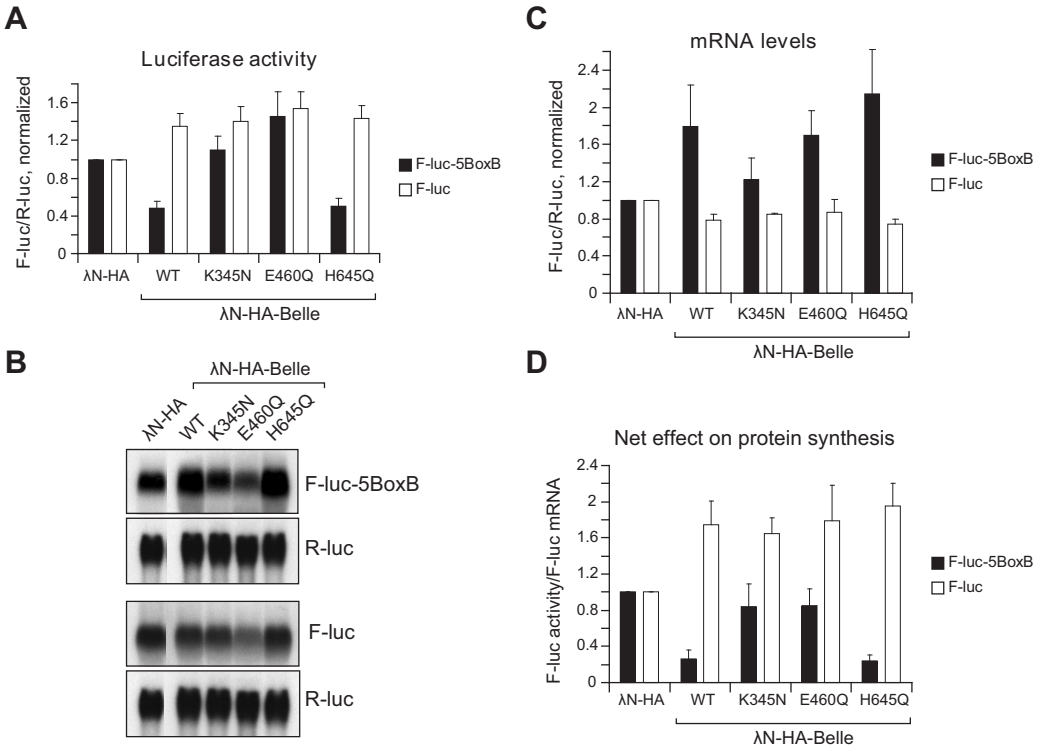

Figure 30. Tethering of λN-HA-Belle represses translation of bound mRNA in ATP-dependant manner.

(A) S2 cells were transfected with the F-luc-5BoxB reporter (black bars) or the F-luc control (reporter lacking the tethering sites, white bars), a plasmid expressing *Renilla* luciferase, and vectors expressing the λN-HA peptide or λN-HA-Belle, either wild type or mutated. Firefly luciferase activity was normalized to that of *Renilla* and set to 1 in cells expressing the λN-HA peptide alone. Mean values ± standard deviations from three independent experiments are shown. **(B)** Firefly luciferase reporter mRNAs and R-luc mRNA levels were analyzed by Northern blot. **(C)** The levels of F-luc-5BoxB (black bars) and F-luc (white bars) reporter mRNAs were normalized to the mRNA levels of R-luc reporter. Normalized values were set to 1 in cells expressing the λN-HA peptide alone. Mean values ± standard deviation of three independent experiments are shown. **(D)** The normalized values of firefly luciferase activity shown in **A** were divided by the normalized mRNA levels shown in **C** to estimate the net effect of tethering Belle on protein synthesis.

mRNAs sediment slowly and appear in the "light" fractions, close to the top of the gradient. Therefore, the position of an mRNA on a gradient is dependent on its translation efficiency.

To understand the mechanism of Belle-mediated translation repression of the bound F-luc-5BoxB mRNA, I analyzed polysome profiles from S2 cells transfected with the F-luc-5BoxB reporter, a *Renilla* luciferase (R-Luc) transfection control and plasmids encoding the λN-HA peptide, λN-HA-Belle wild type or K345N mutant. The distribution of the F-luc-5BoxB and R-luc reporters between different gradient fractions was monitored.

The cells were harvested 48 hours after transfection and lysed in hypertonic, detergent-containing lysis buffer. One half of each lysate was treated with 30 mM ETDA to disassemble the polysomes. The lysates were loaded on 15%-45% sucrose density gradients, and lysate components were separated by ultracentrifugation according to their sedimentation coefficients. The gradients were fractionated and the corresponding UV profiles were recorded (Fig. 31A). The RNA samples extracted from the gradient fractions were analyzed by Northern blot (Fig. 31B).

As was expected, in S2 cells expressing the F-luc-5BoxB reporter, R-luc transfection control and λN-HA peptide alone, the reporter mRNAs were actively translated and appeared in the "heavy" polysome fractions of the gradient (Fig. 31B). EDTA-mediated polysome disruption caused a shift of the reporter mRNAs from the "heavy" to the "light" fractions, close to the top of the gradient.

Tethering of λN-HA-Belle to the F-luc-5BoxB reporter caused a slight shift of the mRNA towards the bottom of the gradient. The distribution of the control R-luc reporter mRNA in the gradient remained unchanged. Interestingly, disruption of polysomes with EDTA in this case did not make the same shift of the F-luc-5BoxB reporter to the top of the gradient, as was the case with tethering of the λN-HA peptide alone. The control R-luc reporter mRNA was shifted to the "light" gradient fractions, as before. Tethering of a λN-HA-Belle K345N mutant, lacking putative ATPase activity, to the F-luc-5BoxB reporter had the same effect on the position of the mRNA in the gradient, with or without EDTA treatment.

I analyzed the protein samples extracted from the gradient fractions by Western blot using anti-Belle polyclonal antibody (Fig. 31C). I found that only a minor fraction of endogenous Belle co-migrates with polysomes in the sucrose gradients. EDTA-mediated polysome disassembly did not dramatically affect the distribution of the protein in the gradient, but a slight shift from the "heavy" fractions was detectable (Fig. 31C). At the same time, λN-HA-Belle co-migrated with the F-luc-5BoxB mRNA in the sucrose gradient. As was expected, this distribution of the protein in the gradient was resistant

to EDTA treatment.

These results indicate that tethering of λN-HA-Belle to the F-luc-5BoxB reporter mRNA induces the formation of a heavy mRNP complex, which is resistant to EDTA treatment at concentrations sufficient for polysome disassembly. Tethering of the λN-HA-Belle K345N mutant also induces the formation of heavy mRNP particles. This process does not depend on the putative ATPase activity of Belle, and is not sufficient for translation repression of the bound mRNA.

3.6 Tandem affinity purification of proteins associated with Belle in *Drosophila* S2 cells

The next step in characterizing the molecular function of Belle was to identify proteins that associate with the protein. I decided to take the approach which involved establishing polyclonal *Drosophila* S2 cell lines expressing C-terminal TAP-tagged wild type Belle and Belle mutants on induction with copper sulfate. Wild type Belle and the K345N mutant, lacking putative ATPase activity, were purified along with interacting proteins by tandem affinity chromatography (Fig. 32).

After colloid Coomassie or silver staining, the gel pieces which contained proteins of interest were excised, proteins were digested in-gel with trypsin, and peptides were extracted from the gel blocks. Peptide mixtures were analyzed using liquid chromatography-tandem mass spectrometry (LC-MS/MS). Raw spectra were processed, and the peak lists searched in-house using Mascot Daemon MS analysis. This identified 213 proteins associated with wild type Belle and 225 proteins associated with the Belle K345N mutant. Proteins identified with a Mascot score $\geq$50 were considered significant, whereas all lower-scoring proteins were either included or discarded after inspection of individual spectra. This resulted in the inclusion of 5 additional proteins with scores of between 43 and 48. By combining the two purification results, and after removal of redundant hits, I identified 336 different proteins which are shown in Table 6. The proteins in the table are listed according to a sum of their Mascot scores, obtained in two different affinity purifications using wild type Belle or Belle K345N mutant.

3.7 Characterization of proteins associated with Belle in *Drosophila* S2 cells using Gene Ontology

Although the chosen approach did not detect proteins stoichiometrically interacting with Belle, it identified many more proteins with the ability to

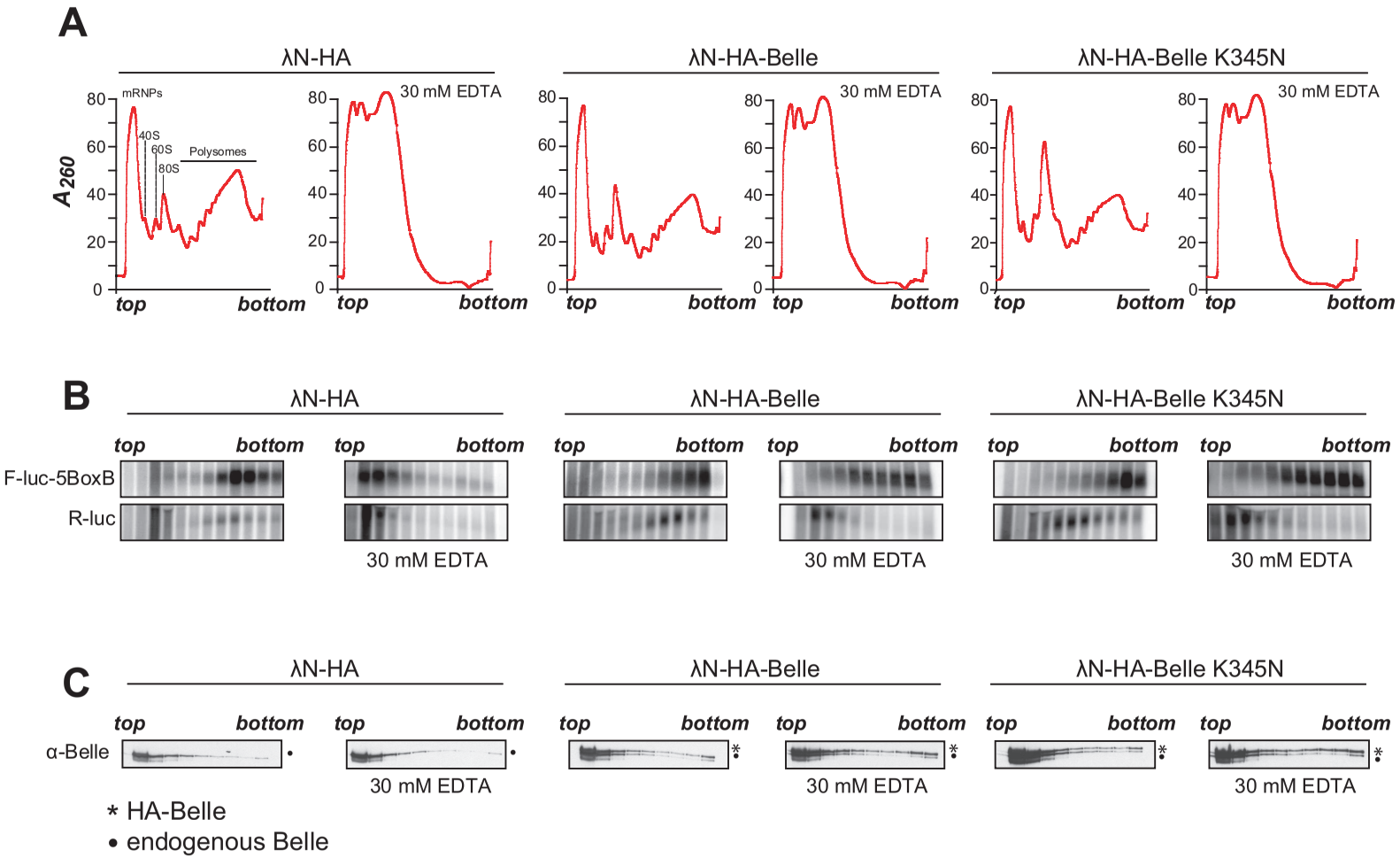

Figure 31. Polysome profiles of S2 cells transfected with λN-HA-Belle tethering reporter system.

(A) Polysome profiles of S2 cells transfected with the F-luc-5BoxB reporter, *Renilla* luciferase (R-Luc) transfection control and plasmids encoding the λN-HA peptide, λN-HA-Belle wild type or K345N mutant. For each condition one half of the lysates prepared from transfected cells was treated with 30 mM EDTA to disassemble polysomes. **(B)** Northern blot analysis of total RNA samples isolated from sucrose gradient fractions with the probes against F-luc and R-luc. **(C)** Western blot analysis of sucrose gradient fractions using anti-Belle antibody.

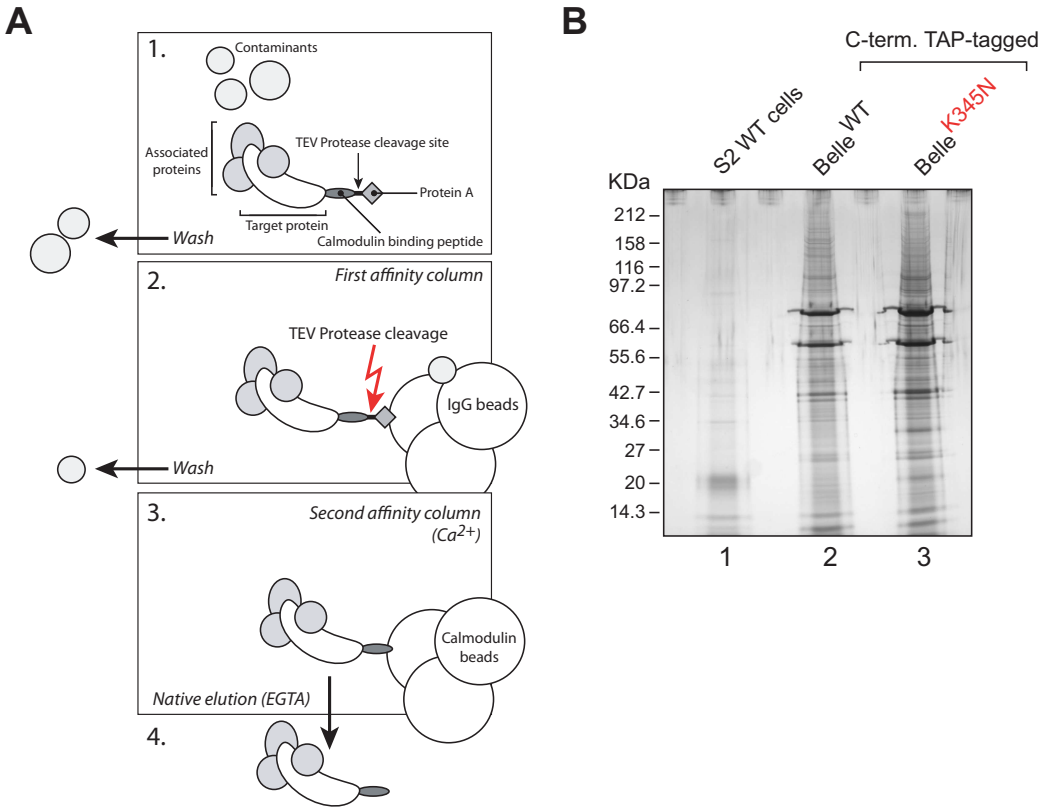

Figure 32. Purification of proteins associated with Belle by tandem affinity chromatography.

(A) Schematic representation of tandem affinity purification principle. **(B)** S2 cells bearing a plasmid encoding C-terminal TAP-tagged Belle under inducible metallothionein promoter were treated with copper sulfate overnight. Twelve hours after addition of copper sulphate, proteins bound to TAP-tagged Belle were purified in presence of RNase A and separated by SDS-PAGE. Lane 1, proteins purified from lysates of wild type S2 cells; lane 2, proteins bound to TAP-tagged Belle wild type, lane 3, proteins bound to TAP-tagged Belle K395N mutant.

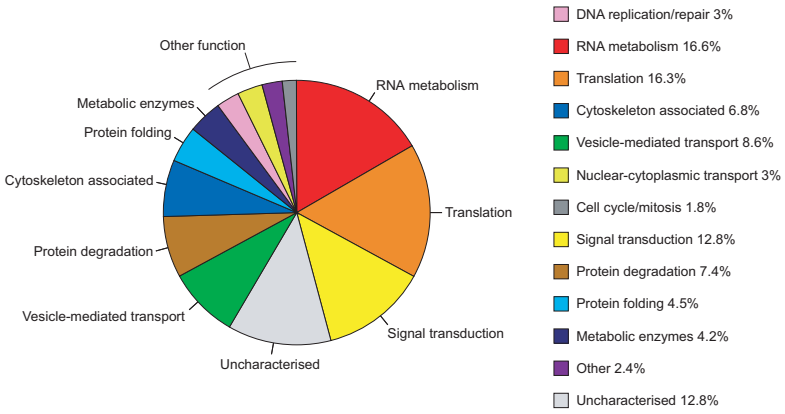

Figure 33. Functional characterization of proteins associated with Belle in *Drosophila* S2 cells.

A pie diagram showing the classification of 336 identified proteins according to Gene Ontology, assisted by manual data mining of references in Flybase and Ensembl. A total of *ca.* 13% of proteins were completely uncharacterised according to the sources. The remaining proteins were grouped by GO function and were encompassed into twelve main categories: DNA replication and repair, RNA metabolism, translation, cytoskeleton associated, vesicle-mediated transport, nuclear-cytoplasmic transport, cell cycle and mitosis, signal transduction, protein degradation, protein folding, metabolic enzymes, and other.

bind Belle than anticipated. To classify the 336 proteins on a functional basis, I characterized them according to the Gene Ontology (GO) database [17] supported by additional manual data mining of previously published work (Fig. 33, Table 6).

A total of 111 proteins (33%) fell within GOs that would be expected to have a function in mRNA translation and turnover, such as those involved in RNA binding, mRNA processing, splicing, localization, translation, decapping, and deadenylation (Fig. 33, Table 6). This percentage remained unchanged when two purifications (with the wild type protein and with the mutant) were inspected separately (Fig. 34A, B) and was even higher (*ca.* 42%) when proteins that came out in both purifications were considered (Fig. 34C, D).

A more formal and detailed functional categorization of proteins interacting with Belle was carried out on the basis of a relatively small number of high-level GO terms. This involves the mapping of a set of annotations for the proteins of interest to a specified subset of high-level GO terms called GO slim ontology. Generic GO slim ontology is updated regularly and is available from the GO website. The GO website provides an algorithm, `map2slim` written by Chris Mungall at Berkeley Drosophila Genome Project, to map

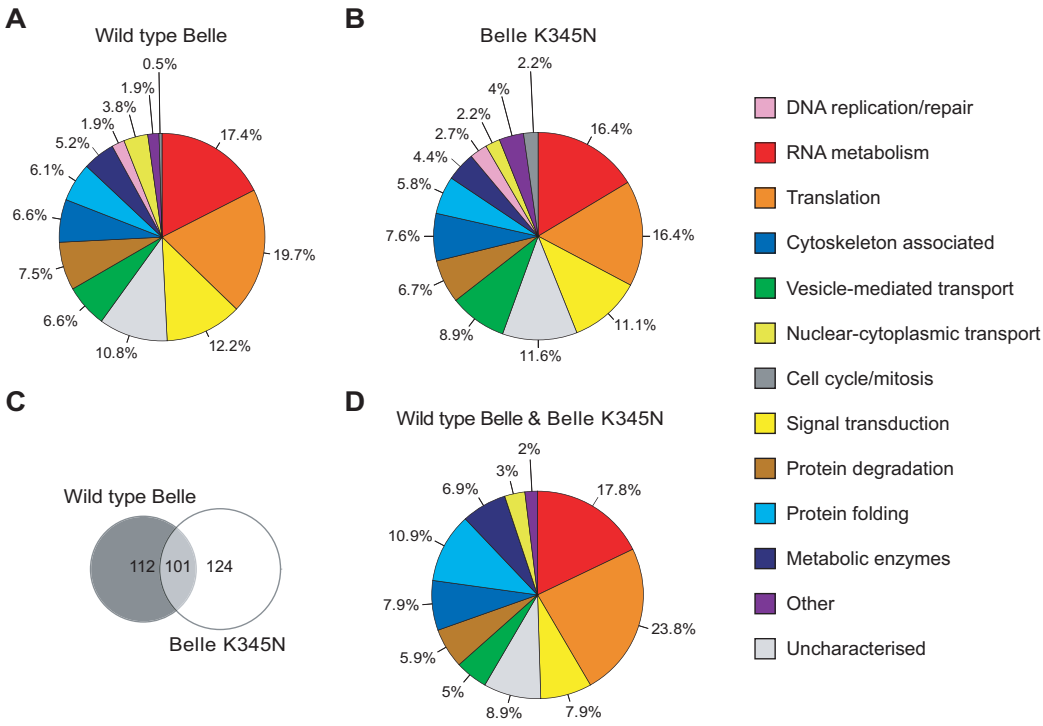

Figure 34. A comparison of the two sets of proteins interacting with wild type Belle and Belle K345N mutant in *Drosophila* S2 cells.

(A) A pie diagram showing the Gene Ontology classification of 213 proteins identified after affinity purification of wild type Belle. **(B)** A GO classification of 225 proteins, identified after affinity purification of Belle K345N mutant. **(C)** Venn diagram showing an overlap between the two experimental data sets. Numbers in circles correspond to the numbers of proteins found in each subset. **(D)** A GO classification of 101 proteins, found in both experimental data sets.

annotations to a slim ontology. I used a web tool developed in Princeton University called *GO Term Mapper* which employs the algorithm `map2slim` and some of the modules included in the *GO-TermFinder* distribution written by Gavin Sherlock and Shuai Weng at Stanford University [43]. *GO Term Mapper* groups proteins from a submitted list into broad categories according to molecular function, biological process, or cellular component. 307 annotated proteins out of 336 proteins associated with wild type Belle or with the K345N mutant were categorized (Fig. 35). Because gene ontology is a directed acyclic graph[3], a GO term used for a specific annotation might be a child of multiple terms in the slim set. Also, individual proteins often have several annotations to different terms to reflect their multiple functions, roles or locations. Because one protein's annotations frequently map to many slim terms, pie diagrams that are traditionally used to illustrate the functional distribution of genes are not a good representation of the data. The sum of the annotations is larger than 100%, that is, proteins are found in more than one slice of the pie [351]. I used a bar diagram as more appropriate here (Fig. 35).

Consistent with the "manual" characterization (Fig. 34), I observed that the main fraction of proteins associated with Belle fell into molecular function and biological process categories related to RNA-binding and translation. Another highly populated molecular function category was nucleotide binding (Fig. 35A). Regarding biological process categories, organelle and cytoskeleton organization and biogenesis together contained more than 60% of proteins associated with Belle. This observation is in line with a study on microtubule interactome, which identified Belle and 59 other proteins that co-purified with Belle in our experiments as microtubule-associated in early *Drosophila* embryos [177].

Interestingly, I found that roughly 15% of proteins associated with Belle were in a cellular component category "lipid particle". According to a mass spectrometry analysis of lipid-droplet proteome reported in [57], Belle was found among proteins significantly represented in the lipid-droplet fraction, together with 32 other proteins (*ca.* 40% of the lipid-droplet proteome) that associated with Belle in our experiments.

To compare coarsely two experimental sets of proteins associated with wild type Belle and the K345N mutant, each set was categorized independently using *GO Term Mapper* (Fig. 36). The goal of such functional profiling is to determine which processes might be different in two particular sets of

[3]Directed acyclic graph (DAG) is a graph in which the GO terms are nodes and the relationships among them are edges. Parent-child relationships are defined, with parent term representing more general entities than their child terms; and unlike a simple tree, a term in a DAG can have multiple parents.

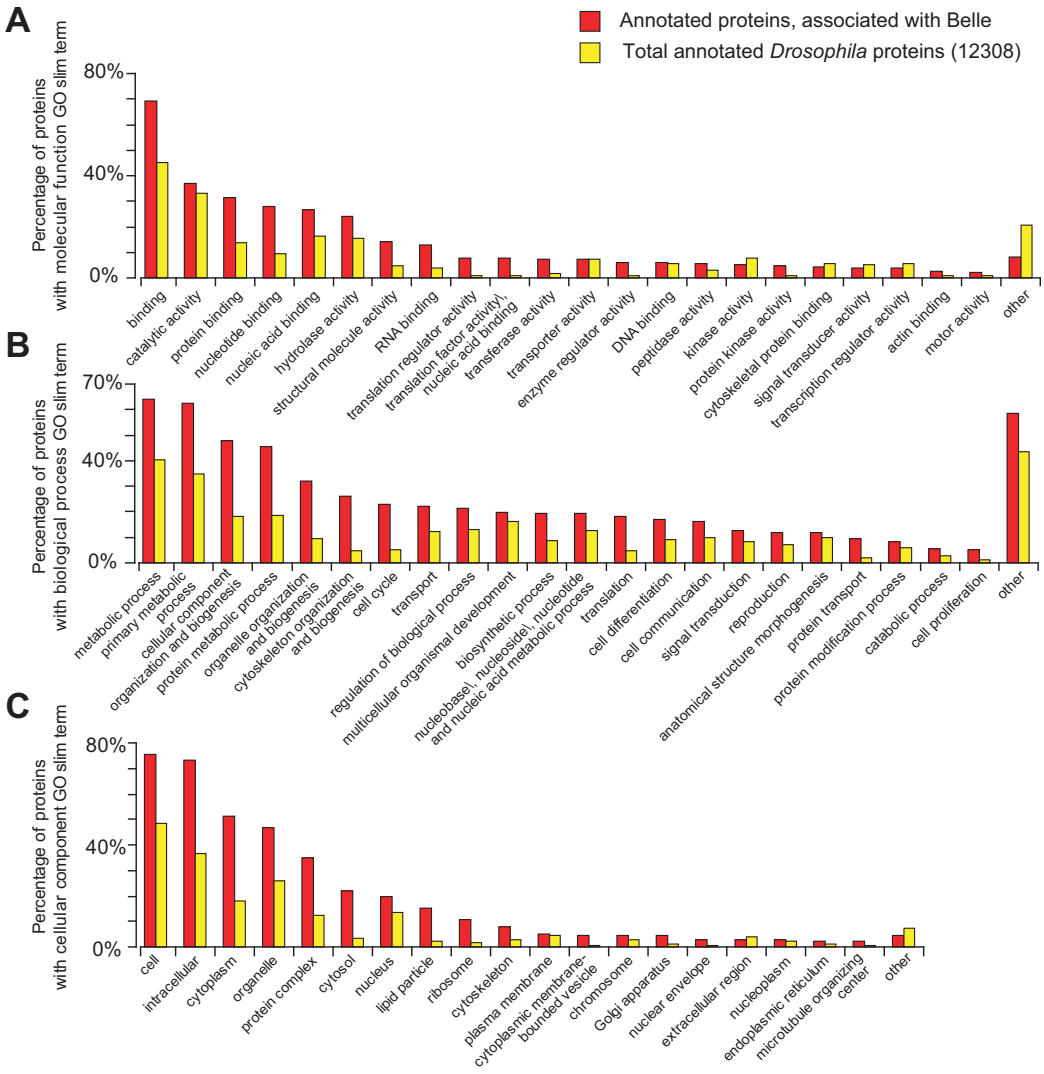

Figure 35. Functional categorization of proteins associated with Belle using generic GO slim terms.

A classification of 307 annotated proteins out of 336 associated with the wild type or K345N mutant Belle according to molecular function **(A)**, biological process **(B)** and cellular component **(C)** GO slim terms. The category "other" consists of all categories that contain less than 2% (molecular function and cellular component) or 5% (biological process) of annotated proteins associated with Belle.

proteins. This can be done by determining which GO slim terms are represented differently within the protein set. By simple comparison of the two GO slim terms profiles we detected a few minor differences between two protein sets obtained from two parallel purifications using either the TAP-tagged wild type Belle or K345N mutant (Fig. 36).

3.8 Functional enrichment analysis

The simple approach of calculating "enrichment/depletion" for each GO slim term (that is, a higher proportion of genes with certain annotations among the protein set than among all of the proteins) is far from perfect because any enrichment value can occur just by chance. Therefore, enrichment (or depletion) alone should not be interpreted as unequivocal evidence implicating the GO term in the phenomenon studied without an appropriate statistical test.

To extract GO terms that are significantly over- and under-represented in the sets of proteins obtained experimentally, I used two different web-based applications, allowing for easy and interactive querying. The reason for using two different functional profiling programs is that the output p-values provided by different applications may vary dramatically (several orders of magnitude for some GO terms). Factors that can cause such wildly different results for the same input data include: the method used to map gene identifiers; sources and versions of annotation files; the method of annotation propagation (for example, direct annotations only versus propagated to parents); the statistical testing method (for example, one-sided versus two sided); and the multiple hypothesis correction method [351].

The first program that was used was *GO Term Finder*. It calculates p-values using hypergeometric distribution [43]. To adjust the p-values for multiple hypothesis testing *GO Term Finder* runs 1000 simulations. The corrected p-value is calculated as the fraction of simulations having any p-value as good or better than the observed p-value. Comparison of simulation corrected p-values with Bonferroni corrected p-values actually suggests that the Bonferroni correction is not conservative enough[4].

An alternative methodology for multiple hypothesis testing is to calculate the false discovery rate (FDR), which is the expected proportion of true

[4]The Bonferroni correction is the most commonly used multiple hypothesis correction method, whereby the α-value is simply divided by the number of tests, and the overall chance of finding any false positive remains the same as in a single hypothesis experiment. The Bonferroni correction assumes that the tests are independent and is considered a conservative adjustment. In our case, the hypotheses (GO terms which are nodes) are not independent, because the nodes themselves structured in a DAG [43].

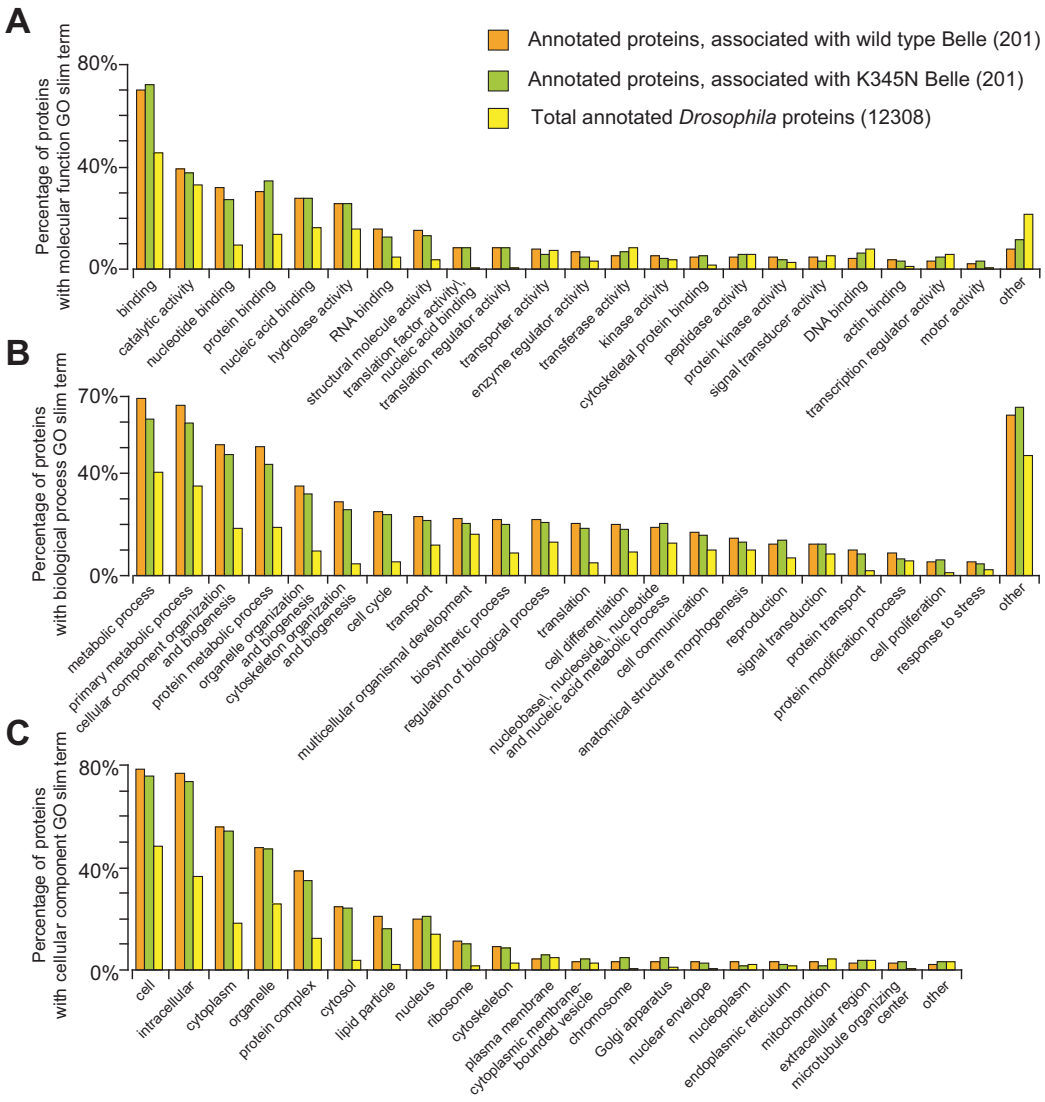

Figure 36. Two sets of proteins associated with wild type Belle or K345N mutant categorized separately from each other.

A classification of annotated proteins (201 out of 213 associated with the wild type Belle and another 201 out of 225 associated with K345N mutant) according to molecular function **(A)**, biological process **(B)** and cellular component **(C)** GO slim terms. The category "other" consists of all categories that contain less than 2% (molecular function and cellular component) or 5% (biological process) of annotated proteins associated with Belle.

null hypotheses rejected out of the total number of null hypotheses rejected. Based on 50 simulations, *GO Term Finder* calculates the FDR for each hypothesis from the real data as the average number of nodes per simulation that have p-values as good or better than the real node's p-value, divided by the number of nodes in the real data that have a p-value as good or better than that p-value. Comparison of p-values corrected by simulation versus the FDR shows that using the corrected p-values is likely to result in more false negatives [43].

The second web application was *FatiGO* [2]. This program first defines the GO level at which the statistical contrast is going to be performed. Deeper terms in the GO hierarchy are more precise, but the number of genes with annotations decreases at deeper GO levels. GO level 3 constitutes a good compromise between information quality and number of genes annotated at this level. For genes annotated at deeper levels than the selected level, *FatiGO* climbs up the GO hierarchy until the terms for the said level are reached. The use of the parent terms increases the size of the classes (genes annotated with a given GO term), making it easier to find relevant differences in distributions of GO terms among clusters of genes. Once the collections of GO terms corresponding to the two data sets of genes are prepared, a Fisher's Exact test for 2×2 contingency tables is applied.

P-value adjustment is based on three different ways of accounting for multiple hypothesis testing. These are the step-down minP method of Westfall and Young [420], the false discovery rate (FDR) method of Benjamini and Hochberg [31], which offers control of the FDR only under independence and some specific types of positive dependence of the test statistics, and the FDR method of Benjamini and Yekutieli [32], which offers strong control under arbitrary dependency of test statistics.

Each program was sequentially provided with two lists of Flybasecgid gene IDs, corresponding to proteins associated with wild type Belle (213 proteins) and the K345N mutant (225 proteins) in the affinity purifications. The background set was the list of Flybasecg IDs of all *Drosophila* protein coding genes, retrieved from BioMart, a query-oriented data management system developed jointly by the Ontario Institute for Cancer Research (OiCR) and the European Bioinformatics Institute (EBI).

The results of this functional profiling performed by two different programs is summarized in Table 5. The p-value cut-off applied to the list of GO terms was 0.01. The output of *GO Term Finder* contained a bigger number of entries with much lower corresponding adjusted p-values (several orders of magnitude) than the output of *FatiGO*, which proved to be more conservative. Only those GO terms that were present in both output files (which in practice included all the results from *FatiGO*) are listed in Table 5.

Enrichment was calculated as a ratio of the percentage of a particular GO term in the experimental data set to the percentage of the same GO term in the list of all *Drosophila* proteins. The discrepancy in the values of enrichment calculated for the same GO terms by two programs are due to the fact that these applications use different methods of annotation propagation. *GO Term Finder* uses direct annotations only, while *FatiGO* uses annotations that are propagated to parents. This leads to a different number of genes being associated with a particular GO term and alters the percentage of the term. The differences in the p-values are due to the statistical testing and multiple hypotheses correction methods.

Regardless of which program was used the results were similar, so that all GO terms that were identified as significantly enriched by *FatiGO* ($p < 0.01$) were also present in the list provided by *GO Term Finder*. This included a set of 54 GO terms significantly enriched in annotations of proteins associated with wild type Belle, and a set of 43 GO terms for the K345N mutant. The overlap between these two sets consisted of 39 GO terms. From the remaining GO terms, 15 were specific to wild type Belle and 4 to K345N mutant (**highlighted** in Table 5).

This specificity reflects the difference between the two sets of proteins associated with wild type Belle and the mutant lacking ATPase activity. Indirectly, this could help to understand what this ATPase activity is most vital for. There were significantly more proteins associated with wild type Belle which were involved in processes such as RNP complex formation, cell cycle and intracellular transport, including cytoskeleton and vesicle organization and biogenesis (Table 5).

Functional enrichment analysis using *FatiGO* was also applied to identify which InterPro terms are over-represented in proteins associated with Belle. Each InterPro term corresponds to a unique entry of the InterPro database, which is a database of protein families, domains, repeats and sites [299]. In addition to Gene Ontology terms, *FatiGO* simultaneously checked for significant over-representation of InterPro terms. This information is important to find out which protein domains or sequence motifs are required for interaction with Belle.

Multiple test correction to account for the multiple hypothesis tested (one for each InterPro term) was performed as described above. The results of this analysis are presented in Table 3.

Table 3. InterPro terms significantly enriched in annotations of proteins associated with Belle.

		Enrichment		Adjusted p-value	
InterPro term	Description	Belle^{wt}	Belle^{K345N}	Belle^{wt}	Belle^{K345N}
IPR000357	HEAT	11.7	15.1	$2.16 \cdot 10^{-5}$	$4.34 \cdot 10^{-9}$
IPR002194	Chaperonin TCP-1, conserved site	38.9	41.9	$2.16 \cdot 10^{-5}$	$8.24 \cdot 10^{-7}$
IPR001844	Chaperonin Cpn60	29.2	31.4	$4.35 \cdot 10^{-5}$	$3.22 \cdot 10^{-6}$
IPR002423	Chaperonin Cpn60/TCP-1	29.2	31.4	$4.35 \cdot 10^{-5}$	$3.22 \cdot 10^{-6}$
IPR000629	RNA helicase, ATP-dependent, DEAD-box, conserved site	16.7	13.8	$9.23 \cdot 10^{-5}$	$1.83 \cdot 10^{-3}$
IPR000225	Armadillo	14.6	7.9	$1.04 \cdot 10^{-3}$	$5.80 \cdot 10^{-1}$

The HEAT repeat is a tandemly repeated module consisting of 37-47 amino acids, occurring in a number of cytoplasmic proteins including huntingtin, the 65 kD alpha regulatory subunit of protein phosphatase 2A (PP2A) and the PI3-kinase TOR [9]. Arrays of HEAT repeats appear to function as protein-protein interaction surfaces. It has been noted that many HEAT repeat-containing proteins are involved in intracellular transport processes. The armadillo (Arm) repeat is an approximately 40 amino acid long tandemly repeated sequence motif. Animal Arm-repeat proteins function in various processes, including intracellular signalling and cytoskeletal regulation, and include such proteins as β-catenin and the nuclear transport factor importin-α, amongst others [163]. The Armadillo repeat was not significantly enriched in proteins associated with the mutant of Belle (Table 3, $p > 0.01$).

Both HEAT and Arm repeats are found in the Armadillo-like helical domain which consists of a multi-helical fold comprised of two curved layers of alpha helices arranged in a regular right-handed superhelix. These superhelical structures present an extensive solvent-accessible surface that is well suited to binding large substrates such as proteins and nucleic acids.

The TCP-1 family of proteins act as molecular chaperones for tubulin, actin and probably some other proteins. They are weakly, but significantly, related to the cpn60/groEL chaperonin family. *Drosophila* proteins that belong to this family have been shown to be associated with microtubules [177].

Interestingly, the DEAD-box ATP-dependent RNA helicase conserved site was found as significantly enriched. This indicates that Belle can interact with other DEAD-box proteins. The DEAD-box helicases are involved in various steps of RNA metabolism, including nuclear transcription, pre-mRNA splicing, ribosome biogenesis, nucleocytoplasmic transport, translation, RNA decay and organellar gene expression.

3.9 Bioinformatic analysis of interactions of proteins associated with Belle

The affinity purification approach identified many proteins involved in translation and mRNA metabolism, but it did not provide information regarding how these proteins work in concert with Belle and each other to elicit their biological functions. To identify functional and structural modules or complexes within the set of proteins associated with Belle I decided to build a network of already known interactions of these proteins.

Protein-protein interactions mapped either by focused studies or by high-throughput techniques are freely available in public repositories. A number of software tools are available for network visualization and analysis. Here I used *Cytoscape* to obtain and process network data. *Cytoscape* is an open source bioinformatic software platform for visualizing molecular interaction networks and biological pathways and integrating these networks with annotations, gene expression profiles and other data [375, 72].

In *Cytoscape*, nodes representing biological entities, such as proteins or genes, are connected with edges representing pairwise interactions, such as determined protein-protein interactions. Nodes and edges can have associated data attributes describing properties of the protein or interaction. Based on attribute values, *Cytoscape* can set visual aspects of nodes and edges. The program also allows users to employ additional software modules, or "plugins" that provide additional functionality in areas such as data query and download services, data integration and filtering, GO enrichment analysis, and protein complex or domain interaction detection [72].

The DroID-Plugin for *Cytoscape* was used, which provides access to the *Drosophila* Interactions Database (DroID) from within the *Cytoscape* environment. The *Drosophila* Interactions Database (DroID) is a "meta" database which assembles gene or protein interaction data from a variety of sources into one location. This database currently includes gene-gene and protein-protein interactions. Because methods used to detect protein interactions rarely record which protein variant from a gene was used, protein interactions in the database are represented by pairs of genes. The precise way to interpret a protein interaction represented as "gene A - gene B" is that one or more proteins encoded by gene A interact with one or more proteins encoded by gene B.

The core of DroID consists of three protein-protein interaction data sets generated mostly in high-throughput yeast two-hybrid (YTH) screens. Finley YTH includes data generated in the Finley laboratory using the LexA yeast two-hybrid system (Zhong, Patel, Zhang, Mangiola, Stanyon, Finley, unpublished; [393], and Schwartz, Yu, Gardenour, Finley, Ideker, submitted).

CuraGen YTH contains interactions detected in a high throughput yeast two-hybrid screen conducted at the CuraGen Corporation [140]. Hybrigenics YTH includes interactions detected in high throughput yeast two-hybrid screens conducted at Hybrigenics [121].

DroID also contains experimentally derived physical interactions other than those from the three major YTH data sets described above. These interactions are collected from the large databases (BioGRID, IntAct, MINT). The ordinal database source and information is available for each interaction.

Gene-gene interactions downloaded from Flybase which represent interactions between two gene alleles are also included in the DroID database. For example, an allele of one gene may enhance or suppress the phenotype of an allele in another gene, or the combination of two alleles may result in a "synthetic" phenotype not observed for either of the individual alleles.

Detected *Drosophila* protein interactions do not cover the whole fly proteome. The DroID database collected and integrated protein-protein interactions for yeast, worm, and human from online interaction databases (BioGRID, IntAct, MINT). Proteins in the obtained interaction sets were then mapped to fly orthologs using *InParanoid* [350], which is an orthology mapping algorithm. Thus, in addition to detected *Drosophila* protein interactions the DroID database covers predicted interactions between *Drosophila* proteins based on experimental evidence for interactions between orthologous proteins in other species.

From the 336 proteins associated with Belle, 221 formed 1402 interactions with each other, including interactions of a protein with itself. The resulting network is shown in Fig. 37. Proteins are indicated by circular nodes and interactions by lines or edges. The colour of an edge corresponds to the nature of the interaction it represents, as shown in the figure legend. The legend is explained below:

- *D.m.* main YTH—interactions of *Drosophila* proteins that were found in the three high-throughput yeast two hybrid screens conducted by the Finley laboratory, CuraGen and Hybrigenics.
- *D.m.* other physical—experimentally derived physical interactions of *Drosophila* proteins collected from the large online databases such as BioGRID, IntAct, and MINT, which were not present in the main YTH data sets.
- *D.m.* genetic—genetic interactions of *Drosophila* genes downloaded from Flybase.
- *S.c.* predicted—high confidence physical interactions of *Saccharomyces cerevisiae* orthologs of *Drosophila* proteins collected from BioGRID,

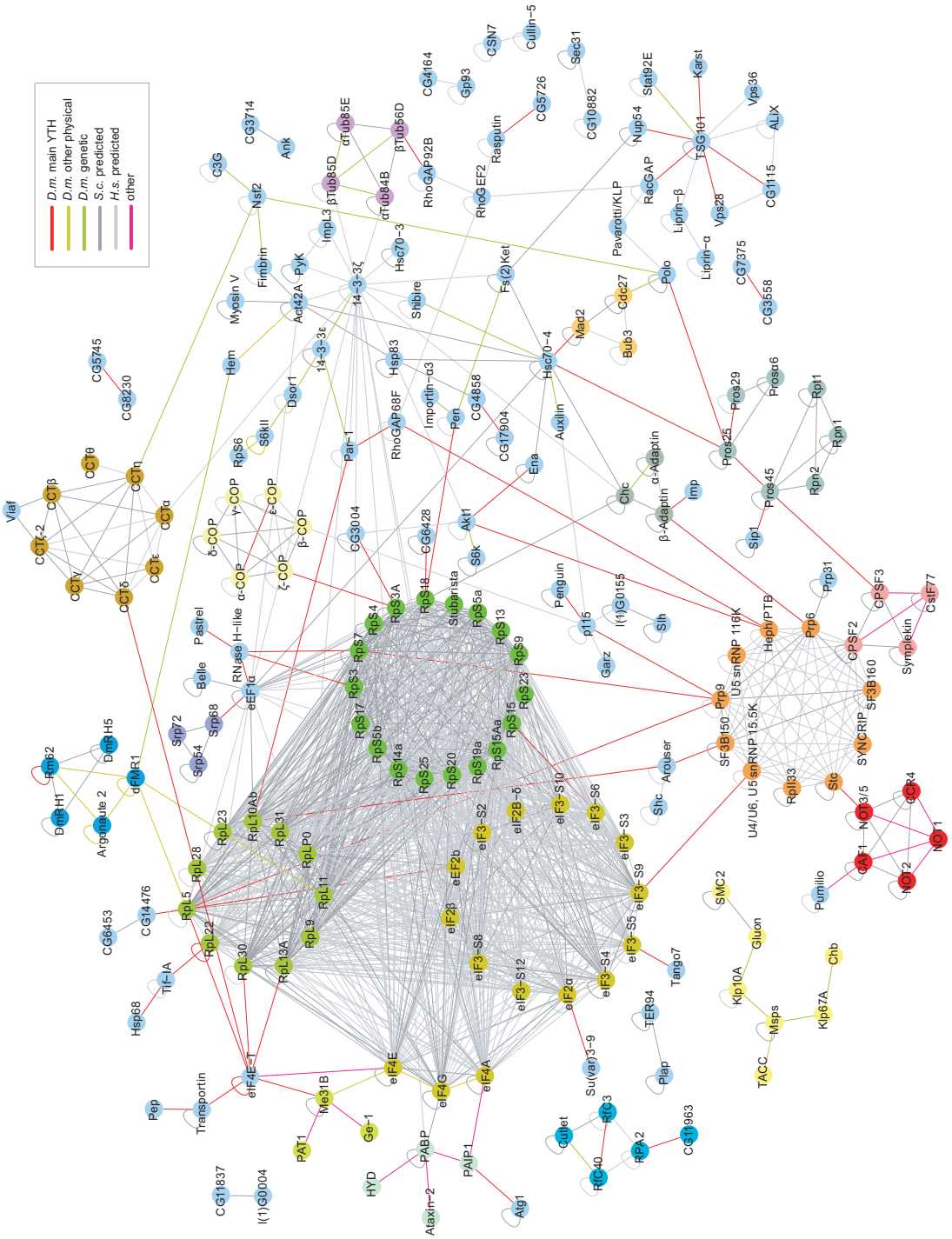

Figure 37. Network of interactions between proteins associated with Belle in *Drosophila* S2 cells.
A total of 221 of the 336 proteins associated with Belle show 1402 interactions with each other, gathered from DroID database; displayed here as an interaction network using *Cytoscape* application. See text for details.

IntAct and MINT databases.

- *H.s.* predicted—high confidence physical interactions of human orthologs of *Drosophila* proteins collected from BioGRID, IntAct and MINT databases.

- Other—physical interactions collected from the literature and from unpublished results from our laboratory.

To identify clusters (highly interconnected regions) I employed the MCODE-Plugin for *Cytoscape* which finds clusters in a network [21]. Clusters in a protein-protein interaction network often represent protein complexes and parts of pathways. I used MCODE with the default parameter settings and identified 11 clusters with number of nodes ≥ 3 and score ≥ 1 (Table 4).

Table 4. Clusters identified using MCODE-Plugin in the network of proteins associated with Belle.

Cluster	Score	Nodes No.	Edges
Ribosome and eIFs	20.93	43	943
Splicing complex	5	11	66
Chaperonin-containing T-complex	2.857	7	20
COPI vesicle coat	2.167	6	19
CCR4-NOT complex	2	5	14
Proteasome	1.429	7	16
Tubulin complex	1.4	5	11
DNA replication factor complex	1.25	4	9
mRNA cleavage and polyadenylation complex	1	3	6
Cell cycle checkpoint complex	1	3	6
Signal recognition particle	1	3	4

Analysis of the Gene Ontology annotations of the proteins that cluster together shows that the clusters represent real protein complexes found in the cell. Proteins that belong to the same cluster are coloured the same on Fig. 37. In addition to these MCODE identified protein complexes, I included complexes that were known from the literature but were only partially present (RISC, decapping enhancer complex, poly(A)-binding complex, microtubule-associated complex and AP-2 clathrin adaptor complex). Taking all these protein complexes into account, the interaction network of proteins associated with Belle could be simplified, as shown in Fig. 38.

3.10 Belle interacts with translation factors and RNA-binding proteins

To confirm the results of the affinity purification, I performed immunoprecipitations from total lysates of wild type S2 cells and cells expressing tagged

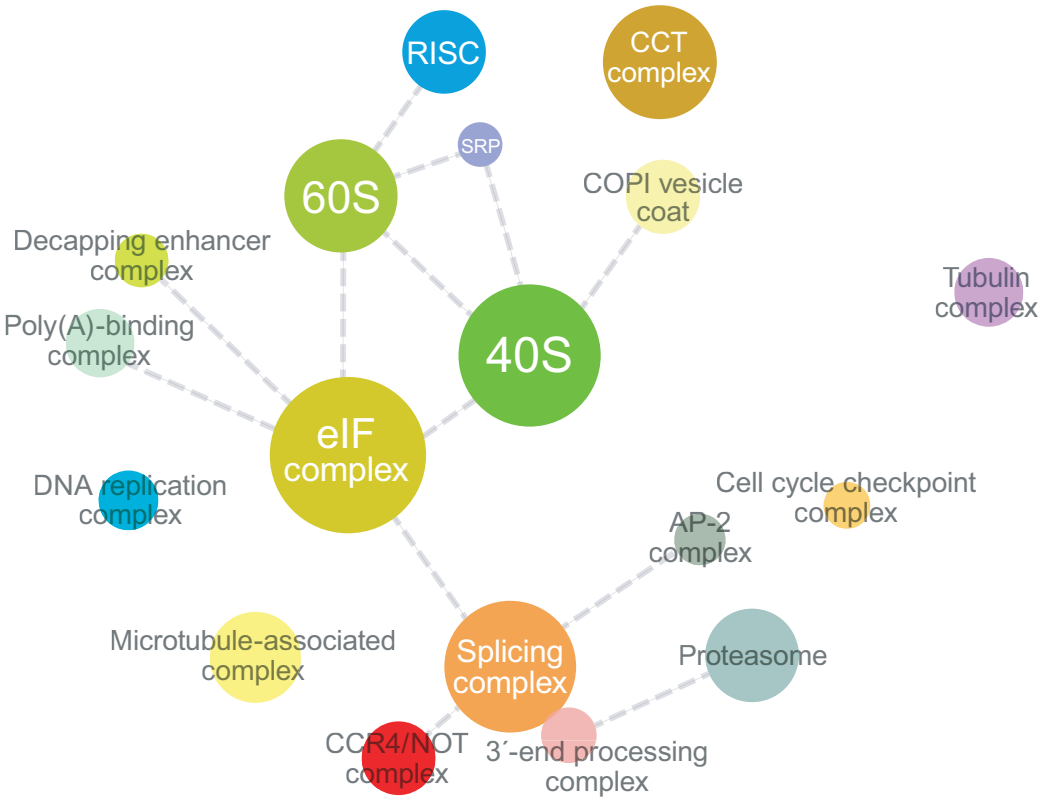

Figure 38. Putative protein complexes identified by the network cluster analysis.

A simplified representation of the interaction network of proteins associated with Belle in *Drosophila* S2 cells. Putative protein complexes (nodes) are coloured as corresponding proteins in Fig. 37. Only direct interactions between complexes are shown (edges).

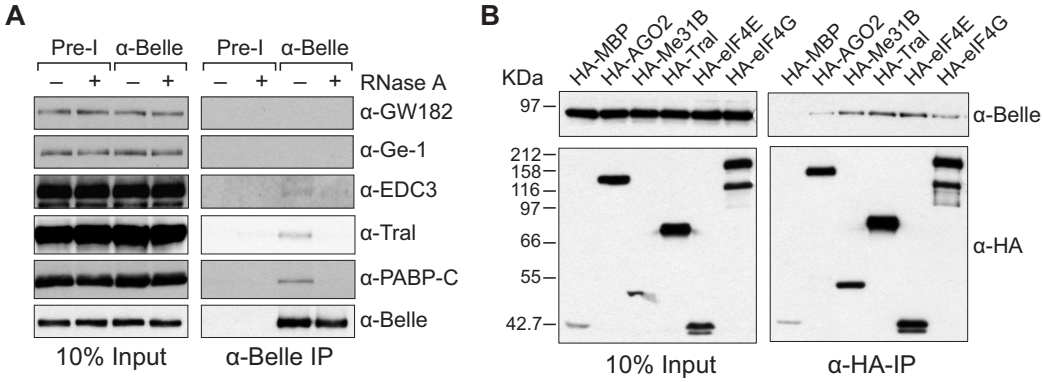

Figure 39. Endogenous Belle interacts with translation initiation factors and RNA binding proteins.

(A) Lysates from S2 cells were immunoprecipitated using anti-Belle rabbit serum (α-Belle) or rabbit pre-immune serum (Pre-I). Inputs (10%) and immunoprecipitates (IPs) were analyzed by Western blotting using polyclonal antibodies against endogenous proteins as indicated on the right. Immunoprecipitates were performed in the presence (+) and absence (-) of RNase A. **(B)** Epitope HA-tagged versions of MBP (maltose binding protein), AGO2, Me31B, Tral, eIF4E and eIF4G were transiently expressed in S2 cells as indicated above the panels. Cell lysates were immunoprecipitated using a monoclonal anti-HA antibody. Inputs (10%) and immunoprecipitates (IPs) were analyzed by Western blotting using a polyclonal anti-HA antibody. The presence of endogenous Belle in the immunoprecipitates was tested by Western blotting with anti-Belle antibody.

versions of proteins identified by mass spectrometry. Using the antibodies available in our laboratory I immunoprecipitated endogenous GW182, a miRNP complex component [347, 30]; PABP-C, the cytoplasmic poly(A)-binding protein; and Tral (Trailer Hitch/Lsm14), EDC3 and GE-1, which are components of the decapping enhancer complex [424, 118, 405]. GW182 was not on the list of Belle-associated proteins and therefore it served as a negative control. EDC3 was not detected either but was nevertheless included because other components of decapping enhancer complex (Me31B and Ge-1) were present amongst proteins associated with Belle. I found that endogenous Belle co-immunoprecipitated with endogenous PABP-C and Tral; the signal of EDC3 was barely above the background level. The interactions were RNA-dependent and were not observed in the presence of RNase A (Fig. 39A).

In cases when antibodies were not available I used an epitope-tagging approach and expressed HA- or EGFP-tagged versions of the proteins of interest. Endogenous Belle was found to co-immunoprecipitate with HA-tagged versions of AGO2, Me31B, Tral, eIF4E and eIF4G although the relative binding efficiency was low (Fig. 39B).

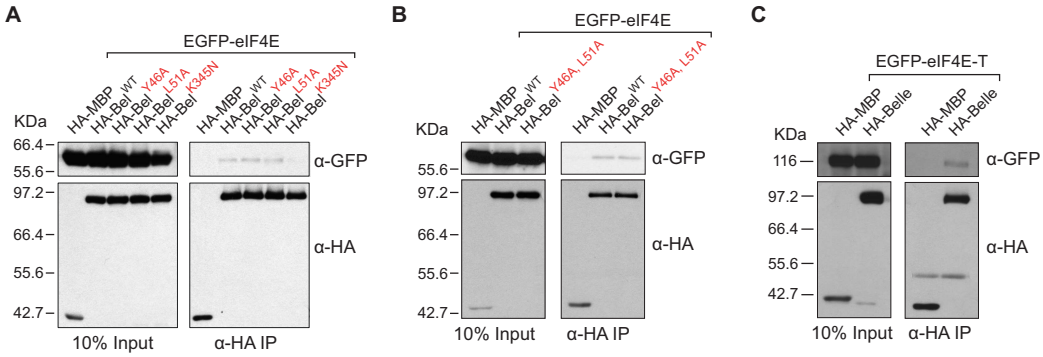

Figure 40. Interaction of Belle with eIF4E and eIF4E-T.

(A, B) HA-tagged wild type Belle or the indicated Belle mutants were cotransfected in S2 cells with EGFP fusions of eIF4E. **(C)** HA-tagged wild type Belle was cotransfected with EGFP fusions of eIF4E-T. Cell lysates were immunoprecipitated using a monoclonal anti-HA antibody. Inputs (10%) and immunoprecipitates were analyzed by Western blotting using polyclonal anti-HA and anti-GFP antibodies. In all panels HA-tagged maltose binding protein (MBP) served as a negative control.

eIF4E binds to the mRNA 5′ cap structure m^7GpppN (where N is any nucleotide), and promotes ribosome binding to the mRNA in the cytoplasm. It has been demonstrated that DDX3, the human ortholog of Belle, is an eIF4E-binding protein [378]. Several eIF4E-binding proteins recognize eIF4E via a consensus YxxxxLΦ motif (the symbol "Φ" represents a hydrophobic residue) [353]. The sequence of DDX3 contains a functional eIF4E-binding motif (YIPPHLR) that interacts with a conserved Y73 residue within the dorsal surface of eIF4E, as occurs with other eIF4E-binding proteins [378].

This motif with a single substitution of I to V is present in *D. melanogaster* Belle at amino-acid residues 46-52 (Fig 29A). To determine whether the interaction of Belle with eIF4E is dependent on this putative eIF4E-binding motif, I introduced amino-acid substitutions in the YVPPHLR motif (Fig. 29A) and examined the effect of the mutations on eIF4E-binding. The mutants of Belle in which the conserved Y64 or L51 residue was replaced with A showed the same level of binding to eIF4E as the wild type Belle (Fig. 40A). Combining these two mutations together also did not change the the ability of Belle to bind eIF4E (Fig. 40B), suggesting that the YVPPHLR motif is not required for the Belle-eIF4E interaction. Interestingly, the K345N mutation which abolishes the putative ATPase activity of Belle also impaired the Belle-eIF4E interaction (Fig. 40A). This finding is consistent with the results of the affinity purification (see Table 6).

eIF4E-T (Transporter) is a nucleocytoplasmic shuttling protein that contains a functional eIF4E-binding motif, which mediates the nuclear import

of eIF4E via the importin-α/β pathway by a piggy-back mechanism [95]. In human cells, eIF4E and eIF4E-T also interact with RCK/p54 (the human ortholog of Me31B) and localize to cytoplasmic P bodies. The *D. melanogaster* ortholog of eIF4E-T is a gene product of CG32016, the protein that was found associated with Belle in my affinity purification. I found that a small fraction of EGFP-tagged CG32012-PC (the longest isoform of *D. melanogaster* eIF4E-T) co-immunoprecipitated with HA-Belle (Fig. 40C). The short isoform CG32012-PE, which lacks the protein's N-terminal fragment with the eIF4E-binding motif, did not co-immunoprecipitate above the background levels observed with the negative control, an HA-tagged version of MBP (data not shown). It is likely that the interaction of Belle and eIF4E-T is not direct and is probably mediated by eIF4E.

The results of the affinity purification of Belle complexes corroborated by immunoprecipitation assays suggest that Belle interacts with Me31B. In the *D. melanogaster* oocyte, Me31B is found within maternal mRNA granules and is required for the proper translational control and localization of the *oskar* mRNA. These mRNP complexes contain the RNA localization protein EXU and Y-box domain protein YPS [303]. EXU contains RNase D-type exonuclease domain that is similar to those found in deadenylases [295]. In the early *Drosophila* embryo Me31B is localized to polar granules where it forms complexes with the Tudor-domain protein TUD or with the DEAD-box helicase VAS. Both complexes also contain the PIWI-like protein AUB, eIF4A and TER94, the transitional ER membrane associated AAA ATPase [402]. In S2 cells, Me31B associates with decapping enzyme DCP2, and with decapping activator DCP1 and enhancer of decapping EDC3 [405]. Another complex that contains Me31B and DCP1 also includes Tral, YPS and translation repressor CUP ([424] and Tritschler *et al.*, in press).

Dhh1p, the *S.cerevisiae* ortholog of Me31B, physically interacts with several proteins involved in mRNA decapping including the decapping enzyme Dcp1p and Pat1p. Dhh1p also associates with Pop2p, a subunit of the CCR4-NOT mRNA deadenylase complex [74]. Moreover, Dhh1p and Pat1p function as translational repressors [73].

Since Me31B is able to interact with many different proteins, I selected several Me31B partners which were identified in the affinity purification of Belle complexes and also included some Me31B partners that were not on the list of Belle-associated proteins. I tested whether EGFP fusions of selected proteins co-immunoprecipitate with HA-tagged Belle when co-expressed in S2 cells.

I found that EGFP-PAT1 (CG5205), the fly ortholog of yeast Pat1p, co-immunoprecipitated with HA-tagged Belle (Fig. 41A). I obtained a similar result for EGFP fusions of EDC3 (Fig. 41C), YPS (Fig. 41E) and CAF1

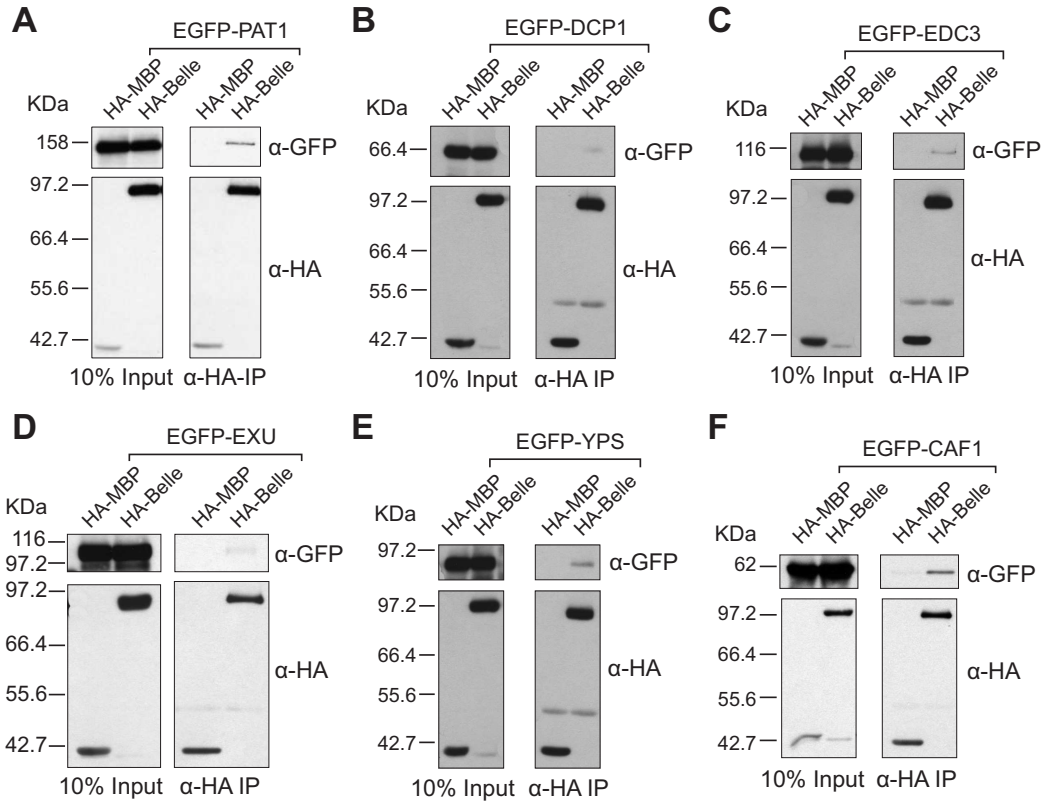

Figure 41. Interaction of Belle with different partners of Me31B.

HA-tagged wild type Belle was cotransfected in S2 cells with EGFP fusions of PAT1 **(A)**, DCP1 **(B)**, EDC3 **(C)**, EXU **(D)**, YPS **(E)** and CAF1 **(F)**. Cell lysates were immunoprecipitated using a monoclonal anti-HA antibody. Inputs (10%) and immunoprecipitates were analyzed by Western blotting using polyclonal anti-HA and anti-GFP antibodies. In all panels HA-MBP served as a negative control.

(CG5684), the *Drosophila* ortholog of yeast Pop2p (Fig. 41F). Only a small fraction of EGPF-DCP1 and EGFP-EXU co-immunoprecipitated with HA-Belle (Fig. 41B and D). Consistent with that, only PAT1 and CAF1 were identified in our affinity purification (Table 6).

Drosophila AGO2 is a key component of the siRNA-mediated gene silencing pathway [180]. In S2 cells AGO2 is associated with dFMR1, the fly ortholog of FMRP, and the DEAD-box helicase Rm62, the fly ortholog of mammalian p68/DDX5 [188]. AGO2 colocalizes with dFMR1, Tral, Me31B and Rm62 in RNP granules in embryos [293]. Mammalian p68 is also found in the Microprocessor complex [149, 125] together with DDX3 and DDX17/p72 (the mammalian orthologs of Belle and CG10077, respectively). AGO2, Rm62 and CG10077 were identified as Belle-associated proteins in the affinity pu-

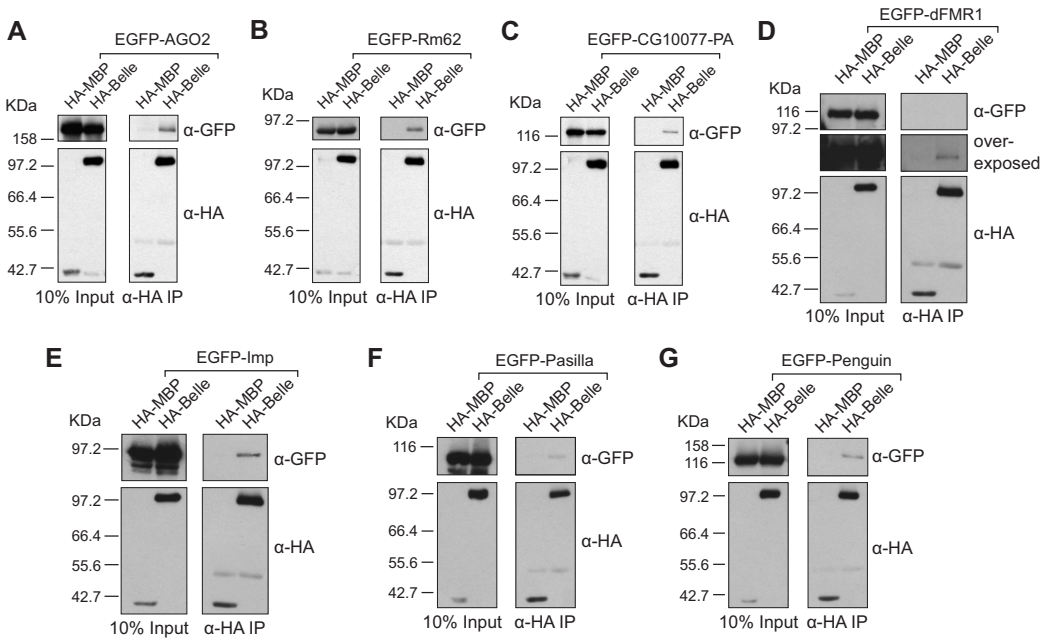

Figure 42. Interaction of Belle with AGO2, DEAD-box helicases and RNA-binding proteins.

HA-tagged wild type Belle was cotransfected in S2 cells with EGFP fusions of AGO2 **(A)**, Rm62 **(B)**, CG10077-PA **(C)**, dFMR1 **(D)**, Imp **(E)**, Pasilla **(F)** and Penguin **(G)**. Cell lysates were immunoprecipitated using a monoclonal anti-HA antibody. Inputs (10%) and immunoprecipitates were analyzed by Western blotting using polyclonal anti-HA and anti-GFP antibodies. In all panels HA-MBP served as a negative control.

rification (Table 6). This result was confirmed by the co-immunoprecipitation assay (Fig. 42A, B, C).

The fragile X mental retardation protein (FMRP) is involved in regulation of mRNA translation, stability and localization [443]. In dendrites, mammalian FMRP is a component of RNA-transporting granules composed of many kinds of proteins, including DDX3, p68/DDX5, translation factors EF-1α, eIF2α, eIF2β and SYNCRIP (proteins which were also identified in the affinity purification, Table 6). These granules are transported by kinesin coordinately with opposite motors, such as dynein [206]. dFMR1 shares the fundamental and characteristic molecular architecture with the mammalian homologues (KH RNA-binding domains), implying functional conservation. In S2 cells, dFMR1-containing RNP granules are transported along microtubules by both kinesin-1 and cytoplasmic dynein [260]. In neuronal cells dFMR1 interacts with Me31B and Tral, where it forms neuronal granules together with AGO2, eIF4E, PABP, DCP1, UPF1, and the translational

regulators YPS, Imp and Pumilio [24]. Although dFMR1 was identified in the affinity purification of Belle protein partners, it was not efficiently co-precipitated with Belle from lysates of cells expressing HA-Belle and an EGFP fusion of dFMR1 (Fig. 42D).

Drosophila IGF-II mRNA binding protein (Imp) is a homolog of the chicken zipcode binding protein ZBP1, and of the human IFG-II mRNA-binding protein, all of which contain four KH RNA-binding domains. Imp RNP particles are actively transported in oogenesis, as well as in neurons by the microtubule motors, dynein and kinesin. In addition, Imp associates with dFMR1 in *Drosophila* ovaries [42].

Pasilla is a *Drosophila* NOVA-like protein that contains two KH RNA-binding domains. Its mammalian homologs are implicated in splicing regulation in neurons [334].

Although both Pasilla and Imp have a rather low Mascot score on the list of proteins associated with Belle (Table 6), both co-precipitated with Belle (Fig. 42E, F).

Pumilio is a member of a widespread PUF protein family of RNA-binding proteins that is implicated in mRNA translation and stability control [422]. Another recently annotated *D. melanogaster* protein that belongs to this family is Penguin. Peptides with a low Mascot score matching Pumilio and Penguin were identified in our mass spectrometry analysis of affinity purified Belle-associated proteins (Table 6). Consistent with this, only the association of Penguin with Belle was confirmed by the co-immunoprecipitation assay (Fig. 42G).

3.11 Belle associates with mRNAs that are regulated at the level of translation

The results of the affinity purification and co-immunoprecipitation assays suggest that endogenous Belle is associated with various types of mRNPs in the cell. If the function of Belle is to regulate translation then it is likely that these mRNPs contain mRNAs that are regulated on a translational level. To test this hypothesis I decided to analyze the RNAs that co-immunoprecipitate with the endogenous protein in lysates from *Drosophila* S2 cells. For this, lysates were immunoprecipitated in presence of RNase inhibitor using anti-Belle or pre-immune rabbit serum. Total RNA was extracted from the immunoprecipitates and an RT-PCR was performed using primer pairs specific for different RNA species. I decided to look for ribosomal 18S RNA; protein-coding mRNAs of *CG2852* and *CG17068* which are expressed at a low level; a highly-abundant *Rp49* mRNA; and mRNAs which expression is regulated

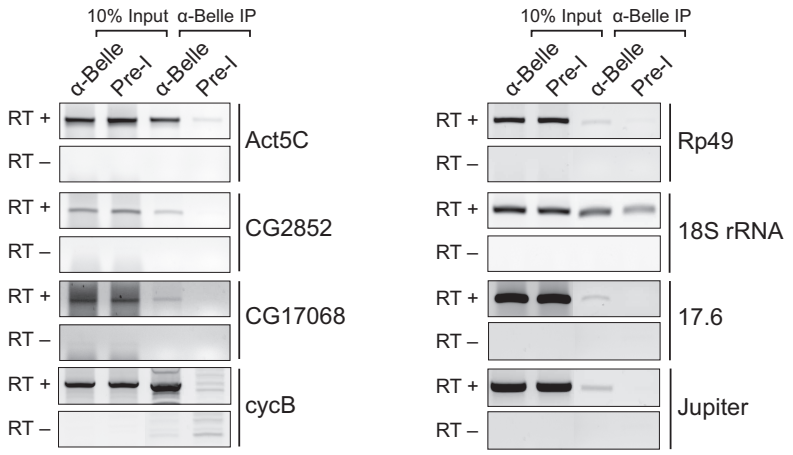

Figure 43. Belle is associated with various mRNAs in S2 cells.

Lysates from S2 cells were immunoprecipitated using anti-Belle rabbit serum (α-Belle) or rabbit pre-immune serum (Pre-I). Total RNA extracted from the immunoprecipitates was analyzed by RT-PCR using primers specific to the genes indicated on the left. The positive or negative signs on the right of the panels indicate that the reverse transcriptase was included (RT+) or omitted (RT-).

at the post-transcriptional level. These included *Act5C* and *cyclin B* mRNAs (translational control), and mRNAs of an LTR (*17.6*) and non-LTR retrotransposon (*Juan*), which are regulated by RNAi (Fig. 43).

Several mRNAs were found to be efficiently and specifically co-immunoprecipitated with endogenous Belle. The efficiency of precipitation was independent of the abundance of a particular mRNA in the cell. This is demonstrated in Fig. 43, based on a comparison of the signals of *Act5C* and *Rp49* mRNAs (highly abundant); *17.6* and *Juan* mRNAs (less abundant); and *CG2852*, *CG17068* and *cyclin B* mRNAs (rare). Ribosomal 18S RNA was present in immunoprecipitates obtained both with anti-Belle and pre-immune serum.

Interestingly, among the seven mRNAs tested, *Act5C* and *cyclin B* mRNAs were the most efficiently precipitated (Fig. 43). β-Actin mRNA is localized near the leading edge in several cell types (reviewed in [75]). The 3′ UTR contains the "zipcode" sequence which is absolutely essential for correct targeting and localized translation of β-actin mRNA. Several regions in the zipcode are conserved among β-actin mRNAs of several species, in particular the sequence `ACACCC`, two copies of which are present in the *Act5C* mRNA 3′ UTR. This sequence is recognized by ZBP1, a KH-domain RNA-binding protein. The *D. melanogaster* ortholog of ZBP1 is Imp, which was found to be associated with Belle (Table 6 and Fig. 42E).

Translation of *cyclin B* mRNA in *Drosophila* is regulated in the embryo by Pumilio, Nanos, and the deadenylase complex and PNG kinase complex [16, 33, 202, 408]. Two *Drosophila* PUF-domain proteins, Pumilio and Penguin, as well as the deadenylase complex components CAF1, CCR4 and NOT proteins were found to be associated with Belle.

Taken together these results suggest that Belle associates with mRNAs that are regulated at the level of translation.

Table 5. GO terms significantly enriched in annotations of proteins associated with Belle.

		FatiGO		*GO Term Finder*		
GO term	Description	Enrichment	Adjusted p-value	Enrichment	Adjusted p-value	FDR rate
Belle wild type						
Molecular function, level 3						
GO:0000166	nucleotide binding	2.7	$5.72 \cdot 10^{-11}$	3.7	$1.91 \cdot 10^{-20}$	0.00%
GO:0003735	structural constituent of ribosome	7.5	$2.11 \cdot 10^{-10}$	7.7	$3.91 \cdot 10^{-12}$	0.00%
GO:0004386	helicase activity	4.7	$4.06 \cdot 10^{-3}$	7.1	$9.38 \cdot 10^{-6}$	0.21%
GO:0008565	protein transporter activity	6.6	$8.40 \cdot 10^{-3}$	11.3	$3.82 \cdot 10^{-8}$	0.00%
Molecular function, level 4						
GO:0017076	purine nucleotide binding	3.0	$4.02 \cdot 10^{-12}$	4.2	$2.47 \cdot 10^{-20}$	0.00%
GO:0008135	translation factor activity, nucleic acid binding	10.9	$1.84 \cdot 10^{-8}$	13.8	$2.66 \cdot 10^{-14}$	0.00%
GO:0003723	RNA binding	4.8	$2.81 \cdot 10^{-7}$	6.2	$3.05 \cdot 10^{-14}$	0.00%
GO:0016817	hydrolase activity, acting on acid anhydrides	3.8	$1.40 \cdot 10^{-6}$	4.5	$1.89 \cdot 10^{-12}$	0.00%
GO:0051082	unfolded protein binding	7.3	$9.64 \cdot 10^{-5}$	10.4	$1.03 \cdot 10^{-7}$	0.00%
Molecular function, level 5						
GO:0030554	adenyl nucleotide binding	2.9	$1.25 \cdot 10^{-8}$	3.7	$2.11 \cdot 10^{-13}$	0.00%
GO:0003743	translation initiation factor activity	13.8	$3.49 \cdot 10^{-7}$	17.1	$3.09 \cdot 10^{-13}$	0.00%
GO:0016818	hydrolase activity, acting on acid anhydrides, in phosphorus-containing anhydrides	3.7	$2.82 \cdot 10^{-6}$	4.5	$1.88 \cdot 10^{-12}$	0.00%
Molecular function, level 6						
GO:0005524	ATP binding	2.9	$3.75 \cdot 10^{-9}$	4.0	$1.01 \cdot 10^{-14}$	0.00%
GO:0016462	pyrophosphatase activity	3.6	$6.94 \cdot 10^{-6}$	4.5	$1.25 \cdot 10^{-12}$	0.00%
Molecular function, level 7						
GO:0017111	nucleoside-triphosphatase activity	3.0	$2.18 \cdot 10^{-5}$	4.6	$6.91 \cdot 10^{-13}$	0.00%
Biological process, level 3						
GO:0009058	biosynthetic process	2.4	$9.17 \cdot 10^{-6}$	2.4	$6.96 \cdot 10^{-8}$	0.00%
GO:0043170	macromolecule metabolic process	1.4	$1.10 \cdot 10^{-5}$	2.6	$3.28 \cdot 10^{-32}$	0.00%
GO:0016043	cellular component organization and biogenesis	1.9	$4.53 \cdot 10^{-5}$	3.5	$8.29 \cdot 10^{-34}$	0.00%
GO:0019953	sexual reproduction	2.6	$4.63 \cdot 10^{-4}$	3.5	$5.44 \cdot 10^{-6}$	0.23%
GO:0044238	primary metabolic process	1.3	$1.46 \cdot 10^{-3}$	2.3	$2.93 \cdot 10^{-29}$	0.00%
GO:0007049	cell cycle	2.6	$2.36 \cdot 10^{-3}$	6.9	$1.48 \cdot 10^{-26}$	0.00%
GO:0051301	cell division	3.4	$3.27 \cdot 10^{-3}$	6.6	$7.35 \cdot 10^{-6}$	0.23%
GO:0048869	cellular developmental process	1.7	$3.80 \cdot 10^{-3}$	2.8	$5.19 \cdot 10^{-6}$	0.24%
GO:0008104	protein localization	2.4	$9.00 \cdot 10^{-3}$	5.0	$6.23 \cdot 10^{-9}$	0.00%

		FatiGO		*GO Term Finder*		
GO term	Description	Enrichment	Adjusted p-value	Enrichment	Adjusted p-value	FDR rate
Biological process, level 4						
GO:0019538	protein metabolic process	2.1	$9.04 \cdot 10^{-13}$	3.4	$2.20 \cdot 10^{-33}$	0.00%
GO:0044260	cellular macromolecule metabolic process	2.0	$1.55 \cdot 10^{-11}$	3.2	$5.39 \cdot 10^{-28}$	0.00%
GO:0044249	cellular biosynthetic process	2.6	$1.08 \cdot 10^{-6}$	2.7	$1.94 \cdot 10^{-9}$	0.00%
GO:0051641	cellular localization	3.3	$6.03 \cdot 10^{-6}$	4.5	$2.01 \cdot 10^{-12}$	0.00%
GO:0007276	gametogenesis	2.5	$3.20 \cdot 10^{-3}$	3.4	$1.38 \cdot 10^{-5}$	0.26%
GO:0022613	ribonucleoprotein complex biogenesis and assembly	4.7	$5.05 \cdot 10^{-3}$	9.7	$3.25 \cdot 10^{-12}$	0.00%
GO:0006996	organelle organization and biogenesis	2.0	$5.38 \cdot 10^{-3}$	4.3	$3.54 \cdot 10^{-26}$	0.00%
GO:0000278	mitotic cell cycle	3.4	$6.29 \cdot 10^{-3}$	9.1	$2.41 \cdot 10^{-30}$	0.00%
GO:0022402	cell cycle process	2.6	$6.62 \cdot 10^{-3}$	7.7	$8.93 \cdot 10^{-28}$	0.00%
GO:0045184	establishment of protein localization	2.8	$6.62 \cdot 10^{-3}$	5.5	$1.58 \cdot 10^{-7}$	0.00%
GO:0030154	cell differentiation	2.6	$8.67 \cdot 10^{-3}$	2.8	$3.06 \cdot 10^{-6}$	0.26%
Biological process, level 5						
GO:0009059	macromolecule biosynthetic process	4.0	$2.57 \cdot 10^{-10}$	2.7	$2.02 \cdot 10^{-9}$	0.00%
GO:0044267	cellular protein metabolic process	2.0	$2.57 \cdot 10^{-10}$	3.3	$3.36 \cdot 10^{-29}$	0.00%
GO:0051649	establishment of cellular localization	3.1	$5.23 \cdot 10^{-5}$	4.4	$5.85 \cdot 10^{-11}$	0.00%
GO:0007010	cytoskeleton organization and biogenesis	3.2	$5.23 \cdot 10^{-4}$	6.9	$9.06 \cdot 10^{-32}$	0.00%
GO:0016050	vesicle organization and biogenesis	11.9	$7.24 \cdot 10^{-3}$	—	—	—
GO:0048468	cell development	1.8	$7.24 \cdot 10^{-3}$	2.9	$2.96 \cdot 10^{-5}$	0.36%
Biological process, level 6						
GO:0006412	translation	5.0	$5.20 \cdot 10^{-13}$	7.6	$1.19 \cdot 10^{-23}$	0.00%
GO:0046907	intracellular transport	3.1	$1.63 \cdot 10^{-3}$	4.9	$4.20 \cdot 10^{-10}$	0.00%
Cellular component, level 3						
GO:0043228	non-membrane-bound organelle	2.6	$6.01 \cdot 10^{-8}$	3.9	$7.05 \cdot 10^{-17}$	0.00%
GO:0044422	organelle part	1.8	$1.28 \cdot 10^{-3}$	2.9	$9.58 \cdot 10^{-18}$	0.00%
Cellular component, level 4						
GO:0005622	intracellular	1.4	$4.17 \cdot 10^{-11}$	2.5	$3.98 \cdot 10^{-45}$	0.00%
GO:0045171	intercellular bridge	10.9	$8.01 \cdot 10^{-3}$	16.5	$8.78 \cdot 10^{-3}$	3.10%
Cellular component, level 5						
GO:0044424	intracellular part	1.3	$3.37 \cdot 10^{-8}$	2.7	$2.94 \cdot 10^{-42}$	0.00%
Cellular component, level 6						
GO:0005737	cytoplasm	2.1	$6.38 \cdot 10^{-11}$	3.8	$1.38 \cdot 10^{-42}1$	0.00%
GO:0030529	ribonucleoprotein complex	4.6	$4.90 \cdot 10^{-9}$	6.3	$1.39 \cdot 10^{-15}$	0.00%
GO:0043229	intracellular organelle	1.3	$5.06 \cdot 10^{-3}$	2.2	$1.75 \cdot 10^{-16}$	0.00%
Cellular component, level 7						
GO:0044444	cytoplasmic part	2.3	$2.75 \cdot 10^{-9}$	4.2	$4.59 \cdot 10^{-37}$	0.00%

		FatiGO		*GO Term Finder*		
GO term	Description	Enrichment	Adjusted p-value	Enrichment	Adjusted p-value	FDR rate
GO:0043232	intracellular non-membrane-bound organelle	2.3	$1.65 \cdot 10^{-6}$	3.9	$7.05 \cdot 10^{-17}$	0.00%
Cellular component, level 8						
GO:0005840	ribosome	4.7	$3.42 \cdot 10^{-7}$	7.9	$5.03 \cdot 10^{-13}$	0.00%
Belle K345N						
Molecular function, level 3						
GO:0003735	structural constituent of ribosome	7.0	$4.16 \cdot 10^{-9}$	6.7	$3.97 \cdot 10^{-10}$	0.00%
GO:0000166	nucleotide binding	2.4	$1.92 \cdot 10^{-7}$	3.0	$4.78 \cdot 10^{-14}$	0.00%
GO:0005515	protein binding	1.3	$4.43 \cdot 10^{-4}$	2.7	$6.81 \cdot 10^{-16}$	0.00%
GO:0004386	helicase activity	4.7	$4.58 \cdot 10^{-3}$	5.6	$6.48 \cdot 10^{-4}$	0.96%
Molecular function, level 4						
GO:0017076	purine nucleotide binding	2.8	$3.30 \cdot 10^{-10}$	3.3	$2.10 \cdot 10^{-14}$	0.00%
GO:0051082	unfolded protein binding	8.7	$3.76 \cdot 10^{-6}$	9.9	$1.05 \cdot 10^{-7}$	0.00%
GO:0008135	translation factor activity, nucleic acid binding	8.5	$1.07 \cdot 10^{-5}$	12.4	$5.47 \cdot 10^{-13}$	0.00%
GO:0016817	hydrolase activity, acting on acid anhydrides	3.1	$3.44 \cdot 10^{-4}$	4.4	$3.54 \cdot 10^{-13}$	0.00%
GO:0003723	RNA binding	3.4	$1.56 \cdot 10^{-3}$	4.5	$3.03 \cdot 10^{-8}$	0.00%
Molecular function, level 5						
GO:0030554	adenyl nucleotide binding	2.9	$1.67 \cdot 10^{-8}$	3.2	$1.22 \cdot 10^{-10}$	0.00%
GO:0003743	translation initiation factor activity	11.6	$3.72 \cdot 10^{-5}$	14.1	$1.84 \cdot 10^{-10}$	0.00%
GO:0016818	hydrolase activity, acting on acid anhydrides, in phosphorus-containing anhydrides	3.2	$4.59 \cdot 10^{-4}$	4.4	$3.54 \cdot 10^{-13}$	0.00%
Molecular function, level 6						
GO:0005524	ATP binding	2.8	$1.75 \cdot 10^{-8}$	3.5	$8.36 \cdot 10^{-12}$	0.00%
GO:0016462	pyrophosphatase activity	3.0	$1.90 \cdot 10^{-3}$	4.4	$2.32 \cdot 10^{-13}$	0.00%
Molecular function, level 7						
GO:0017111	nucleoside-triphosphatase activity	3.1	$1.26 \cdot 10^{-4}$	4.5	$1.25 \cdot 10^{-13}$	0.00%
Biological process, level 3						
GO:0016043	cellular component organization and biogenesis	1.8	$4.53 \cdot 10^{-4}$	3.1	$5.17 \cdot 10^{-28}$	0.00%
GO:0019953	sexual reproduction	2.6	$4.53 \cdot 10^{-4}$	3.8	$1.06 \cdot 10^{-8}$	0.00%
GO:0009058	biosynthetic process	2.0	$1.75 \cdot 10^{-3}$	2.2	$2.39 \cdot 10^{-7}$	0.00%
GO:0051301	cell division	3.6	$1.88 \cdot 10^{-3}$	5.4	$4.31 \cdot 10^{-4}$	0.47%
GO:0008104	protein localization	2.7	$2.64 \cdot 10^{-3}$	4.0	$7.09 \cdot 10^{-6}$	0.09%
GO:0043170	macromolecule metabolic process	1.3	$6.58 \cdot 10^{-3}$	2.2	$5.60 \cdot 10^{-22}$	0.00%
Biological process, level 4						
GO:0019538	protein metabolic process	1.9	$3.70 \cdot 10^{-8}$	2.8	$7.67 \cdot 10^{-22}$	0.00%
GO:0044260	cellular macromolecule metabolic process	1.8	$9.12 \cdot 10^{-7}$	2.5	$8.80 \cdot 10^{-17}$	0.00%

		FatiGO		*GO Term Finder*		
GO term	Description	Enrichment	Adjusted p-value	Enrichment	Adjusted p-value	FDR rate
GO:0044249	cellular biosynthetic process	2.6	$1.03 \cdot 10^{-3}$	2.4	$9.35 \cdot 10^{-8}$	0.00%
GO:0051641	cellular localization	2.6	$2.82 \cdot 10^{-3}$	3.6	$5.26 \cdot 10^{-8}$	0.00%
GO:0007276	gametogenesis	2.4	$3.51 \cdot 10^{-3}$	3.7	$1.42 \cdot 10^{-7}$	0.00%
GO:0045184	establishment of protein localization	2.9	$3.56 \cdot 10^{-3}$	4.7	$6.75 \cdot 10^{-6}$	0.09%
Biological process, level 5						
GO:0009059	macromolecule biosynthetic process	3.4	$4.66 \cdot 10^{-7}$	2.6	$2.23 \cdot 10^{-9}$	0.00%
GO:0044267	cellular protein metabolic process	1.8	$1.47 \cdot 10^{-6}$	2.7	$2.61 \cdot 10^{-18}$	0.00%
Biological process, level 6						
GO:0006412	translation	4.3	$1.97 \cdot 10^{-9}$	6.4	$1.51 \cdot 10^{-18}$	0.00%
Cellular component, level 3						
GO:0043228	non-membrane-bound organelle	2.6	$6.33 \cdot 10^{-8}$	3.5	$1.42 \cdot 10^{-14}$	0.00%
GO:0044422	organelle part	1.7	$2.88 \cdot 10^{-3}$	2.7	$2.74 \cdot 10^{-16}$	0.00%
Cellular component, level 4						
GO:0005622	intracellular	1.4	$1.20 \cdot 10^{-10}$	2.3	$1.84 \cdot 10^{-37}$	0.00%
GO:0045171	intercellular bridge	13.1	$8.64 \cdot 10^{-4}$	19.6	$3.31 \cdot 10^{-4}$	0.88%
Cellular component, level 5						
GO:0044424	intracellular part	1.3	$2.17 \cdot 10^{-7}$	2.4	$1.22 \cdot 10^{-36}$	0.00%
GO:0045172	germline ring canal	11.8	$1.19 \cdot 10^{-3}$	19.6	$3.31 \cdot 10^{-4}$	0.86%
Cellular component, level 6						
GO:0005737	cytoplasm	2.1	$2.66 \cdot 10^{-11}$	3.5	$1.44 \cdot 10^{-39}$	0.00%
GO:0030529	ribonucleoprotein complex	4.3	$3.31 \cdot 10^{-8}$	6.2	$2.02 \cdot 10^{-16}$	0.00%
Cellular component, level 7						
GO:0044444	cytoplasmic part	2.4	$1.76 \cdot 10^{-10}$	12.7	$5.93 \cdot 10^{-25}$	0.00%
GO:0043232	intracellular non-membrane-bound organelle	2.3	$1.37 \cdot 10^{-6}$	3.5	$1.42 \cdot 10^{-14}$	0.00%
Cellular component, level 8						
GO:0005840	ribosome	4.4	$2.17 \cdot 10^{-6}$	6.9	$6.25 \cdot 10^{-11}$	0.00%
GO:0005829	cytosol	4.1	$1.72 \cdot 10^{-3}$	13.5	$4.55 \cdot 10^{-42}$	0.00%
GO:0045169	fusome	12.4	$2.55 \cdot 10^{-3}$	17.9	$5.48 \cdot 10^{-3}$	2.14%

Table 6. Proteins associated with Belle in *Drosophila* S2 cells.

		Mascot score		No. of peptides			
Gene ID	Gene name	wild type	K345N	wild type	K345N	Mol. weight	Function
CG9748	Belle	7215	2557	280	64	85371	DDX3-like DEAD box RNA helicase
CG4264	Hsc70-4 (Heat shock cognate 4)	7656	1475	248	30	71300	Unfolded protein binding, ATPase
CG10811	eIF4G	2548	2965	53	65	184570	Translation initiation factor
CG8977	CCTγ (TCP 1 subunit gamma)	3315	2056	87	46	60043	Chaperonin for tubulin and actin
CG5374	CCTα (TCP 1 subunit alpha)	2618	1399	69	28	60423	Chaperonin for tubulin and actin
CG4257	Stat92E	2601	1126	63	24	86361	Signal transduction
CG8231	CCTζ-2 (TCP 1 subunit zeta-2)	2323	1370	77	32	58495	Chaperonin for tubulin and actin
CG10077	DmRH5	2347	1201	66	33	88497	DDX17/DDX5-like DEAD-box RNA helicase
CG14472	Pushover (Purity of essence)	2713	512	60	10	597892	Ubiquitin cycle, calmodulin binding
CG8258	CCTθ (TCP 1 subunit theta)	1573	1553	31	54	59795	Chaperonin for tubulin and actin
CG8351	CCTη (TCP 1 subunit eta)	1815	1158	41	23	59976	Chaperonin for tubulin and actin
CG7033	CCTβ (TCP 1 subunit beta)	1383	1489	39	33	58483	Chaperonin for tubulin and actin
CG1242	Hsp83 (Heat shock protein 83)	1579	1171	27	22	82099	Unfolded protein binding, ATPase
CG11198	CG11198	891	1837	19	40	279847	Carbamoyl-phosphate synthase, biotin carboxylase, acetyl-CoA carboxylase
CG4147	Hsp70-3 (Heat shock cognate 72)	2256	396	61	11	72304	Unfolded protein binding, ATPase
CG1913	α-Tub84B (α-Tubulin at 84B)	1624	802	46	17	50561	Structural constituent of cytoskeleton
CG1884	Not1	785	1595	17	36	245848	CCR4-NOT deadenylation complex component
CG3210	Drp1 (Dynamin related protein 1)	1092	1187	20	25	83085	Structural constituent of cytoskeleton, GTPase
CG5119	PABPC	2144	90	49	1	69886	Polyadenylate-binding protein
CG7935	Moleskin	932	1011	17	21	120094	Protein import into nucleus, Ran GTPase binding
CG8649	Fimbrin	1768	0	36	0	72382	Cytoskeleton organization and biogenesis, actin binding
CG7070	PyK	222	1528	12	25	57950	Pyruvate kinase activity
CG2168	RpS3A	844	900	18	24	30549	Structural constituent of ribosome
CG32016	eIF4E-T	567	1121	9	22	114390	Translation initiation factor 4E transporter
CG9277	βTub56D (β-Tubulin at 56D)	1687	0	59	0	50571	Structural constituent of cytoskeleton
CG6779	RpS3	720	834	12	19	27682	Structural constituent of ribosome

Gene ID	Gene name	Mascot score		No. of peptides		Mol. weight	Function
		wild type	K345N	wild type	K345N		
CG2146	Didum	662	785	15	19	208656	Motor protein myosin V, mRNA localization
CG5520	Gp93 (Glycoprotein 93)	1332	0	23	0	90296	Unfolded protein binding, ATPase
CG10306	eIF3-S12	408	869	8	18	25820	Translation initiation factor
CG6876	Prp31	1174	72	23	2	55795	U4/U6 snRNP component, pre-mRNA splicing
CG5000	Msps (mini spindles)	374	867	7	19	226743	Structural constituent of cytoskeleton, *bicoid* mRNA localization
CG6718	CG6718	1129	108	28	2	97771	Calcium-independent phospholipase A2
CG32435	Orbit (chb, chromosome bows)	411	820	9	18	166783	Mitotic spindle organization and biogenesis
CG10160	ImpL3	466	727	9	16	35800	L-lactate dehydrogenase
CG5064	Srp68	1134	39	22	1	69593	SRP-dependent cotranslational protein targeting to membrane
CG1486	CG1486	247	919	5	21	92150	Pyridoxal-dependent decarboxylase
CG1515	lethal (1) G0155	267	892	5	17	22576	Vesicle-mediated transport
CG1258	Pavarotti	229	920	5	20	101118	Kinesin motor, microtubule-based movement
CG18102	Shibire	467	639	7	13	98874	Dynamin, vesicle-mediated transport
CG7915	Ect4	399	703	10	17	148989	Transmembrane receptor, RNA binding
CG15112	Enabled	556	542	13	10	88740	Structural constituent of cytoskeleton, actin binding
CG4260	α-Adaptin	507	590	11	11	106352	Vesicle-mediated transport
CG13345	Tumbleweed	1014	47	17	1	70574	Rho protein signal transduction
CG1691	Imp	976	81	23	2	62376	mRNA binding, translation control
CG2097	Symplekin	168	840	4	16	133020	mRNA 3′ end formation, cleavage and polyadenylation complex component
CG1524	RpS14A	551	444	7	8	16312	Structural constituent of ribosome
CG1341	Rpt1	988	0	16	0	48910	Proteasome 26S subunit ATPase 2
CG5800	DmRH14	72	895	2	15	93244	DDX10-like DEAD-box RNA helicase
CG9412	Rasputin	319	633	6	12	75111	G3BP-2-like, mRNA binding, Ras protein signal transduction
CG8571	Smallminded	194	743	4	14	104901	AAA ATPase, S16 ion peptidase
CG9946	eIF2α	643	276	11	4	38850	Translation initiation factor
CG12051	Act42A (actin 42A)	0	911	0	20	42196	Structural constituent of cytoskeleton

Gene ID	Gene name	Mascot score		No. of peptides		Mol. weight	Function
		wild type	K345N	wild type	K345N		
CG10777	DmRH1	192	699	4	17	100698	DEAD/DEAH-box RNA helicase, Eggshell protein
CG14792	Sta (subarista, RpSA)	465	423	10	14	35547	Structural constituent of ribosome
CG8144	Pasilla	709	168	14	3	61498	NOVA-like, mRNA binding
CG32066	CG32066	306	570	5	13	36831	Uncharacterised
CG9484	HYD (Hyperplastic discs)	727	113	15	4	321704	Ubiquitin ligase with Poly(A)-binding (PABC) domain
CG4046	RpS16	357	479	8	10	16878	Structural constituent of ribosome
CG6143	Pep	725	108	11	3	78570	Regulation of pre-mRNA splicing, ssDNA/RNA-binding
CG12876	ALiX	829	0	13	0	92938	Rho GTPase activation
CG7490	RpLP0	322	501	5	9	34295	Structural constituent of ribosome
CG8439	CCTϵ (TCP 1 subunit epsilon)	648	164	16	3	59697	Chaperonin for tubulin and actin
CG1883	RpS7	180	628	4	13	22156	Structural constituent of ribosome
CG1666	Hlc	805	0	12	0	63357	DDX56-like DEAD box RNA helicase
CG17870	14-3-3ζ	147	657	2	9	28324	Diacylglycerol-activated phospholipid-dependent protein kinase C inhibitor
CG9012	Chc (Clathrin heavy chain)	798	0	12	0	192937	Receptor-mediated endocytosis, vesicle-mediated transport
CG5726	CG5726	695	56	9	2	86939	Uncharacterised
CG14695	CG14695	251	486	4	13	33732	Uncharacterised
CG2684	Lodestar	182	552	4	15	118759	SNF2-like DEAH-box helicase, RNAP II transcription termination factor 2
CG17291	PP2A-29B	380	347	9	6	66067	Serine/threonine-protein phosphatase PP2A 65 kDa regulatory subunit
CG11276	RpS4	112	583	3	16	29230	Structural constituent of ribosome
CG9999	RanGAP	694	0	12	0	66613	Ran GTPase activator
CG5525	CCTδ (TCP 1 subunit delta)	0	684	0	13	57764	Chaperonin for tubulin and actin
CG9325	Hts (hu li tai shao)	435	240	8	4	79528	Structural constituent of cytoskeleton, actin binding
CG6428	CG6428	641	0	11	0	69645	Amino acid metabolism
CG6692	Cp1 (Cathepsin L)	150	459	2	7	41974	Proteolysis
CG12008	Karst	499	107	9	2	472720	Signal transduction, cytoskeleton associated
CG8882	eIF3-S2 (Trip1)	592	0	7	0	36365	Translation initiation factor 3 subunit 2
CG9712	TSG101	407	181	8	4	45333	Ubiquitin-protein ligase

		Mascot score		No. of peptides			
Gene ID	Gene name	wild type	K345N	wild type	K345N	Mol. weight	Function
CG8280	EF1α/EF-Tu	525	61	11	1	50535	Translation elongation factor
CG31022	PH4αEFB,	573	0	11	0	63360	Procollagen-proline 4-dioxygenase
CG5434	SRP72	335	225	5	4	73433	Signal recognition particle 72 kDa protein
CG32407	CG32407	277	280	5	5	28227	Retinaldehyde/retinal-binding protein
CG14895	Pak3	554	0	11	0	64506	Protein kinase
CG11804	Ced-6	551	0	10		56220	Signal transduction
CG8309	Tango7	426	123	6	2	44515	Translation initiation factor eIF3-M-like, Golgi biogenesis
CG2708	Tom34	75	471	1	10	106548	Transmembrane transporter activity, ATPase
CG1902	CG1902	163	368	2	6	35883	Uncharacterised
CG8863	CG8863	248	283	5	4	45886	DnaJ-like, heat shock protein
CG17904	CG17904	217	311	4	5	33734	NUBP1-like, AAA ATPase
CG4954	eIF3-S8	115	408	3	10	106158	Translation initiation factor
CG17170	Su(f) (CSTF3/CstF-77)	510	0	7	0	41670	Cleavage stimulation factor 77 kDa subunit , polyadenylate-binding
CG14813	δCOP	500	0	10	0	58010	Vesicle-mediated transport
CG7324	CG7324	0	499	0	7	147970	Rab GTPase activator activity
CG9738	Mkk4	499	0	8	0	48029	MAP kinase kinase activity, JUN kinase kinase activity
CG3714	CG3714	398	92	7	1	62582	Nicotinate phosphoribosyltransferase
CG3572	Vimar	478	0	7	0	71048	Uncharacterised
CG2238	EF2b	471	0	11	0	95424	Translation elongation factor
CG5105	Plap	468	0	8	0	86666	Uncharacterised
CG8266	Sec31	134	330	2	7	137010	Intracellular protein transport
CG1685	Penguin	216	244	4	5	81765	mRNA 3′-UTR binding, translation repressor
CG4464	RpS19A	52	390	2	11	17394	Structural constituent of ribosome
CG6841	Prp6	95	347	2	10	105960	Pre-mRNA splicing, U5 snRNP component
CG17498	Mad2	0	436	0	9	23618	Mitotic cell cycle checkpoint
CG31196	14-3-3ε	77	356	1	7	29951	Ras protein signal transduction
CG8922	RpS5A	0	429	0	8	25760	Structural constituent of ribosome
CG3661	RpL23	423	0	10	0	15041	Structural constituent of ribosome
CG1422	p115	422	0	7	0	93094	Intracellular protein transport
CG1059	Importin-β 3	98	321	4	8	125078	Protein import into nucleus

Gene ID	Gene name	Mascot score		No. of peptides		Mol. weight	Function
		wild type	K345N	wild type	K345N		
CG11324	Homer	0	413	0	5	42906	G-protein coupled receptor protein signaling
CG8947	26-29-p	45	363	2	6	62661	Proteolysys
CG11148	CG11148	165	234	2	4	173973	Uncharacterised
CG9677	Int6 (eIF3-S6)	181	217	4	4	51756	Translation initiation factor
CG3356	CG3356	0	393	0	8	129831	Ubiquitin ligase
CG7726	RpL11	203	190	3	3	21270	Structural constituent of ribosome
CG9359	βTub85D (β-Tubulin at 85D)	386	0	18	0	50418	Structural constituent of cytoskeleton
CG1528	γCop	374	0	8	0	98498	Vesicle-mediated transport
CG9155	Myosin 61F	0	363	0	7	118410	Myosin IB, structural constituent of cytoskeleton
CG9543	εCOP	0	363	0	5	34825	Vesicle-mediated transport
CG9075	eIF4A	181	175	3	2	46149	Translation initiation factor
CG6223	βCop	153	202	2	5	108308	Vesicle-mediated transport
CG8636	eIF3-S4	67	283	1	7	30155	Translation initiation factor
CG1821	RpSL31	339	0	6	0	14581	Structural constituent of ribosome
CG8014	Rme-8	0	334	0	8	274770	Vesicle-mediated transport
CG17219	CG17219	0	331	0	6	35280	Uncharacterised
CG11738	lethal (1) G0004	43	287	1	7	26774	mRNA binding, rRNA processing
CG8611	CG8611	0	329	0	5	108002	DDX31-like DEAD box RNA helicase
CG17514	GCN1	0	327	0	8	296460	eIF2α-kinase binding and activation, translation activation
CG10206	Nop5	320	0	4	0	57349	rRNA processing
CG17838	SYNCRIP	317	0	7	0	63607	HnRNP R and Q splicing factor
CG8831	CG8831	315	0	7	0	64642	Nucleoporin
CG3221	CG3221	314	0	5	0	63164	Uncharacterised
CG3126	C3G	0	313	0	6	173561	Regulation of small GTPase mediated signal transduction
CG7283	RpL10Ab	0	306	0	5	24429	Structural constituent of ribosome
CG5269	Vibrator	0	305	0	8	31495	Phosphatidylinositol transfer protein
CG2747	CG2747	0	302	0	7	234071	Uncharacterised
CG32210	ZNF294	0	300	0	6	201061	Uncharacterised
CG3248	Cog3 (Sec34)	0	296	0	5	102032	Vesicle-mediated transport
CG7014	RpS5b	0	296	0	5	25985	Structural constituent of ribosome
CG10279	DmRH8 (Rm62, Dmp68)	293	0	7	0	78956	DDX5-like DEAD-box RNA helicase
CG1107	Auxillin	0	292	0	7	129154	Serine/threonine kinase activity, ATP binding.

Gene ID	Gene name	Mascot score		No. of peptides		Mol. weight	Function
		wild type	K345N	wild type	K345N		
CG4878	eIF3-S9	291	0	6	0	80733	Translation initiation factor
CG9476	α-Tub85E (α-Tubulin at 85E)	291	0	10	0	50631	Structural constituent of cytoskeleton
CG15797	Ric8a	290	0	6	0	66587	G-protein alpha-subunit binding
CG17489	RpL5	0	289	0	5	34244	Structural constituent of ribosome
CG5602	CG5602	287	0	5	0	85407	DNA ligase
CG11963	CG11963	285	0	5	0	55172	Succinyl-CoA ligase
CG2706	fs(1)Yb (female sterile (1) Yb)	0	284	0	4	118745	Stem-cells maintenance, oogenesis
CG5366	CAND1	0	283	0	7	140806	Transcription factor binding
CG4552	TBC1D23	275	0	5	0	78440	RabGAP/TBC
CG9755	Pumilio	95	180	2	5	158171	mRNA 3′-UTR binding, translation repressor
CG3395	RpS9	0	273	0	7	22610	Structural constituent of ribosome
CG4658	CG4658	0	271	0	5	59124	Uncharacterised
CG13389	RpS13	52	217	1	7	17168	Structural constituent of ribosome
CG4035	eIF4E	265	0	5	0	29320	Translation initiation factor
CG8715	Lingerer	0	260	0	5	135935	Uncharacterised
CG3278	Tif-IA	258	0	4	0	71331	RNAP I specific transcription initiation factor RRN3, RNAP II general factor
CG10973	CG10973	0	257	0	4	34226	Hsp70-binding protein 1 (HspBP1)
CG31453	CG31453	250	0	3	0	46819	AAA ATPase
CG1559	Upf1	0	247	0	5	131256	DEAD/DEAH box helicase, regulator of NMD
CG5266	Pros25	0	246	0	3	26004	Threonine endopeptidase, proteasome subunit
CG7238	Sip1 (septin interacting protein 1)	0	246	0	4	95110	Pre-mRNA-splicing factor SPP382
CG4916	Me31B	245	0	5	0	52663	DDX6-like DEAD box RNA helicase
CG5436	Hsp68 (Heat shock protein 68)	242	0	4	0	70043	Unfolded protein binding, ATPase
CG5684	Pop2 (CAF1)	0	240	0	4	34232	CCR4-NOT deadenylase complex subunit
CG6453	CG6453	185	55	4	1	62414	Alpha-glucosidase activity, calcium ion binding
CG18593	Viaf	0	236	0	3	27541	Phosducin-like protein
CG11943	CG11943	0	232	0	5	237335	Nucleoporin
CG32165	Importin 4	0	230	0	6	122234	Protein import into nucleus
CG4276	Arouser	227	0	5	0	85251	EGF receptor signaling

		Mascot score		No. of peptides			
Gene ID	Gene name	wild type	K345N	wild type	K345N	Mol. weight	Function
CG18495	Prosα6	107	118	2	2	27460	Threonine endopeptidase, proteasome subunit
CG6831	Rhea	222	0	5	0	308914	Structural constituent of cytoskeleton, actin binding
CG10882	Sec24D	0	220	0	4	130328	Vesicle-mediated transport
CG2331	TER94	218	0	5	0	89518	DEAD box helicase, AAA ATPase
CG4858	CG4858	48	170	1	4	28688	AAA ATPase
CG4968	CG4968	0	217	0	4	30524	Ubiquitin thioesterase
CG10652	RpL30	215	0	4	0	12398	Structural constituent of ribosome
CG5077	CG5077	0	214	0	4	92404	Oxysterol-binding protein
CG6877	Aut1	0	212	0	3	37274	Autophagy
CG3226	CG3226	0	209	0	3	25824	Calcyclin binding
CG1475	RpL13A	0	208	0	6	23803	Structural constituent of ribosome
CG1548	Cathepsin D	208	0	3	0	42788	Peptidase
CG10743	CG10743	206	0	3		76057	Uncharacterised
CG3922	RpS17	206	0	4	0	15332	Structural constituent of ribosome
CG8368	CG8368	204	0	4	0	77128	Riboexonuclease, RNaseH-like
CG7762	Rpn1	203	0	4	0	103010	Proteolysis
CG5166	Ataxin-2	55	147	1	3	117734	mRNA binding, PABP interacting
CG7439	Argonaute 2	0	201	0	5	137677	RNA-mediated gene silencing
CG6141	RpL9	0	199	0	4	21563	Structural constituent of ribosome
CG7002	Homolectin	198	0	4	0	443460	Chitin metabolic process
CG3040	CG3040	0	195	0	4	27200	Uncharacterised
CG6476	Su(var)3-9	0	191	0	2	52080	Establishment and/or maintenance of chromatin architecture
CG4799	Pendulin	83	105	3	2	58055	Importin-α-like, protein import into nucleus
CG9247	MUT7	186	0	3	0	72876	3′-5′ exonuclease (Rnase H fold)
CG14476	CG14446	0	185	0	4	106064	Glucosidase II subunit alpha
CG6203	dFMR1	185	0	4	0	75967	mRNA binding, translation repression
CG4153	eIF2β	110	74	2	1	35481	Translation initiation factor
CG3715	Shc (SHC-adaptor protein)	0	180	0	3	45405	EGF receptor signaling
CG8828	CG8828	180	0	3	0	78442	Uncharacterised
CG8201	Par-1	0	179	0	4	89237	Protein serine/threonine kinase activity
CG2637	Fs(2)Ket (Female sterile (2) Ketel)	177	0	2	0	99886	Importin-β 1, protein import into nucleus

Gene ID	Gene name	Mascot score		No. of peptides		Mol. weight	Function
		wild type	K345N	wild type	K345N		
CG9327	Pros29	0	175	0	6	29735	Threonine endopeptidase, proteasome subunit
CG33101	Nsf2	174	0	3	0	83781	AAA ATPase
CG7398	Transportin	174	0	3	0	102934	Importin-β 2, protein import into nucleus
CG9206	Glued	0	172	0	3	141701	Dynactin subunit p150, structural constituent of cytoskeleton
CG15445	CG15445	171	0	2	0	69838	Uncharacterised
CG7878	Rm26	171	0	7	0	78975	DEAD-box RNA helicase
CG17611	eIF6	0	170	0	5	26649	Translation initiation factor
FBgn0013437	*copia* GIP (gag-int-pol)	0	170	0	3	48649	Transposon protein
CG3647	Shuttle craft	0	168	0	3	128769	Regulation of transcription from RNAP II promoter
CG5313	RfC3	0	167	0	2	37840	DNA replication, DNA repair
CG10923	Klp67A	166	0	2	0	92863	Kinesin motor, microtubule-based movement
CG12770	Vps28	0	163	0	5	24781	Vesicle-mediated transport
CG7581	Bub3	162	0	3	0	37791	Mitotic checkpoint protein
CG31256	Brf	161	0	3	0	74341	Transcription factor IIIB
CG17766	CG17766	0	153	0	4	170592	GTPase activity
CG11199	Liprin-α	0	151	0	4	135100	Receptor binding, anterograde synaptic vesicle transport
CG12737	Crag	0	149	0	3	161912	Vesicle-mediated transport
CG9829	Poly (did)	0	148	0	3	28209	Uncharacterised
CG10711	Vps36	0	147	0	1	44471	*bicoid* mRNA 3′ UTR binding and localization
CG33106	Mask	147	0	2	0	425153	Structural constituent of cytoskeleton, RNA binding
CG8465	lethal (1) G0222	0	147	0	3	129615	Uncharacterised
CG10212	SMC2	0	146	0	3	135050	Structural maintenance of chromosomes
CG4215	Spellchecker1	0	144	0	4	104102	DNA mismatch repair protein MutS
CG3004	CG3004	0	137	0	2	35952	GTPase activity, mRNA binding, rRNA metabolic process
CG9528	Retm	136	0	2	0	76201	Cellular retinaldehyde-binding/triple function

		Mascot score		No. of peptides			
Gene ID	Gene name	wild type	K345N	wild type	K345N	Mol. weight	Function
CG32485	CG32485	0	135	0	4	26370	Retinaldehyde/retinal-binding proteins
CG1115	CG1115	0	132	0	3	24361	Vesicle-mediated transport
CG5787	CG5787	0	127	0	2	100425	Wnt signalling
CG11761	Translin	0	126	0	2	27123	DNA binding, recombination
CG8588	Pastrel	50	76	1	1	72085	Uncharacterised
CG8230	CG8230	125	0	2	0	79702	Dymeclin (Dyggve-Melchior-Clausen syndrome protein)
CG1651	Ankyrin	0	124	0	3	172000	Structural constituent of cytoskeleton
CG18572	Rudimentary	0	124	0	4	248796	Carbamoyl-phosphate synthase
CG9360	CG9360	45	78	1	1	27348	2,3-dihydro-2,3-dihydroxybenzoate dehydrogenase
CG8400	Casper	122	0	2	0	78905	Signal transduction, apoptosis
CG15693	RpS20	121	0	3	0	13593	Structural constituent of ribosome
CG4755	RhoGAP92B	121	0	2	0	83547	GTPase activator activity
CG9635	RhoGEF2	117	0	4	0	282202	Rho guanyl-nucleotide exchange factor activity
CG1957	CPSF2	116	0	2	0	85935	Cleavage and polyadenylation specificity factor subunit 2
CG6811	RhoGAP68F	116	0	2	0	55220	Rho GTPase activator
CG11397	Gluon	0	115	0	3	160639	Structural maintenance of chromosomes
CG5208	PAT1	0	115	0	2	108322	Decapping activator, P body component
CG12241	CG12241	114	0	1	0	92532	Regulation of Rab GTPase
CG12244	Licorne	112	0	2	0	38512	Tyrosine protein kinase
CG6406	CG6406	112	0	2	0	60166	Uncharacterised
CG2033	RpS15A	109	0	3	0	14933	Structural constituent of ribosome
CG3948	ζCOP	0	108	0	1	20151	Vesicle-mediated transport
CG1401	Cullin-5	107	0	3	0	97268	Proteolysis
CG9273	RPA2	0	107	0	3	26565	DNA recombination and repair
CG1489	Pros45	0	106	0	2	45480	26S protease regulatory subunit 8
CG1951	CG1951	106	0	2	0	93854	Vesicle-associated kinase
CG7375	CG7375	106	0	2	0	21067	NEDD8-conjugating enzyme Ubc12
CG8478	CG8478	106	0	2	0	60865	Nucleic acid binding; zinc ion binding
CG8830	CG8830	105	0	2	0	96140	Ubiquitin cycle

		Mascot score		No. of peptides			
Gene ID	Gene name	wild type	K345N	wild type	K345N	Mol. weight	Function
CG4849	U5-116 kDa	0	104	0	2	111606	Pre-mRNA splicing, U5 snRNP component
CG5837	Hem (HEM-protein)	0	103	0	2	130665	Cytoskeleton organization and biogenesis
CG4659	Srp54k	0	102	0	2	56172	SRP-dependent cotranslational protein targeting to membrane
CG8963	PAIP1	102	0	2	0	63589	Polyadenylate-binding protein-interacting protein 1 homolog
CG1227	CG1227	0	101	0	2	37053	Serine/threonine protein kinase
CG7434	RpL22	100	0	1	0	30649	Structural constituent of ribosome
CG10539	S6k	0	99	0	1	55677	Ribosomal S6 protein serine/threonine kinase
CG5974	Pelle	0	99	0	2	56467	Protein serine/threonine kinase
CG7698	CPSF3	99	0	1	0	77688	Cleavage and polyadenylation specificity factor 73 kDa subunit
CG12306	Polo	96	0	1	0	67614	Serine/threonine kinase
CG1977	α-Spectrin	0	95	0	3	279101	Cytoskeletal protein binding, organelle organization and biogenesis
CG4164	CG4164	0	91	0	1	40585	DnaJ-like, heat shock protein
CG7885	RpII33 (RNAP II 33kD subunit)	0	91	0	2	31566	DNA-directed RNA polymerase
CG11837	CG11837	0	89	0	3	35254	rRNA (adenine-N6,N6-)-dimethyltransferase
CG11888	Rpn2	0	89	0	2	113754	26S proteasome regulatory subunit RPN2
CG10967	Atg1	88	0	2	0	91501	Serine/threonine protein kinase
CG6303	Bruce	88	0	1	0	545829	Ubiquitin-conjugating enzyme, E2
CG31137	Twin (CCR4)	0	87	0	1	65450	CCR4-NOT deadenylase complex component
CG3558	CG3558	0	87	0	3	114743	Uncharacterised
CG10732	PCM1	0	86	0	2	184338	Pericentriolar Material 1protein (PCM1) homolog
CG8415	RpS23	86	0	1	0	16064	Structural constituent of ribosome
CG8900	RpS18	86	0	1	0	17658	Structural constituent of ribosome
CG2034	CG2034	0	85	0	1	29094	Uncharacterised
CG31426	Ligatin	83	0	1	0	62206	Translation initiation factor
CG6181	Ge-1 (EDC4)	0	82	0	2	150525	Enhancer of decapping

Gene ID	Gene name	Mascot score		No. of peptides		Mol. weight	Function
		wild type	K345N	wild type	K345N		
CG8426	l(2)NC136 (NOT3)	0	82	0	1	92596	CCR4-NOT deadenylase complex component
CG2213	CG2213	0	81	0	1	28500	Uncharacterised
CG2038	CSN7	0	80	0	1	31219	Protein deneddylation
CG3980	CG3980	80	0	1	0	90899	Protein phosphatase type 1 regulator
CG8487	Gartenzwerg	0	79	0	1	222049	Vesicle-mediated transport
CG9143	CG9143	0	79	0	1	91804	DDX24-like DEAD box RNA helicase
CG14999	RfC40	78	0	2	0	37549	AAA ATPase
CG9769	eIF3-S5	0	78	0	1	31370	Translation initiation factor
CG12233	lethal (1) G0156	77	0	1	0	38902	Isocitrate dehydrogenase (NAD^+) activity
CG31000	Hephaestus (PTB/hnRNP I)	77	0	2	0	61391	Polypyrimidine Tract Binding protein, pre-mRNA splicing
CG2161	Regena (NOT2)	76	0	1	0	59434	CCR4-NOT deadenylase complex subunit 2
CG6684	RpS25	76	0	2	0	13193	Structural constituent of ribosome
CG12740	RpL28	0	75	0	2	16019	Structural constituent of ribosome
CG3029	Orange	75	0	1	0	21924	Vesicle-mediated transport
CG9641	CG9641	75	0	2	0	60924	Uncharacterised
CG9765	Tacc	0	75	0	1	132897	Negative regulation of microtubule depolymerization
CG11883	CG11883	74	0	1	0	79155	Nucleotide metabolism, proteolysis
CG10189	CG10189	0	73	0	1	45486	Uncharacterised
CG4006	Akt1	71	0	2	0	60282	Serine/threonine kinase
CG8981	Microcephalin	0	71	0	1	91362	Cell cycle checkpoint
CG1453	Klp10A	0	70	0	2	89300	Kinesin motor, microtubule-based movement
CG3605	SF3B150/SAP145	0	70	0	1	84786	Pre-mRNA splicing, U2 snRNP component
CG32479	CG32479	0	69	0	2	164934	Ubiquitin cycle
CG10315	eIF2B-δ	67	0	1	0	68311	Translation initiation factor
CG17492	Mib2 (mind bomb 2)	0	67	0	2	116847	E3 ubiquitin-protein ligase MIB2
CG2671	LGL (lethal (2) giant larvae)	0	67	0	2	127845	Cell polarization, regulation of actomyosin cytoskeleton, exocitosis
CG1412	RhoGAP19D	0	66	0	3	230711	Small GTPase regulator activity
CG3949	Hoip (hoi-polloi)	66	0	1	0	14045	U4/U6.U5 tri-snRNP 15.5 kDa protein, pre-mRNA splicing

Gene ID	Gene name	Mascot score		No. of peptides		Mol. weight	Function
		wild type	K345N	wild type	K345N		
CG2925	Noisette (SF3a60/SAP61/Prp9)	0	65	0	1	58670	Pre-mRNA splicing, U2 snRNP component
CG5745	CG5745	65	0	2	0	61872	RabGAP/TBC
CG1503	CG1503	0	63	0	1	34681	Proteolysis
CG7961	αCop	0	63	0	2	141003	Vesicle-mediated transport
CG8332	RpS15	63	0	1	0	17026	Structural constituent of ribosome
CG9124	eIF3-S3	63	0	1	0	38725	Translation initiation factor
CG8003	CG8003	0	62	0	1	46537	Uncharacterised
CG17596	RpS6PKII	61	0	1	0	101143	Ribosomal protein S6 kinase activity
CG9423	Importin-α 3	61	0	1	0	57360	Protein import into nucleus
CG10392	Ogt	0	60	0	1	119943	Amino acid glycosylation
CG8184	CG8184	60	0	1	0	560049	Ubiquitin-protein ligase, mRNA transport
CG12532	Bap (β-adaptin)	0	59	0	1	101914	Vesicle-mediated transport
CG10223	Top2	58		1		165034	DNA topoisomerase
CG10944	RpS6	0	57	0	1	28561	Structural constituent of ribosome
CG3539	Slh (SLY-1 homologous)	57	0	1	0	74856	Vesicle-mediated transport
CG8709	CG8709	57	0	1	0	121346	Lipid metabolism
CG12321	CG12321	54	0	1	0	28014	Uncharacterised
CG31012	CG31012	0	54	0	1	57268	SH3/SH2 adaptor activity
CG33122	Cutlet	0	52	0	1	112273	DNA replication, AAA ATPase
CG7546	CG7546	52	0	1	0	142601	Ubiquitin cycle
CG8610	Cdc27	0	51	0	3	98566	Anaphase-promoting complex subunit
CG10363	TepIV	0	50	0	1	169129	Endopeptidase inhibitor activity
CG17704	Nipped-B	0	50	0	2	239145	Mitotic sister chromatid cohesion, regulation of transcription
CG9805	eIF3-S10	0	50	0	1	134481	Translation initiation factor
CG2807	SF3B160/SAP155	0	48	0	1	150284	Pre-mRNA splicing, U2 snRNP component
CG15793	Dsor1	0	47	0	1	44127	MAP kinase kinase
CG6509	CG6509	0	47	0	1	211045	Cytoskeleton organization and biogenesis
CG9044	CG9044	0	45	0	2	146310	Uncharacterised
CG3983	CG3983	43	0	1	0	66457	GTP binding

Part III

Discussion

4 Genome-wide analysis of mRNAs regulated by Drosha and Argonaute proteins in *Drosophila*

The first part of my thesis work was dedicated to identification of mRNAs regulated by Drosha and Argonaute proteins at the genomic level. In this chapter I will discuss in more detail the results published in [348] and described in § 2, taking into account the progress that was achieved in the miRNA field after these results have been published.

4.1 Transcripts regulated by Drosha and Argonaute proteins

Using microarray analysis of *Drosophila* cells depleted of Drosha and Argonaute proteins, we show that transcripts whose levels are likely to be directly regulated by silencing pathways (up-regulated transcripts) represent less than 20% of the *Drosophila* S2 cells transcriptome (Fig. 15 D, Fig. 16 and [348], Supplementary Tables). However, computational predictions of miRNA targets indicate that more than 30% of the transcriptome is targeted by miRNAs [106, 256, 356, 395, 394]. There are several possible explanations for these seemingly contradictory results. Firstly, I observed that not all authentic targets change levels in a detectable manner (Fig. 18). This indicates that although microarrays are a valuable tool to identify miRNA targets (see also [256]), many targets may escape detection using this approach. Second, some miRNAs and targets are expressed in a tissue specific manner, so it is likely that only a subset of miRNA/target pairs is expressed in S2 cells [106, 115, 238, 244, 394]. Finally, current models of miRNA function suggest that miRNAs expressed in a given cell type target transcripts that are already expressed at low levels, but avoid house keeping genes or genes that are expressed in these cells at high levels [115, 256, 394]. Targets which are expressed at low levels may escape detection by microarray analysis. Nevertheless, among transcripts regulated by the Argonaute proteins we found several that are expressed at relatively high levels, suggesting that miRNAs not only silence the expression of undesirable low abundance transcripts, but may also play a role in fine-tuning the expression of abundant mRNAs.

4.2 Crosstalk between AGO1 and AGO2

AGO1 and AGO2 are thought to have non-overlapping functions in *Drosophila* [318, 344]. In this study we show that these proteins regulate the

expression levels of a common set of miRNA targets (Fig. 16). The observation that Drosha also regulates these transcripts strongly supports the idea that regulation is mediated by miRNAs. In agreement with this, it was observed that AGO2 can associate with endogenous miRNAs, although less efficiently than AGO1 (Fig. 20). In this way, AGO2 may also regulate the expression levels of a subset of miRNA targets. Nonetheless, when miRNA function was assayed by over-expressing miRNAs together with luciferase-based mRNA reporters, it was observed that miRNA-mediated translational repression requires AGO1, but not AGO2. It is therefore possible that in this assay the fraction of miRNAs incorporated into AGO2-containing RISCs is too small to observe changes in the expression levels of the reporter. Dicer-1 is involved in miRNA biogenesis and is also required for the assembly of RISCs [250], so our observations suggest that Dicer-1 may load AGO2-containing RISCs with miRNAs, at least to some extent.

A partial functional overlap between AGO1 and AGO2 is also suggested by the observation that these proteins regulate the expression of a common set of transposable elements (Fig. 23).

Apart from the commonly regulated transcripts, we have also identified transcripts individually regulated by AGO2, but not by Drosha or AGO1, suggesting that AGO2 may regulate the expression of these transcripts by an miRNA-independent mechanism that might involve endogenous siRNAs.

Recent studies on an endogenous small interfering RNA pathway have led to the discovery of diverse intramolecular and intermolecular substrates that generate endo-siRNAs in *Drosophila* [137, 315, 316, 208, 80, 69]. These findings suggest broad and possibly conserved roles for endogenous RNAi in regulating host-gene expression and transposable element (TE) transcripts (reviewed in [319]). Most of these endo-siRNA classes are derived from TE, from complementary annealed transcripts, and from long "fold-back" transcripts called hairpin RNAs (Fig. 44).

Consistent with my observation that AGO2 regulates the expression of TEs, deep sequencing of the small RNAs that directly associate with AGO2 revealed that TEs are a substantial source of endo-siRNAs of precisely 21 nt [208, 80]. A similar result has been obtained by sequencing small RNAs enriched for AGO2-loaded RNAs [137] or by analyzing total head or cultured-cell RNAs [69].

It has also been demonstrated that siRNAs can be produced from *cis*-natural antisense transcript (*cis*-NAT) arrangements, genomic regions that encode exons on both DNA strands and can involve 5′, 3′ or internal exons. Only a subset of co-expressed *cis*-NAT pairs are selected for endo-siRNA production (*ca.* 140), presumably reflecting endogenous functional use. Virtually all *cis*-NAT-siRNAs in flies are derived from 3′ UTR overlaps

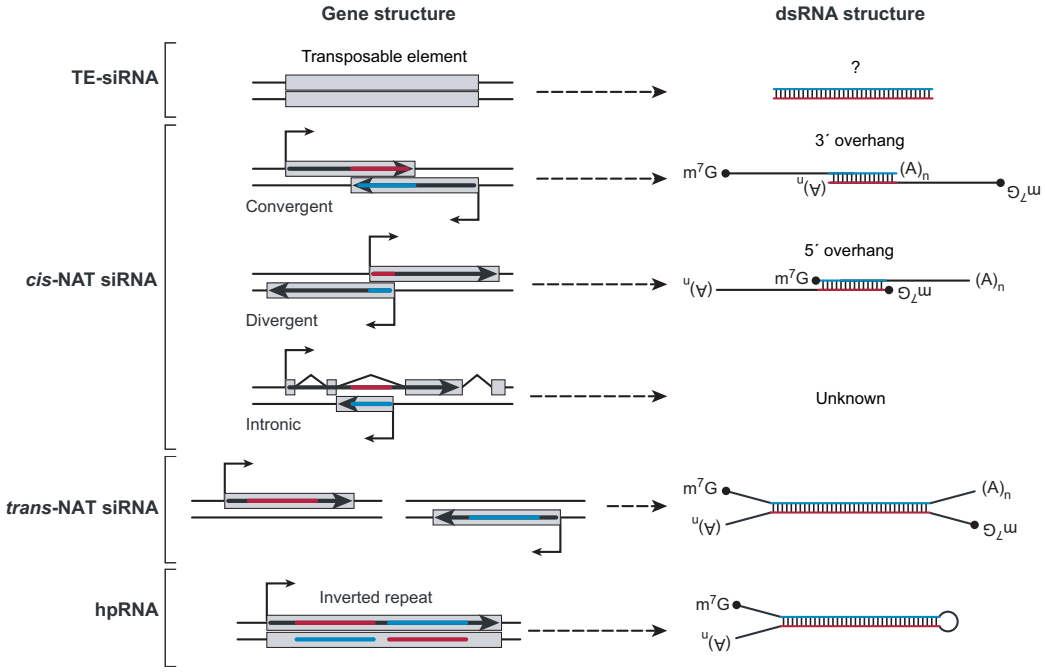

Figure 44. Substrates for endo-siRNA production in *D. melanogaster*. Modified from [319].

[137, 315, 208, 80].

Bioinformatic studies in *Drosophila* revealed a number of loci that produce endo-siRNAs from extended inverted repeats transcribed into hairpin RNAs (hpRNAs), the stems of which were up to 400 base pairs in length [316]. At least seven distinct loci generate endo-siRNAs [316, 208, 80]. As with siRNAs from artificial long-inverted repeats, the siRNA duplexes derived from hpRNAs are phased and direct AGO2 to carry out target transcript cleavage.

Generation of endo-siRNAs is dependent on Dicer-2 and, surprisingly, on the Dicer-1 partner Loquacious [315, 316, 208, 80, 69]. The endogenous siRNA biogenesis pathway is shown in Fig. 45.

In agreement with the results obtained in our study, known miRNAs comprised more than 97% of AGO1-associated RNAs and up to 8% of the AGO2-bound species in S2 cells. The contribution of transposons and satellite repeats to AGO2-associated endo-siRNAs is 27% and just 0.5% in the case of AGO1-associated RNAs.

The remaining endo-siRNAs are derived from hpRNAs or from *cis*-NATs [80]. Relative levels of endo-siRNAs generated from each convergent *cis*-NAT were low, and no or little change (up to a $\sim$ 1.3-fold increase) in the

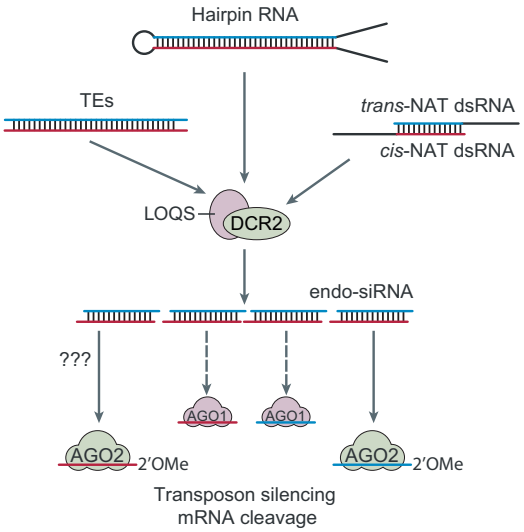

Figure 45. Endo-siRNA pathway in *D. melanogaster*. Modified from [319].

Drosophila cells produce several sources of endogenous dsRNA—transposable elements (TEs), *cis*-natural antisense transcripts, *trans*-natural antisense transcripts and hairpin RNA transcripts—that are processed into endo-siRNAs that load mostly AGO2. These repress transposon transcripts or endogenous mRNAs.

expression of such genes was detected in *AGO2* mutant ovaries. This result explains why genes regulated by endo-siRNAs were not considered regulated in our AGO2 knock-down experiments.

4.3 miRNAs affect mRNA expression levels

The levels of *hid* and *reaper* mRNAs (two experimentally validated miRNA targets [46, 395]), increase in cells in which the miRNA pathway is impaired. Moreover, by analyzing changes in mRNA levels, additional miRNA targets in *Drosophila* have been identified and validated (Table 1, Fig. 17, 18). The observation that miRNA targets change levels following inhibition of the miRNA pathway lends further support to the idea that miRNAs can reduce the levels of the targeted transcripts, and not just the expression of the translated protein [22, 256, 368]. Along these lines, it has recently been shown that miRNAs can trigger a strong reduction in target levels in mammals, zebrafish, *Drosophila* and *C. elegans* [432, 141, 30, 22]. It was observed that among the 136 core transcripts, 21% are between 1.5 and 2-fold up-regulated, 73% exhibited changes in the 2-5-fold range and 6% were at least 5-fold up-regulated in AGO1-depleted cells ([348], Supplementary Table VI). Thus, although changes in transcript levels can be used to validate miRNA targets

[256], the effects can be modest and, as mentioned above, not all targets can be identified using this approach.

In human cells the Argonaute proteins localize to P bodies [262, 341, 361, 374]. These are specialized cytoplasmic foci in which the enzymes involved in mRNA degradation in the 5′ to 3′ direction co-localize (*e.g.* the DCP1:DCP2 decapping complex, and the 5′ to 3′ exonuclease XRN1 [361, 374]). In addition, mRNA decay intermediates, miRNA-targets and miRNAs have been observed in P-bodies suggesting a functional link between P-bodies and RNA silencing pathways [361, 374]. Consistent with this, several groups have recently shown that P body components play a crucial role in silencing pathways [91, 191, 261, 347]. In particular, the RNA-binding protein GW182 (a P body component in metazoa) and the DCP1:DCP2 decapping complex are required for miRNA-mediated gene silencing in *Drosophila* cells [347]. Likewise, human GW182 plays a role in silencing mediated by miRNAs and siRNAs [190, 261]. Finally, the *C. elegans* protein AIN-1, which is related to GW182, is also required for regulation of a subset of miRNA targets [91]. Together with the observation that miRNAs inhibit cap-dependent, but not cap-independent, translation initiation [341], these observations suggest a model in which miRNA targets are stored in P-bodies after translation inhibition, where they are maintained in a silenced state by associating with proteins that prevent translation or possibly by removal of the cap structure [91, 261, 341, 347, 361, 374]. Decapping or simply the storage of miRNA targets in P-bodies may make these mRNAs susceptible to degradation, providing a possible explanation for the reduction in mRNA levels [262, 347, 361, 374]. In agreement with this, depletion of a 5′ to 3′ exonuclease in *C. elegans* partially restores the levels of miRNA targets [22].

More recent studies have demonstrated that in animal cells, miRNAs cause decay of mRNA targets by directing mRNAs to the general mRNA degradation machinery. This hypothesis is supported by studies in zebrafish embryos, *C. elegans*, *Drosophila* and human cells showing that miRNAs accelerate deadenylation and decapping of their targets [30, 141, 434, 113].

Nevertheless, not all authentic miRNA-targets change expression levels. Thus it is possible that the extent of the degradation depends on the number of miRNA binding sites and/or the stability of the miRNA:mRNA duplexes. It is also possible that the rate of mRNA decay triggered by miRNAs for some targets does not exceed the rate of transcription, and thus the steady-state levels of these targets remain unchanged. It would therefore be of interest to determine whether miRNAs generally cause a reduction in the half-life of targeted transcripts.

4.4 Drosha regulate mRNAs independently of Argonaute proteins

DsRNA stem-loop structures found within intronic regions or the coding sequence of some transcripts are cleaved by the RNase III enzyme Rnt1p in *S. cerevisiae* [83, 131]. This cleavage triggers degradation of pre-mRNAs and lariat introns or mature mRNAs, therefore inhibiting gene expression. Human and *Drosophila* Drosha forms a large complex (500 kDa in *Drosophila*) known as "Microprocessor", in which it interacts with its cofactor, DGCR8 (or Pasha in *Drosophila*) [85, 149]. Both proteins are essential for pri-miRNA processing [149, 160] (Fig. 13). Several studies suggest that the Drosha complex may also cleave preribosomal RNA [124, 149, 247, 431], but whether Microprocessor is able to cleave pre-mRNAs remains unknown.

Two transcripts (*CG15861* and *CG31642*) were clearly found to be exclusively up-regulated in Drosha-depleted cells (Fig. 21A, E). I found that these genes were also up-regulated in Pasha depleted cells (Fig. 22A), consistent with a role for Pasha in promoting Drosha-mediated cleavage of dsRNA hairpins of pri-miRNA [85]. The fact that the expression levels of these genes were not up-regulated in AGO1- and AGO2-depleted cells argues for their independence from miRNA/siRNA-mediated repression. In addition, pre-mRNA levels of *CG15861*, and *CG31642*, as well as *Stathmin-14* which contains the complete sequence of *CG31642* within its fourth intron, were increased in Drosha- and Pasha-depleted cells, suggesting that Drosha cleaves unspliced pre-mRNAs. However, an indirect effect on transcription of these genes can not be completely ruled out. It remains to be established whether Drosha indeed cleaves the *CG15861* and *CG31642* pre-mRNAs.

5 A role for *Drosophila* RNA-helicase Belle in translational control

As a result of numerous studies, RNA helicases of the DEAD-box family have been linked to different stages of RNA metabolism (reviewed in [77, 259]). They have been implemented in transcription, processing, splicing, export, localization, translational control and decay of mRNAs [357]. In all these processes, inappropriate or transitory RNA-RNA or RNA-protein interactions can be deleterious for subsequent steps, and therefore they require energy-driven helicases to allow the correct assembly of the complexes.

Although most DEAD-box helicases have similar enzymatic activities, it is often difficult to assign a defined molecular function to a given DEAD-box helicase in a particular cellular process [357]. In addition, the same DEAD-box protein can be involved in several diverse processes [357, 77] and even have a dual function in promoting two opposite activities. For example Ded1p, the *S. cerevisiae* ortholog of Belle, has been suggested to promote translation initiation [68, 84], while other observations raise the possibility that Ded1p has both a positive and negative role in translation [28].

Similar data are accumulating regarding the role of DDX3, the human ortholog of Belle, in translation. A potential function for DDX3 in translation initiation was suggested by the observation that human DDX3 (as well as *Drosophila* Belle and the mouse ortholog PL10) can rescue the lethal phenotype of a *ded1* null mutant [269, 68, 201]. A homolog of DDX3 was detected both in free mRNP and polysome fractions in *Chironomus tetans* [306]. Moreover, human DDX3 associates with the translation initiation complex components eIF4A, eIF2α and PABP1, and promotes translation of mRNAs containing a long or structured 5′ UTR [240]. A complementary study has shown that DDX3 interacts with the cytoplasmic multi-subunit translation initiation factor eIF3 in an RNase insensitive manner and promotes translation [245].

However, experiments involving RNAi knock-down and over-expression of DDX3 in mammalian cells have led to the view that this protein does not function in translation initiation, but instead represses cap-dependent translation by acting as an eIF4E-inhibitory protein [378]. It has been also demonstrated that in HeLa cells under stress conditions DDX3 is recruited to stress granules and that over-expression of DDX3 induces relocalization of its interacting partners (eIF4A, eIF4E, PABP) to stress granules [240]. Stress granules are cytoplasmic mRNP granules that are formed by aggregation of non-translating mRNAs as a response to stress [8].

In addition, mammalian DDX3 has been identified as a component of

RNA-transporting granules in neurons together with ribosomal proteins, RNA-binding proteins, transported mRNAs and transporting motor proteins [206, 105]. Although not proven, it is thought that the mRNAs are transported in a translationally quiescent state [44].

Taken together, these observations indicate that mammalian DDX3 and its yeast ortholog Ded1p have conserved roles both in translation initiation and repression. In this work I have tried to delineate a possible role for *Drosophila* Belle in translational control using several different approaches.

5.1 The subcellular localization of Belle

The subcellular localization of mammalian DDX3 has been difficult to establish. Several previous studies reported that DDX3 was found mainly in the nucleus with only low levels in the cytoplasm [325, 441]. In another study, however, DDX3 was detected in endoplasmic reticulum in discrete foci [269]. A further, more recent study has shown that DDX3 shuttles between the nucleus and the cytoplasm, binds the export receptor CRM1, and locates to nuclear pores [437]. DDX3 and other DEAD-box helicases were also found among proteins associated with the spliceosome [448, 286].

DEAD-box RNA helicases often localize to various RNA granules (see [109, 7] and references wherein). P bodies in many species, including *S. cerevisiae*, *D. melanogaster* and mammals contain the helicase Dhh1 (Me31B or RCK/DDX6) [376, 439], which is also concentrated in sponge bodies, maternal mRNPs and neuronal transport RNA granules [303, 24]. Germline-specific RNA granules in *Drosophila* such as nuage and polar granules contain the DDX4-like helicase Vasa [253].

As mentioned above, DDX3 along with the DDX5/p68, DDX6/RCK and DDX17/p72 DEAD-box helicases was detected in neuronal transport mRNP granules [206, 105] and in stress granules under stress conditions [240]. A recent study from R. Parker's laboratory has shown that *S. cerevisiae* Ded1p is a component of yeast P bodies. Moreover, it was observed that *Drosophila* Belle colocalizes with dFMR1 in foci in the neurites [28]. These results argue that DDX3 and its orthologs are conserved components of P bodies and related RNA granules.

In the original immunofluorescence study in *Drosophila* ovaries, Belle was found to be concentrated in the perinuclear region of nurse cells (nuage) and in the posterior pole of oocytes [201].

I used HA- and EGFP-tagged versions of Belle to localize the protein in *Drosophila* S2 cells. I observed that Belle forms large aggregates in the cytoplasm (Fig. 24). The distribution of the HA-tagged protein in the cytoplasm was remarkably similar to the localization of endogenous Belle in cell bodies

of *Drosophila* neurons [28]. Moreover, the EGFP-fusion of Belle showed less diffused cytoplasmic staining and formed discrete foci of varying number and size. Interestingly, these foci were different from P bodies, since no colocalization with P body markers Me31B, DCP1 and Ge1 was observed (Fig. 24B, C, D). The deviance of localization patterns of HA- and EGFP-Belle might be due to the difference in the expression levels of the fusion proteins, or alternatively, due to the properties of the tag.

The nature of Belle heterogenous distribution in the cytoplasm is not clear. Stress granules are dynamic cytoplasmic sites containing aggregates of mRNAs bound to the 48S preinitiation complex and proteins involved in translation repression, RNA metabolism and signaling pathways (reviewed in [8, 7, 6]). I found that known stress granule components such as translation factors (eIF4A, eIF4E, eIF4G, eIF2, eIF3), 40S ribosomal subunit components, PABP, and translational regulators (Me31B, Ataxin-2, Pumilio, dFMR1, G3BP2, AGO2, UPF1) were associated with Belle (Table 6; § 3.10). This observation raises the possibility that Belle is a component of *Drosophila* RNA granules that are similar to mammalian stress granules.

Another possible explanation could be that a considerable fraction of over-expressed Belle is localized to lipid droplets. Lipid droplets are ubiquitous organelles found in yeast, plants and animals, which serve as storage sites for energy-rich lipids [277]. Recently, a general role for lipid droplets as transient storage depots for proteins in temporary excess has been proposed [57]. This study has characterized the lipid-droplet proteome and identified Belle as a protein significantly represented in the lipid-droplet fraction [57]. Interestingly, I found that *ca.* 26% (33 of 126) of the proteins described in the study by Cermelli *et al.* as "represented abundantly and significantly in the lipid-droplet fraction" were associated with Belle in the tandem affinity purification.

5.2 Belle is required for cell viability and general translation efficiency

It has been demonstrated that *bel* is an essential gene that is required for larval growth as well as male and female fertility [201]. Belle can rescue the lethal phenotype of a *ded1* null mutant [201]. Depletion of Ded1p inhibits translation in yeast cells where this protein has a role in promoting translation initiation [68, 84, 28]. In contrast to these observations, two independent studies have provided evidence that depletion of human DDX3 either does not significantly affect [240] or enhances protein synthesis up to 150% in HeLa cells [378]. It has been also shown that over-expression of DDX3 ex-

erts an inhibitory effect on cell growth [60] and inhibits general translation efficiency in a dosage-dependent manner (27-50%) in HuH7 cells [378].

Therefore, it was important to determine whether *Drosophila* Belle is required for cell proliferation and general translation efficiency or functions as translational repressor. In the latter case, Belle could function in a similar way to Dhh1p, the yeast ortholog of Me31B, and Pat1p which are required for global translational repression of the vast majority of mRNAs in response to stress (glucose deprivation or amino acid starvation) [73].

I have observed that proliferation was significantly inhibited in *Drosophila* S2 cells depleted of Belle, Me31B, eIF4E and eIF4A, indicating that these proteins are required for cell proliferation (Fig. 25A). Using *in vivo* labeling experiments, I have demonstrated that the efficiency of protein synthesis is decreased in such cells both at normal growth conditions (25°C) and during heat-shock-induced stress (at 37°C), when the expression of heat shock proteins is induced (Fig. 26A).

Inhibition of cell proliferation leads to a certain decrease in protein synthesis. Interestingly, although all knock-down cells showed similar growth inhibition, depletion of Belle had the strongest effect on protein synthesis, comparable to depletion of the essential translation initiation factor eIF4A (Fig. 26A, Fig. 27). This indicates that Belle is required for efficient translation in S2 cells.

Depletion of eIF4E (CG4035) does not have such a strong effect on protein synthesis as eIF4A depletion (Fig. 26A, Fig. 27). The *D. melanogaster* genome contains seven genes encoding eight eIF4E isoforms [168]. In *Drosophila* embryos, cap-dependent translation relies mainly on the eIF4E-1 isoform encoded by CG4035 which also encodes the eIF4E-2 isoform [168]. However, it is likely that eIF4E isoforms are partially redundant and can substitute for the missing isoform eIF4E-1 and eIF4E-2 in S2 cells depleted of CG4035.

During the stress induced by heat-shock, protein synthesis was efficiently inhibited in control cells and cells depleted of Belle, Me31B and translation factors (Fig. 26A). This result suggests that Belle and Me31B, unlike yeast Dhh1p, are not required for global translational repression in response to stress. Moreover, the expression of HSP70 protein in Belle-depleted cells was also reduced in comparison to control cells (Fig. 26A, lane 10 versus lane 8 and 9), although Hsp70 mRNA was strongly induced (Fig. 26B). This observation lends support to the idea that Belle is required for translation and its depletion does not affect transcription and nuclear processing of mRNA.

Analysis of polysome profiles of S2 cells depleted of Belle, eIF4A and eIF4E demonstrates a similarity between them. All three profiles are characterized by an increase of the peaks corresponding to the 40S and the 60S

ribosomal subunits and the monosome peak, and a decrease of the polysome peaks. These features are the hallmarks of a translation initiation defect.

Moreover, I observed that Belle is associated with translation initiation factors eIF4G, eIF4E, eIF4A, multi-subunit factors eIF2 and eIF3 as well as translation elongation factor EF1α (Table 6, Fig. 39, 40). At least some of these interactions are conserved in mammals [245, 240, 105, 206]. Consistent with these observations, endogenous Belle was found mainly in free mRNP fractions and only a small fraction of the protein co-migrates with polysomes after sedimentation in sucrose gradients (Fig. 31C).

Taken together, these results suggest that Belle has an essential function in the cell to promote general translation initiation.

5.3 Belle functions as a translational repressor

Apart from its role in translation activation, Belle is able to repress translation of a bound mRNA in the tethering assay described in [30]. I observed that tethering of Belle to the 3′ UTR of an F-luc 5BoxB reporter mRNA caused translational repression and stabilization of the mRNA (Fig. 28). The translational repression activity of Belle was dependent on its putative ATPase activity (Fig. 30).

Although the observation that Belle is required for translation, but acts as a translational repressor in the tethering assay may seem contradictory, they might reflect the dual function of Belle in translational control. One possible explanation would be that Belle is required for general translation initiation but can also repress translation of a subset of mRNAs containing *cis*-regulatory sequences in the 3′ UTR. In the latter case, additional *trans*-acting proteins which are able to interact with Belle and bind these *cis*-regulatory sequences would be required for the repression. The observation that Belle interacts with several mRNA-binding proteins implemented in translational control (Table 6, Fig. 41, 42) supports this possibility. Tethering of Belle directly to the reporter 3′ UTR circumvents the need for such *trans*-acting proteins and puts Belle in the context required for translational repression.

The mechanism of this translational repression is not clear. Polysome profile analysis demonstrated that tethering of λN-HA-Belle to the reporter mRNA induces the formation of heavy mRNP complexes which are different to polysomes and contain λN-HA-Belle (Fig. 31B, C). The putative ATPase activity of Belle was required for translational repression but was dispensable for the formation of the heavy mRNPs. This suggests that heavy mRNPs may represent precursors of the repressed mRNPs but their formation may not be necessary for inhibition of translation.

The assembly of heavy mRNPs as an initial step in the translational repression mechanism in *Drosophila* is not without precedent. It has been reported for miRNA-mediated silencing ("pseudo-polysomes", [400]) and for the repression of *oskar* mRNA translation by Bruno ("silencing particles", [61]). Whether Belle mediates translational repression via assembly of heavy mRNPs *in vivo* is an open question.

There are two observations that argue that the answer to this question is positive. First, Belle localizes to nuage in nurse cells and the posterior pole of *Drosophila* oocytes which contain maternal mRNPs [201]. Second, Belle colocalizes with dFMR1 in foci in the neurites which are likely to be large transport RNA granules [28, 24, 206, 105]. It is widely accepted that mRNAs are transported as part of large mRNPs. Although not proven, it is thought that the maternal and other localized mRNAs are transported in a translationally quiescent state [44]. Therefore, in order for specific mRNAs to be transported and localized, they must first be sequestered from the translational machinery in the cytoplasm and organized into mRNPs. The sequestration from translation is likely to start in the nucleus or right after the export of the mRNAs to the cytoplasm. Consistent with this, Belle was found concentrated in the perinuclear region of nurse cells (nuage) in *Drosophila* ovaries [201]. DDX3, the human ortholog of Belle, also concentrates at the cytoplasmic side of the nuclear pore complex [437]. Finally, I found several RNA-binding proteins involved in translational control to be associated with Belle in S2 cells (Table 6, Fig. 41, 42). Thus, it is possible that Belle, in concert with various RNA-binding proteins, mediates the formation of large translationally dormant mRNPs from mRNAs targeted for translational repression or localization.

5.4 The association of Belle with various protein complexes reflects its functional diversity

Functional proteomics relies on the hypothesis that the association of proteins suggests their common involvement in a biological function. Thus, characterization of the molecular partners of a protein has become a critical part of analyzing its biological function, alongside knocking down its expression by RNAi and studying its subcellular localization. In order to characterize proteins associated with Belle, I made use of a tandem affinity purification approach followed by mass spectrometry analysis. This approach permitted the identification of potential partners of Belle in *Drosophila* S2 cells and helped to delineate its role in translational control.

In total, 336 proteins were found to be associated either with wild type

Belle or the K345N mutant (Table 6), with 101 proteins present in both purifications (Fig. 34). Because mass spectrometry is such a sensitive technique, an undesired side effect is that contaminating proteins such as keratins and highly abundant or "sticky" proteins are also identified in purification experiments. The large number of Belle-associated proteins raised the question of the specificity of their interactions with Belle.

To address this question, I performed a detailed bioinformatic analysis of the obtained protein set. This included protein annotation using Gene Ontology (§ 3.7), functional enrichment analysis (§ 3.8) and protein interaction network cluster analysis (§ 3.9). Interactions of a small subset of Belle-associated proteins were evaluated by a complementary co-immunoprecipitation assay (Fig. 39–42).

As shown in Fig. 33 and 34, the majority of annotated proteins associated with Belle are either directly implemented in translation (translation factors and ribosome structural components), or involved in translational control and other aspects of mRNA metabolism, including splicing, processing, 3′-end formation, localization and degradation (RNA-binding proteins, DEAD-box helicases, nucleases).

Categorization of Belle-associated proteins using GO slim terms was consistent with this observation (Fig. 35, 36). Functional enrichment analysis has demonstrated that the sets of proteins associated either with wild type Belle or the K345N mutant are significantly ($p < 0.01$) enriched in translation factors, structural constituents of ribosomes, RNA-binding proteins and ATPases (Table 5). At this point, a distinction was observed between proteins associated with wild type Belle or the K345N mutant. Significantly more proteins associated with wild type Belle were involved in RNP complex biogenesis and assembly, the cell cycle, intracellular transport, organization and biogenesis of the cytoskeleton and vesicles (Table 5). This indicates that the putative ATPase activity of Belle is required for some specific interactions.

Finally, I analyzed all the protein interactions with Belle which were previously known and/or predicted with high level of confidence. An interaction network was built which consisted of 221 proteins showing 1402 interactions with each other (Fig. 37). This result indicates that the set of proteins associated with Belle is not a random set, but most of these proteins are functionally and physically connected.

A machine-algorithm-assisted search for highly interconnected regions (clusters) in the network has revealed the presence of several previously known biological complexes (Table 4, Fig. 37, 38). Consistent with the role of Belle in promoting translation, translation initiation factors, PABP, and components of large and small ribosomal subunits formed the largest cluster.

The poly(A)-binding protein (PABP) is thought to stimulate translation

by mechanisms which are complex and may involve redundant or alternative pathways [86]. These include promoting mRNA circularization through simultaneous interactions with eIF4G and the 3′ poly(A) tail and stimulation independent of PABP poly(A)-binding activity. mRNA circularization promotes the recycling of terminating ribosomes by bridging two ends of an mRNA. Alternatively, PABP can promote 48S initiation complex formation, 60S ribosomal subunit joining and interaction of eIF4E with the cap structure [204]. The PABP C-terminal region (PABC) is also found in members of the hyperplastic discs protein (HYD) family of E3 ubiquitin-protein ligases [270].

PAIP1 binds to PABP and acts as a translational enhancer. It also interacts with eIF4A and eIF3 facilitating the bridging of the 5′ and 3′ ends of mRNA. PAM2, the domain of PAIP1 which interacts with the PABP C-terminal region, is also found in Ataxin-2. Human Ataxin-2 interacts with DDX6/RCK/p54 and localizes to stress granules.

PABP, PAIP1, HYD and Ataxin-2 were found associated with Belle (Table 6, Fig. 39). The interaction of Belle with PABP was RNase sensitive, suggesting that it is mediated by mRNA (Fig. 39A). Thus, it is likely that Belle is a component of mRNPs that contain circularized mRNA.

HYD mediates ubiquitin-dependent proteolysis of specific protein targets (reviewed in [86]). Thus, another PABP-binding protein PAIP2A is ubiquitinated upon binding to HYD through its PAM2 motif. The affinity of PAIP2A to the HYD PABC domain is significantly weaker than to that of PABP; therefore, under physiological conditions, the higher affinity of PAIP2 for PABP protects PAIP2A from HYD-dependent proteolysis. However, upon reduction in PABP levels, PAIP2A becomes free to associate with HYD and is subsequently ubiquitinated and degraded by the proteasome. Although PAIP1 also binds to the PABC domain of HYD, it is not degraded upon reduction in PABP levels, suggesting that an additional unknown factor is required for specific ubiquitination of PAIP1 [86]. Consistent with the role of HYD in ubiquitination and proteasome-mediated proteolysis, several proteasome subunits were found to be associated with Belle (Table 4, Fig. 37, 38).

Interestingly, the next largest cluster was comprised of RNA-binding proteins implicated in splicing (Table 4, Fig. 37, 38). In addition to this, a cluster of proteins involved in mRNA cleavage and polyadenylation was identified. It raises a possibility that Belle might possess some functions in the nucleus. For example, Belle could participate in export of a subset of mRNAs. The observation that human DDX3 is a nucleo-cytoplasmic shuttling protein which binds to CRM1, localizes to nuclear pores and participates in Rev-dependent export of intron-containing HIV-1 RNA supports this possibility [437].

Translation and mRNA turnover are strongly linked together. Inhibition of translation initiation diverts mRNAs to P bodies for decay, whereas inhibition of translation elongation stabilizes mRNAs on polysomes. These observations indicate that translation competes with mRNA decay [127, 109]. The poly(A) tail is both a determinant of mRNA stability and of translation efficiency. The first step in mRNA decay, deadenylation, is therefore also a means to inhibit the translation of mRNAs.

Consistent with this, a cluster formed by components of the CCR4-CAF1-NOT deadenylase complex was identified (Table 4, Fig. 37, 38). Interaction of Belle and CAF1 was confirmed by co-immunoprecipitation (Fig. 41F). In *Drosophila*, translational repression mediated by miRNAs and the PUF-domain translational regulator Pumilio is coupled with the recruitment of the CCR4-CAF1-NOT complex and subsequent deadenylation [30, 202]. Two annotated *Drosophila* PUF-domain proteins Pumilio and Penguin were found to be associated with Belle (Table 6, Fig. 42G). These observations support the hypothesis that Belle is involved in translation repression and deadenylation mediated by RNA-binding proteins.

In the normal mRNA degradation pathway, decapping follows deadenylation. The core decapping complex is a dimer that consists of DCP1 and DCP2. DCP2 contains the MutT domain and supplies the catalytic activity [397]. In higher eukaryotes, there are additional components (Ge-1, EDC3, Tral, PAT1, Me31B) which modulate decapping activity and link decapping to translation control and mRNA localization ([40, 74, 118, 258] and Tritschler *et al.*, in press). However, decapping activity is separable from localization function at least in the case of *oskar* mRNA since DCP2 is absent from the localized mRNPs [258]. Components of the decapping enhancer complex were found to be associated with Belle (Table 6, Fig. 39, 41), providing additional support to the view that Belle is a component of translationally repressed mRNPs.

Finally, the observation that translationally regulated *cyclin B* mRNA co-immunoprecipitates with Belle fits with this hypothesis (Fig. 43). In *Drosophila* embryos, translational repression of *cyclin B* mRNA occurs via a poly(A)-dependent mechanism [409]. In the pole cells, Pumilio binds to the *cis*-regulatory element NRE in the *cyclin B* mRNA 3′ UTR and recruits Nanos [16]. Nanos has been shown to recruit the CCR4-CAF1-NOT deadenylation complex to the mRNA, which results in shortening of the poly(A) tail and in translational repression [202].

A considerable number of proteins (60) found to be associated with Belle (including Belle itself) were also found among 270 previously identified microtubule-associated proteins (MAPs) [177]. Tubulin, actin and many actin-binding proteins were also identified in the affinity purification (Table 6).

This is not surprising, since about 50% of the translational machinery is associated with the cytoskeleton in eukaryotic cells [169]. Different experiments demonstrated that the association of polysomes with the cytoskeleton depends on the integrity of actin filaments. The translation elongation factor EF1α is involved in β-actin binding, bundling and anchoring mRNA to actin filaments (reviewed in [75]). Given that EF1α and Belle were found to be associated together (Table 6), it is likely that Belle is present in actin-anchored mRNPs involved in localized translation. EF1α associates with actin filaments in regions where actin mRNA is anchored. Consistently, I found that *Act5C* mRNA was co-immunoprecipitating with Belle (Fig. 43). Finally, the CCT complex which interacts with the β-actin nascent chain [161] and serves as a chaperonin for actin and tubulin, was found to be associated with Belle in the affinity purification (Table 6, Fig. 37, 38).

Interestingly, the CCT chaperon complex and nascent peptide associated complex subunit-α (NACα) were identified as protein components of DDX3-containing RNA granules purified from developing brain [105]. It was proposed that these complexes stabilize nascent proteins which are attached to ribosomes arrested at the stage of elongation [105]. Although I did not find any NAC components to be associated with Belle, three subunits of the signal-recognition particle (SRP) were identified in the affinity purification (Table 6, Fig. 37, 38). SRP mediates translational arrest only of ribosomes synthesizing proteins possessing an N-terminal signal peptide that targets them to the endoplasmic reticulum. However, it is unlikely that SRP and the CCT chaperon complex mediate a general translation arrest in transported mRNP granules.

Act5C mRNA 3′ UTR contains two copies of the conserved "zipcode" sequence, `ACACCC`, which is essential for correct targeting and localized translation of β-actin mRNA in many species (reviewed in [75]). This sequence is recognized by the zipcode-binding protein ZBP1, a KH-domain RNA-binding protein. The *D. melanogaster* ortholog of ZBP1 is Imp, which was found to be associated with Belle (Table 6 and Fig. 42E).

Therefore, another possible explanation of the association of Belle with cytoskeleton and cytoskeleton-binding proteins could be that Belle is present in transport mRNP granules. Transport of different populations of mRNP granules requires different motor proteins to specify the site of localization. mRNP granules are moved by microtubule-dependent motors such as kinesin-1 and 2 [221, 15, 206], acting coordinately with actin-based myosin II and V [263, 242, 440], since both microtubules and actin filaments are involved in rapid linear transport of mRNA in the same cell [144]. In *Drosophila* S2 cells, dFMR1 is able to form transport RNA granules that are moved by kinesin-1 and cytoplasmic dynein [260]. Consistent with this, dFMR1, a

kinesin motor protein Pavarotti (MKLP1), a myosin V motor protein Didum, and a dynactin complex component Glued were found associated with Belle (Table 6).

Plus- and minus-end-directed motors are also required for bidirectional vesicle transport. In *Drosophila*, mutations in kinesin, dynein or Glued block bidirectional vesicle transport in axons [179, 276]. Similarly, plus-end movement of lipid droplets in *Drosophila* embryos was severely impaired when either dynein or Glued was mutated [155]. Belle and many Belle-associated proteins are protein components of lipid droplets in *Drosophila* [57]. Therefore, it is likely that a fraction of Belle is localized to lipid droplets that are transported along microtubules in a dynein- and dynactin-dependent manner.

In yeast, the endoplasmic reticulum (ER) couples mRNA trafficking and local translation (reviewed in [328]). Several localized mRNAs code for membrane-bound proteins which undergo translocation to the ER upon translation, to be properly sorted through the secretory pathway. ER vesicles with such localized mRNAs attached to them are transported by myosin V via the actin filaments linking mRNA localization to ER transport.

I found that 6 of 7 coatomer subunits of the COPI vesicle coat were associated with Belle (Table 6, Fig. 37, 38). In animal cells, COPI-coated vesicles mediate traffic between the ER and the Golgi complex and within the Golgi complex (for the review see [264]).

Some proteins synthesized in the ER are retained there by a diarginine (RR) motif that is "recognized" by the COPI retention machinery [264, 296]. 14-3-3ε and ζ were identified as interacting proteins for the diarginine motif of the C-terminus of the potassium channel α subunit, Kir6.2. 14-3-3 proteins competed for binding to the dibasic region with the COPI machinery, which suggests that bound 14-3-3 masks the COPI interaction site and thus causes the release of Kir6.2 from the ER [49]. Interestingly, the two isoforms of the 14-3-3 protein, ε and ζ, were found to be associated with Belle, as well as other known partners of 14-3-3, including clathrin coat components, coat recruitment GTPases, Rab GTPases, GTPase-activating proteins (GAPs), guanine-nucleotide exchange factors (GEFs) as well as actin and heat shock proteins (Table 6; Fig. 37, 38). Enabled, the voltage-dependent potassium channel subunit with a C-terminal RR motif which can serve as a putative ligand of 14-3-3 proteins and COPI machinery, was also identified in the affinity purification of Belle (Table 6).

The biological meaning of the interaction of Belle with the components of the ER protein sorting system is not clear. The proteins identified in various 14-3-3 interactome studies differ greatly [49]. Consistent with my results, DDX3, PABP, translation factors, ribosomal proteins, the CCT complex and

other chaperons have been identified as 14-3-3-binding proteins in human cells [283].

The observation that Belle is associated with protein kinases involved in signal transduction is not surprising. According to recent data, higher levels of control exist to monitor RNA binding proteins and translational regulators [408]. It is likely that many RNA binding proteins are sensitive to signalling cascades that monitor the local and external environment of the cell, which enable them to modulate mRNA translation at an appropriate rate to suit changing cellular circumstances.

An intriguing connection between Belle and the RNAi pathway comes from the observation that Belle is associated with AGO2, the key component of the siRNA-mediated silencing machinery (Table 6; Fig. 42A). Previously, it was demonstrated that AGO2, RpL5, RpL11 and Rm62 (the *Drosophila* ortholog of human DDX5/p68) interact directly and form a complex with dFMR1 in *Drosophila* S2 cells [188]. Consistent with this result, I identified all the components of the dFMR1 complex in the affinity purification of Belle and confirmed some interactions by a co-immunoprecipitation assay (Table 6; Fig. 42A, C, and D). The function of dFMR1 in the RNAi pathway is yet to be determined, whereas RNA-helicases such as Belle and Rm62 may facilitate ATP-dependent unwinding of the siRNA duplex to generate active RISC of AGO2 and the small RNA. It is also conceivable that Belle and Rm62 may be involved in downstream events such as target RNA recognition, as an RNA chaperon or an RNPase. In agreement with these possibilities, it was shown that Belle and Rm62, but not dFMR1 alone, are required for efficient RNAi in S2 cells [406, 188]. It is likely that Belle (and Rm62) functions redundantly and can be substituted by other RNA-helicases. Consistent with this, proteomic analysis of AGO1- and AGO2-containing mRNPs in human cells revealed the presence of a large number of different DEAD-box RNA-helicases, including DDX5/p86 [164].

5.5 Concluding remarks

Diverse regulatory mechanisms are used redundantly to regulate mRNA translation and stability with the required precision. Many *trans*-acting proteins and *cis*-regulatory sequences play multiple specific roles in these mechanisms. This study on the function of Belle in translational control has revealed a perfect example of such versatility. In an attempt to integrate my results into the general picture of post-transcriptional gene regulation, I propose the following model of Belle function (Fig. 46).

Belle is an essential *Drosophila* protein which is required for general translation efficiency. In a certain molecular context, Belle can function as a

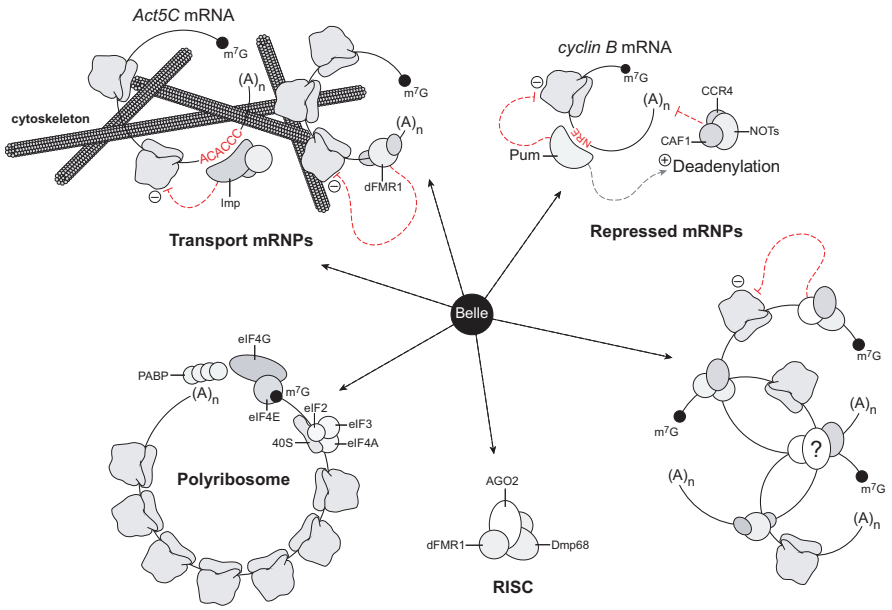

Figure 46. Hypothetical model of Belle function in translational control

Belle interacts with translation initiation machinery (eIFs, PABP, ribosomal components) and promotes general protein synthesis. In addition, Belle associates with proteins that bind 3′ UTRs and repress translation (dFMR1, Imp) by mechanisms which are not completely clear. This repression is required for mRNP assembly, transport, and localized translation on polysomes associated with cytoskeleton. At least in the case of Pumilio, translational repression is dependent on mRNA deadenylation by the CCR4-CAF1-NOT complex. Belle was also found to be associated with P body and stress granule components (Me31B, decapping enhancers, RNA-binding proteins). These mRNP granules contain aggregated mRNPs which are translationally inactivated by an unknown mechanism. Finally, Belle interacts with the RISC complex components and may function in the RNAi pathway. The grey dashed arrow corresponds to an activating signals; red blunted lines correspond to inhibitory signals.

translational repressor and mediate the assembly of heavy mRNPs. Consistent with its function in translation activation and repression, Belle associates with various proteins involved in translational control and a subset of mRNAs in the cytoplasm, although a specific nuclear function for Belle cannot be excluded. Several observations suggest that Belle may be involved in mRNP assembly and transport as well as localized mRNA translation. Finally, Belle may function as an auxiliary factor in the RNA interference pathway.

Part IV

Materials and methods

6 Materials

6.1 Chemicals and reagents

Inorganic salts, acids and alkali, as well as organic buffers (HEPES, MOPS, Tris), chelating agents (EDTA and EGTA), detergents (deoxycholate, NP-40, *Triton* X-100, *TWEEN* 20, SDS) antibiotics (ampicillin, kanamycin, cycloheximide, puromycin), DTT, β-mercaptoethanol, glyoxal, ammonium persulfate, TEMED, heparin, Ficoll, and sucrose were supplied by *Merck*, *Fluka*, *SIGMA*, and *Carl Roth*, Germany. Organic solvents (MeOH, EtOH, *i*PrOH, $CHCl_3$, formaldehyde) and acetic acid were obtained from *Merck*, Germany. Phenol and an equilibrated mixture of phenol, $CHCl_3$, isoamyl alcohol (25:24:1) was purchased from *AppliChem*, Germany. Formamide was from *Ambion*, USA. *peqGOLD TriFast*^{TM} reagent and deoxynucleotides were supplied by *PeqLab*, Germany. *Illustra*^{TM} NTP set (100 mM solutions) was purchased from *GE Healthcare*, USA.

All reagents for cell culture, electrophoresis-grade agarose and pre-cast gels for protein PAGE were purchased from *Invitrogen*, USA. Acrylamide/*bis*-acrylamid (37.5:1) mixture for protein electrophoresis was obtained from *Bio-Rad*, USA. Protein pre-stained and broad range markers, as well as DNA size markers (100 bp and 1 kb ladder) were supplied by *New England Biolabs*. RNase inhibitor *RNasin* was purchased from *Promega*, USA. Complete protease inhibitor cocktail, EDTA-free, was obtained from *Roche Applied Science*, Germany.

Kits for DNA isolation (*QIAprep* Spin Miniprep and QIAfilter Plasmid Purification Kits, *QIAquick* Gel Extraction Kit and PCR Purification Kit) and the transfection reagent *Effectine* were from *QIAGEN*. The TOPO-cloning kit was from *Invitrogen*, USA. The kit for the *Dual-luciferase*^{TM} assay was purchased from *Promega*. The chemiluminescence immunoblot detection system was from *TROPIX*, USA.

Isotope-labeled compounds were supplied by *Amersham Biosciences*^{TM} and Hartmann, Germany. *Fluoromount-G*^{TM} was from *Southern Biotechnologies*, USA. Glycogen which was used to enhance RNA precipitation was obtained from *Fermentas*, Germany.

6.2 Enzymes

All restriction enzymes, T4 DNA ligase and the Klenow fragment of DNA polymerase I were purchased from *New England Biolabs*, USA. Shrimp AP was supplied by *Roche Applied Science*, Germany. DNase I (RNA quality) for the removal of DNA from total RNA preparations and AMV reverse

transcriptase were obtained from *Promega*. In special cases, the TURBO DNA-*free*™ DNA removal system from *Ambion* was used. The reverse transcriptase for the generation of cDNA libraries and for the semi-quantitative RT-PCR, *RevertAid*™ *H Minus M-MuLV*, was purchased from *Fermentas*, Germany. The enzyme mix used for the amplification of cDNA for the purpose of cloning was part of the *Expand High Fidelity PCR System*, *Roche Applied Science*, Germany. For PCR mutagenesis, *PfuTurbo* polymerase (*STRATAGENE*, USA) was used. Routine PCR and asymmetrical PCR for the generation of radiolabeled probes were carried out using *Tag* polymerase that was produced and purified in our laboratory. T7 RNA polymerase for the *in vitro* transcription was also produced in house.

6.3 DNA oligonucleotides

DNA oligonucleotides were ordered from *SIGMA*, Germany. Primers for PCR purified with reverse phase cartridge were obtained in lyophilized form and were dissolved in water.

6.4 Membranes and filter paper

The nylon-based membrane for Northern blotting (*GeneScreen Plus*) was obtained from *PerkinElmer*™ Life Sciences, USA. Nitrocellulose membrane for Western blotting (*Protran* BA) was supplied by *Whatman* (Schleicher & Schuel), Germany. Blotting paper (3MM Chr) was obtained from *Whatman*, England.

6.5 Chromatography resins and columns

For the co-immunoprecipitation experiments Protein A-agarose was used, purchased from *Roche Applied Science*, Germany. Recombinant GST-fusion proteins were purified using glutathione-agarose from *SIGMA*, Germany. His-tagged recombinant proteins were purified using Ni-NTA Superflow resin from *QIAGEN*, Germany. *Sephadex* G-50 from *SIGMA*, Germany, was used for purification of radiolabeled DNA. Tandem affinity purification was performed using IgG *Sepharose*™ 6 Fast Flow and Calmodulin *Sepharose*™ 4B, purchased from *GE Healthcare*, Sweden. Ion-exchange resin AG-510-X8 for the de-ionization of glyoxal was purchased from *BioRad*, USA.

Columns for chromatography were supplied by *BioRad*, USA and *MoBiTec*, Germany.

6.6 Antibodies

Polyclonal rabbit anti-HA antibody and monoclonal anti-tubulin mouse antibody were purchased from *SIGMA*. Monoclonal mouse anti-V5 antibody was supplied by *Invitrogen*, USA. Monoclonal mouse anti-HA.11 antibody, used for immunofluorescence and for the co-immunoprecipitation experiments was from *COVANCE*, USA.

The following antibodies were generated in house by Michaela Rode, Daniel Schweizer, Andreas Lingel, Isao Kashima and Regina Büttner: polyclonal antibodies against GW182, Tral (Lsm14), EDC3 (Lsm16) and Ge-1 (EDC4) were raised in rats immunized with recombinant GST-fusion proteins; polyclonal antibodies against AGO2, PABPC, Upf1, GFP and Belle were raised in rabbits immunized with recombinant GST-fusion proteins.

Secondary antibodies coupled to AP (goat anti-rabbit and goat anti-mouse) were supplied with the *TROPIX* chemiluminescence immunoblot detection system, goat ant-rat antibody was from *SIGMA*.

6.7 DNA oligonucleotide microarrays

High-density DNA oligonucleotide microarrays that were used in this study were purchased from *Affymetrix*. The *GeneChip* Drosophila Genome 2.0 Array was largely based on the content from the annotation (release 3.1) of the *Drosophila melanogaster* genome by Flybase and the Berkeley Drosophila Genome Project (BDGP). In addition, other published gene predictions from the Drosophila Research community were included. In total, the array uses over 500,000 data points (14 probe pairs per probe set) to measure the expression of 18,500 transcripts and variants. The array also contains control sequences including:

- Hybridization controls: *bioB, bioC, bioD* from *E. coli* and *cre* from P1 bacteriophage
- Poly-A controls: *dap, lys, phe, thr, trp* from *B. subtilis*
- Housekeeping/Control genes: Actin (Actin 42A), GAPDH (Glyceraldehyde 3 phosphate dehydrogenase 2), Eif-4a (Eukaryotic translation initiation factor 4a)

6.8 Bacterial strains

For the propagation of plasmid DNA, the *E.coli* strains DH5-α or XL1-Blue were used. For recombinant protein expression BL21-Gold and *Rosetta*^{TM} 2

strains were used. The genotypes are as follows. DH5-α: *endA1 glnV44 thi-1 recA1 relA1 gyrA96 deoR nupG* Δ*(lacZYA-argF)U169* Δ*(lacZ)M15 nsdR17*. XL1-Blue: *recA1 endA1 gyrA96 thi-1 hsdR17 supE44 relA1 lac glnV44* F′[*proAB*$^+$ *lacI*^{q} Δ*(lacZ)M15*::Tn*10*(Tet^R)]. BL21-Gold: *ompT hsdS* (r_B^- m_B^-) *dcm*$^+$ Tet^R *gal endA* Hte. *Rosetta*$^{\text{TM}}$ 2: *ompT hsdS* (r_B^- m_B^-) *dcm*$^+$ (DE3) pRARE2 (Cam^R).

7 Methods

7.1 DNA cloning

7.1.1 Generation of cDNA library

A *D. melanogaster* cDNA library was prepared for the amplification of genes of interest, when plasmid templates were not available. For this, total RNA was isolated from *Drosophila* Schneider 2 cells and treated with DNase I, as described in § 7.3.1 and § 7.3.3. The RNA was reverse transcribed using an oligo(dT)$_{15}$ or random hexamer primer and M-MuLV reverse transcriptase, engineered to lack RNase H activity. The reaction was performed under RNase-free conditions. All reagents and plasticware were sterile and RNase-free. Equipment and work surfaces were cleaned with 1% SDS prior to use and gloves were worn throughout all manipulations.

4 μg of DNase treated total RNA was mixed with 0.5 μg of oligo(dT)$_{15}$ or random hexamer primer in a total volume of 11 μL. The RNA was denatured for 5 min at 70°C, and then chilled on ice for 2 min. Subsequently, 5 μL of 5× reaction buffer (250 mM Tris-HCl, pH 8.3, 250 mM KCl, 20 mM $MgCl_2$, 50 mM DTT), 2.5 μL of dNTP mix (dATP, dCTP, dGTP and dTTP, 10 mM each), 0.5 μL of RNase inhibitor *RNasin* (40 u/μL) and 6 μL of H_2O were added. The mixture was incubated for 5 min at 25°C before addition of 1 μL of *RevertAid*$^{\text{TM}}$ H minus M-MuLV reverse transcriptase (200 U/μL). If random hexamer was used, the reaction mixture was incubated for 10 min more at 25°C. Then the reaction was allowed to proceed for 1 hour at 42°C, and after that the enzyme was inactivated by heating the reaction mix for 10 min at 70°C.

7.1.2 Amplification of DNA by PCR

For the purpose of cloning, genes or gene fragments of interest were amplified from plasmid templates or from a *Drosophila* cDNA library. In both cases, the *Expand High Fidelity PCR System* was employed, which makes use of

an enzyme mix containing thermostable *Taq* polymerase and a proofreading polymerase optimized to amplify DNA fragments up to 5 kb.

The following reaction mixture was used:

38 μL	H_2O
3 μL	cDNA template or *ca.* 50 ng of plasmid
5 μL	10× reaction buffer
1 μL	dNTP mix (dATP, dCTP, dGTP, dTTP, 10 mM each)
0.5 μL	sense primer (10 μM)
0.5 μL	anti-sense primer (10 μM)
1 μL	*Expand High Fidelity* enzyme mix
50 μL	Total

The reaction mix was prepared in thick-walled 0.5 mL PCR tubes on ice. The dNTP mix contained 10 mM of each nucleotide, dissolved in H_2O. The 10× reaction buffer (unspecified composition, containing 15 mM $MgCl_2$) and the enzyme mix were part of the *Expand High Fidelity PCR System*. If cDNA served as the template, 3 μL of the 25 μL reverse transcription reaction described in § 7.1.1 was used. This corresponds to cDNA generated from *ca.* 0.48 μg of total *Drosophila* S2 cells RNA. A *DNA Engine* (PTC-200) Peltier Thermal Cycler (*BioRad*) was used, employing the following programm:

01	2:00	94°C	denaturation
02	0:30	94°C	denaturation
03	0:30	56°C	primers annealing
04	0:30	72°C	elongation
05	GOTO 02	34 times	
06	7:00	72°C	elongation

The extension time varied, depending on the length of the DNA fragment being amplified: 30 s was used for fragments of *ca.* 500 bp; for each additional 1 kb, the extension time was increased by 1 min.

For the semi-quantitative RT-PCR, in-house produced and purified *Taq* polymerase was used together with 10× *AmpliTaq* polymerase buffer (15 mM $MgCl_2$) from *Applied Biosystems*. The amounts of reaction components were adjusted to the final volume of 25 μL and mixed on ice in thin-walled 0.2 mL PCR tubes. A *RoboCycler Gradient 96* thermal cycler from *STRATAGENE* was used, employing appropriate cycling parameters. Extension time and primer annealing temperature varied, depending on the primers and DNA fragment being amplified.

Tables 12 and 10 specify the DNA templates and PCR primers used in each amplification reaction.

7.1.3 DNA agarose gel electrophoresis

DNA fragments generated by PCR or restriction digest were separated according to size by agarose gel electrophoresis, using a minigel system produced in the EMBL mechanical workshop. Agarose was melted in 1× TBE buffer (90 mM Tris base, pH 8.3, 90 mM boric acid, 1 mM EDTA), at a final concentration of 1%. After cooling to 65°C, ethidium bromide was added (0.5 μg/mL final concentration), and the gel was allowed to solidify in a minigel chamber with an appropriate comb. Before loading, the samples were mixed with 5× DNA dye (20% Ficoll, 1 mM EDTA, 0.1% SDS, 0.05% Bromophenol Blue). A DNA size marker (100 bp or 1kb ladder) was loaded on a separate lane. Gel electrophoresis was performed at 15 V/cm in 1× TBE buffer containing 0.5 μg/mL of ethidium bromide. DNA fragments were visualized under UV light and documented using the gel documentation system from *PeqLab*.

7.1.4 Purification of DNA fragments

DNA fragments generated by PCR or by restriction digest were purified using the *QIAquick* PCR Purification Kit or Gel Extraction Kit (*QIAGEN*) according to the manufacturer's instructions.

Restriction fragments were purified from an agarose gel. For this, slices containing the fragment of interest were excised from the gel, and the agarose slice was solubilized in an appropriate amount of buffer QG (unspecified composition). DNA fragments generated by PCR were purified directly from the reaction mixture, after the addition of 5 volumes of binding buffer PB (unspecified composition). In either case, the solutions containing the solubilized gel slice or the PCR mixture were applied to the silica-based purification column. The DNA selectively adsorbs to the silica membrane in the presence of high-salt while contaminants pass through the column during a centrifugation step. After washing the column with EtOH-containing buffer PE (unspecified composition), the pure DNA was eluted with 30 μL Tris buffer EB or water.

7.1.5 Restriction endonuclease digest of DNA

Plasmids and DNA fragments generated by PCR were digested with appropriate enzymes supplied by *New England Biolabs*. Optimal reaction buffers, as recommended by the supplier, were used. Reactions were typically carried out in a total volume of 50 μL, using 10-20 units of each enzyme (1 μL), 5 μL of the appropriate 10× buffer and 5 μL of BSA (1 mg/mL). The reaction was incubated from 45 min to 15 hours (overnight) at 37°C. Restriction

fragments were separated by agarose gel electrophoresis, visualized by UV light and purified from the gel using the *QIAquick* Gel Extraction Kit from *QIAGEN* as described in §§ 7.1.3 and 7.1.4.

7.1.6 Ligation of DNA fragments

A linearized plasmid and a gene fragment with compatible ends were ligated using T4 DNA ligase, *New England Biolabs*. Generally, 5-6 μL of the gel-purified digested PCR product and 50 ng of linearized plasmid vector were ligated. Ligation reaction was performed in 10 μL containing 200 units of T4 DNA ligase and 1 μL of 10× T4 DNA ligase buffer (500 mM Tris-HCl, pH 7.5, 100 mM $MgCl_2$, 100 mM DTT, 10 mM ATP, 250 μg/mL BSA). The reactions were performed either at room temperature for 10-20 min or at 16°C over night.

7.1.7 Preparation of transformation-competent *E. coli* cells

To allow high efficiency transformation with DNA, *E.coli* strains XL1-Blue and DH5α were treated as described in [185].

Bacteria from a frozen glycerol stock were streaked out on LB agar (10 g/L tryptone, 5 g/L yeast extract, 10 g/L NaCl, 15 g/L agarose), and incubated overnight at 37°C. A colony was used to inoculate 2 mL of LB medium (10 g/L trypton, 5 g/L yeast extract, 10 g/L NaCl), and bacteria were allowed to grow for 9 hours at 37°C with vigorous shaking. 1 mL of the bacterial suspension was transferred to a 2 L Erlenmeyer flask containing 500 mL of LB medium supplemented with 10 mM $MgCl_2$. The bacteria were grown at 18°C while shaking at 100 rpm, until they reached an OD of 0.3 units. This would typically take about 48 hours. Once the desired OD was reached, the culture was cooled on ice, and the bacterial cells were pelleted by centrifugation at 2500×g in a pre-cooled rotor. The subsequent steps were performed at 4°C in a cold room, using pre-cooled reagents. The pellet was resuspended in 150 mL of ice-cold transformation buffer (10mM PIPES, 250 mM KCl, 15 mM $CaCl_2$, 55 mM $MnCl_2$), pelleted again as above, and finally resuspended again in 40 mL of transformation buffer. 3 mL DMSO was added, while gently swirling the bacterial suspension. The transformation-competent cells were dispensed in 200 μL aliquots and immediately frozen in liquid nitrogen and stored at −80°C. Aliquots were tested by transformation with serial dilutions of plasmid DNA to ensure a transformation efficiency of at least 10^6 colonies per 1 μg of plasmid DNA.

7.1.8 Transformation of *E. coli* cells

Transformation-competent bacteria (*E. coli* strains, prepared as described in § 7.1.7), were thawed on ice. The ligation reaction or 100 ng of a plasmid were added to 50 μL of the competent bacteria, and incubated on ice for 30 min. The cells were then heat-shocked for 1 min at 42°C and chilled on ice. 500 μL of LB medium was added, and the bacteria suspension was incubated for 30 min at 37°C to allow the expression of antibiotic resistance genes if required. The bacteria were then pelleted by brief centrifugation in a table-top centrifuge and resuspended in 100 μL of LB medium. The cells were plated onto LB agar plates containing the appropriate selective antibiotic (*e.g.* 25 μg/mL kanamycin or 100 μg/mL ampicillin), and were incubated overnight at 37°C.

7.1.9 Isolation of plasmid DNA from *E. coli* cells

Plasmids were propagated in *E. coli* XL1-Blue or DH5α strains. For the evaluation of cloning results, a small-scale plasmid preparation (miniprep) was used. For this, 2-4 colonies were picked from an agar plate, and each was used to inoculate 3 mL of LB medium containing the appropriate selective antibiotic (*e.g.* 25 μg/mL kanamycin or 100 μg/mL ampicillin). After incubation at 37°C for at least 9 hours, bacteria were pelleted from 2 mL of the suspension by centrifugation at 6800×g for 3 min. Plasmids were purified from the bacterial pellet using *QIAprep* Spin Miniprep Plasmid Purification Kit (*QIAGEN*) according to manufacturer's instructions. The bacterial pellet was resuspended in 250 μL of ice-cold buffer P1 (50 mM Tris-HCl, pH 8.0, 10 mM EDTA, 100 μL/mL RNase A). Then, an equal amount of lysis buffer P2 (200 mM NaOH, 1% SDS) was added and mixed gently by inverting the tubes. After lysing the cells for no more than 5 min, 350 μL of neutralization buffer N3 (confidential composition) was added and mixed immediately. The resulting lysate was cleared by centrifugation for 10 min at 16100×g, and the clear supernatant was applied on the spin column by decanting. Plasmid DNA was adsorbed on silica membrane, washed with EtOH-containing buffer PE, and eluted with 50 μL of elution buffer EB (10 mM Tris-HCl, pH 8.5).The plasmids were analyzed by restriction digest and agarose gel electrophoresis as described in §§ 7.1.5 and 7.1.3.

In order to produce larger amounts of plasmid, cultures of bacteria harbouring the desired plasmid were used to inoculate 100 mL of LB medium containing the appropriate selective antibiotic in 300 mL Erlenmeyer flask. The suspension was incubated with vigorous shaking overnight at 37°C. The cells were pelleted by centrifugation at 6800×g, 4°C, for 15 min. To extract

the plasmid from the bacterial cells, the QIAfilter Plasmid Purification Kit from *QIAGEN* was used according to the manufacturer's instructions. The bacterial pellet was resuspended in 4 mL of buffer P1 (see above). Then, 4 mL lysis buffer P2 (see above) was added. The mixture was incubated at room temperature for 5 min. The lysis was terminated by addition of 4 mL of ice-cold neutralization buffer P3 (3 M KOAc, pH 5.5). The lysate was poured into the barrel of the QIAfilter Cartridge and incubated at room temperature for 10 min. In the meantime, the purification column (QIAGEN-tip 100) was equilibrated with 4 mL of buffer QBT (50 mM MOPS, pH 7.0, 750 mM NaCl, 15% *i*PrOH, 0.15% *Triton* X-100). The lysate was cleared by passing it through the Cartridge filter. The cleared lysate was applied to the previously equilibrated column and was allowed to enter the resin by gravity flow. The column was washed twice with 10 mL of wash buffer QC (50 mM MOPS, pH 7.0, 1 M NaCl, 15% *i*PrOH). Plasmid DNA was finally eluted with 5 mL of elution buffer QF (50 mM Tris-HCl, pH 8.5, 1.25 M NaCl, 15% *i*PrOH), and precipitated by adding 3.5 mL of *i*PrOH followed by centrifugation at 15000×g, 4°C, for 15 min. The pellet was washed with 1 mL of 70% EtOH, and centrifuged again for 5 min at 16100×g. The air-dried pellet was dissolved in 150 μL of water. The concentration of DNA in the solution was determined by measuring its absorbance at 260 nm (A_{260}). An A_{260} value of 1 unit corresponds to a concentration of 50 μg/mL of double-stranded DNA.

7.1.10 PCR mutagenesis

For the generation of point mutants and for the insertion or deletion of short DNA fragments, PCR mutagenesis was performed. The mutagenesis strategy involves the amplification of the target plasmid with sense and anti-sense oligonucleotide primers that contain the desired mutation. *PfuTurbo* polymerase was used to replicate both plasmid strands without displacing the mutant oligonucleotide primers. This generated a mutant plasmid with staggered nicks. After amplification, the parental DNA template was digested with the restriction endonuclease *Dpn* I, which is specific for methylated and hemimethylated DNA (target sequence Gm^6ATC). The remaining, newly synthesised mutated plasmid was used to transform *E. coli* cells, which repaired the nicks and propagated the plasmid.

Oligonucleotide primers (30-45 nt long) were designed to contain the desired mutation, flanked on both sides by 15-20 nt of gene-specific sequences. Both sense and anti-sense primers contained the desired mutation and annealed to the same sequence on opposite strands of the template plasmid. Oligonucleotide sequences are listed in Table 10.

The following reaction mixture was prepared for the mutagenesis PCR:

40 μL	H_2O
1 μL	plasmid template (200 ng/μL)
5 μL	10× Pfu buffer
1 μL	dNTP mix (dATP, dCTP, dGTP, dTTP, 10 mM each)
1 μL	sense primer (2 μM)
1 μL	anti-sense primer (2 μM)
1 μL	*PfuTurbo* polymerase (2.5 U/μL)
50 μL	Total

The amplification reaction was performed using the following PCR programme:

01	5:00	94°C	denaturation
02	1:00	94°C	denaturation
03	1:00	56°C	primers annealing
04	16:00	68°C	elongation
05	GOTO 02	19 times	
06	16:00	68°C	elongation

Following the amplification, 1 μL of *Dpn* I enzyme (20 U/μL) was added to the PCR mixture, and incubated for 2 hours at 37°C. 50 μL of transformation-competent *E. coli* XL1-Blue or DH5α cells were transformed with 2 μL of the digestion reaction, as described in § 7.1.8. The cells were plated on an LB agar plate containing the appropriate selective antibiotic, and the plates were incubated at 37°C overnight. Plasmids were purified as described in § 7.1.9, and the presence of the desired mutation was verified by DNA sequencing.

7.1.11 Genetic constructs

The plasmids used in this study are listed in Table 12; cloning restriction sites and origins of the inserts are indicated. The sequences of primers used for the amplification of the inserts are listed in Table 10.

7.2 Cell culture and transfection

All cell culture experiments in this study were performed on *Drosophila melanogaster* Schneider 2 (S2 or SL2) cells. This line was established in 1969 by I. Schneider from several hundred Oregon R embryos on the verge of hatching (20 to 24 hours) [369]. The cells are male, by the criterion of MSL (male specific lethal) complex assembly. This versatile cell line grows rapidly at room temperature without CO_2 and is easily adapted to suspension culture.

7.2.1 Propagation of *D. melanogaster* S2 cells

Drosophila Schneider cells were grown in *GIBCO*™ Revised Schneider's *Drosophila* medium (with L-Glutamine), purchased from *Invitrogen*. The medium was supplemented with 10% heat-inactivated fœtal bovine serum (FBS), 50 U/mL penicillin and 50 μg/mL streptomycin (*Invitrogen*).

The cells were propagated under sterile conditions as a loose, semi-adherent monolayer in tissue culture flasks and in suspension in spinners at 25°C without CO_2. For general maintenance, the cells were passed into fresh flasks when the cell density was between 2 to 7×10^6 cells/mL, and split at a 1:2 to 1:5 dilution. Some conditioned medium (that in which the cells had been growing) was carried over when transferring the cells. S2 cells do not grow well when seeded at a density below 5×10^5 cells/mL, so the density was kept above 1×10^6 cells/mL.

7.2.2 Transfection

Transfection of S2 cells was performed in 6-well dishes using *Effectene* non-liposomal lipid transfection reagent (*QIAGEN*) according to the manufacturer's instructions.

One hour before transfection, 2.5×10^6 cells per well were seeded in a 6-well plate and incubated under normal growth conditions. In the meantime, the plasmid DNA mixture was prepared. 1 μg of plasmid DNA, combined in the desired ratio in a total volume of 10 μL, was diluted in DNA-condensation buffer, buffer EC (unspecified composition), to a final volume of 150 μL. Then, 8 μL of Enhancer was added and mixed by vortexing for 1 s. After incubation of the mixture at room temperature for 5 min, 25 μL of Effectene Reagent was added and mixed by pipetting up and down 5 times, or by vortexing for 10 s. The samples were incubated at room temperature for 15 min to allow transfection-complex formation. During this incubation, the adhered S2 cells were washed once with PBS, and then covered with 1.6 mL of complete Schneider's medium. 0.6 mL of the growth medium was also added to the tube containing the transfection complexes, and then mixed by pipetting up and down twice. The mixture was added drop-wise onto the adhered S2 cells.

The cells were incubated with the transfection complexes under their normal growth conditions for an appropriate amount of time for expression of the transfected genes (48-72 hours).

7.2.3 RNA interference

To deplete endogenous proteins from S2 cells, double dsRNA interference was performed, essentially as described in [71]. DsRNA was synthesized and prepared as described in § 7.3.4.

Drosophila S2 cells were pelleted by centrifugation at $210\times g$ for 5 min, washed once and resuspended in serum-free Schneider's medium (without FBS, penicillin and streptomycin). The cell density was adjusted to 2×10^6 cells/mL, and 1-3 mL was put into a sterile 25 mL screw-cap *Sarsted* tube. Then, 10 μg of dsRNA (3 μg/μL) per 10^6 cells was added. The cells were incubated at 25°C on an orbital shaker for 1-2 hours. After the incubation, equal volume of "2×" Schneider's medium containing 20% FBS, 100 U/mL penicillin and 100 μg/mL streptomycin was added. Cells treated with dsRNA were incubated on the shaker at 25°C until further analysis on day 6-9. In most cases, a second dsRNA treatment was performed on day 3 to ensure efficient depletion of the targeted protein.

7.2.4 Generation of stable cell lines

Stably transfected S2 cell lines were generated as follows. The cells were transfected as described in § 7.2.2, using two wells of a 6-well dish per genetic construct. The construct contained the gene of interest under an inducible metallothionein promoter, and a hygromycin B-resistance gene. 72 hours after transfection the cells were harvested, washed twice and diluted in 24 mL of selection medium (complete Schneider's growth medium supplemented with 300 μg/mL of hygromycin B). The cells were seeded in a 24-well plate (1 mL per well), and incubated for 14 days (after 7 days the selection medium was placed). The wells were checked regularly to see if transfectants were growing. After this initial selection stage, polyclonal populations of cells resistant to hygromycin B were expanded and tested for expression of the transgene by a Western blot, as described in § 7.5. To induce expression of the transgene, cells were treated with 2.5 mM $CuSO_4$ overnight.

The positive cell lines expressing the desired transgene were frozen as follows. 150×10^6 cells were pelleted and resuspended in 5 mL of ice-cold "freezing media" (15% DMSO in selective media). Then, the cells were aliquoted into sterile cryotubes (1 mL per tube) and frozen gradually by shifting the tubes from 4°C to −20°C (2 hours), and finally to −80°C (overnight). After freezing, the cells were stored in liquid nitrogen.

7.3 RNA isolation and analysis

All work involving RNA was performed under RNase-free conditions, using specially prepared reagents, pipettes, plastic- and glassware. Gloves were worn throughout all manipulations.

7.3.1 RNA extraction with *TriFast*™ reagent

Total RNA was extracted from *Drosophila melanogaster* Schneider 2 cells using *peqGOLD TriFast*™ reagent (*PeqLab*) according to the manufacturer's instructions. The TriFast reagent, a mono-phasic solution of phenol and guanidine isothiocyanate, is an improvement to the single-step RNA isolation method, described in [67]. During sample homogenization and lysis, the reagent maintains the stability of RNA, while disrupting cells and dissolving cell components.

To isolate RNA, the suspension of cells in growth medium was centrifuged at 210×g for 5 min and the cell pellet washed once with ice-cold PBS. The cell suspension was distributed into 2 mL tubes, centrifuged once again, and 1 mL of TriFast reagent was added (packed cell volume was equal or less than 10% of the volume of TriFast reagent used for lysis). Cell were lysed by repetitive pipetting or by vigourous shaking for 30 s, followed by incubation at room temperature for 5 min to permit the complete dissociation of nucleoprotein complexes. Then, 200 μL of chloroform was added. After vigorous shaking for 15 s, the tubes were incubated at room temperature for 5 min. The aqueous and the organic phases were separated by centrifugation for 15 min at 12000×g, 4°C. The upper aqueous phase was transferred to a fresh 1.5 mL tube, and the RNA was precipitated by mixing with 500 μL of iPrOH followed by incubation at −20°C for at least 20 min. The RNA was pelleted by centrifugation for 20 min at 12000×g, 4°C. The pellet was washed with 1 mL of 75% EtOH, centrifuged at 7500×g, 4°C, and allowed to air-dry for 5 min. The RNA was dissolved in the appropriate volume of water.

The concentration of RNA in the solution was determined by measuring its absorbance at 260 nm (A_{260}). An A_{260} value of 1 unit corresponds to a concentration of 40 μg/mL of single-stranded RNA.

7.3.2 RNA extraction with phenol-chloroform-isoamyl alcohol

To extract RNA from various protein solutions (*e.g.* sucrose gradient fractions, *in vitro* transcription reaction mixtures), the phenol-chloroform-isoamyl alcohol method was used. For this, typically 200 μL of the RNA-containing mixture was taken (or the volume was adjusted to 200 μL with water). One volume of TE-saturated (pH 4.5) phenol-chloroform-isoamyl

alcohol mixture (25:24:1) was added. The RNA was extracted by vigorous shaking for 20 s, and the phases were separated by centrifugation for 5 min at 12000×g, 4°C. The upper aqueous phase containing RNA was then transferred to a fresh tube and an equal volume of chloroform was added, to remove the residual phenol. After another shaking and centrifugation step (same as above), the upper phase was transferred to a fresh tube and precipitated with 0.75 volumes of iPrOH or with 2.5 volumes of EtOH, 0.1 volume of 3 M NaOAc (pH 5.2), 10 μg glycogen (NaOAc and glycogen were added only if a low yield of the RNA was expected). The concentration of the RNA solution was determined as described in § 7.3.1.

7.3.3 DNase treatment of RNA preparations

To remove the remnants of genomic and plasmid DNA from RNA preparations (*e.g.* before reverse transcription, or to reduce background signal in Northern blots), the RNA solutions were treated with RNase-free DNase. Routinely, RQ1 RNase-free DNase (*Promega*) was used in the following reaction:

37.5 μL	RNA (10-50 μg) in H_2O
10 μL	5× transcription buffer
0.5 μL	*RNasin* (40 U/μL)
2 μL	RNase-free DNase I
50 μL	Total

5× transcription buffer contained 400 mM HEPES-KOH, 120 mM $MgCl_2$, 10 mM spermidine, 200 mM DTT. The reaction mixture was incubated for 30 min at 37°C. After incubation, the RNA was purified as described in § 7.3.2.

For semi-quantitative RT-PCR, RNA samples were treated with TURBO DNase (*Ambion*). For this, the RNA pellet was dissolved in 21.5 μL of H_2O. 2.5 μL of 10× reaction buffer (unspecified composition) and 1 μL of TURBO DNase (2 U/μL) were added. The mixture was incubated at 37°C for 30 min, and then 2.5 μL of DNase Inactivation Reagent was added followed by incubation with occasional mixing for 2 min at room temperature. The DNase Inactivation Reagent was removed by centrifugation for 1.5 min at 10000×g, room temperature. The supernatant, containing DNA-free RNA ready for downstream applications, was transferred to a fresh tube and used directly for reverse transcription.

7.3.4 Preparation of double-stranded RNA

Depletion of endogenous proteins was performed by RNA interference (RNAi) as described in § 7.2.3. For this, long double-stranded RNA (dsRNA) was used. DsRNAs corresponding to *Drosophila* genes were transcribed *in vitro* from DNA templates about 700 base pairs long. To generate the templates for dsRNA synthesis, fragments of cDNA were amplified by PCR as described in § 7.1.2 from a Schneider cell cDNA library. The primers which were used for the amplification carried a 24 nt T7 polymerase promoter sequence on its 5′-end. The sequences of the primers are listed in Table 11. The PCR products were purified from an agarose gel as described in § 7.1.4. The purified DNA was examined by agarose gel electrophoresis prior to transcription to ensure the presence of a clean (nondegraded) DNA fragment of the expected size. *In vitro* transcription was performed in the following reaction mixture:

10 μL	H_2O
30 μL	DNA template ($\geq$50 ng/μL)
20 μL	5$\times$ transcription buffer (see § 7.3.3)
30 μL	NTP mix (ATP, CTP, GTP, UTP, 25 mM each)
10 μL	T7 polymerase (in-house produced)
100 μL	Total

The reaction mixture was incubated overnight at 37°C. The DNA template was removed by digestion with DNase following the transcription reaction. 2 μL of RQ1 RNase-free DNase from *Promega* was added to the transcription reaction, and the tube was incubated for another 30 min at 37°C. After that, *in vitro* transcripts were extracted with phenol-chloroform-isoamyl alcohol as described in § 7.3.2. The RNA pellet was dissolved in 150 μL of water by vigorous shaking at 30°C. To anneal the opposite RNA strands and obtain dsRNA, the RNA from the transcription reaction was denatured at 80°C for 10 min and then the tube was placed into a beaker containing 500 mL of water heated to 80°C. The RNA solution was allowed to cool down gradually to the room temperature with the water bath. The concentration of the RNA solution was determined as described in § 7.3.1. An A_{260} value of 1 unit corresponds to a concentration of 45 μg/mL of dsRNA. The concentration was adjusted to 3 μg/μL and 0.3 μg was mixed with DNA dye and loaded on a 1% agarose gel to assess the quality of the preparation.

7.3.5 Northern blot

Denaturing agarose gel electrophoresis Total RNA isolated from S2 cells was separated according to size by denaturing agarose gel electrophoresis

in the presence of glyoxal. For a 1.2% agarose gel (size: 20 cm×20 cm), 3.6 g of agarose was melted in 270 mL of RNase-free water, and the solution was allowed to cool down to 65°C. Then, 30 mL of 10× MOPS running buffer (200 mM MOPS, 80 mM NaOAc, 10 mM EDTA, pH 7.0) was added. The gel was allowed to solidify in a gel tray with an appropriate comb (19 or 21 wells). 6 to 14 μg of RNA was loaded per lane.

To start the glyoxal denaturing reaction, 6.75 μL of RNA in H_2O was combined with 23.25 μL of glyoxal reaction mixture. The glyoxal reaction mixture was prepared beforehand according to the following recipe:

1.2 mL	DMSO
0.4 mL	deionized glyoxal
0.24 mL	10× MOPS running buffer
0.12 mL	80% glycerol
40 μL	H_2O
2 mL	Total

The RNA samples were incubated at 74°C for 10 min, and chilled on ice. Then, 3 μL of RNA gel loading dye (95% formamide, 0.05% SDS, 0.05% xylene cyanol FF, 0.05% Bromphenol Blue, 0.5 mg/mL ethidium bromide) was added. The gel was pre-run for 10 min at 2 V/cm in 1× MOPS running buffer (see above), before the samples were loaded. Gel electrophoresis was performed over 12-16 hours at 2 V/cm, 4°C.

Transfer of RNA to membranes After electrophoresis, the agarose gel was rinsed once with water. The RNA was blotted onto a positively charged nylon membrane (GeneScreen Plus) by upward capillary transfer. The transfer setup was assembled as follows:

The gel was placed on a large strip of filter paper (Whatman, 3MM) situated on a glass plate, with the ends of the filter paper in a reservoir with 10× SSC buffer (1.5 M NaCl, 0.15 M tri-sodium citrate dihydrate, pH 7.0). The nylon membrane was soaked in 10× SSC buffer and placed on top of the gel, surrounded by plastic film to prevent the buffer from bypassing the membrane. Two pieces of Whatman filter paper soaked in 2× SSC buffer were then placed on top, followed by an assembly of dry filter paper to create the upward capillary action. The transfer was allowed to proceed for 5-6 hours.

After transfer, the membrane was rinsed in 2× SSC buffer, and the RNA cross-linked to the membrane by UV light using a *Stratalinker 2400* (*Stratagene*). The ethidium bromide-stained ribosomal RNA was visualized under UV light, and the membrane was marked and cut at the 18S rRNA band, so that the two halves could be hybridized independently.

Preparation of [^{32}P]-labeled DNA probes Labeled DNA probes for Northern hybridization were prepared by asymmetric PCR or by random priming. The template for asymmetric PCR, as well as for random priming, was produced by PCR or restriction digest, followed by purification of the product from an agarose gel as described in § 7.1.4. Linear PCR was performed in the presence of [^{32}P]-dATP and [^{32}P]-dCTP (*Hartmann*), using the anti-sense primer to initiate the synthesis of single-stranded DNA molecules which were complementary to the mRNA of interest. The following reaction mixture was used:

30 μL	H_2O
2 μL	DNA template (50-100 ng)
5 μL	10× reaction buffer
1 μL	dNTP mix (0.1 mM dATP, dCTP; 10 mM dGTP, dTTP)
1 μL	anti-sense primer (10 μM)
1 μL	*Taq* polymerase (in-house produced)
5 μL	[^{32}P]-dATP (10 Ci/μL)
5 μL	[^{32}P]-dCTP (10 Ci/μL)
50 μL	Total

The reaction mix was prepared in thin-walled 0.2 mL PCR tubes on ice. A *DNA Engine* (PTC-200) Peltier Thermal Cycler (*BioRad*) was used, employing the following programm:

01	2:00	94°C	denaturation
02	0:30	94°C	denaturation
03	0:30	56°C	primers annealing
04	0:45	72°C	elongation
05	GOTO 02	39 times	
06	7:00	72°C	elongation

To label DNA fragments by random priming (as described in [116]), at least 30 ng of DNA template was taken and combined with 2 μg of random nonamer in a total of 13 μL of water. The mixture was denatured for 5 min at 94°C and chilled on ice. Then, the following reagents were added:

5 μL	N9 buffer
1 μL	BSA (10 μg/μL)
1 μL	Klenow polymerase (5 U/μL)
5 μL	[^{32}P]-dCTP (10 Ci/μL)
25 μL	Total

The composition of N9 buffer was as follows: 1 M HEPES, pH 6.6, 250 mM Tris-HCl, pH 8.0, 25 mM $MgCl_2$, 5 mM β-mercaptoethanol, dATP, dCTP, dGTP, dTTP, 2 mM each. The reaction mixture was incubated for 30 min at 37°C.

The [^{32}P]-labeled probes were purified by size-exclusion chromatography, using a *Sephadex* G50 column. To prepare the G50 column, the plunger was removed from a 2 mL syringe, and a small amount of siliconized glass wool was inserted at the tip of the syringe. The syringe was then filled with *Sephadex* G50 slurry (1:1) in water, and centrifuged for 5 min at 840×g in a 15 mL polypropylene Falcon tube. The flow-through was discarded, and a 1.5 mL reaction tube with the cap removed was placed below the tip of the syringe. Then, the the labeling reaction, diluted in 100 μL of water, was applied to the column. After centrifugation for 5 min at 840×g, the flow-through containing the radiolabeled probe was collected, while any unincorporated nucleotides were retained on the column. The specific activity of 1 μL of the probe solution was measured using a scintillation counter, and 10^6 cpm were used per 1 mL of hybridization buffer.

Northern hybridization Reporter transcripts and endogenous mRNAs were detected by hybridization of [^{32}P]-labeled probes, generated as described in above. Membranes were placed in glass hybridization tubes, rinsed once with 2× SSC buffer, and pre-hybridized at 65°C in 12.5 mL of Church hybridization buffer (500 mM sodium phosphate, pH 7.0, 7% SDS, 1 mM EDTA) containing 100 μg/mL salmon testis DNA. The salmon testis DNA was denatured for 5 min at 96°C and chilled on ice before it was added to the hybridization buffer. After one hour of pre-hybridization, the purified [^{32}P]-labeled probe was added (10^6 cpm per 1 mL of Church buffer). Hybridization was carried out overnight at 65°C. Membranes were washed 5 times for 20 min at 65°C with 20 mL of Church wash buffer (40 mM sodium phosphate, pH 7.0, 1% SDS, 1 mM EDTA), and sealed between two transparent films. Radioactive bands were visualized using *BioMax* MS and MR films (*Kodak*$^{\text{TM}}$), and their intensity was quantified using the *Storm*$^{\text{TM}}$ 820 Gel and Blot Imaging system (*GE Healthcare*, USA).

7.3.6 Preparation of RNA for microarray analysis

Total RNA from 18×10^6 *Drosophila* Schneider 2 cells transfected with dsRNA (see § 7.2.3) was extracted as described in § 7.3.1. Two RNA preparations for each type of knock down were performed in parallel. The RNA preparations were treated with DNase (see § 7.3.3). After that, the RNA was precipitated, dissolved in 20 μL of water and concentrations and A_{260}/A_{280} ratios were de-

termined. Ratios between 1.9 and 2.1 were considered to be acceptable. The concentrations were adjusted to 2 μg/μL. 2 μg from each RNA sample were analyzed by agarose gel electrophoresis (see § 7.1.3) to ensure the presence of two bands of nondegraded ribosomal RNA. For this, 1 μL of RNA solution was mixed with 19 μL of RNA gel loading dye, and loaded on a 1% agarose gel. Then equal amounts of RNA from two separate preparations of each knock down were combined ("Pool I") and the concentration of this pooled RNA sample was adjusted to 1.5 μg/μL.

Each type of knock down experiment was repeated again. Two RNA preparations for each type of knock down were performed and processed in parallel, in essentially the same way, to obtain "Pool II". RNA from each pool was tested separately by RT-PCR, using random hexamer and AMV reverse transcriptase (*Promega*) for reverse transcription (§ 7.1.1) and primers specific for RpL49 mRNA during 18 cycles of PCR (§ 7.1.2).

Equal amounts of RNA from "Pool I" and "Pool II" were combined in the final RNA sample, and the concentration was adjusted to 1 μg/μL. RNA integrity was tested as described above by measuring the A_{260}/A_{280} ratios and running an agarose gel electrophoresis.

10 μg of total RNA obtained from each type of knock down experiment were sent to *Affymetrix GeneChip* Array Services at the European Molecular Biology Laboratory CeneCore facility. The samples were processed according to *Affymetrix* protocols and the cRNAs thus obtained were hybridized to the *GeneChip* Drosophila Genome 2.0 Array.

7.4 Immunoprecipitation

For immunoprecipitations of tagged proteins, transfections of *Drosophila* Scheinder 2 cells were performed in 6-well dishes as described in § 7.2.2. Cells were collected 3 days after transfection, washed with PBS, and resuspended in ice-cold lysis buffer (50 mM HEPES-KOH, pH 7.6, 150 mM KCl, 1 mM EDTA and 0.1% *Triton* X-100), supplemented with Complete protease inhibitor cocktail (*Roche Applied Science*). The cells were lysed for 15 min on ice in 200 μL of buffer per 5×10^6 cells. Cell lysate was spun at $16000\times g$ for 15 min at 4°C, and the supernatant was transferred to a fresh tube. 10% of the lysate was taken aside and mixed with an equal volume of 2× SDS sample buffer (10% input). Mouse monoclonal anti-HA antibody (*COVANCE*) was added to the supernatant (2.5 μL/5×10^6 cells), and the tube was rotated for one hour at 4°C. After that, 25 μL of Protein G-agarose (*Roche Applied Science*) were added and the mixture was rotated for another hour at 4°C. Protein G-agarose beads were pelleted by centrifugation for 2 min at $500\times g$, 4°C, washed three times with lysis buffer and once with lysis

Table 7. Resolving gels for denaturing SDS-PAGE

Volume of components (mL) per gel mould volume of 40 mL			
8%	10%	12%	Components
18.5	15.9	13.2	H_2O
10.7	13.3	16	30% acrylamide/bis-acrylamide (37.5:1)
10	10	10	1.5 M Tris-HCl, pH 8.7
0.4	0.4	0.4	10% SDS
0.4	0.4	0.4	10% APS
0.024	0.016	0.016	TEMED

buffer without *Triton* X-100. Bound proteins were eluted by incubating the beads in 100 μL of 2× SDS sample buffer at 96°C for 5 min with occasional vigorous mixing.

7.5 Protein gel electrophoresis and Western blot

Total-cell extracts for Western blot were prepared as follows. *Drosophila* Schneider 2 cells grown as a layer or in suspension were collected, washed once with ice-cold PBS, and lysates obtained by re-suspending the cell pellet in 2× SDS sample buffer (41.6 mM Tris-HCl, pH 6.8, 6% SDS, 30% glycerol, 100 mM DTT, 0.05% Bromophenol Blue) at a concentration of 30000 cells per 1 μL.

7.5.1 Polyacrylamide gel electrophoresis

Proteins were separated according to size by SDS-polyacrylamide gel electrophoresis (SDS-PAGE). Polyacrylamide gels contained an upper stacking gel to ensure that all proteins in the sample entered the lower separating gel simultaneously. In the lower gel, the proteins were separated according to molecular weight, as the amino acid chains were denatured in the presence of SDS. Separating gels were prepared according to the recipes summarized in Table 7.

APS and TEMED were the last reagents to be added to the mixture, just before pouring the gel. The lower separating gel was overlaid with *i*PrOH, and allowed to solidify for 15 min. The upper stacking gel had the following composition:

6.8 mL	H_2O
1.7 mL	30% acrylamide/bis-acrylamide (37.5:1)
1.25 mL	1.5 M Tris-HCl (pH 6.8)
0.1 mL	10% SDS
0.1 mL	10% APS
0.01 mL	TEMED
10 mL	Total

The *i*PrOH was aspirated from the lower gel, and a layer of stacking gel was poured on top. A comb was inserted, and the gel was allowed to solidify for 10 min. Gel electrophoresis was performed in Læmmli buffer (25 mM Tris base, 192 mM glycin, 1% SDS). The gel was run at 15 V/cm until the Bromophenol Blue dye front had migrated out of the gel.

7.5.2 Transfer of proteins to nitrocellulose membranes

To transfer proteins from the polyacrylamide gel onto a nitrocellulose membrane (*Protran* BA), a wet transfer system (*BioRad*) was used. The membrane, the gel and 4 pieces of Whatman 3MM filter paper were soaked in transfer buffer (20 mM Tris base, 150 mM glycine, 20% MeOH, 0.1% SDS). A transfer sandwich was assembled as follows (from the side of the cathode—the negative electrode): a porous pad, two pieces of filter paper and the gel. The nitrocellulose membrane was placed on top of the gel, and air bubbles between the membrane and the gel were removed. Two pieces of filter paper and the second porous pad completed the transfer assembly. The wet transfer was performed in the transfer buffer (see above) for 2 hours at 50 V, 4°C.

7.5.3 Western blot

After transfer, the membrane was rinsed with water and stained with 0.05% Ponceau Red to assess the efficiency of the transfer, washed in water, and blocked overnight at 4°C in blocking buffer (PBS, 0.3% *TWEEN* 20, 5% desiccated milk). Immunoblotting was performed using the Western-*Star*™ chemiluminescent immunoblot detection system (*TROPIX*). The system utilizes enzyme-linked immunodetection of antigen-specific antibodies with secondary antibodies conjugated to alkaline phosphatase (AP). The immobilized AP enzyme dephosphorylates the CDP-*Star*™ substrate. Upon dephosphorylation, the substrate decomposes, producing a prolonged emission of light that is imaged on X-ray or instant photographic film.

For the Western blot, the blocked membrane was incubated for 1 hour with primary antibody diluted in the blocking buffer on a rocking platform at

room temperature. Antibodies and working antibody dilutions are listed in Table 8. The membrane was washed three times for 5 min in washing buffer (PBS, 0.3% *TWEEN* 20), and then incubated for 1 hour with a secondary antibody coupled to alkaline phosphatase, diluted in the blocking buffer. After four washes for 15 min in the washing buffer, the membrane was washed twice for 2 min in assay buffer (20 mM Tris-HCl, pH 9.8, 1 mM $MgCl_2$), then the excess buffer removed. The membrane was placed on a glass plate and covered with a thin layer of CDP-*Star*™ substrate solution followed by 5 min incubation at room temperature. Then the substrate was removed and the blot was sealed between two transparent films and exposed to *BioMax* MR film (*Kodak*™).

Table 8. Antibodies used for Western blot

Antigen	Properties	Source	Dilution
Belle	Rabbit polyclonal	Our laboratory	1:50000
UPF1	Rabbit polyclonal	Our laboratory	1:1000
AGO2	Rabbit polyclonal	Our laboratory	1:1000
GW182	Rat polyclonal	Our laboratory	1:1000
Tral/Lsm14	Rat polyclonal	Our laboratory	1:2000
EDC3/Lsm16	Rat polyclonal	Our laboratory	1:1000
EDC4/Ge-1	Rat polyclonal	Our laboratory	1:1000
EGFP	Rabbit polyclonal	Our laboratory	1:2000
Tubulin	Mouse polyclonal	*SIGMA*	1:10000
HA tag	Rabbit polyclonal	*SIGMA*	1:1000
V5 tag	Mouse monoclonal	*Invitrogen*	1:5000
Rabbit IgG	Goat polyclonal, AP-coupled	*TROPIX*	1:50000
Mouse IgG	Goat polyclonal, AP-coupled	*TROPIX*	1:20000
Rat IgG	Goat polyclonal, AP-coupled	*SIGMA*	1:20000

7.6 *In vivo* metabolic labeling of cells

Drosophila Schneider 2 cells, transfected with dsRNA as described in § 7.2.3, were transferred to 15-mL Falcon tubes, washed once with serum-free Sf-900 II SFM *Drosophila* medium lacking methionine and cystine (*Invitrogen*), and incubated in 200 μL of this medium for 20 min at 25°C. After this preincubation period, 200 μL of Sf-900 II SFM medium, supplemented with 125 mCi/mL of [^{35}S]-labeled methionine and cysteine (*Redivue*™ *PRO-MIX*™ *in vitro* cell labeling mix; *Amersham Biosciences*™), were added. Cells were either kept at 25°C or immediately shifted to 37°C by immersing the tubes in a water bath. After 1 hour, cells were washed twice with ice-cold PBS and directly resuspended in 100 μL of 2× SDS sample buffer (see above). Aliquots of 25 mL were analyzed by SDS-PAGE (see § 7.5.1). The gel was stained with Coomassie solution (45% MeOH, 10% AcOH, 1 g/L Brilliant

Blue R-250) for 15 min, and destained with destaining solution (25% *i*PrOH, 10% AcOH). Then, the gel was photographed using gel documentation system (*PeqLab*), and dried in a *BioRad* gel dryer for 45 min at 65°C. The dried gel was exposed to *BioMax* MR film (*Kodak*^{TM}).

7.7 Analysis of polysomes by sedimentation in sucrose gradients

The following protocol for the analysis of polysome profiles of *Drosophila* S2 cells in sucrose gradients was developed in our laboratory based on similar protocols for yeast and mammalian cells.

Cells intended for polysome profile analysis were harvested at a cell density of 3-4×10^6 cells/mL. It was important to keep the cell population in the logarithmic phase (cell density below 5×10^6 cells/mL), since translation is most efficient at this stage. Approximately, 30×10^6 cells were taken per gradient.

To stabilize the polysomes, cycloheximide[5] was added to the growth medium at 0.1 mg/mL final concentration, and the cells were incubated at 25°C for 20-30 min. During the incubation with cycloheximide, lysis buffer and sucrose gradients[6] were prepared.

Hypertonic buffer[7] was used for lysing the cells. The buffer composition was as follows: 40 mM HEPES-KOH, pH 7.6, 300 mM KCl, 5 mM $Mg(OAc)_2$, 2 mM DTT, 1% NP-40, 1% sodium deoxycholate, 1× Complete protease inhibitor cocktail (*Roche Applied Science*), 0.5 U/μL *RNasin*, 0.1 mg/mL cycloheximide.

11×60 mm ultracentrifuge tubes were used in conjunction with an SW 60 Ti rotor. Pairs of tubes were selected that differed in mass by less than 50 mg. The tubes were rinsed once with 0.1% DEPC and twice with H_2O. 2 mL of 15% sucrose in gradient buffer (40 mM HEPES-KOH, pH 7.6, 150 mM KCl, 5 mM $Mg(OAc)_2$, 2 mM DTT, 0.1 mg/mL cycloheximide) was underlaid with 2 mL of 45% sucrose, without disturbing the interface. This was done by gently inserting the tip of a blunt stainless steel needle to the

[5]Cycloheximide inhibits the peptidyl transferase reaction on the 60S ribosomal subunit preventing ribosomes from completing the translation cycle and falling off the mRNA during extraction.

[6]The sucrose concentration range for the gradient is determined by the goals of the experiment. 15%-45% gradient gives fairly good resolution of free mRNPs, ribosome subunits, monosome and polysome peaks.

[7]The choice of the lysis buffer is determined by the mRNA of interest, since some mRNAs get extracted more efficiently with hypotonic buffer, some with hypertonic, etc. This has to be tested for each particular mRNA.

bottom of the tube and slowly releasing the 45% sucrose solution from the syringe to displace the 15% sucrose solution upwards. The tubes were finally equilibrated by adding 15% sucrose on top.

To form a linear gradient of sucrose concentration, the tubes with two layers (15% and 45%) of sucrose were capped and placed in the *BioComp Gradient Master*. The instrument was run according to the manufacturer's programme, so the gradient was formed and stored at 4°C.

After incubation with cycloheximide, the cells were pelleted by centrifugation at $210\times g$ for 5 min. After centrifugation, the cells were placed on ice and all further manipulations were performed at 4°C. The pellet was resuspended in ice-cold PBS, containing 0.1 mg/mL cycloheximide, and the cells were transferred to 1.5 mL tube. The cells were pelleted again, resuspended in the lysis buffer (200 μL per 30×10^6 cells) by pipetting up and down, and lysed on ice for 10 min. The cell lysate was cleared by centrifugation at $10{,}000\times g$ for 10 min, 4°C. The supernatant was transferred to a fresh tube and EDTA was added (30 mM final concentration) to a control sample to disrupt the polysomes.

The cleared lysate was carefully layered on top of the sucrose gradient and centrifuged for 55 min at 45,000 rpm in a *Beckman* SW 60 Ti rotor, 4°C.

The gradient was fractionated using an *ISCO Teledyne* gradient fractionator. The gradient's $A_2 60$ profile was recorded during the fractionation. 12 fractions were collected and kept at −80°C.

One half of each fraction was used to precipitate proteins with MeOH-chloroform (see below), and the other to extract total RNA with phenol-chloroform-isoamyl alcohol (§ 7.3.2). Samples for RNA isolation were treated with Proteinase K (stock solution: 10 mg/mL in 50 mM Tris-HCl, pH 8, 10 mM $CaCl_2$) prior to RNA extraction. For this, the samples were mixed with 0.1 volume of 10× digestion buffer (100 mM Tris-HCl, pH 7.5, 50 mM EDTA, 5% SDS) and Proteinase K up to 100 μg/mL. The tubes were incubated with vigourous shaking for 45 min at 37°C, and then total RNA was extracted as described in § 7.3.2 (phenol-chloroform-isoamyl alcohol extraction was performed twice). The RNA content of different gradient fractions was analyzed by Northern blot, as described in § 7.3.5.

Proteins contained in gradient fractions were extracted as follows. Samples were mixed with 4 volumes of MeOH by vortexing for 20 s. Then, one sample volume of chloroform was added, followed by vortexing for 20 s. To separate the organic and the aqueous phases, 3 sample volumes of water were added, followed by vortexing for 20 s and centrifugation for 5 min at $16{,}100\times g$, room temperature. The upper phase was carefully removed, leaving the lower phase and the interphase intact. To precipitate the proteins, 3 sample volumes of MeOH were added to the lower phase and the interphase.

After vortexing for 20 s, the proteins were pelleted by centrifugation for 10 min at 16,100×g, room temperature. The pellet was air-dried and resuspended directly in 2× SDS sample buffer. The protein content of different gradient fractions was analyzed by Western blot, as described in § 7.5.

7.8 Tandem affinity purification and mass spectrometry analysis of protein complexes

Stably transfected *Drosophila* S2 cell lines, expressing TAP-tagged proteins, were used for tandem affinity purification. The expression of the transgene was induced overnight by addition of $CuSO_2$ to the growth media[8].

7.8.1 Tandem affinity purification

For each purification, 450 mL of culture was used with cell density of 4-5×10^6 cells/mL. The cells were harvested in 50 mL *Falcon*™ tubes and pelleted by centrifugation for 5 min at 210×g, room temperature. All further work was performed at 4°C (in a cold room), using ice-cold reagents. The cells were washed twice with 10 pcv (packed cell volume) of PBS. Then, the pellet was resuspended in 7 mL of buffer A (10 mM HEPES-KOH, pH 7.9, 10 mM KCl, 1.5 mM $MgCl_2$, 0.5 mM DTT, 0.5 mM EDTA, 2 mM EGTA, 1× Complete protease inhibitor cocktail) and allowed to swell for 10-15 min on ice. After that, the cells were disrupted with 40 strokes in a Dounce "B" homogenizer. The lysate was centrifuged for 20 min at 740×g, 4°C, to remove nuclei and cell debris. The supernatant was transferred to a fresh tube and KCl was added to a final concentration of 200 mM. To increase the stringency of the purification, NP-40 was added at this stage up to 0.5%. Then, the extract was centrifuged for 15 min at 15,700×g, 4°C. The supernatant was collected and cytochalasin B was added up to 5 μg/mL to avoid actin unspecific binding. To disrupt RNA-mediated interactions in some experiments, RNase A was added to the final concentration of 200 μg/mL.

100 μL of cross-linked IgG *Sepharose* 6 Fast Flow beads (*GE Healthcare*) was added to the extract. Proteins were bound to the beads for 2 hours on a rotating wheel at 4°C. Then the beads were pelleted by centrifugation for 2 min at 300×g, resuspended in 800 μL of buffer B (20 mM HEPES-KOH, pH 7.9, 200 mM KCl, 2 mM EGTA, 0.5 mM DTT, 0.5 mM EDTA, 1× Complete protease inhibitor cocktail, 0.5% NP-40, 20% glycerol), and transferred into a fresh 1.5 mL tube. After that, the beads were washed four times with 800

[8]The amount of $CuSO_2$ was determined experimentally to ensure that the transgene protein level was similar to the endogenous protein level.

μL of buffer B, four times with 800 μL of buffer C (20 mM HEPES-KOH, pH 7.9, 200 mM KCl, 0.5 mM DTT, 0.5 mM EDTA, 0.1% NP-40, 20% glycerol), and finally two times with TEV cleavage buffer (10 mM Tris-HCl, pH 8, 150 mM NaCl, 0.5 mM DTT, 0.5 mM EDTA, 0.1% NP-40).

The beads were pelleted (2 min at 300×g, 4°C), resuspended in 200 μL of TEV cleavage buffer, and 3 μg of TEV protease was added (1 mg/mL stock solution) to cleave off the protein complexes that were bound to the IgG beads. The cleavage was carried out overnight at 4°C, on a rotating wheel.

Next day the beads were pelleted and washed twice with 50 μL of TEV cleavage buffer. The supernatant was transferred to a fresh tube, combined with the two washes (*ca.* 300 μL in total), and $CaCl_2$ was added up to 2 mM. The supernatant was mixed with 900 μL of calmodulin binding buffer (10 mM Tris-HCl, pH 8, 150 mM NaCl, 1 mM $Mg(OAc)_2$, 2 mM $CaCl_2$, 0.5 mM EDTA, 1 mM imidazole, 10 mM β-mercaptoethanol, 0.1% NP-40), and applied to 70 μL of calmodulin beads (equilibrated beforehand with calmodulin binding buffer). Protein binding to calmodulin beads was carried out for 2 hours at 4°C, on a rotating wheel. The beads were next washed seven times with 800 μL of calmodulin binding buffer, and transferred into precleaned (with 1× LDS sample buffer[9] and calmodulin binding buffer) micro-columns (*MoBiTec*, 35 μm pores, No. M2135). The remaining buffer was removed by brief centrifugation of the column. Then, the proteins were eluted from the beads with 40 μL of 1× LDS sample buffer after 20 min of shaking at room temperature. This step was repeated once with additional 15 μL of 1× LDS sample buffer and a further 10 min of shaking at room temperature. The eluate was collected by centrifugation for 30 s at 16,000×g, room temperature.

The proteins were separated by PAGE, using *NuPAGE* Novex Bis-Tris precast 4-12% gradient gels from *Invitrogen* with MOPS buffer, according to the manufacturer's instructions.

7.8.2 Silver staining of protein gels

The staining of the gel was performed using the *SilverQuest*™ Silver Staining Kit from *Invitrogen* according to the manufacturer's instructions.

After electrophoresis, the gel was removed from the cassette and placed in a clean staining tray of the appropriate size. The gel was rinsed briefly with ultrapure water and fixed in 100 mL of fixative (40% EtOH, 10% AcOH in ultrapure) for 20 min with gentle rotation. The fixative solution was decanted and the gel washed in 30% EtOH for 10 min. The EtOH was

[9]Provided with *NuPAGE* Novex Bis-Tris precast gels from *Invitrogen*.

decanted and 100 mL of Sensitizing solution (30% EtOH, 10% Sensitizer of unspecified composition in ultrapure water) added to the washed gel in the staining container. The gel was incubated in the Sensitizing solution for 10 min. The Sensitizing solution was decanted and the gel washed for 10 min each in 100 mL of 30% EtOH, then in 100 mL of ultrapure water. The gel was next incubated in 100 mL of Staining solution (1% Stainer of unspecified composition in ultrapure water) for 15 minutes. After staining was complete, the Staining solution was decanted and the gel washed with 100 mL of ultrapure water for 20-60 s. Then, the gel was incubated in 100 mL of Developing solution (10% Developer, 0.05% Development enhancer in ultrapure water) for 4-8 min until bands started to appear and the desired band intensity was reached. Once the appropriate staining intensity was achieved, 10 mL of Stopper (unspecified composition) was added directly to the gel still immersed in Developing solution, and the gel gently agitated for 10 min. The Stopper solution was decanted and the gel was finally washed with 100 mL of ultrapure water for 10 min.

The gel was photographed using a digital gel documentation system from *PeqLab*.

7.8.3 Destaining the gel and preparing samples for mass spectrometry analysis

All manipulations for preparing the samples for mass spectrometry analysis and the analysis itself were performed by Guido Sauer in our laboratory.

The gel was thoroughly washed with ultrapure water. The bands of interest were carefully excised using a clean scalpel and placed into a 1.5 mL sterile tube. 50 μL of Destainer A and 50 μL of Destainer B (provided with the *SilverQuest*^{TM} Kit) were added to the tube. The contents of the tube were thoroughly mixed and incubated for 15 min at room temperature. The supernatant was removed, 200 μL of ultrapure water was added to the tube, mixed, and incubated for 10 min at room temperature. The last washing step was repeated 3 times.

After destaining, the bands of interest were in-gel digested with trypsin (*Promega*) and extracted essentially as described in [377].

7.8.4 Mass spectrometry analysis of purified proteins

The extracted peptides were separated by reversed-phase HPLC (*NanoLC-2D*^{TM}, Eksigent) using *SilicaTip*^{TM} (*PicoTips*, New Objective) capillary column with 15 cm length and 75 μm inner diameter, self-packed with *ReproSil-Pur* C18-AQ, 3 μm (Dr. Maisch GmbH).

A stepwise gradient with buffer A (0.1% formamide in ultrapure water) and buffer B (0.1% formamide in acetonitrile) was applied in a run time of 90 min:

- 6 min at 5% of buffer B
- 67 min linear gradient from 5% to 30% of buffer B
- 6 min linear gradient from 30% to 80% of buffer B
- 5 min at 80% of buffer B
- 6 min linear gradient from 80% to 4% of buffer B

Mass spectrometric analysis was performed on an ion trap (HCT_{ultra}™, *Bruker Daltonics*) equipped with a nano-electrospray ion source from *Proxeon*. 4-8 scans were acquired for precursor ion scans in Standard Enhanced scan mode and Ultrascan mode for MS/MS fragmentation, respectively. Scan range was 300 to 1100 m/z in MS mode. Up to 4 precursors were fragmented per parent ion scanning with active exclusion activated for 30 sec.

A Mascot generic data file was generated using DataAnalysis software (*Bruker*) and peptides were searched against the NCBInr protein database using an in-house Mascot Server (V2.2). The following settings were used: digestion with trypsin allowing 1 miss cleavage, carbamylation of cysteine as fixed modification, oxidation of methionine as variable, 0.6 Da peptide mass accuracy and 0.3 Da for fragmentation masses. Proteins with a score of > 50 and at least two unique peptides were regarded as identified.

7.9 Immunofluorescence and confocal microscopy

7.9.1 Immunofluorescence

For localization studies, S2 cells were transfected with HA- and EGFP-tagged proteins as described in § 7.2.2. 24 hours after transfection the cells were collected, washed once and resuspended in serum-free Schneider's medium (without FBS, penicillin and streptomycin). The suspension was pipetted on poly-Lysine coated glass coverslips placed in a 24-well plate and cells were allowed to adhere for 10 min. After that, the cells were washed once with serum-free medium and fixed in 4% paraformaldehyde, 4% sucrose in PBS for 10 min. Then, the coverslips were washed once with PBS for 5 min, incubated for 5 min in MeOH at $-20°C$, and washed again three times with PBS for 5 min. To detect HA-tagged or endogenous proteins, the cells were permeabilized with 0.1% *Triton* X-100 in PBS for 10 min, followed

by three washes in PBS for 5 min. To avoid unspecific signal, the cells were blocked for 30 min in 1% BSA (w/v) in PBS, then incubated with an appropriate antibody (see Table 9) diluted in PBS containing 1% BSA for 1 hour. Antibody incubation was carried out at room temperature in a humidified chamber. The cells were washed three times in PBS and incubated with secondary antibody in PBS containing 1% BSA as described above. To stain nuclear envelope, 2 μg/mL Alexa *Fluor* 488 conjugated to the lectin wheat germ agglutinin (*Molecular Probes*$^{\text{TM}}$) was also applied to the the cells together with the secondary antibody solution. After two washes with PBS, the coverslips were incubated for 3 min in 10 μg/mL Hoechst 33342 in PBS (*Molecular Probes*$^{\text{TM}}$) to stain the DNA, washed again twice and mounted on a glass slide using *Fluoromount-G*$^{\text{TM}}$(*Southern Biotechnologies*).

Table 9. Antibodies used for immunofluorescence

Antigen	Properties	Source	Dilution
Belle	Rabbit polyclonal	Our laboratory	1:100
HA tag	Mouse monoclonal	*COVANCE*	1:1000
Mouse IgG	Goat polyclonal, TRITC-coupled	*Southern Biotech*	1:250
Rabbit IgG	Goat polyclonal, TRITC-coupled	*Southern Biotech*	1:250

7.9.2 Confocal fluorescence microscopy

Confocal images were accquired using a *Carl Zeiss* LSM510 confocal scanning microscope fitted with a 63× oil immersion objective (*Carl Zeiss Plan-Apochromat*). A UV laser was used at 405 nm for excitation of Hoechst 33342 dye (excitation maximum 346 nm), an Ar laser at 488 nm for excitation of EGFP (excitation maximum 488 nm), and HeNe laser at 543 nm for excitation of TRITC (excitation maximum 554 nm). In co-localization experiments, an emission filter set was used to collect emissions at non-overlapping frequency intervals, surrounding each fluorophore's emission maximum to minimize the crosstalk between channels: 420-280 nm for Hoechst 33342, 505-550 nm for EGFP, 560-657 nm for TRITC.

The LSM-FCS software (*Carl Zeiss* in collaboration with the Advanced Light Microscopy Facility, EMBL) was used for image acquisition. Confocal sections were obtained as optical slices of < 1 μm, with pixel time 1.6 μs and stack size 512×512 pixels (16.2 μm×16.2 μm). Images were generated as a mean of four linear scans to improve the signal-to-noise ratio.

Table 10. Oligonucleotide sequences used for cloning, mutagenesis and RT-PCR

No.	Primer name	Sequence	Transcript ID
9	HMGzLBamHI	CGGGATCCCAAGGCGGTAAAGGAGTACG	CG17921-RB
10	HMGzREcoRI	CGGAATTCACTTGACGCGATCGAAAGTT	CG17921-RB
41	CG15861XbaL	CTCTAGATACGAAATGCTGGTGGTCAA	CG1586-RA
42	CG15861NcoR	TACCATGGCCGTTGTGAGCATAATGGTG	CG1586-RA
45	CG15825BamL	CGGGATCCTGGAAGTTCCTTCGGCTCTA	CG15825-RB
46	CG15825EcoR	CGGAATTCGGTGGTCACCTTTCGTTGAT	CG15825-RB
47	CG18522BamL	CGGGATCCATGTACGGCCTGCTGAAGTC	CG18522-RA
48	CG18522EcoR	CGGAATTCGACACAGCTCCATGGTTTCA	CG18522-RA
71	17.6L	GCCGCATACGTCAACAATAA	X01472
72	17.6R	GAGAAGCCTCTGTGCTTGCT	X01472
75	TranspacL	ACACATGGCGCTAAGCTTTT	AF222049
76	TranspacR	AAGATCGTTGCCTCCAGAAA	AF222049
77	JuanL	CTGTAAAGGCGACCATCCAT	AY180919
78	JuanR	TGCTTTGGGATTAGGCAAAG	AY180919
100	CG31642L	ACCAAGGAATTGATGGAACG	CG31642-RA
101	CG31642R	CCGAGGCTTATTTCCTACAAA	CG31642-RA
110	CG15861Int1L	TGATTCTTGCTCCTCACCTT	CG15861-RA
111	CG15861Int1R	TGAGAAAGGGCACATAAACG	CG15861-RA
112	CG15861Int2L	CGCTATATCTTTTCGCCACA	CG15861-RA
113	CG31642Int1L	GCCGCTCACATTTCAATTTT	CG31642-RA
114	CG31642Ex2R	TTGCCGCACAAAGTGTATTC	CG31642-RA
121	CG31641IntL	GACCTTTAACGCGAGCCATA	CG31641
122	CG31641IntR	TCCCGCACTTTAGGTGAAAC	CG31641
125	Dm-miR-7-s	TGGAAGACTAGTGATTTTGTTGT	AJ421767
126	Dm-miR-7-as	ACAACAAAATCACTAGTCTTC	AJ421767
127	Dm-miR-9b-as	CATACAGCTAAAATCACCAAAGA	CG31782-RA
128	Dm-miR-14-as	TAGGAGAGAGAAAAAGACTGA	AJ421776
129	Dm-miR-bantam-as	AATCAGCTTTCAAAATGATCTCA	AJ550546
130	18-S-157-S	TCTTTCAAATGTCTGCCCTATCAAC	FBgn0061475
131	18-S-329-AS	GAGTCCTGTATTGTTATTTTTCGTCAC	FBgn0061475
231	belleFL-HindIII-L	CGCAAGCTTGATGAGTAATGCTATTAACCAA	CG9748-RA
232	belleFL-NotI-R	ATGCGGCCGCTCATTGAGCCCACCAGTCGGG	CG9748-RA
244	AGO2-FL-NotI-R	ATGCGGCCGCTCAGACAAAGTACATGGGGTT	CG7439-RB/C
246	AGO1-RB-FL-EcoRI-L	CGGAATTCCATGTATCCAGTTGGACAACAGTC	CG6671-RB
247	AGO1-FL-NotI-R	ATGCGGCCGCTTAGGCAAAGTACATGACCTTCTTGG	CG6671
250	CG10077-RA-FL-HindIII-L	CGCAAGCTTAATGAACATGTACAACGGACAGATG	CG10077-RA
251	CG10077-RA-FL-NotI-R	ATGCGGCCGCCTAGTTCTGCACAGGCAGCG	CG10077-RA
256	Dmp68FL-NotI-R	ATGCGGCCGCCTAGTCGAAGCGCGAGTGTC	CG10279-RD
257	Dmp68FL-HindIII-L	CGCAAGCTTAATGGCACCACACGATCG	CG10279-RD
259	MBP-FL-HindIII-L	CGCAAGCTTCATGAAAATCGAAGAAGGTAAAC	pETM-41
260	MBP-FL-NotI-R	ATGCGGCCGCCTAGTCTTTCAGGGCTTCATCG	pETM-41
265	CG10686-FL-HindIII-L	CGCAAGCTTGATGAGCGGGGGATTACC	CG10686-RA
266	CG10686-FL-NotI-R	ATGCGGCCGCCTATTGTGAAACTGCCGCC	CG10686-RA
267	AGO2-RC-FL-EcoRV-L	GCGATATCATGCACTTTCCAATTACCACCCCAG	CG7439-RC
272	bel-K345N-L	CCCAGACTGGATCAGGCAACACGGCCGCCTTCCT	CG9748-RA
273	bel-K345N-R	AGGAAGGCGGCCGTGTTGCCTGATCCAGTCTGGG	CG9748-RA
274	bel-E459Q-L	TTCCTTGTACTGGATCAGGCTGATCGTATGT	CG9748-RA
275	bel-E459Q-R	ACATACGATCAGCCTGATCCAGTACAAGGAA	CG9748-RA
276	bel-H645Q-L	GGAGGAGTATGTCCAGCGTATCGGGCGTACC	CG9748-RA
277	bel-H645Q-R	GGTACGCCCGATACGCTGGACATACTCCTCC	CG9748-RA
284	belle-FL-NcoI-L	ATCCATGGCAATGAGTAATGCTATTAACCAA	CG9748-RA
286	Dmp68FL-NcoI-L	TATCCATGGCACCACACGATCG	CG10279-RD
287	Dmp68FL-KpnI-R	ATGGTACCCTAGTCGAAGCGCGAGTGTC	CG10279-RA
295	Act-5C-L	AAATGTGTGACGAAGAAGTTGC	CG4027-RA
296	Act-5C-R	TCTTCATCAGGTAGTCGGTCAA	CG4027-RA
310	Pum-RA-FL-XbaI-R	TATCTAGATTACAGCACAACGTTGCCG	CG9755-RA

No.	Primer name	Sequence	Transcript ID
317	cycB-RA-3'UTR-EcoRI-L	TAGAATTCTGCGGTCCAAGGCGGACTG	CG3510-RA
318	cycB-RA-3'UTR-SalI-R	GACGTCGACCTATGTATTGTTCAGAGAC	CG3510-RA
321	bel-230-KpnI-R	ATGGTACCTTAGCCGCGATTGTTGTAGCTTC	CG9748-RA
327	Pum-RE-extraFL-HindIII-L	TAGAAGCTTGATGGTGGTTTTAGAAACTG	CG9755-RE
330	belle-FL-XhoI-L	GCCTCGAGATGAGTAATGCTATTAACCAA	CG9748-RA
331	belle-FL-EcoRV-R	ATGATATCTTGAGCCCACCAGTCGGGT	CG9748-RA
368	yps-RA-HindIII-L	TATAAGCTTGATGGCTGATGCCGCGGAGAG	CG5654-RA
369	yps-RA-NotI-R	ATGCGGCCGCCTATGCAGTGCTCTCTGTGG	CG5654-RA
374	exu-RA-EcoRI-L	CGGAATTCAATGGTTGCCGATAACATCGATG	CG8994-RA
375	exu-RA-XbaI-R	GCTCTAGATTAGTTGGAGGCCGTGATGGC	CG8994-RA
386	Belle-Y46A-L	CTCGGTCACCGGTGGTGTGGCTGTGCCCCCGCACCTTCGTG	CG9748-RA
387	Belle-Y46A-R	CACGAAGGTGCGGGGGCACAGCCACACCACCGGTGACCGAG	CG9748-RA
388	Belle-L51A-L	TGTGTATGTGCCCCCGCACGCTCGTGGTGGTGGTGGCAATAAC	CG9748-RA
389	Belle-L51A-R	GTTATTGCCACCACCACCACGAGCGTGCGGGGGCACATACACA	CG9748-RA
390	Pasilla-RD-EcoRI-L	TAGAATTCAATGTTGTTCGCCAGAACCAC	CG8144-RD
391	Pasilla-RD-XbaI-R	GCTCTAGATTAATTCACAACAGTGGTTAATG	CG8144-RD
392	Imp-RA-EcoRI-L	CAGAATTCAATGCACAGCAACAATAATAG	CG1619-RA
393	Imp-RA-XbaI-R	GCTCTAGATTACTGTTGTGAGCTCGCCAG	CG1619-RA
394	dFMR-RA-HindIII-L	TATAAGCTTGATGGAAGATCTCCTCGTGG	CG6203-RA
395	dFMR-RA-XhoI-R	GCCTCGAGTTAGGACGTGCCATTGACCAG	CG6203-RA
396	Penguin-HindII-L	TATAAGCTTGATGGTTAGCTCGGAGCCGAAAG	CG1685-RA
397	Penguin-XhoI-R	GCCTCGAGTCATTTGCCAATGTCCAG	CG1685-RA

Table 11. Oligonucleotide sequences used for dsRNA preparation

No.	Primer name	Sequence	ID/Source
1	T7Ago1Left	ttaatacgactcactatagggagaCATTAAAAAGCTGACCGATATGC	CG6671-RA
2	T7Ago1Right	ttaatacgactcactatagggagaTTGACGTTGATCTTCAGACACAG	CG6671-RA
3	T7AubLeft	ttaatacgactcactatagggagaGTGGGTCCCTCGATAGAGAAAT	CG6137-RA
4	T7AubRight	ttaatacgactcactatagggagaGTGGCATATCTCGGAACAAAGT	CG6137-RA
5	T7PiwiLeft	ttaatacgactcactatagggagaCGAACTTTTTCCGATTAAAAACC	CG6122-RA
6	T7PiwiRight	ttaatacgactcactatagggagaAGTTTGTCCAAAGTCGACATCAT	CG6122-RA
31	T7Ago1L	ttaatacgactcactatagggagaCCCAAGTGCCCAGAATGT	CG6671-RA
32	T7Ago1R	ttaatacgactcactatagggagaAACTGAAGAAGCTACGTCCCACT	CG6671-RA
33	T7Ago2L	ttaatacgactcactatagggagaAGGGTGGACTAAACAAGGTCAAC	CG7439-RB
34	T7Ago2R	ttaatacgactcactatagggagaGCTGTTGGTAGCCACCTTCTT	CG7439-RB
35	T7AubL	ttaatacgactcactatagggagaCAGAAGGAGTCTTTCCGCTACTT	CG6137-RA
36	T7AubR	ttaatacgactcactatagggagaACTCGTATGGTTCCGCTGTAAT	CG6137-RA
37	T7PiwiL	ttaatacgactcactatagggagaTATGCGTGCCATGAGCAGTTA	CG6122-RA
38	T7PiwiR	ttaatacgactcactatagggagaTTTCGGCGTTATCATTGGGTA	CG6122-RA
39	T7Ago2cL	ttaatacgactcactatagggagaAAAGAGTACCGTAACGCCTATCC	CG7439-RB
40	T7Ago2cR	ttaatacgactcactatagggagaACTCCTTCTTCAAATCCAGGAAC	CG7439-RB
360	T7belle-Boutros-L	ttaatacgactcactatagggagaTTTGACGGTAATCCCTGGAG	CG9748-RA
361	T7belle-Boutros-R	ttaatacgactcactatagggagaATCCCGTCACTAGCATCCAC	CG9748-RA
Oligonucleotides from other sources			
	GFP-UT7	ttaatacgactcactatagggaggATGGTGAGCAAGGGCGAGGAG	E. Izaurralde
	GFP-LT7	ttaatacgactcactatagggaggCTTGTACAGCTCGTCCATGCCG	E. Izaurralde
	T7U-Drosha	taatacgactcactatagggaggATGTACCAGCCGCCTTTGCCACCG	E. Izaurralde
	T7L741-Dros	taatacgactcactatagggaggGCAGAAGTTAGAACACCACTGTCTC	E. Izaurralde
	Me31B-T7U	taatacgactcactatagggaggATGATGACTGAAAAGTTAAATTCTGGG	E. Izaurralde
	Me31B-T7L	taatacgactcactatagggaggCTTGACTGTTAGTGGAAATGTTGCGG	E. Izaurralde
	eIF4E-UT7-171	ttaatacgactcactatagggaggAGCAGGCAACACTGCAAC	A. Eulálio
	eIF4E-T7L650	ttaatacgactcactatagggaggGCTTCCTCGTTGTTTCCG	A. Eulálio
	eIF4A-UT7	ttaatacgactcactatagggaggATGGATGACCGAAATGAGATACC	A. Eulálio
	eIF4A-T7Low700	ttaatacgactcactatagggaggGACGGGATCACGCATGAAGC	A. Eulálio

Table 12. Details of plasmid construction

Plasmid name	Insert	Origin of insert/Source	Primer No.	Parent plasmid
GST-Belle 1-230	Belle ORF (aa. 1-230)	S2 cells cDNA library	284/321	pETM-30
λN-HA-Bel	Belle ORF	S2 cells cDNA library	231/232	λN-HA pAc5.1
λN-HA-Bel K345N	Belle ORF, K345N	Mutagenesis of λN-HA-Bel	272/273	λN-HA-Bel
λN-HA-Bel E459Q	Belle ORF, E459Q	Mutagenesis of λN-HA-Bel	274/275	λN-HA-Bel
λN-HA-Bel H645Q	Belle ORF, H645Q	Mutagenesis of λN-HA-Bel	276/277	λN-HA-Bel
λN-HA-Bel Y46A	Belle ORF, Y46A	Mutagenesis of λN-HA-Bel	386/387	λN-HA-Bel
λN-HA-Bel L51A	Belle ORF, L51A	Mutagenesis of λN-HA-Bel	388/389	λN-HA-Bel
λN-HA-Bel Y46A, L51A	Belle ORF, Y46A, L51A	Mutagenesis of λN-HA-Bel Y46A	388/389	λN-HA-Bel Y46A
EGFP-Belle	Belle ORF	S2 cells cDNA library	231/232	EGFP pAc5.1
EGFP-Bel K345N	Belle ORF, K345N	Mutagenesis of EGFP-Bel	272/273	EGFP-Bel
EGFP-Bel E459Q	Belle ORF, E459Q	Mutagenesis of EGFP-Bel	274/275	EGFP-Bel
EGFP-Bel H645Q	Belle ORF, H645Q	Mutagenesis of EGFP-Bel	276/277	EGFP-Bel
EGFP-Bel Y46A	Belle ORF, Y46A	Mutagenesis of EGFP-Bel	386/387	EGFP-Bel
EGFP-Bel L51A	Belle ORF, L51A	Mutagenesis of EGFP-Bel	388/389	EGFP-Bel
EGFP-Bel Y46A, L51A	Belle ORF, Y46A, L51A	Mutagenesis of EGFP-Bel Y46A	388/389	EGFP-Bel Y46A
Bel-TAP	Belle ORF	S2 cells cDNA library	330/331	pSD135
Bel-K345N-TAP	Belle ORF	Mutagenesis of Bel-TAP	272/273	Bel-TAP
λN-HA-Rm62	Rm62 ORF	S2 cells cDNA library	257/256	λN-HA pAc5.1
EGFP-Rm62	Rm62 ORF	S2 cells cDNA library	257/256	EGFP pAc5.1
λN-HA-CG10077	CG10077 ORF	S2 cells cDNA library	250/251	λN-HA pAc5.1
EGFP-CG10077	CG10077 ORF	S2 cells cDNA library	250/251	EGFP pAc5.1
λN-HA-Tral	Tral ORF	S2 cells cDNA library	265/266	λN-HA pAc5.1
EGFP-Tral	Tral ORF	S2 cells cDNA library	265/266	EGFP pAc5.1
λN-HA-Imp	Imp ORF	S2 cells cDNA library	392/393	λN-HA pAc5.1
EGFP-Imp	Imp ORF	S2 cells cDNA library	392/393	EGFP pAc5.1
λN-HA-Ps	Pasilla ORF	S2 cells cDNA library	390/391	λN-HA pAc5.1
EGFP-Ps	Pasilla ORF	S2 cells cDNA library	390/391	EGFP pAc5.1
λN-HA-dFMR1	dFMR1 ORF	S2 cells cDNA library	394/395	λN-HA pAc5.1
EGFP-dFMR1	dFMR1 ORF	S2 cells cDNA library	394/395	EGFP pAc5.1
λN-HA-YPS	YPS ORF	S2 cells cDNA library	368/369	λN-HA pAc5.1
EGFP-YPS	YPS ORF	S2 cells cDNA library	368/369	EGFP pAc5.1
λN-HA-EXU	Exuperantia ORF	S2 cells cDNA library	374/375	λN-HA pAc5.1
EGFP-EXU	Exuperantia ORF	S2 cells cDNA library	374/375	EGFP pAc5.1
λN-HA-Pum	Pumilio ORF	S2 cells cDNA library	327/310	λN-HA pAc5.1
EGFP-Pum	Pumilio ORF	S2 cells cDNA library	327/310	EGFP pAc5.1

Plasmid name	Insert	Origin of insert/Source	Primer No.	Parent plasmid
λN-HA-Pen	Penguin ORF	S2 cells cDNA library	396/397	λN-HA pAc5.1
EGFP-Pen	Penguin ORF	S2 cells cDNA library	396/397	EGFP pAc5.1
λN-HA-AGO1	AGO1 ORF	S2 cells cDNA library	246/247	λN-HA pAc5.1
EGFP-AGO1	AGO1 ORF	S2 cells cDNA library	246/247	EGFP pAc5.1
λN-HA-AGO2	AGO2 ORF	S2 cells cDNA library	267/244	λN-HA pAc5.1
EGFP-AGO2	AGO2 ORF	S2 cells cDNA library	267/244	EGFP pAc5.1
λN-HA-MBP	MBP ORF	pETM-41	259/260	λN-HA pAc5.1
Plasmids from other sources				
λN-HA-eIF4E	eIF4E ORF	A. Eulálio		λN-HA pAc5.1
EGFP-eIF4E	eIF4E ORF	A. Eulálio		EGFP pAc5.1
EGFP-eIF4E-T	eIF4E-T ORF	A. Eulálio		EGFP pAc5.1
λN-HA-eIF4G	eIF4G ORF	A. Eulálio		λN-HA pAc5.1
λN-HA-Me31B	Me31B ORF	E. Izaurralde		λN-HA pAc5.1
EGFP-PAT1	PAT1 ORF	A. Eulálio		EGFP pAc5.1
EGFP-DCP1	DCP1 ORF	E. Izaurralde		EGFP pAc5.1
EGFP-EDC3	EDC3 ORF	E. Izaurralde		EGFP pAc5.1
EGFP-CAF1	CAF1 ORF	A. Eulalio		EGFP pAc5.1
R-luc	*Renilla* luciferase ORF	[347]		pAc5.1
F-luc-5BoxB	3′ UTR with 5 BoxB elements	[347]		F-luc pAc5.1
F-luc-Nerfin	Nerfin 3′ UTR	[394]		pJ-Luc
F-luc-CG12403	CG12403 3′ UTR	[347]		pJ-Luc
F-luc-CG10011	CG10011 3′ UTR	[347]		pJ-Luc
F-luc-CG3401	CG3401 3′ UTR	[347]		pJ-Luc
F-luc-CG4851	CG4851 3′ UTR	[347]		pJ-Luc
F-luc-CG6446	CG6446 3′ UTR	[347]		pJ-Luc
F-luc-CG12505	CG12505 3′ UTR	[347]		pJ-Luc
F-luc-CG30337	CG30337 3′ UTR	[347]		pJ-Luc
F-luc-CG31886	CG31886 3′ UTR	[347]		pJ-Luc
F-luc-CG33087	CG33087 3′ UTR	[347]		pJ-Luc
F-luc-CG1172	CG1172 3′ UTR	[348]		pJ-Luc
F-luc-CG2928	CG2928 3′ UTR	[348]		pJ-Luc
F-luc-CG3799	CG3799 3′ UTR	[348]		pJ-Luc
F-luc-CG5977	CG5977 3′ UTR	[348]		pJ-Luc
F-luc-CG7417	CG7417 3′ UTR	[348]		pJ-Luc
F-luc-CG9995	CG9995 3′ UTR	[348]		pJ-Luc
F-luc-CG10719	CG10719 3′ UTR	[348]		pJ-Luc

Plasmid name	Insert	Origin of insert/Source	Primer No.	Parent plasmid
F-luc-CG18604	CG18604 3′ UTR	[348]		pJ-Luc
F-luc-CG31712	CG31712 3′ UTR	[348]		PJ-Luc
miR-2b	200 nt genomic miR-2b sequence	[348]		pAc5.1
miR-9a	200 nt genomic miR-9a sequence	[348]		pAc5.1
miR-9b	200 nt genomic miR-9b sequence	[348]		pAc5.1
miR-12	200 nt genomic miR-12 sequence	[348]		pAc5.1
miR-13a/b	200 nt genomic miR-13a/b sequence	[348]		pAc5.1
miR-14	200 nt genomic miR-14 sequence	[348]		pAc5.1

References

[1] Abaza, I., Coll, O., Patalano, S. & Gebauer, F. Drosophila UNR is required for translational repression of male-specific lethal 2 mRNA during regulation of X-chromosome dosage compensation. *Genes Dev* **20**, 380–389 (2006).

[2] Al-Shahrour, F., Díaz-Uriarte, R. & Dopazo, J. FatiGO: a web tool for finding significant associations of Gene Ontology terms with groups of genes. *Bioinformatics* **20**, 578–580 (2004).

[3] Alderete, J. P., Child, S. J. & Geballe, A. P. Abundant early expression of gpUL4 from a human cytomegalovirus mutant lacking a repressive upstream open reading frame. *J Virol* **75**, 7188–7192 (2001).

[4] Alekhina, O. M., Vassilenko, K. S. & Spirin, A. S. Translation of non-capped mRNAs in a eukaryotic cell-free system: acceleration of initiation rate in the course of polysome formation. *Nucleic Acids Res* **35**, 6547–6559 (2007).

[5] Alemán, L. M., Doench, J. & Sharp, P. A. Comparison of siRNA-induced off-target RNA and protein effects. *RNA* **13**, 385–395 (2007).

[6] Anderson, P. & Kedersha, N. Stressful initiations. *J Cell Sci* **115**, 3227–3234 (2002).

[7] Anderson, P. & Kedersha, N. RNA granules. *J Cell Biol* **172**, 803–808 (2006).

[8] Anderson, P. & Kedersha, N. Stress granules: the Tao of RNA triage. *Trends Biochem Sci* **33**, 141–150 (2008).

[9] Andrade, M. A. & Bork, P. HEAT repeats in the Huntington's disease protein. *Nat Genet* **11**, 115–116 (1995).

[10] Antar, L. N., Afroz, R., Dictenberg, J. B., Carroll, R. C. & Bassell, G. J. Metabotropic glutamate receptor activation regulates fragile x mental retardation protein and FMR1 mRNA localization differentially in dendrites and at synapses. *J Neurosci* **24**, 2648–2655 (2004).

[11] Antar, L. N., Dictenberg, J. B., Plociniak, M., Afroz, R. & Bassell, G. J. Localization of FMRP-associated mRNA granules and requirement of microtubules for activity-dependent trafficking in hippocampal neurons. *Genes Brain Behav* **4**, 350–359 (2005).

[12] Aravin, A. A., Hannon, G. J. & Brennecke, J. The Piwi-piRNA pathway provides an adaptive defense in the transposon arms race. *Science* **318**, 761–764 (2007).

[13] Aravin, A. A., Klenov, M. S., Vagin, V. V., Bantignies, F., Cavalli, G. & Gvozdev, V. A. Dissection of a natural RNA silencing process in the Drosophila melanogaster germ line. *Mol Cell Biol* **24**, 6742–6750 (2004).

[14] Aravin, A. A., Lagos-Quintana, M., Yalcin, A., Zavolan, M., Marks, D., Snyder, B., Gaasterland, T., Meyer, J. & Tuschl, T. The small RNA profile during Drosophila melanogaster development. *Dev Cell* **5**, 337–350 (2003).

[15] Aronov, S., Aranda, G., Behar, L. & Ginzburg, I. Visualization of translated tau protein in the axons of neuronal P19 cells and characterization of tau RNP granules. *J Cell Sci* **115**, 3817–3827 (2002).

[16] Asaoka-Taguchi, M., Yamada, M., Nakamura, A., Hanyu, K. & Kobayashi, S. Maternal Pumilio acts together with Nanos in germline development in Drosophila embryos. *Nat Cell Biol* **1**, 431–437 (1999).

[17] Ashburner, M., Ball, C. A., Blake, J. A., Botstein, D., Butler, H., Cherry, J. M., Davis, A. P., Dolinski, K., Dwight, S. S., Eppig, J. T., Harris, M. A., Hill, D. P., Issel-Tarver, L., Kasarskis, A., Lewis, S., Matese, J. C., Richardson, J. E., Ringwald, M., Rubin, G. M. & Sherlock, G. Gene ontology: tool for the unification of biology. The Gene Ontology Consortium. *Nat Genet* **25**, 25–29 (2000).

[18] Ashley, C. T., Wilkinson, K. D., Reines, D. & Warren, S. T. FMR1 protein: conserved RNP family domains and selective RNA binding. *Science* **262**, 563–566 (1993).

[19] Aviv, T., Lin, Z., Lau, S., Rendl, L. M., Sicheri, F. & Smibert, C. A. The RNA-binding SAM domain of Smaug defines a new family of post-transcriptional regulators. *Nat Struct Biol* **10**, 614–621 (2003).

[20] Bablanian, R., Goswami, S. K., Esteban, M., Banerjee, A. K. & Merrick, W. C. Mechanism of selective translation of vaccinia virus mRNAs: differential role of poly(A) and initiation factors in the translation of viral and cellular mRNAs. *J Virol* **65**, 4449–4460 (1991).

[21] Bader, G. D. & Hogue, C. W. V. An automated method for finding molecular complexes in large protein interaction networks. *BMC Bioinformatics* **4**, 2 (2003).

[22] Bagga, S., Bracht, J., Hunter, S., Massirer, K., Holtz, J., Eachus, R. & Pasquinelli, A. E. Regulation by let-7 and lin-4 miRNAs results in target mRNA degradation. *Cell* **122**, 553–563 (2005).

[23] Bagni, C. & Greenough, W. T. From mRNP trafficking to spine dysmorphogenesis: the roots of fragile X syndrome. *Nat Rev Neurosci* **6**, 376–387 (2005).

[24] Barbee, S. A., Estes, P. S., Cziko, A.-M., Hillebrand, J., Luedeman, R. A., Coller, J. M., Johnson, N., Howlett, I. C., Geng, C., Ueda, R., Brand, A. H., Newbury, S. F., Wilhelm, J. E., Levine, R. B., Nakamura, A., Parker, R. & Ramaswami, M. Staufen- and FMRP-containing neuronal RNPs are structurally and functionally related to somatic P bodies. *Neuron* **52**, 997–1009 (2006).

[25] Barker, D. D., Wang, C., Moore, J., Dickinson, L. K. & Lehmann, R. Pumilio is essential for function but not for distribution of the Drosophila abdominal determinant Nanos. *Genes Dev* **6**, 2312–2326 (1992).

[26] Bartel, D. P. MicroRNAs: genomics, biogenesis, mechanism, and function. *Cell* **116**, 281–297 (2004).

[27] Bashaw, G. J. & Baker, B. S. The msl-2 dosage compensation gene of Drosophila encodes a putative DNA-binding protein whose expression is sex specifically regulated by Sex-lethal. *Development* **121**, 3245–3258 (1995).

[28] Beckham, C., Hilliker, A., Cziko, A.-M., Noueiry, A., Ramaswami, M. & Parker, R. The DEAD-Box RNA Helicase Ded1p Affects and Accumulates in Saccharomyces cerevisiae P-Bodies. *Mol Biol Cell* **19**, 984–993 (2008).

[29] Beckmann, K., Grskovic, M., Gebauer, F. & Hentze, M. W. A dual inhibitory mechanism restricts msl-2 mRNA translation for dosage compensation in Drosophila. *Cell* **122**, 529–540 (2005).

[30] Behm-Ansmant, I., Rehwinkel, J., Doerks, T., Stark, A., Bork, P. & Izaurralde, E. mRNA degradation by miRNAs and GW182 requires both CCR4:NOT deadenylase and DCP1:DCP2 decapping complexes. *Genes Dev* **20**, 1885–1898 (2006).

[31] Benjamini, Y. & Hochberg, Y. Controlling the False Discovery Rate: a Practical and Powerful Approach to Multiple Testing. *Journal of the Royal Statistical Society B* **57**, 289 –300 (1995).

[32] Benjamini, Y. & Yekutieli, D. The control of the false discovery rate in multiple testing under dependency. *The Annals of Statistics* **29**, 1165–118 (2001).

[33] Benoit, B., Mitou, G., Chartier, A., Temme, C., Zaessinger, S., Wahle, E., Busseau, I. & Simonelig, M. An essential cytoplasmic function for the nuclear poly(A) binding protein, PABP2, in poly(A) tail length control and early development in Drosophila. *Dev Cell* **9**, 511–522 (2005).

[34] Berezikov, E., Chung, W.-J., Willis, J., Cuppen, E. & Lai, E. C. Mammalian mirtron genes. *Mol Cell* **28**, 328–336 (2007).

[35] Bergsten, S. E. & Gavis, E. R. Role for mRNA localization in translational activation but not spatial restriction of nanos RNA. *Development* **126**, 659–669 (1999).

[36] Berthelot, K., Muldoon, M., Rajkowitsch, L., Hughes, J. & McCarthy, J. E. G. Dynamics and processivity of 40S ribosome scanning on mRNA in yeast. *Mol Microbiol* **51**, 987–1001 (2004).

[37] Bertholet, C., Meir, E. V., ten Heggeler-Bordier, B. & Wittek, R. Vaccinia virus produces late mRNAs by discontinuous synthesis. *Cell* **50**, 153–162 (1987).

[38] Bhattacharyya, S. N., Habermacher, R., Martine, U., Closs, E. I. & Filipowicz, W. Relief of microRNA-mediated translational repression in human cells subjected to stress. *Cell* **125**, 1111–1124 (2006).

[39] Bohnsack, M. T., Czaplinski, K. & Gorlich, D. Exportin 5 is a RanGTP-dependent dsRNA-binding protein that mediates nuclear export of pre-miRNAs. *RNA* **10**, 185–191 (2004).

[40] Bonnerot, C., Boeck, R. & Lapeyre, B. The two proteins Pat1p (Mrt1p) and Spb8p interact in vivo, are required for mRNA decay, and are functionally linked to Pab1p. *Mol Cell Biol* **20**, 5939–5946 (2000).

[41] Borchert, G. M., Lanier, W. & Davidson, B. L. RNA polymerase III transcribes human microRNAs. *Nat Struct Mol Biol* **13**, 1097–1101 (2006).

[42] Boylan, K. L. M., Mische, S., Li, M., Marqués, G., Morin, X., Chia, W. & Hays, T. S. Motility screen identifies Drosophila IGF-II mRNA-binding protein–zipcode-binding protein acting in oogenesis and synaptogenesis. *PLoS Genet* **4**, e36 (2008).

[43] Boyle, E. I., Weng, S., Gollub, J., Jin, H., Botstein, D., Cherry, J. M. & Sherlock, G. GO::TermFinder–open source software for accessing Gene Ontology information and finding significantly enriched Gene Ontology terms associated with a list of genes. *Bioinformatics* **20**, 3710–3715 (2004).

[44] Bramham, C. R. & Wells, D. G. Dendritic mRNA: transport, translation and function. *Nat Rev Neurosci* **8**, 776–789 (2007).

[45] Breitwieser, W., Markussen, F. H., Horstmann, H. & Ephrussi, A. Oskar protein interaction with Vasa represents an essential step in polar granule assembly. *Genes Dev* **10**, 2179–2188 (1996).

[46] Brennecke, J., Hipfner, D. R., Stark, A., Russell, R. B. & Cohen, S. M. bantam encodes a developmentally regulated microRNA that controls cell proliferation and regulates the proapoptotic gene hid in Drosophila. *Cell* **113**, 25–36 (2003).

[47] Brennecke, J., Stark, A., Russell, R. B. & Cohen, S. M. Principles of microRNA-target recognition. *PLoS Biol* **3**, e85 (2005).

[48] Brenner, S., Jacob, F. & Meselson, M. An unstable intermediate carrying information from genes to ribosomes for protein synthesis. *Nature* **190**, 576 – 581 (1961).

[49] Bridges, D. & Moorhead, G. B. G. 14-3-3 proteins: a number of functions for a numbered protein. *Sci STKE* **2005**, re10 (2005).

[50] Bushati, N. & Cohen, S. M. microRNA functions. *Annu Rev Cell Dev Biol* **23**, 175–205 (2007).

[51] Cai, X., Hagedorn, C. H. & Cullen, B. R. Human microRNAs are processed from capped, polyadenylated transcripts that can also function as mRNAs. *RNA* **10**, 1957–1966 (2004).

[52] Cao, Q. & Richter, J. D. Dissolution of the maskin-eIF4E complex by cytoplasmic polyadenylation and poly(A)-binding protein controls cyclin B1 mRNA translation and oocyte maturation. *EMBO J* **21**, 3852–3862 (2002).

[53] Carlberg, U., Nilsson, A. & Nygård, O. Functional properties of phosphorylated elongation factor 2. *Eur J Biochem* **191**, 639–645 (1990).

[54] Castagnetti, S. & Ephrussi, A. Orb and a long poly(A) tail are required for efficient oskar translation at the posterior pole of the Drosophila oocyte. *Development* **130**, 835–843 (2003).

[55] Castagnetti, S., Hentze, M. W., Ephrussi, A. & Gebauer, F. Control of oskar mRNA translation by Bruno in a novel cell-free system from Drosophila ovaries. *Development* **127**, 1063–1068 (2000).

[56] Caudy, A. A., Myers, M., Hannon, G. J. & Hammond, S. M. Fragile X-related protein and VIG associate with the RNA interference machinery. *Genes Dev* **16**, 2491–2496 (2002).

[57] Cermelli, S., Guo, Y., Gross, S. P. & Welte, M. A. The lipid-droplet proteome reveals that droplets are a protein-storage depot. *Curr Biol* **16**, 1783–1795 (2006).

[58] Chagnovich, D. & Lehmann, R. Poly(A)-independent regulation of maternal hunchback translation in the Drosophila embryo. *Proc Natl Acad Sci U S A* **98**, 11359–11364 (2001).

[59] Chang, T.-C., Yamashita, A., Chen, C.-Y. A., Yamashita, Y., Zhu, W., Durdan, S., Kahvejian, A., Sonenberg, N. & Shyu, A.-B. UNR, a new partner of poly(A)-binding protein, plays a key role in translationally coupled mRNA turnover mediated by the c-fos major coding-region determinant. *Genes Dev* **18**, 2010–2023 (2004).

[60] Chao, C.-H., Chen, C.-M., Cheng, P.-L., Shih, J.-W., Tsou, A.-P. & Lee, Y.-H. W. DDX3, a DEAD box RNA helicase with tumor growth-suppressive property and transcriptional regulation activity of the p21waf1/cip1 promoter, is a candidate tumor suppressor. *Cancer Res* **66**, 6579–6588 (2006).

[61] Chekulaeva, M., Hentze, M. W. & Ephrussi, A. Bruno acts as a dual repressor of oskar translation, promoting mRNA oligomerization and formation of silencing particles. *Cell* **124**, 521–533 (2006).

[62] Chen, C. Y. & Sarnow, P. Initiation of protein synthesis by the eukaryotic translational apparatus on circular RNAs. *Science* **268**, 415–417 (1995).

[63] Chendrimada, T. P., Finn, K. J., Ji, X., Baillat, D., Gregory, R. I., Liebhaber, S. A., Pasquinelli, A. E. & Shiekhattar, R. MicroRNA silencing through RISC recruitment of eIF6. *Nature* **447**, 823–828 (2007).

[64] Chendrimada, T. P., Gregory, R. I., Kumaraswamy, E., Norman, J., Cooch, N., Nishikura, K. & Shiekhattar, R. TRBP recruits the Dicer complex to Ago2 for microRNA processing and gene silencing. *Nature* **436**, 740–744 (2005).

[65] Cho, P. F., Gamberi, C., Cho-Park, Y. A., Cho-Park, I. B., Lasko, P. & Sonenberg, N. Cap-dependent translational inhibition establishes two opposing morphogen gradients in Drosophila embryos. *Curr Biol* **16**, 2035–2041 (2006).

[66] Cho, P. F., Poulin, F., Cho-Park, Y. A., Cho-Park, I. B., Chicoine, J. D., Lasko, P. & Sonenberg, N. A new paradigm for translational control: inhibition via 5'-3' mRNA tethering by Bicoid and the eIF4E cognate 4EHP. *Cell* **121**, 411–423 (2005).

[67] Chomczynski, P. & Sacchi, N. Single-step method of RNA isolation by acid guanidinium thiocyanate-phenol-chloroform extraction. *Anal Biochem* **162**, 156–159 (1987).

[68] Chuang, R. Y., Weaver, P. L., Liu, Z. & Chang, T. H. Requirement of the DEAD-Box protein ded1p for messenger RNA translation. *Science* **275**, 1468–1471 (1997).

[69] Chung, W.-J., Okamura, K., Martin, R. & Lai, E. C. Endogenous RNA interference provides a somatic defense against Drosophila transposons. *Curr Biol* **18**, 795–802 (2008).

[70] Clark, I. E., Wyckoff, D. & Gavis, E. R. Synthesis of the posterior determinant Nanos is spatially restricted by a novel cotranslational regulatory mechanism. *Curr Biol* **10**, 1311–1314 (2000).

[71] Clemens, J. C., Worby, C. A., Simonson-Leff, N., Muda, M., Maehama, T., Hemmings, B. A. & Dixon, J. E. Use of double-stranded RNA interference in Drosophila cell lines to dissect signal transduction pathways. *Proc Natl Acad Sci U S A* **97**, 6499–6503 (2000).

[72] Cline, M. S., Smoot, M., Cerami, E., Kuchinsky, A., Landys, N., Workman, C., Christmas, R., Avila-Campilo, I., Creech, M., Gross, B., Hanspers, K., Isserlin, R., Kelley, R., Killcoyne, S., Lotia, S., Maere, S., Morris, J., Ono, K., Pavlovic, V., Pico, A. R., Vailaya, A., Wang, P.-L., Adler, A., Conklin, B. R., Hood, L., Kuiper, M., Sander, C., Schmulevich, I., Schwikowski, B., Warner, G. J., Ideker, T. & Bader, G. D. Integration of biological networks and gene expression data using Cytoscape. *Nat Protoc* **2**, 2366–2382 (2007).

[73] Coller, J. & Parker, R. General translational repression by activators of mRNA decapping. *Cell* **122**, 875–886 (2005).

[74] Coller, J. M., Tucker, M., Sheth, U., Valencia-Sanchez, M. A. & Parker, R. The DEAD box helicase, Dhh1p, functions in mRNA decapping and interacts with both the decapping and deadenylase complexes. *RNA* **7**, 1717–1727 (2001).

[75] Condeelis, J. & Singer, R. H. How and why does beta-actin mRNA target? *Biol Cell* **97**, 97–110 (2005).

[76] Cook, H. A., Koppetsch, B. S., Wu, J. & Theurkauf, W. E. The Drosophila SDE3 homolog armitage is required for oskar mRNA silencing and embryonic axis specification. *Cell* **116**, 817–829 (2004).

[77] Cordin, O., Banroques, J., Tanner, N. K. & Linder, P. The DEAD-box protein family of RNA helicases. *Gene* **367**, 17–37 (2006).

[78] Cox, D. N., Chao, A., Baker, J., Chang, L., Qiao, D. & Lin, H. A novel class of evolutionarily conserved genes defined by piwi are essential for stem cell self-renewal. *Genes Dev* **12**, 3715–3727 (1998).

[79] Crucs, S., Chatterjee, S. & Gavis, E. R. Overlapping but distinct RNA elements control repression and activation of nanos translation. *Mol Cell* **5**, 457–467 (2000).

[80] Czech, B., Malone, C. D., Zhou, R., Stark, A., Schlingeheyde, C., Dus, M., Perrimon, N., Kellis, M., Wohlschlegel, J. A., Sachidanandam, R., Hannon, G. J. & Brennecke, J. An endogenous small interfering RNA pathway in Drosophila. *Nature* **453**, 798–802 (2008).

[81] Dahanukar, A., Walker, J. A. & Wharton, R. P. Smaug, a novel RNA-binding protein that operates a translational switch in Drosophila. *Mol Cell* **4**, 209–218 (1999).

[82] Dahanukar, A. & Wharton, R. P. The Nanos gradient in Drosophila embryos is generated by translational regulation. *Genes Dev* **10**, 2610–2620 (1996).

[83] Danin-Kreiselman, M., Lee, C. Y. & Chanfreau, G. RNAse III-mediated degradation of unspliced pre-mRNAs and lariat introns. *Mol Cell* **11**, 1279–1289 (2003).

[84] de la Cruz, J., Iost, I., Kressler, D. & Linder, P. The p20 and Ded1 proteins have antagonistic roles in eIF4E-dependent translation in Saccharomyces cerevisiae. *Proc Natl Acad Sci U S A* **94**, 5201–5206 (1997).

[85] Denli, A. M., Tops, B. B. J., Plasterk, R. H. A., Ketting, R. F. & Hannon, G. J. Processing of primary microRNAs by the Microprocessor complex. *Nature* **432**, 231–235 (2004).

[86] Derry, M. C., Yanagiya, A., Martineau, Y. & Sonenberg, N. Regulation of poly(A)-binding protein through PABP-interacting proteins. *Cold Spring Harb Symp Quant Biol* **71**, 537–543 (2006).

[87] Deshpande, G., Calhoun, G. & Schedl, P. Drosophila argonaute-2 is required early in embryogenesis for the assembly of centric/centromeric heterochromatin, nuclear division, nuclear migration, and germ-cell formation. *Genes Dev* **19**, 1680–1685 (2005).

[88] Dever, T. E., Arvin, C. D. & Sicheri, F. The eIF2α Kinases. In *Translational control in biology and medicine*, edited by M. Mathews, N. Sonenberg & J. Hershey, chap. 12. Cold Spring Harbor Laboratory Press, New York (2007).

[89] Dictenberg, J. B., Swanger, S. A., Antar, L. N., Singer, R. H. & Bassell, G. J. A direct role for FMRP in activity-dependent dendritic mRNA transport links filopodial-spine morphogenesis to fragile X syndrome. *Dev Cell* **14**, 926–939 (2008).

[90] Ding, L. & Han, M. GW182 family proteins are crucial for microRNA-mediated gene silencing. *Trends Cell Biol* **17**, 411–416 (2007).

[91] Ding, L., Spencer, A., Morita, K. & Han, M. The developmental timing regulator AIN-1 interacts with miRISCs and may target the argonaute protein ALG-1 to cytoplasmic P bodies in C. elegans. *Mol Cell* **19**, 437–447 (2005).

[92] Doench, J. G., Petersen, C. P. & Sharp, P. A. siRNAs can function as miRNAs. *Genes Dev* **17**, 438–442 (2003).

[93] Doench, J. G. & Sharp, P. A. Specificity of microRNA target selection in translational repression. *Genes Dev* **18**, 504–511 (2004).

[94] Dorokhov, Y. L., Skulachev, M. V., Ivanov, P. A., Zvereva, S. D., Tjulkina, L. G., Merits, A., Gleba, Y. Y., Hohn, T. & Atabekov, J. G. Polypurine (A)-rich sequences promote cross-kingdom conservation of internal ribosome entry. *Proc Natl Acad Sci U S A* **99**, 5301–5306 (2002).

[95] Dostie, J., Ferraiuolo, M., Pause, A., Adam, S. A. & Sonenberg, N. A novel shuttling protein, 4E-T, mediates the nuclear import of the mRNA 5' cap-binding protein, eIF4E. *EMBO J* **19**, 3142–3156 (2000).

[96] Doudna, J. & Sarnow, P. Translation initiation by viral IRES. In *Translational control in biology and medicine*, edited by M. Mathews, N. Sonenberg & J. Hershey, chap. 5. Cold Spring Harbor Laboratory Press, New York (2007).

[97] Dreyfuss, G., Kim, V. N. & Kataoka, N. Messenger-RNA-binding proteins and the messages they carry. *Nat Rev Mol Cell Biol* **3**, 195–205 (2002).

[98] Du, T. & Zamore, P. D. microPrimer: the biogenesis and function of microRNA. *Development* **132**, 4645–4652 (2005).

[99] Du, T.-G., Schmid, M. & Jansen, R.-P. Why cells move messages: the biological functions of mRNA localization. *Semin Cell Dev Biol* **18**, 171–177 (2007).

[100] Dubnau, J. & Struhl, G. RNA recognition and translational regulation by a homeodomain protein. *Nature* **379**, 694–699 (1996).

[101] Duncan, K., Grskovic, M., Strein, C., Beckmann, K., Niggeweg, R., Abaza, I., Gebauer, F., Wilm, M. & Hentze, M. W. Sex-lethal imparts a sex-specific function to UNR by recruiting it to the msl-2 mRNA 3' UTR: translational repression for dosage compensation. *Genes Dev* **20**, 368–379 (2006).

[102] Eberhart, D. E., Malter, H. E., Feng, Y. & Warren, S. T. The fragile X mental retardation protein is a ribonucleoprotein containing both nuclear localization and nuclear export signals. *Hum Mol Genet* **5**, 1083–1091 (1996).

[103] Edwards, T. A., Pyle, S. E., Wharton, R. P. & Aggarwal, A. K. Structure of Pumilio reveals similarity between RNA and peptide binding motifs. *Cell* **105**, 281–289 (2001).

[104] Elroy-Stein, O. & Merrick, W. Translation initiation via cellular internal ribosome entry sites. In *Translational control in biology and medicine*, edited by M. Mathews, N. Sonenberg & J. Hershey, chap. 6. Cold Spring Harbor Laboratory Press, New York (2007).

[105] Elvira, G., Wasiak, S., Blandford, V., Tong, X.-K., Serrano, A., Fan, X., del Rayo Sánchez-Carbente, M., Servant, F., Bell, A. W., Boismenu, D., Lacaille, J.-C., McPherson, P. S., DesGroseillers, L. & Sossin, W. S. Characterization of an RNA granule from developing brain. *Mol Cell Proteomics* **5**, 635–651 (2006).

[106] Enright, A. J., John, B., Gaul, U., Tuschl, T., Sander, C. & Marks, D. S. MicroRNA targets in Drosophila. *Genome Biol* **5**, R1 (2003).

[107] Ephrussi, A. & Johnston, D. S. Seeing is believing: the bicoid morphogen gradient matures. *Cell* **116**, 143–152 (2004).

[108] Estes, P. S., O'Shea, M., Clasen, S. & Zarnescu, D. C. Fragile X protein controls the efficacy of mRNA transport in Drosophila neurons. *Mol Cell Neurosci* **39**, 170–179 (2008).

[109] Eulalio, A., Behm-Ansmant, I. & Izaurralde, E. P bodies: at the crossroads of post-transcriptional pathways. *Nat Rev Mol Cell Biol* **8**, 9–22 (2007).

[110] Eulalio, A., Behm-Ansmant, I., Schweizer, D. & Izaurralde, E. P-body formation is a consequence, not the cause, of RNA-mediated gene silencing. *Mol Cell Biol* **27**, 3970–3981 (2007).

[111] Eulalio, A., Huntzinger, E. & Izaurralde, E. Getting to the root of miRNA-mediated gene silencing. *Cell* **132**, 9–14 (2008).

[112] Eulalio, A., Huntzinger, E. & Izaurralde, E. GW182 interaction with Argonaute is essential for miRNA-mediated translational repression and mRNA decay. *Nat Struct Mol Biol* **15**, 346–353 (2008).

[113] Eulalio, A., Rehwinkel, J., Stricker, M., Huntzinger, E., Yang, S.-F., Doerks, T., Dorner, S., Bork, P., Boutros, M. & Izaurralde, E. Target-specific requirements for enhancers of decapping in miRNA-mediated gene silencing. *Genes Dev* **21**, 2558–2570 (2007).

[114] Fang, P., Spevak, C. C., Wu, C. & Sachs, M. S. A nascent polypeptide domain that can regulate translation elongation. *Proc Natl Acad Sci U S A* **101**, 4059–4064 (2004).

[115] Farh, K. K.-H., Grimson, A., Jan, C., Lewis, B. P., Johnston, W. K., Lim, L. P., Burge, C. B. & Bartel, D. P. The widespread impact of mammalian MicroRNAs on mRNA repression and evolution. *Science* **310**, 1817–1821 (2005).

[116] Feinberg, A. P. & Vogelstein, B. A technique for radiolabeling DNA restriction endonuclease fragments to high specific activity. *Anal Biochem* **132**, 6–13 (1983).

[117] Feng, Y., Absher, D., Eberhart, D. E., Brown, V., Malter, H. E. & Warren, S. T. FMRP associates with polyribosomes as an mRNP, and the I304N mutation of severe fragile X syndrome abolishes this association. *Mol Cell* **1**, 109–118 (1997).

[118] Fenger-Grøn, M., Fillman, C., Norrild, B. & Lykke-Andersen, J. Multiple processing body factors and the ARE binding protein TTP activate mRNA decapping. *Mol Cell* **20**, 905–915 (2005).

[119] Filipowicz, W., Bhattacharyya, S. N. & Sonenberg, N. Mechanisms of post-transcriptional regulation by microRNAs: are the answers in sight? *Nat Rev Genet* **9**, 102–114 (2008).

[120] Findley, S. D., Tamanaha, M., Clegg, N. J. & Ruohola-Baker, H. Maelstrom, a Drosophila spindle-class gene, encodes a protein that colocalizes with Vasa and RDE1/AGO1 homolog, Aubergine, in nuage. *Development* **130**, 859–871 (2003).

[121] Formstecher, E., Aresta, S., Collura, V., Hamburger, A., Meil, A., Trehin, A., Reverdy, C., Betin, V., Maire, S., Brun, C., Jacq, B., Arpin, M., Bellaiche, Y., Bellusci, S., Benaroch, P., Bornens, M., Chanet, R., Chavrier, P., Delattre, O., Doye, V., Fehon, R., Faye, G., Galli, T., Girault, J.-A., Goud, B., de Gunzburg, J., Johannes, L., Junier, M.-P., Mirouse, V., Mukherjee, A., Papadopoulo, D., Perez, F., Plessis, A., Rossé, C., Saule, S., Stoppa-Lyonnet, D., Vincent, A., White, M., Legrain, P., Wojcik, J., Camonis, J. & Daviet, L. Protein interaction mapping: a Drosophila case study. *Genome Res* **15**, 376–384 (2005).

[122] Forrest, K. M., Clark, I. E., Jain, R. A. & Gavis, E. R. Temporal complexity within a translational control element in the nanos mRNA. *Development* **131**, 5849–5857 (2004).

[123] Förstemann, K., Tomari, Y., Du, T., Vagin, V. V., Denli, A. M., Bratu, D. P., Klattenhoff, C., Theurkauf, W. E. & Zamore, P. D. Normal microRNA maturation and germ-line stem cell maintenance requires Loquacious, a double-stranded RNA-binding domain protein. *PLoS Biol* **3**, e236 (2005).

[124] Fukuda, T., Yamagata, K., Fujiyama, S., Matsumoto, T., Koshida, I., Yoshimura, K., Mihara, M., Naitou, M., Endoh, H., Nakamura, T., Akimoto, C., Yamamoto, Y., Katagiri, T., Foulds, C., Takezawa, S., Kitagawa, H., ichi Takeyama, K., O'Malley, B. W. & Kato, S. DEAD-box RNA helicase subunits of the Drosha complex are required for processing of rRNA and a subset of microRNAs. *Nat Cell Biol* **9**, 604–611 (2007).

[125] Fukuhara, N., Ebert, J., Unterholzner, L., Lindner, D., Izaurralde, E. & Conti, E. SMG7 is a 14-3-3-like adaptor in the nonsense-mediated mRNA decay pathway. *Mol Cell* **17**, 537–547 (2005).

[126] Galgano, A., Forrer, M., Jaskiewicz, L., Kanitz, A., Zavolan, M. & Gerber, A. P. Comparative analysis of mRNA targets for human PUF-family proteins suggests extensive interaction with the miRNA regulatory system. *PLoS ONE* **3**, e3164 (2008).

[127] Garneau, N. L., Wilusz, J. & Wilusz, C. J. The highways and byways of mRNA decay. *Nat Rev Mol Cell Biol* **8**, 113–126 (2007).

[128] Gavis, E. R. & Lehmann, R. Localization of nanos RNA controls embryonic polarity. *Cell* **71**, 301–313 (1992).

[129] Gavis, E. R. & Lehmann, R. Translational regulation of nanos by RNA localization. *Nature* **369**, 315–318 (1994).

[130] Gavis, E. R., Lunsford, L., Bergsten, S. E. & Lehmann, R. A conserved 90 nucleotide element mediates translational repression of nanos RNA. *Development* **122**, 2791–2800 (1996).

[131] Ge, D., Lamontagne, B. & Elela, S. A. RNase III-mediated silencing of a glucose-dependent repressor in yeast. *Curr Biol* **15**, 140–145 (2005).

[132] Gebauer, F., Corona, D. F., Preiss, T., Becker, P. B. & Hentze, M. W. Translational control of dosage compensation in Drosophila by Sex-lethal: cooperative silencing via the 5' and 3' UTRs of msl-2 mRNA is independent of the poly(A) tail. *EMBO J* **18**, 6146–6154 (1999).

[133] Gebauer, F., Grskovic, M. & Hentze, M. W. Drosophila sex-lethal inhibits the stable association of the 40S ribosomal subunit with msl-2 mRNA. *Mol Cell* **11**, 1397–1404 (2003).

[134] Gebauer, F., Merendino, L., Hentze, M. W. & Valcárcel, J. The Drosophila splicing regulator sex-lethal directly inhibits translation of male-specific-lethal 2 mRNA. *RNA* **4**, 142–150 (1998).

[135] Gerber, A. P., Luschnig, S., Krasnow, M. A., Brown, P. O. & Herschlag, D. Genome-wide identification of mRNAs associated with the translational regulator PUMILIO in Drosophila melanogaster. *Proc Natl Acad Sci U S A* **103**, 4487–4492 (2006).

[136] Gesteland, C. T., R.F. & Atkins, J. (eds.). *The RNA World*. Cold Spring Harbor Laboratory Press, New York, 3rd ed. (2006).

[137] Ghildiyal, M., Seitz, H., Horwich, M. D., Li, C., Du, T., Lee, S., Xu, J., Kittler, E. L. W., Zapp, M. L., Weng, Z. & Zamore, P. D. Endogenous siRNAs derived from transposons and mRNAs in Drosophila somatic cells. *Science* **320**, 1077–1081 (2008).

[138] Gilbert, W. V., Zhou, K., Butler, T. K. & Doudna, J. A. Cap-independent translation is required for starvation-induced differentiation in yeast. *Science* **317**, 1224–1227 (2007).

[139] Gingras, A. C., Svitkin, Y., Belsham, G. J., Pause, A. & Sonenberg, N. Activation of the translational suppressor 4E-BP1 following infection with encephalomyocarditis virus and poliovirus. *Proc Natl Acad Sci U S A* **93**, 5578–5583 (1996).

[140] Giot, L., Bader, J. S., Brouwer, C., Chaudhuri, A., Kuang, B., Li, Y., Hao, Y. L., Ooi, C. E., Godwin, B., Vitols, E., Vijayadamodar, G., Pochart, P., Machineni, H., Welsh, M., Kong, Y., Zerhusen, B., Malcolm, R., Varrone, Z., Collis, A., Minto, M., Burgess, S., McDaniel, L., Stimpson, E., Spriggs, F., Williams, J., Neurath, K., Ioime, N., Agee, M., Voss, E., Furtak, K., Renzulli, R., Aanensen, N., Carrolla, S., Bickelhaupt, E., Lazovatsky, Y., DaSilva, A., Zhong, J., Stanyon, C. A., Finley, R. L., White, K. P., Braverman, M., Jarvie, T., Gold, S., Leach, M., Knight, J., Shimkets, R. A., McKenna, M. P., Chant, J. & Rothberg, J. M. A protein interaction map of Drosophila melanogaster. *Science* **302**, 1727–1736 (2003).

[141] Giraldez, A. J., Mishima, Y., Rihel, J., Grocock, R. J., Dongen, S. V., Inoue, K., Enright, A. J. & Schier, A. F. Zebrafish MiR-430 promotes deadenylation and clearance of maternal mRNAs. *Science* **312**, 75–79 (2006).

[142] Goldstrohm, A. C., Hook, B. A., Seay, D. J. & Wickens, M. PUF proteins bind Pop2p to regulate messenger RNAs. *Nat Struct Mol Biol* **13**, 533–539 (2006).

[143] Goldstrohm, A. C., Seay, D. J., Hook, B. A. & Wickens, M. PUF protein-mediated deadenylation is catalyzed by Ccr4p. *J Biol Chem* **282**, 109–114 (2007).

[144] Gonsalvez, G. B., Urbinati, C. R. & Long, R. M. RNA localization in yeast: moving towards a mechanism. *Biol Cell* **97**, 75–86 (2005).

[145] Goossen, B., Caughman, S. W., Harford, J. B., Klausner, R. D. & Hentze, M. W. Translational repression by a complex between the iron-responsive element of ferritin mRNA and its specific cytoplasmic binding protein is position-dependent in vivo. *EMBO J* **9**, 4127–4133 (1990).

[146] Green, J. B., Edwards, T. A., Trincao, J., Escalante, C. R., Wharton, R. P. & Aggarwal, A. K. Crystallization and characterization of Smaug: a novel RNA-binding motif. *Biochem Biophys Res Commun* **297**, 1085–1088 (2002).

[147] Green, J. B., Gardner, C. D., Wharton, R. P. & Aggarwal, A. K. RNA recognition via the SAM domain of Smaug. *Mol Cell* **11**, 1537–1548 (2003).

[148] Gregory, R. I., Chendrimada, T. P., Cooch, N. & Shiekhattar, R. Human RISC couples microRNA biogenesis and posttranscriptional gene silencing. *Cell* **123**, 631–640 (2005).

[149] Gregory, R. I., Yan, K.-P., Amuthan, G., Chendrimada, T., Doratotaj, B., Cooch, N. & Shiekhattar, R. The Microprocessor complex mediates the genesis of microRNAs. *Nature* **432**, 235–240 (2004).

[150] Grewal, S. I. S. & Elgin, S. C. R. Transcription and RNA interference in the formation of heterochromatin. *Nature* **447**, 399–406 (2007).

[151] Griffiths-Jones, S., Bateman, A., Marshall, M., Khanna, A. & Eddy, S. R. Rfam: an RNA family database. *Nucleic Acids Res* **31**, 439–441 (2003).

[152] Griffiths-Jones, S., Saini, H. K., van Dongen, S. & Enright, A. J. miRBase: tools for microRNA genomics. *Nucleic Acids Res* **36**, D154–D158 (2008).

[153] Grimson, A., Farh, K. K.-H., Johnston, W. K., Garrett-Engele, P., Lim, L. P. & Bartel, D. P. MicroRNA targeting specificity in mammals: determinants beyond seed pairing. *Mol Cell* **27**, 91–105 (2007).

[154] Gros, F., Hiatt, H., Gilbert, W., Kurland, C. G., Risebrough, R. W. & Watson, J. D. Unstable ribonucleic acid revealed by pulse labelling of Escherichia coli. *Nature* **190**, 581–585 (1961).

[155] Gross, S. P., Welte, M. A., Block, S. M. & Wieschaus, E. F. Coordination of opposite-polarity microtubule motors. *J Cell Biol* **156**, 715–724 (2002).

[156] Grskovic, M., Hentze, M. W. & Gebauer, F. A co-repressor assembly nucleated by Sex-lethal in the 3'UTR mediates translational control of Drosophila msl-2 mRNA. *EMBO J* **22**, 5571–5581 (2003).

[157] Gudkov, A. T., Ozerova, M. V., Shiryaev, V. M. & Spirin, A. S. 5'-poly(A) sequence as an effective leader for translation in eukaryotic cell-free systems. *Biotechnol Bioeng* **91**, 468–473 (2005).

[158] Gupta, Y. K., Nair, D. T., Wharton, R. P. & Aggarwal, A. K. Structures of human Pumilio with noncognate RNAs reveal molecular mechanisms for binding promiscuity. *Structure* **16**, 549–557 (2008).

[159] Hachet, O. & Ephrussi, A. Drosophila Y14 shuttles to the posterior of the oocyte and is required for oskar mRNA transport. *Curr Biol* **11**, 1666–1674 (2001).

[160] Han, J., Lee, Y., Yeom, K.-H., Kim, Y.-K., Jin, H. & Kim, V. N. The Drosha-DGCR8 complex in primary microRNA processing. *Genes Dev* **18**, 3016–3027 (2004).

[161] Hansen, W. J., Cowan, N. J. & Welch, W. J. Prefoldin-nascent chain complexes in the folding of cytoskeletal proteins. *J Cell Biol* **145**, 265–277 (1999).

[162] Hartig, J. V., Tomari, Y. & Förstemann, K. piRNAs–the ancient hunters of genome invaders. *Genes Dev* **21**, 1707–1713 (2007).

[163] Hatzfeld, M. The armadillo family of structural proteins. *Int Rev Cytol* **186**, 179–224 (1999).

[164] Höck, J., Weinmann, L., Ender, C., Rüdel, S., Kremmer, E., Raabe, M., Urlaub, H. & Meister, G. Proteomic and functional analysis of Argonaute-containing mRNA-protein complexes in human cells. *EMBO Rep* **8**, 1052–1060 (2007).

[165] Hellen, C. U. & Sarnow, P. Internal ribosome entry sites in eukaryotic mRNA molecules. *Genes Dev* **15**, 1593–1612 (2001).

[166] Hentze, M. W., Muckenthaler, M. U. & Andrews, N. C. Balancing acts: molecular control of mammalian iron metabolism. *Cell* **117**, 285–297 (2004).

[167] Herbert, T. & Proud, C. G. Regulation of translation elongation and the cotranslational protein targeting pathway. In *Translational control in biology and medicine*, edited by M. Mathews, N. Sonenberg & J. Hershey, chap. 21. Cold Spring Harbor Laboratory Press, New York (2007).

[168] Hernández, G., Altmann, M., Sierra, J. M., Urlaub, H., del Corral, R. D., Schwartz, P. & Rivera-Pomar, R. Functional analysis of seven genes encoding eight translation initiation factor 4E (eIF4E) isoforms in Drosophila. *Mech Dev* **122**, 529–543 (2005).

[169] Hesketh, J. E. & Pryme, I. F. Interaction between mRNA, ribosomes and the cytoskeleton. *Biochem J* **277 I**, 1–10 (1991).

[170] Hinnebusch, A., Dever, T. & Asano, K. Mechanism of translation initiation in the yeast Saccharomyces cerevisiae. In *Translational control in biology and medicine*, edited by M. Mathews, N. Sonenberg & J. Hershey, chap. 9. Cold Spring Harbor Laboratory Press, New York (2007).

[171] Hinnebusch, A. G. Translational regulation of yeast GCN4. A window on factors that control initiator-trna binding to the ribosome. *J Biol Chem* **272**, 21661–21664 (1997).

[172] Hinnebusch, A. G. & Natarajan, K. Gcn4p, a master regulator of gene expression, is controlled at multiple levels by diverse signals of starvation and stress. *Eukaryot Cell* **1**, 22–32 (2002).

[173] Hülskamp, M., Schröder, C., Pfeifle, C., Jäckle, H. & Tautz, D. Posterior segmentation of the Drosophila embryo in the absence of a maternal posterior organizer gene. *Nature* **338**, 629–632 (1989).

[174] Holcik, M. & Sonenberg, N. Translational control in stress and apoptosis. *Nat Rev Mol Cell Biol* **6**, 318–327 (2005).

[175] Huang, J., Liang, Z., Yang, B., Tian, H., Ma, J. & Zhang, H. Derepression of microRNA-mediated protein translation inhibition by apolipoprotein B mRNA-editing enzyme catalytic polypeptide-like 3G (APOBEC3G) and its family members. *J Biol Chem* **282**, 33632–33640 (2007).

[176] Huang, Y.-S., Carson, J. H., Barbarese, E. & Richter, J. D. Facilitation of dendritic mRNA transport by CPEB. *Genes Dev* **17**, 638–653 (2003).

[177] Hughes, J. R., Meireles, A. M., Fisher, K. H., Garcia, A., Antrobus, P. R., Wainman, A., Zitzmann, N., Deane, C., Ohkura, H. & Wakefield, J. G. A microtubule interactome: complexes with roles in cell cycle and mitosis. *PLoS Biol* **6**, e98 (2008).

[178] Humphreys, D. T., Westman, B. J., Martin, D. I. K. & Preiss, T. MicroRNAs control translation initiation by inhibiting eukaryotic initiation factor 4E/cap and poly(A) tail function. *Proc Natl Acad Sci U S A* **102**, 16961–16966 (2005).

[179] Hurd, D. D., Stern, M. & Saxton, W. M. Mutation of the axonal transport motor kinesin enhances paralytic and suppresses Shaker in Drosophila. *Genetics* **142**, 195–204 (1996).

[180] Hutvagner, G. & Simard, M. J. Argonaute proteins: key players in RNA silencing. *Nat Rev Mol Cell Biol* **9**, 22–32 (2008).

[181] Hutvágner, G., McLachlan, J., Pasquinelli, A. E., Bálint, E., Tuschl, T. & Zamore, P. D. A cellular function for the RNA-interference enzyme Dicer in the maturation of the let-7 small temporal RNA. *Science* **293**, 834–838 (2001).

[182] Hutvágner, G. & Zamore, P. D. A microRNA in a multiple-turnover RNAi enzyme complex. *Science* **297**, 2056–2060 (2002).

[183] Huynh, J.-R., Munro, T. P., Smith-Litière, K., Lepesant, J.-A. & Johnston, D. S. The Drosophila hnRNPA/B homolog, Hrp48, is specifically required for a distinct step in osk mRNA localization. *Dev Cell* **6**, 625–635 (2004).

[184] Iacoangeli, A., Rozhdestvensky, T. S., Dolzhanskaya, N., Tournier, B., Schütt, J., Brosius, J., Denman, R. B., Khandjian, E. W., Kindler, S. & Tiedge, H. On BC1 RNA and the fragile X mental retardation protein. *Proc Natl Acad Sci U S A* **105**, 734–739 (2008).

[185] Inoue, H., Nojima, H. & Okayama, H. High efficiency transformation of Escherichia coli with plasmids. *Gene* **96**, 23–28 (1990).

[186] Iost, I., Dreyfus, M. & Linder, P. Ded1p, a DEAD-box protein required for translation initiation in Saccharomyces cerevisiae, is an RNA helicase. *J Biol Chem* **274**, 17677–17683 (1999).

[187] Irish, V., Lehmann, R. & Akam, M. The Drosophila posterior-group gene nanos functions by repressing hunchback activity. *Nature* **338**, 646–648 (1989).

[188] Ishizuka, A., Siomi, M. C. & Siomi, H. A Drosophila fragile X protein interacts with components of RNAi and ribosomal proteins. *Genes Dev* **16**, 2497–2508 (2002).

[189] Jacob, F. & Monod, J. Genetic regulatory mechanisms in the synthesis of proteins. *J Mol Biol* **3**, 318–356 (1961).

[190] Jakymiw, A., Lian, S., Eystathioy, T., Li, S., Satoh, M., Hamel, J. C., Fritzler, M. J. & Chan, E. K. L. Disruption of GW bodies impairs mammalian RNA interference. *Nat Cell Biol* **7**, 1267–1274 (2005).

[191] Jakymiw, A., Pauley, K. M., Li, S., Ikeda, K., Lian, S., Eystathioy, T., Satoh, M., Fritzler, M. J. & Chan, E. K. L. The role of GW/P-bodies in RNA processing and silencing. *J Cell Sci* **120**, 1317–1323 (2007).

[192] Jan, E. Divergent IRES elements in invertebrates. *Virus Res* **119**, 16–28 (2006).

[193] Jang, S. K. Internal initiation: IRES elements of picornaviruses and hepatitis c virus. *Virus Res* **119**, 2–15 (2006).

[194] Jang, S. K., Davies, M. V., Kaufman, R. J. & Wimmer, E. Initiation of protein synthesis by internal entry of ribosomes into the 5' nontranslated region of encephalomyocarditis virus RNA in vivo. *J Virol* **63**, 1651–1660 (1989).

[195] Jang, S. K., Kräusslich, H. G., Nicklin, M. J., Duke, G. M., Palmenberg, A. C. & Wimmer, E. A segment of the 5' nontranslated region of encephalomyocarditis virus RNA directs internal entry of ribosomes during in vitro translation. *J Virol* **62**, 2636–2643 (1988).

[196] Jiang, F., Ye, X., Liu, X., Fincher, L., McKearin, D. & Liu, Q. Dicer-1 and R3D1-L catalyze microRNA maturation in Drosophila. *Genes Dev* **19**, 1674–1679 (2005).

[197] Jin, P., Zarnescu, D. C., Ceman, S., Nakamoto, M., Mowrey, J., Jongens, T. A., Nelson, D. L., Moses, K. & Warren, S. T. Biochemical and genetic interaction between the fragile X mental retardation protein and the microRNA pathway. *Nat Neurosci* **7**, 113–117 (2004).

[198] Johnston, D. S. Moving messages: the intracellular localization of mRNAs. *Nat Rev Mol Cell Biol* **6**, 363–375 (2005).

[199] Johnston, D. S., Beuchle, D. & Nüsslein-Volhard, C. Staufen, a gene required to localize maternal RNAs in the Drosophila egg. *Cell* **66**, 51–63 (1991).

[200] Johnston, D. S. & Nüsslein-Volhard, C. The origin of pattern and polarity in the Drosophila embryo. *Cell* **68**, 201–219 (1992).

[201] Johnstone, O., Deuring, R., Bock, R., Linder, P., Fuller, M. T. & Lasko, P. Belle is a Drosophila DEAD-box protein required for viability and in the germ line. *Dev Biol* **277**, 92–101 (2005).

[202] Kadyrova, L. Y., Habara, Y., Lee, T. H. & Wharton, R. P. Translational control of maternal Cyclin B mRNA by Nanos in the Drosophila germline. *Development* **134**, 1519–1527 (2007).

[203] Kahvejian, A., Roy, G. & Sonenberg, N. The mRNA closed-loop model: the function of PABP and PABP-interacting proteins in mRNA translation. *Cold Spring Harb Symp Quant Biol* **66**, 293–300 (2001).

[204] Kahvejian, A., Svitkin, Y. V., Sukarieh, R., M'Boutchou, M.-N. & Sonenberg, N. Mammalian poly(A)-binding protein is a eukaryotic translation initiation factor, which acts via multiple mechanisms. *Genes Dev* **19**, 104–113 (2005).

[205] Kaminker, J. S., Bergman, C. M., Kronmiller, B., Carlson, J., Svirskas, R., Patel, S., Frise, E., Wheeler, D. A., Lewis, S. E., Rubin, G. M., Ashburner, M. & Celniker, S. E. The transposable elements of the Drosophila melanogaster euchromatin: a genomics perspective. *Genome Biol* **3**, RESEARCH0084 (2002).

[206] Kanai, Y., Dohmae, N. & Hirokawa, N. Kinesin transports RNA: isolation and characterization of an RNA-transporting granule. *Neuron* **43**, 513–525 (2004).

[207] Kapitonov, V. V. & Jurka, J. Molecular paleontology of transposable elements in the Drosophila melanogaster genome. *Proc Natl Acad Sci U S A* **100**, 6569–6574 (2003).

[208] Kawamura, Y., Saito, K., Kin, T., Ono, Y., Asai, K., Sunohara, T., Okada, T. N., Siomi, M. C. & Siomi, H. Drosophila endogenous small RNAs bind to Argonaute 2 in somatic cells. *Nature* **453**, 793–797 (2008).

[209] Keene, J. D. RNA regulons: coordination of post-transcriptional events. *Nat Rev Genet* **8**, 533–543 (2007).

[210] Keene, J. D. & Lager, P. J. Post-transcriptional operons and regulons co-ordinating gene expression. *Chromosome Res* **13**, 327–337 (2005).

[211] Keene, J. D. & Tenenbaum, S. A. Eukaryotic mRNPs may represent posttranscriptional operons. *Mol Cell* **9**, 1161–1167 (2002).

[212] Kelley, R. L., Wang, J., Bell, L. & Kuroda, M. I. Sex lethal controls dosage compensation in Drosophila by a non-splicing mechanism. *Nature* **387**, 195–199 (1997).

[213] Ketting, R. F., Fischer, S. E., Bernstein, E., Sijen, T., Hannon, G. J. & Plasterk, R. H. Dicer functions in RNA interference and in synthesis of small RNA involved in developmental timing in C. elegans. *Genes Dev* **15**, 2654–2659 (2001).

[214] Khvorova, A., Reynolds, A. & Jayasena, S. D. Functional siRNAs and miRNAs exhibit strand bias. *Cell* **115**, 209–216 (2003).

[215] Kim, J., Krichevsky, A., Grad, Y., Hayes, G. D., Kosik, K. S., Church, G. M. & Ruvkun, G. Identification of many microRNAs that copurify with polyribosomes in mammalian neurons. *Proc Natl Acad Sci U S A* **101**, 360–365 (2004).

[216] Kim, S. H., Dong, W. K., Weiler, I. J. & Greenough, W. T. Fragile X mental retardation protein shifts between polyribosomes and stress granules after neuronal injury by arsenite stress or in vivo hippocampal electrode insertion. *J Neurosci* **26**, 2413–2418 (2006).

[217] Kim, Y.-K. & Kim, V. N. Processing of intronic microRNAs. *EMBO J* **26**, 775–783 (2007).

[218] Kim-Ha, J., Kerr, K. & Macdonald, P. M. Translational regulation of oskar mRNA by bruno, an ovarian RNA-binding protein, is essential. *Cell* **81**, 403–412 (1995).

[219] Kiriakidou, M., Tan, G. S., Lamprinaki, S., Planell-Saguer, M. D., Nelson, P. T. & Mourelatos, Z. An mRNA m7G cap binding-like motif within human Ago2 represses translation. *Cell* **129**, 1141–1151 (2007).

[220] Klenov, M. S., Lavrov, S. A., Stolyarenko, A. D., Ryazansky, S. S., Aravin, A. A., Tuschl, T. & Gvozdev, V. A. Repeat-associated siRNAs cause chromatin silencing of retrotransposons in the Drosophila melanogaster germline. *Nucleic Acids Res* **35**, 5430–5438 (2007).

[221] Knowles, R. B., Sabry, J. H., Martone, M. E., Deerinck, T. J., Ellisman, M. H., Bassell, G. J. & Kosik, K. S. Translocation of RNA granules in living neurons. *J Neurosci* **16**, 7812–7820 (1996).

[222] Kolch, W. Coordinating ERK/MAPK signalling through scaffolds and inhibitors. *Nat Rev Mol Cell Biol* **6**, 827–837 (2005).

[223] Komar, A. A. & Hatzoglou, M. Internal ribosome entry sites in cellular mRNAs: mystery of their existence. *J Biol Chem* **280**, 23425–23428 (2005).

[224] Konarska, M., Filipowicz, W., Domdey, H. & Gross, H. J. Binding of ribosomes to linear and circular forms of the 5'-terminal leader fragment of tobacco-mosaic-virus RNA. *Eur J Biochem* **114**, 221–227 (1981).

[225] Kondrashov, A. V., Kiefmann, M., Ebnet, K., Khanam, T., Muddashetty, R. S. & Brosius, J. Inhibitory effect of naked neural BC1 RNA or BC200 RNA on eukaryotic in vitro translation systems is reversed by poly(A)-binding protein (PABP). *J Mol Biol* **353**, 88–103 (2005).

[226] Kontos, H., Napthine, S. & Brierley, I. Ribosomal pausing at a frameshifter RNA pseudoknot is sensitive to reading phase but shows little correlation with frameshift efficiency. *Mol Cell Biol* **21**, 8657–8670 (2001).

[227] Kozak, M. Inability of circular mRNA to attach to eukaryotic ribosomes. *Nature* **280**, 82–85 (1979).

[228] Kozak, M. Constraints on reinitiation of translation in mammals. *Nucleic Acids Res* **29**, 5226–5232 (2001).

[229] Kozak, M. New ways of initiating translation in eukaryotes? *Mol Cell Biol* **21**, 1899–1907 (2001).

[230] Kozak, M. Pushing the limits of the scanning mechanism for initiation of translation. *Gene* **299**, 1–34 (2002).

[231] Kozak, M. How strong is the case for regulation of the initiation step of translation by elements at the 3' end of eukaryotic mRNAs? *Gene* **343**, 41–54 (2004).

[232] Kozak, M. Regulation of translation via mRNA structure in prokaryotes and eukaryotes. *Gene* **361**, 13–37 (2005).

[233] Kozak, M. A second look at cellular mRNA sequences said to function as internal ribosome entry sites. *Nucleic Acids Res* **33**, 6593–6602 (2005).

[234] Kozak, M. Rethinking some mechanisms invoked to explain translational regulation in eukaryotes. *Gene* **382**, 1–11 (2006).

[235] Kozak, M. Lessons (not) learned from mistakes about translation. *Gene* **403**, 194–203 (2007).

[236] Kozak, M. Some thoughts about translational regulation: forward and backward glances. *J Cell Biochem* **102**, 280–290 (2007).

[237] Kuersten, S. & Goodwin, E. B. The power of the 3' UTR: translational control and development. *Nat Rev Genet* **4**, 626–637 (2003).

[238] Lagos-Quintana, M., Rauhut, R., Lendeckel, W. & Tuschl, T. Identification of novel genes coding for small expressed RNAs. *Science* **294**, 853–858 (2001).

[239] Lai, E. C., Tomancak, P., Williams, R. W. & Rubin, G. M. Computational identification of Drosophila microRNA genes. *Genome Biol* **4**, R42 (2003).

[240] Lai, M.-C., Lee, Y.-H. W. & Tarn, W.-Y. The DEAD-box RNA helicase DDX3 associates with export messenger ribonucleoproteins as well as tip-associated protein and participates in translational control. *Mol Biol Cell* **19**, 3847–3858 (2008).

[241] Landthaler, M., Yalcin, A. & Tuschl, T. The human DiGeorge syndrome critical region gene 8 and Its D. melanogaster homolog are required for miRNA biogenesis. *Curr Biol* **14**, 2162–2167 (2004).

[242] Latham, V. M., Yu, E. H., Tullio, A. N., Adelstein, R. S. & Singer, R. H. A Rho-dependent signaling pathway operating through myosin localizes beta-actin mRNA in fibroblasts. *Curr Biol* **11**, 1010–1016 (2001).

[243] Law, G. L., Raney, A., Heusner, C. & Morris, D. R. Polyamine regulation of ribosome pausing at the upstream open reading frame of S-adenosylmethionine decarboxylase. *J Biol Chem* **276**, 38036–38043 (2001).

[244] Leaman, D., Chen, P. Y., Fak, J., Yalcin, A., Pearce, M., Unnerstall, U., Marks, D. S., Sander, C., Tuschl, T. & Gaul, U. Antisense-mediated depletion reveals essential and specific functions of microRNAs in Drosophila development. *Cell* **121**, 1097–1108 (2005).

[245] Lee, C.-S., Dias, A. P., Jedrychowski, M., Patel, A. H., Hsu, J. L. & Reed, R. Human DDX3 functions in translation and interacts with the translation initiation factor eIF3. *Nucleic Acids Res* **36**, 4708–4718 (2008).

[246] Lee, R. C., Feinbaum, R. L. & Ambros, V. The C. elegans heterochronic gene lin-4 encodes small RNAs with antisense complementarity to lin-14. *Cell* **75**, 843–854 (1993).

[247] Lee, Y., Ahn, C., Han, J., Choi, H., Kim, J., Yim, J., Lee, J., Provost, P., Rådmark, O., Kim, S. & Kim, V. N. The nuclear RNase III Drosha initiates microRNA processing. *Nature* **425**, 415–419 (2003).

[248] Lee, Y., Hur, I., Park, S.-Y., Kim, Y.-K., Suh, M. R. & Kim, V. N. The role of PACT in the RNA silencing pathway. *EMBO J* **25**, 522–532 (2006).

[249] Lee, Y., Kim, M., Han, J., Yeom, K.-H., Lee, S., Baek, S. H. & Kim, V. N. MicroRNA genes are transcribed by RNA polymerase II. *EMBO J* **23**, 4051–4060 (2004).

[250] Lee, Y. S., Nakahara, K., Pham, J. W., Kim, K., He, Z., Sontheimer, E. J. & Carthew, R. W. Distinct roles for Drosophila Dicer-1 and Dicer-2 in the siRNA/miRNA silencing pathways. *Cell* **117**, 69–81 (2004).

[251] Leung, A. K. L., Calabrese, J. M. & Sharp, P. A. Quantitative analysis of Argonaute protein reveals microRNA-dependent localization to stress granules. *Proc Natl Acad Sci U S A* **103**, 18125–18130 (2006).

[252] Leung, A. K. L. & Sharp, P. A. microRNAs: a safeguard against turmoil? *Cell* **130**, 581–585 (2007).

[253] Liang, L., Diehl-Jones, W. & Lasko, P. Localization of vasa protein to the Drosophila pole plasm is independent of its RNA-binding and helicase activities. *Development* **120**, 1201–1211 (1994).

[254] Lie, Y. S. & Macdonald, P. M. Apontic binds the translational repressor Bruno and is implicated in regulation of oskar mRNA translation. *Development* **126**, 1129–1138 (1999).

[255] Lim, A. K. & Kai, T. Unique germ-line organelle, nuage, functions to repress selfish genetic elements in Drosophila melanogaster. *Proc Natl Acad Sci U S A* **104**, 6714–6719 (2007).

[256] Lim, L. P., Lau, N. C., Garrett-Engele, P., Grimson, A., Schelter, J. M., Castle, J., Bartel, D. P., Linsley, P. S. & Johnson, J. M. Microarray analysis shows that some microRNAs downregulate large numbers of target mRNAs. *Nature* **433**, 769–773 (2005).

[257] Lin, D., Pestova, T. V., Hellen, C. U. T. & Tiedge, H. Translational control by a small RNA: dendritic BC1 RNA targets the eukaryotic initiation factor 4A helicase mechanism. *Mol Cell Biol* **28**, 3008–3019 (2008).

[258] Lin, M.-D., Fan, S.-J., Hsu, W.-S. & Chou, T.-B. Drosophila decapping protein 1, dDcp1, is a component of the oskar mRNP complex and directs its posterior localization in the oocyte. *Dev Cell* **10**, 601–613 (2006).

[259] Linder, P. Yeast RNA helicases of the DEAD-box family involved in translation initiation. *Biol Cell* **95**, 157–167 (2003).

[260] Ling, S.-C., Fahrner, P. S., Greenough, W. T. & Gelfand, V. I. Transport of Drosophila fragile X mental retardation protein-containing ribonucleoprotein granules by kinesin-1 and cytoplasmic dynein. *Proc Natl Acad Sci U S A* **101**, 17428–17433 (2004).

[261] Liu, J., Rivas, F. V., Wohlschlegel, J., Yates, J. R., Parker, R. & Hannon, G. J. A role for the P-body component GW182 in microRNA function. *Nat Cell Biol* **7**, 1261–1266 (2005).

[262] Liu, J., Valencia-Sanchez, M. A., Hannon, G. J. & Parker, R. MicroRNA-dependent localization of targeted mRNAs to mammalian P-bodies. *Nat Cell Biol* **7**, 719–723 (2005).

[263] Long, R. M., Gu, W., Lorimer, E., Singer, R. H. & Chartrand, P. She2p is a novel RNA-binding protein that recruits the Myo4p-She3p complex to ASH1 mRNA. *EMBO J* **19**, 6592–6601 (2000).

[264] Lowe, M. & Kreis, T. E. Regulation of membrane traffic in animal cells by COPI. *Biochim Biophys Acta* **1404**, 53–66 (1998).

[265] Lu, P. D., Harding, H. P. & Ron, D. Translation reinitiation at alternative open reading frames regulates gene expression in an integrated stress response. *J Cell Biol* **167**, 27–33 (2004).

[266] Lund, E., Güttinger, S., Calado, A., Dahlberg, J. E. & Kutay, U. Nuclear export of microRNA precursors. *Science* **303**, 95–98 (2004).

[267] Lytle, J. R., Yario, T. A. & Steitz, J. A. Target mRNAs are repressed as efficiently by microRNA-binding sites in the 5' UTR as in the 3' UTR. *Proc Natl Acad Sci U S A* **104**, 9667–9672 (2007).

[268] Mahone, M., Saffman, E. E. & Lasko, P. F. Localized Bicaudal-C RNA encodes a protein containing a KH domain, the RNA binding motif of FMR1. *EMBO J* **14**, 2043–2055 (1995).

[269] Mamiya, N. & Worman, H. J. Hepatitis C virus core protein binds to a DEAD box RNA helicase. *J Biol Chem* **274**, 15751–15756 (1999).

[270] Mangus, D. A., Evans, M. C. & Jacobson, A. Poly(A)-binding proteins: multifunctional scaffolds for the post-transcriptional control of gene expression. *Genome Biol* **4**, 223 (2003).

[271] Maniataki, E. & Mourelatos, Z. A human, ATP-independent, RISC assembly machine fueled by pre-miRNA. *Genes Dev* **19**, 2979–2990 (2005).

[272] Mansfield, J. H., Wilhelm, J. E. & Hazelrigg, T. Ypsilon Schachtel, a Drosophila Y-box protein, acts antagonistically to Orb in the oskar mRNA localization and translation pathway. *Development* **129**, 197–209 (2002).

[273] Markussen, F. H., Breitwieser, W. & Ephrussi, A. Efficient translation and phosphorylation of Oskar require Oskar protein and the RNA helicase Vasa. *Cold Spring Harb Symp Quant Biol* **62**, 13–17 (1997).

[274] Marín, I., Siegal, M. L. & Baker, B. S. The evolution of dosage-compensation mechanisms. *Bioessays* **22**, 1106–1114 (2000).

[275] Maroney, P. A., Yu, Y., Fisher, J. & Nilsen, T. W. Evidence that microRNAs are associated with translating messenger RNAs in human cells. *Nat Struct Mol Biol* **13**, 1102–1107 (2006).

[276] Martin, M., Iyadurai, S. J., Gassman, A., Gindhart, J. G., Hays, T. S. & Saxton, W. M. Cytoplasmic dynein, the dynactin complex, and kinesin are interdependent and essential for fast axonal transport. *Mol Biol Cell* **10**, 3717–3728 (1999).

[277] Martin, S. & Parton, R. G. Caveolin, cholesterol, and lipid bodies. *Semin Cell Dev Biol* **16**, 163–174 (2005).

[278] Martinez, J. & Tuschl, T. RISC is a 5' phosphomonoester-producing RNA endonuclease. *Genes Dev* **18**, 975–980 (2004).

[279] Mathews, M., Sonenberg, N. & Hershey, J. Origins and principles of translational control. In *Translational control in biology and medicine*, edited by M. Mathews, N. Sonenberg & J. Hershey, chap. 1. Cold Spring Harbor Laboratory Press, New York (2007).

[280] Mathews, M., Sonenberg, N. & Hershey, J. (eds.). *Translational control in biology and medicine*. Cold Spring Harbor Laboratory Press, New York (2007).

[281] Mathonnet, G., Fabian, M. R., Svitkin, Y. V., Parsyan, A., Huck, L., Murata, T., Biffo, S., Merrick, W. C., Darzynkiewicz, E., Pillai, R. S., Filipowicz, W., Duchaine, T. F. & Sonenberg, N. MicroRNA inhibition of translation initiation in vitro by targeting the cap-binding complex eIF4F. *Science* **317**, 1764–1767 (2007).

[282] Mazroui, R., Huot, M.-E., Tremblay, S., Filion, C., Labelle, Y. & Khandjian, E. W. Trapping of messenger RNA by Fragile X Mental Retardation protein into cytoplasmic granules induces translation repression. *Hum Mol Genet* **11**, 3007–3017 (2002).

[283] Meek, S. E. M., Lane, W. S. & Piwnica-Worms, H. Comprehensive proteomic analysis of interphase and mitotic 14-3-3-binding proteins. *J Biol Chem* **279**, 32046–32054 (2004).

[284] Meister, G., Landthaler, M., Peters, L., Chen, P. Y., Urlaub, H., Lührmann, R. & Tuschl, T. Identification of novel argonaute-associated proteins. *Curr Biol* **15**, 2149–2155 (2005).

[285] Meister, G. & Tuschl, T. Mechanisms of gene silencing by double-stranded RNA. *Nature* **431**, 343–349 (2004).

[286] Merz, C., Urlaub, H., Will, C. L. & Lührmann, R. Protein composition of human mRNPs spliced in vitro and differential requirements for mRNP protein recruitment. *RNA* **13**, 116–128 (2007).

[287] Micklem, D. R., Adams, J., Grünert, S. & Johnston, D. S. Distinct roles of two conserved Staufen domains in oskar mRNA localization and translation. *EMBO J* **19**, 1366–1377 (2000).

[288] Minshall, N., Reiter, M. H., Weil, D. & Standart, N. CPEB interacts with an ovary-specific eIF4E and 4E-T in early Xenopus oocytes. *J Biol Chem* **282**, 37389–37401 (2007).

[289] Mirth, C. K. & Riddiford, L. M. Size assessment and growth control: how adult size is determined in insects. *Bioessays* **29**, 344–355 (2007).

[290] Mishima, Y., Giraldez, A. J., Takeda, Y., Fujiwara, T., Sakamoto, H., Schier, A. F. & Inoue, K. Differential regulation of germline mRNAs in soma and germ cells by zebrafish miR-430. *Curr Biol* **16**, 2135–2142 (2006).

[291] Miyoshi, K., Tsukumo, H., Nagami, T., Siomi, H. & Siomi, M. C. Slicer function of Drosophila Argonautes and its involvement in RISC formation. *Genes Dev* **19**, 2837–2848 (2005).

[292] Mohr, S. E., Dillon, S. T. & Boswell, R. E. The RNA-binding protein Tsunagi interacts with Mago Nashi to establish polarity and localize oskar mRNA during Drosophila oogenesis. *Genes Dev* **15**, 2886–2899 (2001).

[293] Monzo, K., Papoulas, O., Cantin, G. T., Wang, Y., Yates, J. R. & Sisson, J. C. Fragile X mental retardation protein controls trailer hitch expression and cleavage furrow formation in Drosophila embryos. *Proc Natl Acad Sci U S A* **103**, 18160–18165 (2006).

[294] Morris, A. R., Mukherjee, N. & Keene, J. D. Ribonomic analysis of human Pum1 reveals cis-trans conservation across species despite evolution of diverse mRNA target sets. *Mol Cell Biol* **28**, 4093–4103 (2008).

[295] Moser, M. J., Holley, W. R., Chatterjee, A. & Mian, I. S. The proofreading domain of Escherichia coli DNA polymerase I and other DNA and/or RNA exonuclease domains. *Nucleic Acids Res* **25**, 5110–5118 (1997).

[296] Mrowiec, T. & Schwappach, B. 14-3-3 proteins in membrane protein transport. *Biol Chem* **387**, 1227–1236 (2006).

[297] Muckenthaler, M., Gray, N. K. & Hentze, M. W. IRP-1 binding to ferritin mRNA prevents the recruitment of the small ribosomal subunit by the cap-binding complex eIF4F. *Mol Cell* **2**, 383–388 (1998).

[298] Mulder, J., Robertson, M. E., Seamons, R. A. & Belsham, G. J. Vaccinia virus protein synthesis has a low requirement for the intact translation initiation factor eIF4F, the cap-binding complex, within infected cells. *J Virol* **72**, 8813–8819 (1998).

[299] Mulder, N. J., Apweiler, R., Attwood, T. K., Bairoch, A., Barrell, D., Bateman, A., Binns, D., Biswas, M., Bradley, P., Bork, P., Bucher, P., Copley, R. R., Courcelle, E., Das, U., Durbin, R., Falquet, L., Fleischmann, W., Griffiths-Jones, S., Haft, D., Harte, N., Hulo, N., Kahn, D., Kanapin, A., Krestyaninova, M., Lopez, R., Letunic, I., Lonsdale, D., Silventoinen, V., Orchard, S. E., Pagni, M., Peyruc, D., Ponting, C. P., Selengut, J. D., Servant, F., Sigrist, C. J. A., Vaughan, R. & Zdobnov, E. M. The InterPro Database, 2003 brings increased coverage and new features. *Nucleic Acids Res* **31**, 315–318 (2003).

[300] Murata, Y. & Wharton, R. P. Binding of pumilio to maternal hunchback mRNA is required for posterior patterning in Drosophila embryos. *Cell* **80**, 747–756 (1995).

[301] Naarmann, I. S., Harnisch, C., Flach, N., Kremmer, E., Kühn, H., Ostareck, D. H. & Ostareck-Lederer, A. mRNA silencing in human erythroid cell maturation: heterogeneous nuclear ribonucleoprotein K controls the expression of its regulator c-Src. *J Biol Chem* **283**, 18461–18472 (2008).

[302] Nakahata, S., Kotani, T., Mita, K., Kawasaki, T., Katsu, Y., Nagahama, Y. & Yamashita, M. Involvement of Xenopus Pumilio in the translational regulation that is specific to cyclin B1 mRNA during oocyte maturation. *Mech Dev* **120**, 865–880 (2003).

[303] Nakamura, A., Amikura, R., Hanyu, K. & Kobayashi, S. Me31B silences translation of oocyte-localizing RNAs through the formation of cytoplasmic RNP complex during Drosophila oogenesis. *Development* **128**, 3233–3242 (2001).

[304] Nakamura, A., Sato, K. & Hanyu-Nakamura, K. Drosophila cup is an eIF4E binding protein that associates with Bruno and regulates oskar mRNA translation in oogenesis. *Dev Cell* **6**, 69–78 (2004).

[305] Napoli, I., Mercaldo, V., Boyl, P. P., Eleuteri, B., Zalfa, F., Rubeis, S. D., Marino, D. D., Mohr, E., Massimi, M., Falconi, M., Witke, W., Costa-Mattioli, M., Sonenberg, N., Achsel, T. & Bagni, C. The fragile X syndrome protein represses activity-dependent translation through CYFIP1, a new 4E-BP. *Cell* **134**, 1042–1054 (2008).

[306] Nashchekin, D., Zhao, J., Visa, N. & Daneholt, B. A novel Ded1-like RNA helicase interacts with the Y-box protein ctYB-1 in nuclear mRNP particles and in polysomes. *J Biol Chem* **281**, 14263–14272 (2006).

[307] Nelson, M. R., Leidal, A. M. & Smibert, C. A. Drosophila Cup is an eIF4E-binding protein that functions in Smaug-mediated translational repression. *EMBO J* **23**, 150–159 (2004).

[308] Nelson, P. T., Hatzigeorgiou, A. G. & Mourelatos, Z. miRNP:mRNA association in polyribosomes in a human neuronal cell line. *RNA* **10**, 387–394 (2004).

[309] Newmark, P. A. & Boswell, R. E. The mago nashi locus encodes an essential product required for germ plasm assembly in Drosophila. *Development* **120**, 1303–1313 (1994).

[310] Noble, S. L., Allen, B. L., Goh, L. K., Nordick, K. & Evans, T. C. Maternal mRNAs are regulated by diverse P body-related mRNP granules during early Caenorhabditis elegans development. *J Cell Biol* **182**, 559–572 (2008).

[311] Nomoto, A., Kitamura, N., Golini, F. & Wimmer, E. The 5'-terminal structures of poliovirion RNA and poliovirus mRNA differ only in the genome-linked protein VPg. *Proc Natl Acad Sci U S A* **74**, 5345–5349 (1977).

[312] Norvell, A., Debec, A., Finch, D., Gibson, L. & Thoma, B. Squid is required for efficient posterior localization of oskar mRNA during Drosophila oogenesis. *Dev Genes Evol* **215**, 340–349 (2005).

[313] Nottrott, S., Simard, M. J. & Richter, J. D. Human let-7a miRNA blocks protein production on actively translating polyribosomes. *Nat Struct Mol Biol* **13**, 1108–1114 (2006).

[314] O'Donnell, K. A. & Boeke, J. D. Mighty Piwis defend the germline against genome intruders. *Cell* **129**, 37–44 (2007).

[315] Okamura, K., Balla, S., Martin, R., Liu, N. & Lai, E. C. Two distinct mechanisms generate endogenous siRNAs from bidirectional transcription in Drosophila melanogaster. *Nat Struct Mol Biol* **15**, 581–590 (2008).

[316] Okamura, K., Chung, W.-J., Ruby, J. G., Guo, H., Bartel, D. P. & Lai, E. C. The Drosophila hairpin RNA pathway generates endogenous short interfering RNAs. *Nature* **453**, 803–806 (2008).

[317] Okamura, K., Hagen, J. W., Duan, H., Tyler, D. M. & Lai, E. C. The mirtron pathway generates microRNA-class regulatory RNAs in Drosophila. *Cell* **130**, 89–100 (2007).

[318] Okamura, K., Ishizuka, A., Siomi, H. & Siomi, M. C. Distinct roles for Argonaute proteins in small RNA-directed RNA cleavage pathways. *Genes Dev* **18**, 1655–1666 (2004).

[319] Okamura, K. & Lai, E. C. Endogenous small interfering RNAs in animals. *Nat Rev Mol Cell Biol* **9**, 673–678 (2008).

[320] Olsen, D. S., Jordan, B., Chen, D., Wek, R. C. & Cavener, D. R. Isolation of the gene encoding the Drosophila melanogaster homolog of the Saccharomyces cerevisiae GCN2 eIF-2alpha kinase. *Genetics* **149**, 1495–1509 (1998).

[321] Olsen, P. H. & Ambros, V. The lin-4 regulatory RNA controls developmental timing in Caenorhabditis elegans by blocking LIN-14 protein synthesis after the initiation of translation. *Dev Biol* **216**, 671–680 (1999).

[322] Ostareck, D. H., Ostareck-Lederer, A., Shatsky, I. N. & Hentze, M. W. Lipoxygenase mRNA silencing in erythroid differentiation: The 3'UTR regulatory complex controls 60S ribosomal subunit joining. *Cell* **104**, 281–290 (2001).

[323] Ostareck, D. H., Ostareck-Lederer, A., Wilm, M., Thiele, B. J., Mann, M. & Hentze, M. W. mRNA silencing in erythroid differentiation: hnRNP K and hnRNP E1 regulate 15-lipoxygenase translation from the 3' end. *Cell* **89**, 597–606 (1997).

[324] Ostareck-Lederer, A., Ostareck, D. H., Standart, N. & Thiele, B. J. Translation of 15-lipoxygenase mRNA is inhibited by a protein that binds to a repeated sequence in the 3' untranslated region. *EMBO J* **13**, 1476–1481 (1994).

[325] Owsianka, A. M. & Patel, A. H. Hepatitis C virus core protein interacts with a human DEAD box protein DDX3. *Virology* **257**, 330–340 (1999).

[326] Pal-Bhadra, M., Leibovitch, B. A., Gandhi, S. G., Rao, M., Bhadra, U., Birchler, J. A. & Elgin, S. C. R. Heterochromatic silencing and HP1 localization in Drosophila are dependent on the RNAi machinery. *Science* **303**, 669–672 (2004).

[327] Palacios, I. M., Gatfield, D., Johnston, D. S. & Izaurralde, E. An eIF4AIII-containing complex required for mRNA localization and nonsense-mediated mRNA decay. *Nature* **427**, 753–757 (2004).

[328] Paquin, N. & Chartrand, P. Local regulation of mRNA translation: new insights from the bud. *Trends Cell Biol* **18**, 105–111 (2008).

[329] Park, H. S., Himmelbach, A., Browning, K. S., Hohn, T. & Ryabova, L. A. A plant viral "reinitiation" factor interacts with the host translational machinery. *Cell* **106**, 723–733 (2001).

[330] Patel, D. D. & Pickup, D. J. Messenger RNAs of a strongly-expressed late gene of cowpox virus contain 5'-terminal poly(A) sequences. *EMBO J* **6**, 3787–3794 (1987).

[331] Pause, A. & Sonenberg, N. Mutational analysis of a DEAD box RNA helicase: the mammalian translation initiation factor eIF-4A. *EMBO J* **11**, 2643–2654 (1992).

[332] Pelletier, J. & Sonenberg, N. Internal initiation of translation of eukaryotic mRNA directed by a sequence derived from poliovirus RNA. *Nature* **334**, 320–325 (1988).

[333] Penalva, L. O. F. & Sánchez, L. RNA binding protein sex-lethal (Sxl) and control of Drosophila sex determination and dosage compensation. *Microbiol Mol Biol Rev* **67**, 343–59, table of contents (2003).

[334] Perrone-Bizzozero, N. & Bolognani, F. Role of HuD and other RNA-binding proteins in neural development and plasticity. *J Neurosci Res* **68**, 121–126 (2002).

[335] Pestova, T., Lorsch, J. & Hellen, C. The mechanism of translation initiation in eukaryotes. In *Translational control in biology and medicine*, edited by M. Mathews, N. Sonenberg & J. Hershey, chap. 4. Cold Spring Harbor Laboratory Press, New York (2007).

[336] Pestova, T. V., Hellen, C. U. & Shatsky, I. N. Canonical eukaryotic initiation factors determine initiation of translation by internal ribosomal entry. *Mol Cell Biol* **16**, 6859–6869 (1996).

[337] Pestova, T. V., Shatsky, I. N., Fletcher, S. P., Jackson, R. J. & Hellen, C. U. A prokaryotic-like mode of cytoplasmic eukaryotic ribosome binding to the initiation codon during internal translation initiation of hepatitis C and classical swine fever virus RNAs. *Genes Dev* **12**, 67–83 (1998).

[338] Pestova, T. V., Shatsky, I. N. & Hellen, C. U. Functional dissection of eukaryotic initiation factor 4F: the 4A subunit and the central domain of the 4G subunit are sufficient to mediate internal entry of 43S preinitiation complexes. *Mol Cell Biol* **16**, 6870–6878 (1996).

[339] Peters, L. & Meister, G. Argonaute proteins: mediators of RNA silencing. *Mol Cell* **26**, 611–623 (2007).

[340] Petersen, C. P., Bordeleau, M.-E., Pelletier, J. & Sharp, P. A. Short RNAs repress translation after initiation in mammalian cells. *Mol Cell* **21**, 533–542 (2006).

[341] Pillai, R. S., Bhattacharyya, S. N., Artus, C. G., Zoller, T., Cougot, N., Basyuk, E., Bertrand, E. & Filipowicz, W. Inhibition of translational initiation by Let-7 MicroRNA in human cells. *Science* **309**, 1573–1576 (2005).

[342] Pomar, N., Berlanga, J. J., Campuzano, S., Hernández, G., Elías, M. & de Haro, C. Functional characterization of Drosophila melanogaster PERK eukaryotic initiation factor 2alpha (eIF2alpha) kinase. *Eur J Biochem* **270**, 293–306 (2003).

[343] Rajkowitsch, L., Vilela, C., Berthelot, K., Ramirez, C. V. & McCarthy, J. E. G. Reinitiation and recycling are distinct processes occurring downstream of translation termination in yeast. *J Mol Biol* **335**, 71–85 (2004).

[344] Rand, T. A., Ginalski, K., Grishin, N. V. & Wang, X. Biochemical identification of Argonaute 2 as the sole protein required for RNA-induced silencing complex activity. *Proc Natl Acad Sci U S A* **101**, 14385–14389 (2004).

[345] Raught, B. & Gingras, A. Signaling to translation initiation. In *Translational control in biology and medicine*, edited by M. Mathews, N. Sonenberg & J. Hershey, chap. 14. Cold Spring Harbor Laboratory Press, New York (2007).

[346] Redpath, N. T. & Proud, C. G. The tumour promoter okadaic acid inhibits reticulocyte-lysate protein synthesis by increasing the net phosphorylation of elongation factor 2. *Biochem J* **262**, 69–75 (1989).

[347] Rehwinkel, J., Behm-Ansmant, I., Gatfield, D. & Izaurralde, E. A crucial role for GW182 and the DCP1:DCP2 decapping complex in miRNA-mediated gene silencing. *RNA* **11**, 1640–1647 (2005).

[348] Rehwinkel, J., Natalin, P., Stark, A., Brennecke, J., Cohen, S. M. & Izaurralde, E. Genome-wide analysis of mRNAs regulated by Drosha and Argonaute proteins in Drosophila melanogaster. *Mol Cell Biol* **26**, 2965–2975 (2006).

[349] Reiling, J. H. & Sabatini, D. M. Stress and mTORture signaling. *Oncogene* **25**, 6373–6383 (2006).

[350] Remm, M., Storm, C. E. & Sonnhammer, E. L. Automatic clustering of orthologs and in-paralogs from pairwise species comparisons. *J Mol Biol* **314**, 1041–1052 (2001).

[351] Rhee, S. Y., Wood, V., Dolinski, K. & Draghici, S. Use and misuse of the gene ontology annotations. *Nat Rev Genet* **9**, 509–515 (2008).

[352] Richter, J. D. CPEB: a life in translation. *Trends Biochem Sci* **32**, 279–285 (2007).

[353] Richter, J. D. & Sonenberg, N. Regulation of cap-dependent translation by eIF4E inhibitory proteins. *Nature* **433**, 477–480 (2005).

[354] Riechmann, V. & Ephrussi, A. Axis formation during Drosophila oogenesis. *Curr Opin Genet Dev* **11**, 374–383 (2001).

[355] Rivera-Pomar, R., Niessing, D., Schmidt-Ott, U., Gehring, W. J. & Jäckle, H. RNA binding and translational suppression by bicoid. *Nature* **379**, 746–749 (1996).

[356] Robins, H., Li, Y. & Padgett, R. W. Incorporating structure to predict microRNA targets. *Proc Natl Acad Sci U S A* **102**, 4006–4009 (2005).

[357] Rocak, S. & Linder, P. DEAD-box proteins: the driving forces behind RNA metabolism. *Nat Rev Mol Cell Biol* **5**, 232–241 (2004).

[358] Romero, N. M., Dekanty, A. & Wappner, P. Cellular and developmental adaptations to hypoxia: a Drosophila perspective. *Methods Enzymol* **435**, 123–144 (2007).

[359] Ron, D. & Harding, H. P. eIF2α phosphorylation in cellular stress responses and disease. In *Translational control in biology and medicine*, edited by M. Mathews, N. Sonenberg & J. Hershey, chap. 13. Cold Spring Harbor Laboratory Press, New York (2007).

[360] Rongo, C., Gavis, E. R. & Lehmann, R. Localization of oskar RNA regulates oskar translation and requires Oskar protein. *Development* **121**, 2737–2746 (1995).

[361] Rossi, J. J. RNAi and the P-body connection. *Nat Cell Biol* **7**, 643–644 (2005).

[362] Ruby, J. G., Jan, C. H. & Bartel, D. P. Intronic microRNA precursors that bypass Drosha processing. *Nature* **448**, 83–86 (2007).

[363] Ryabova, L., Park, H.-S. & Hohn, T. Control of translation reinitiation on the cauliflower mosaic virus (CaMV) polycistronic RNA. *Biochem Soc Trans* **32**, 592–596 (2004).

[364] Ryazanov, A. G., Shestakova, E. A. & Natapov, P. G. Phosphorylation of elongation factor 2 by EF-2 kinase affects rate of translation. *Nature* **334**, 170–173 (1988).

[365] Saffman, E. E., Styhler, S., Rother, K., Li, W., Richard, S. & Lasko, P. Premature translation of oskar in oocytes lacking the RNA-binding protein bicaudal-C. *Mol Cell Biol* **18**, 4855–4862 (1998).

[366] Saito, K., Ishizuka, A., Siomi, H. & Siomi, M. C. Processing of pre-microRNAs by the Dicer-1-Loquacious complex in Drosophila cells. *PLoS Biol* **3**, e235 (2005).

[367] Santoyo, J., Alcalde, J., Méndez, R., Pulido, D. & de Haro, C. Cloning and characterization of a cDNA encoding a protein synthesis initiation factor-2alpha (eIF-2alpha) kinase from Drosophila melanogaster. Homology To yeast GCN2 protein kinase. *J Biol Chem* **272**, 12544–12550 (1997).

[368] Schmitter, D., Filkowski, J., Sewer, A., Pillai, R. S., Oakeley, E. J., Zavolan, M., Svoboda, P. & Filipowicz, W. Effects of Dicer and Argonaute down-regulation on mRNA levels in human HEK293 cells. *Nucleic Acids Res* **34**, 4801–4815 (2006).

[369] Schneider, I. Cell lines derived from late embryonic stages of Drosophila melanogaster. *J Embryol Exp Morphol* **27**, 353–365 (1972).

[370] Schratt, G. M., Tuebing, F., Nigh, E. A., Kane, C. G., Sabatini, M. E., Kiebler, M. & Greenberg, M. E. A brain-specific microRNA regulates dendritic spine development. *Nature* **439**, 283–289 (2006).

[371] Schwarz, D. S., Hutvágner, G., Du, T., Xu, Z., Aronin, N. & Zamore, P. D. Asymmetry in the assembly of the RNAi enzyme complex. *Cell* **115**, 199–208 (2003).

[372] Schwer, B., Visca, P., Vos, J. C. & Stunnenberg, H. G. Discontinuous transcription or RNA processing of vaccinia virus late messengers results in a 5' poly(A) leader. *Cell* **50**, 163–169 (1987).

[373] Seggerson, K., Tang, L. & Moss, E. G. Two genetic circuits repress the Caenorhabditis elegans heterochronic gene lin-28 after translation initiation. *Dev Biol* **243**, 215–225 (2002).

[374] Sen, G. L. & Blau, H. M. Argonaute 2/RISC resides in sites of mammalian mRNA decay known as cytoplasmic bodies. *Nat Cell Biol* **7**, 633–636 (2005).

[375] Shannon, P., Markiel, A., Ozier, O., Baliga, N. S., Wang, J. T., Ramage, D., Amin, N., Schwikowski, B. & Ideker, T. Cytoscape: a software environment for integrated models of biomolecular interaction networks. *Genome Res* **13**, 2498–2504 (2003).

[376] Sheth, U. & Parker, R. Decapping and decay of messenger RNA occur in cytoplasmic processing bodies. *Science* **300**, 805–808 (2003).

[377] Shevchenko, A., Wilm, M., Vorm, O. & Mann, M. Mass spectrometric sequencing of proteins silver-stained polyacrylamide gels. *Anal Chem* **68**, 850–858 (1996).

[378] Shih, J.-W., Tsai, T.-Y., Chao, C.-H. & Lee, Y.-H. W. Candidate tumor suppressor DDX3 RNA helicase specifically represses cap-dependent translation by acting as an eIF4E inhibitory protein. *Oncogene* **27**, 700–714 (2008).

[379] Shirokikh, N. E. & Spirin, A. S. Poly(A) leader of eukaryotic mRNA bypasses the dependence of translation on initiation factors. *Proc Natl Acad Sci U S A* **105**, 10738–10743 (2008).

[380] Siomi, H., Choi, M., Siomi, M. C., Nussbaum, R. L. & Dreyfuss, G. Essential role for KH domains in RNA binding: impaired RNA binding by a mutation in the KH domain of FMR1 that causes fragile X syndrome. *Cell* **77**, 33–39 (1994).

[381] Sittler, A., Devys, D., Weber, C. & Mandel, J. L. Alternative splicing of exon 14 determines nuclear or cytoplasmic localisation of fmr1 protein isoforms. *Hum Mol Genet* **5**, 95–102 (1996).

[382] Smibert, C. A., Lie, Y. S., Shillinglaw, W., Henzel, W. J. & Macdonald, P. M. Smaug, a novel and conserved protein, contributes to repression of nanos mRNA translation in vitro. *RNA* **5**, 1535–1547 (1999).

[383] Smibert, C. A., Wilson, J. E., Kerr, K. & Macdonald, P. M. smaug protein represses translation of unlocalized nanos mRNA in the Drosophila embryo. *Genes Dev* **10**, 2600–2609 (1996).

[384] Snee, M., Benz, D., Jen, J. & Macdonald, P. M. Two distinct domains of Bruno bind specifically to the oskar mRNA. *RNA Biol* **5**, 1–9 (2008).

[385] Sonoda, J. & Wharton, R. P. Recruitment of Nanos to hunchback mRNA by Pumilio. *Genes Dev* **13**, 2704–2712 (1999).

[386] Sonoda, J. & Wharton, R. P. Drosophila Brain Tumor is a translational repressor. *Genes Dev* **15**, 762–773 (2001).

[387] Sood, R., Porter, A. C., Ma, K., Quilliam, L. A. & Wek, R. C. Pancreatic eukaryotic initiation factor-2alpha kinase (PEK) homologues in humans, Drosophila melanogaster and Caenorhabditis elegans that mediate translational control in response to endoplasmic reticulum stress. *Biochem J* **346 II**, 281–293 (2000).

[388] Spassov, D. S. & Jurecic, R. The PUF family of RNA-binding proteins: does evolutionarily conserved structure equal conserved function? *IUBMB Life* **55**, 359–366 (2003).

[389] Spirin, A. S., Belitsina, N. V. & Aitkhozhin, M. A. [Messenger RNA in early embryogenesis] In Russian. *Zh Obshch Biol* **25**, 321–338 (1964).

[390] Spirin, A. S. & Nemer, M. Messenger RNA in early sea-urchin embryos: cytoplasmic particles. *Science* **150**, 214–217 (1965).

[391] Standart, N. & Jackson, R. J. MicroRNAs repress translation of m7Gppp-capped target mRNAs in vitro by inhibiting initiation and promoting deadenylation. *Genes Dev* **21**, 1975–1982 (2007).

[392] Standart, N. & Minshall, N. Translational control in early development: CPEB, P-bodies and germinal granules. *Biochem Soc Trans* **36**, 671–676 (2008).

[393] Stanyon, C. A., Liu, G., Mangiola, B. A., Patel, N., Giot, L., Kuang, B., Zhang, H., Zhong, J. & Finley, R. L. A Drosophila protein-interaction map centered on cell-cycle regulators. *Genome Biol* **5**, R96 (2004).

[394] Stark, A., Brennecke, J., Bushati, N., Russell, R. B. & Cohen, S. M. Animal MicroRNAs confer robustness to gene expression and have a significant impact on 3'UTR evolution. *Cell* **123**, 1133–1146 (2005).

[395] Stark, A., Brennecke, J., Russell, R. B. & Cohen, S. M. Identification of Drosophila MicroRNA targets. *PLoS Biol* **1**, E60 (2003).

[396] Stebbins-Boaz, B., Cao, Q., de Moor, C. H., Mendez, R. & Richter, J. D. Maskin is a CPEB-associated factor that transiently interacts with elF-4E. *Mol Cell* **4**, 1017–1027 (1999).

[397] Steiger, M., Carr-Schmid, A., Schwartz, D. C., Kiledjian, M. & Parker, R. Analysis of recombinant yeast decapping enzyme. *RNA* **9**, 231–238 (2003).

[398] Stripecke, R., Oliveira, C. C., McCarthy, J. E. & Hentze, M. W. Proteins binding to 5' untranslated region sites: a general mechanism for translational regulation of mRNAs in human and yeast cells. *Mol Cell Biol* **14**, 5898–5909 (1994).

[399] Struhl, G. Differing strategies for organizing anterior and posterior body pattern in Drosophila embryos. *Nature* **338**, 741–744 (1989).

[400] Thermann, R. & Hentze, M. W. Drosophila miR2 induces pseudo-polysomes and inhibits translation initiation. *Nature* **447**, 875–878 (2007).

[401] Thiele, B. J., Andree, H., Höhne, M. & Rapoport, S. M. Lipoxygenase mRNA in rabbit reticulocytes. Its isolation, characterization and translational repression. *Eur J Biochem* **129**, 133–141 (1982).

[402] Thomson, T., Liu, N., Arkov, A., Lehmann, R. & Lasko, P. Isolation of new polar granule components in Drosophila reveals P body and ER associated proteins. *Mech Dev* **125**, 865–873 (2008).

[403] Tolia, N. H. & Joshua-Tor, L. Slicer and the argonautes. *Nat Chem Biol* **3**, 36–43 (2007).

[404] Tomari, Y., Du, T., Haley, B., Schwarz, D. S., Bennett, R., Cook, H. A., Koppetsch, B. S., Theurkauf, W. E. & Zamore, P. D. RISC assembly defects in the Drosophila RNAi mutant armitage. *Cell* **116**, 831–841 (2004).

[405] Tritschler, F., Eulalio, A., Truffault, V., Hartmann, M. D., Helms, S., Schmidt, S., Coles, M., Izaurralde, E. & Weichenrieder, O. A divergent Sm fold in EDC3 proteins mediates DCP1 binding and P-body targeting. *Mol Cell Biol* **27**, 8600–8611 (2007).

[406] Ulvila, J., Parikka, M., Kleino, A., Sormunen, R., Ezekowitz, R. A., Kocks, C. & Rämet, M. Double-stranded RNA is internalized by scavenger receptor-mediated endocytosis in Drosophila S2 cells. *J Biol Chem* **281**, 14370–14375 (2006).

[407] van Eeden, F. J., Palacios, I. M., Petronczki, M., Weston, M. J. & Johnston, D. S. Barentsz is essential for the posterior localization of oskar mRNA and colocalizes with it to the posterior pole. *J Cell Biol* **154**, 511–523 (2001).

[408] Vardy, L. & Orr-Weaver, T. L. The Drosophila PNG kinase complex regulates the translation of cyclin B. *Dev Cell* **12**, 157–166 (2007).

[409] Vardy, L. & Orr-Weaver, T. L. Regulating translation of maternal messages: multiple repression mechanisms. *Trends Cell Biol* **17**, 547–554 (2007).

[410] Vaucheret, H., Vazquez, F., Crété, P. & Bartel, D. P. The action of ARGONAUTE1 in the miRNA pathway and its regulation by the miRNA pathway are crucial for plant development. *Genes Dev* **18**, 1187–1197 (2004).

[411] Wakiyama, M., Takimoto, K., Ohara, O. & Yokoyama, S. Let-7 microRNA-mediated mRNA deadenylation and translational repression in a mammalian cell-free system. *Genes Dev* **21**, 1857–1862 (2007).

[412] Wang, B., Love, T. M., Call, M. E., Doench, J. G. & Novina, C. D. Recapitulation of short RNA-directed translational gene silencing in vitro. *Mol Cell* **22**, 553–560 (2006).

[413] Wang, C., Dickinson, L. K. & Lehmann, R. Genetics of nanos localization in Drosophila. *Dev Dyn* **199**, 103–115 (1994).

[414] Wang, C. & Lehmann, R. Nanos is the localized posterior determinant in Drosophila. *Cell* **66**, 637–647 (1991).

[415] Wang, H., Dictenberg, J. B., Ku, L., Li, W., Bassell, G. J. & Feng, Y. Dynamic association of the fragile X mental retardation protein as a messenger ribonucleoprotein between microtubules and polyribosomes. *Mol Biol Cell* **19**, 105–114 (2008).

[416] Wang, H., Iacoangeli, A., Lin, D., Williams, K., Denman, R. B., Hellen, C. U. T. & Tiedge, H. Dendritic BC1 RNA in translational control mechanisms. *J Cell Biol* **171**, 811–821 (2005).

[417] Wang, X., Zamore, P. D. & Hall, T. M. Crystal structure of a Pumilio homology domain. *Mol Cell* **7**, 855–865 (2001).

[418] Webster, P. J., Liang, L., Berg, C. A., Lasko, P. & Macdonald, P. M. Translational repressor bruno plays multiple roles in development and is widely conserved. *Genes Dev* **11**, 2510–2521 (1997).

[419] Wells, S. E., Hillner, P. E., Vale, R. D. & Sachs, A. B. Circularization of mRNA by eukaryotic translation initiation factors. *Mol Cell* **2**, 135–140 (1998).

[420] Westfall, Y.-S. S., Peter H. *Resampling-based Multiple Testing.* Wiley Series in Probability and Statistics. John Wiley & Sons, New York (1993).

[421] Wharton, R. P. & Aggarwal, A. K. mRNA regulation by Puf domain proteins. *Sci STKE* **2006**, pe37 (2006).

[422] Wickens, M., Bernstein, D. S., Kimble, J. & Parker, R. A PUF family portrait: 3'UTR regulation as a way of life. *Trends Genet* **18**, 150–157 (2002).

[423] Wightman, B., Ha, I. & Ruvkun, G. Posttranscriptional regulation of the heterochronic gene lin-14 by lin-4 mediates temporal pattern formation in C. elegans. *Cell* **75**, 855–862 (1993).

[424] Wilhelm, J. E., Buszczak, M. & Sayles, S. Efficient protein trafficking requires trailer hitch, a component of a ribonucleoprotein complex localized to the ER in Drosophila. *Dev Cell* **9**, 675–685 (2005).

[425] Wilhelm, J. E., Hilton, M., Amos, Q. & Henzel, W. J. Cup is an eIF4E binding protein required for both the translational repression of oskar and the recruitment of Barentsz. *J Cell Biol* **163**, 1197–1204 (2003).

[426] Wilhelm, J. E. & Smibert, C. A. Mechanisms of translational regulation in Drosophila. *Biol Cell* **97**, 235–252 (2005).

[427] Williams, R. W. & Rubin, G. M. ARGONAUTE1 is required for efficient RNA interference in Drosophila embryos. *Proc Natl Acad Sci U S A* **99**, 6889–6894 (2002).

[428] Wilson, J. E., Pestova, T. V., Hellen, C. U. & Sarnow, P. Initiation of protein synthesis from the A site of the ribosome. *Cell* **102**, 511–520 (2000).

[429] Wreden, C., Verrotti, A. C., Schisa, J. A., Lieberfarb, M. E. & Strickland, S. Nanos and pumilio establish embryonic polarity in Drosophila by promoting posterior deadenylation of hunchback mRNA. *Development* **124**, 3015–3023 (1997).

[430] Wright, C. F. & Moss, B. In vitro synthesis of vaccinia virus late mRNA containing a 5' poly(A) leader sequence. *Proc Natl Acad Sci U S A* **84**, 8883–8887 (1987).

[431] Wu, H., Xu, H., Miraglia, L. J. & Crooke, S. T. Human RNase III is a 160-kDa protein involved in preribosomal RNA processing. *J Biol Chem* **275**, 36957–36965 (2000).

[432] Wu, L. & Belasco, J. G. Micro-RNA regulation of the mammalian lin-28 gene during neuronal differentiation of embryonal carcinoma cells. *Mol Cell Biol* **25**, 9198–9208 (2005).

[433] Wu, L. & Belasco, J. G. Let me count the ways: mechanisms of gene regulation by miRNAs and siRNAs. *Mol Cell* **29**, 1–7 (2008).

[434] Wu, L., Fan, J. & Belasco, J. G. MicroRNAs direct rapid deadenylation of mRNA. *Proc Natl Acad Sci U S A* **103**, 4034–4039 (2006).

[435] Xie, Z., Kasschau, K. D. & Carrington, J. C. Negative feedback regulation of Dicer-Like1 in Arabidopsis by microRNA-guided mRNA degradation. *Curr Biol* **13**, 784–789 (2003).

[436] Yano, T., de Quinto, S. L., Matsui, Y., Shevchenko, A., Shevchenko, A. & Ephrussi, A. Hrp48, a Drosophila hnRNPA/B homolog, binds and regulates translation of oskar mRNA. *Dev Cell* **6**, 637–648 (2004).

[437] Yedavalli, V. S. R. K., Neuveut, C., Chi, Y.-H., Kleiman, L. & Jeang, K.-T. Requirement of DDX3 DEAD box RNA helicase for HIV-1 Rev-RRE export function. *Cell* **119**, 381–392 (2004).

[438] Yi, R., Qin, Y., Macara, I. G. & Cullen, B. R. Exportin-5 mediates the nuclear export of pre-microRNAs and short hairpin RNAs. *Genes Dev* **17**, 3011–3016 (2003).

[439] ying Chu, C. & Rana, T. M. Translation repression in human cells by microRNA-induced gene silencing requires RCK/p54. *PLoS Biol* **4**, e210 (2006).

[440] Yoshimura, A., Fujii, R., Watanabe, Y., Okabe, S., Fukui, K. & Takumi, T. Myosin-Va facilitates the accumulation of mRNA/protein complex in dendritic spines. *Curr Biol* **16**, 2345–2351 (2006).

[441] You, L. R., Chen, C. M., Yeh, T. S., Tsai, T. Y., Mai, R. T., Lin, C. H. & Lee, Y. H. Hepatitis C virus core protein interacts with cellular putative RNA helicase. *J Virol* **73**, 2841–2853 (1999).

[442] Zaessinger, S., Busseau, I. & Simonelig, M. Oskar allows nanos mRNA translation in Drosophila embryos by preventing its deadenylation by Smaug/CCR4. *Development* **133**, 4573–4583 (2006).

[443] Zalfa, F., Achsel, T. & Bagni, C. mRNPs, polysomes or granules: FMRP in neuronal protein synthesis. *Curr Opin Neurobiol* **16**, 265–269 (2006).

[444] Zalfa, F., Giorgi, M., Primerano, B., Moro, A., Penta, A. D., Reis, S., Oostra, B. & Bagni, C. The fragile X syndrome protein FMRP associates with BC1 RNA and regulates the translation of specific mRNAs at synapses. *Cell* **112**, 317–327 (2003).

[445] Zamore, P. D., Williamson, J. R. & Lehmann, R. The Pumilio protein binds RNA through a conserved domain that defines a new class of RNA-binding proteins. *RNA* **3**, 1421–1433 (1997).

[446] Zappavigna, V., Piccioni, F., Villaescusa, J. C. & Verrotti, A. C. Cup is a nucleocytoplasmic shuttling protein that interacts with the eukaryotic translation initiation factor 4E to modulate Drosophila ovary development. *Proc Natl Acad Sci U S A* **101**, 14800–14805 (2004).

[447] Zhang, B., Gallegos, M., Puoti, A., Durkin, E., Fields, S., Kimble, J. & Wickens, M. P. A conserved RNA-binding protein that regulates sexual fates in the C. elegans hermaphrodite germ line. *Nature* **390**, 477–484 (1997).

[448] Zhou, Z., Licklider, L. J., Gygi, S. P. & Reed, R. Comprehensive proteomic analysis of the human spliceosome. *Nature* **419**, 182–185 (2002).